BIODEGRADATION OF POLY(ETHYLENE TEREPHTHALATE) MICROPLASTICS BY BACTERIAL COMMUNITIES FROM ACTIVATED SLUDGE

by

Patricia Torena, BSc.

University of Carabobo, 2011

A thesis presented to

Ryerson University

in partial fulfilment of the

requirements for the degree of

Master of Applied Science

in the program of

Chemical Engineering

Toronto, Ontario, Canada, 2019

AUTHOR'S DECLARATION

I hereby declare that I am the sole author of this thesis. This is a true copy of the thesis, including any required final revisions, as accepted by my examiners.

I authorize Ryerson University to lend this thesis to other institutions or individuals for the purpose of scholarly research.

I further authorize Ryerson University to reproduce this thesis by photocopying or by other means, in total or in part, at the request of other institutions or individuals for the purpose of scholarly research.

I understand that my thesis may be made electronically available to the public.

ABSTRACT

BIODEGRADATION OF POLY(ETHYLENE TEREPHTHALATE) MICROPLASTICS BY BACTERIAL COMMUNITIES FROM ACTIVATED SLUDGE

Patricia Torena, 2019

Master of Applied Science
Chemical Engineering
Ryerson University
Toronto, Ontario, Canada

The emerging accumulation of microplastics (MPs) within global waters and the risks they pose to both humans and aquatic species are of increasing concern, yet suitable technologies to remove MPs are lacking. In this study, bacteria with potential to degrade MPs were isolated from activated sludge as promising biocatalysts for the removal of MPs in water. The bacterial communities in activated sludge were first screened for their potential to degrade thermally-treated MPs from PET. The consortium exhibited growth on a mineral medium with PET MPs as the sole carbon and energy source, indicating the presence of degrading bacteria. To further assess its biodegradability potential, the consortium was put through a CO_2 evolution test where the degradation of MPs was monitored through measuring the CO_2 evolved. The test was carried out in an experimental device that was engineered and constructed according to ISO 14852. The biodegradation extent was further validated through assessment of morphological and structural changes on the MPs by means of scanning electron microscopy, differential scanning calorimetry and Fourier transform infrared spectroscopy analyses. Upon incubation, the consortium degraded 17 % of PET MPs. Three bacterial strains within the consortium were isolated and identified as *Lysinibacillus macroides* RW13-2, *Bacillus cereus* SEHD031MH and *Agromyces mediolanus* PNP3. The latter two thrived individually with PET while only *B. cereus* showed enzymatic activity during a clear-zone test. The examined bacterial strains possess a promising PET-degrading activity that can be further investigated and applied to the elimination of MPs in water/wastewater through innovative and effective technologies.

ACKNOWLEDGEMENTS

I would like to express my deepest gratitude and admiration to Dr. Manuel Alvarez Cuenca, my supervisor and mentor throughout the realization of this work. I would like to thank Dr. Manuel Alvarez Cuenca for giving me the opportunity to work on a very innovative and interesting experimental research that opened my frontiers in the field of wastewater treatment and environmental remediation. More than a leader, Dr. Manuel Alvarez Cuenca has been my mentor and I am grateful that he always invested in my professional growth and encouraged me to go beyond my own expectations. Without his extensive knowledge, dedicated guidance and financial support, this thesis would not have been possible. I am forever thankful for everything he has done and for all he has taught me.

I also would like to extend my thanks to the technicians from the Chemical Engineering Department at Ryerson University, Mr. Ali Hemmati, Mr. Daniel Boothe and Mr. Tondar Tajrobehkar for their support and help in the construction and troubleshooting of the experimental unit.

I would like to express my special thanks to Dr. Kimberley Gilbride in the Department of Biology/Chemistry for providing us with the tools to perform the microbial analysis and to her graduate students Farhan Yusuf and Amir Tehrani, for their enthusiastic support and mentorship. This analysis involved extensive work that took a lot of dedication and expertise, which helped us to complete this thesis successfully. Thanks also to Dr. Maryam Reza, for her constant willingness to advise and provide precious feedback throughout this entire research work.

I would like to thank the technologists from the Biology/Chemistry Department, Robert Denning and Shawn McFadden, and from the Mechanical Engineering Department, Qiang Li, for all their assistance in the analytical techniques performed in this research work.

Finally, I would like to thank my family, specially my husband for his unconditional love, understanding and support that gave me the courage and strength to overcome the difficulties and accomplish this research work.

Special thanks to the Department of Chemical Engineering for the financial support provided throughout the development of this investigation. The facilities used for the analytical techniques required in this work, Scanning Electron Microscopy, High Performance Liquid Chromatography and Differential Scanning Calorimetry, were kindly provided by the Mechanical Engineering Department at Ryerson University and the Ryerson University Analytical Centre. The DNA sequencing involved in the microbial analysis was performed by the ACGT Corporation (Toronto, ON).

TABLE OF CONTENTS

LIST OF TABLES

LIST OF FIGURES

LIST OF ACRONYMS

A: absorbance

$Ba(OH)_2$: barium hydroxide

BLAST: Basic Local Assignment Search Tool

BHET: bis(hydroxyethyl) terephthalate

Ca: calcium

Cc: carbon content

CFU: colony-forming unit

Cl: chlorine

CO_2: carbon dioxide

DAD: photodiode array detector

DDTs: dichlorodiphenyltrichloroethane

DEHP: di-(2-ethylhexyl) phthalate

DMT: dimethyl terephthalate

DSC: Differential Scanning Calorimetry

Dt: percentage biodegradation

EG: ethylene glycol

EPS: extracellular polymeric substance

Expon: predicted exponential curve

F_{O2}: oxygen flow rate

FTIR: Fourier-transform infrared spectroscopy

GPC: Gel permeation chromatography

GTA: Greater Toronto Area

HCl: hydrochloric acid

HDPE: high-density polyethylene

HPLC: High performance liquid chromatography

H_2O: water

I.D.: inside diameter

I: intensity

ISO: International Organization for Standardization

LDPE: low-density polyethylene

LB: Luria broth

M: mean

MHET: mono(2-hydroxyethyl) terephthalate acid

MPs: microplastics

Na: sodium

NaOH: sodium hydroxide

Na_2CO_3: sodium carbonate

NCBI: National Center for Biotechnology Information

O_2: oxygen

O.D.: outside diameter

OD: optical density

PAHs: polycyclic aromatic hydrocarbons

PBS: phosphate buffer saline solution

PCBs: polychlorinated biphenyls

PCL: polycaprolactone

PCR: polymerase chain reaction process

PE: polyethylene

PET: poly(ethylene terephthalate)

PET_o: poly(ethylene terephthalate) before incubation

PET_i: poly(ethylene terephthalate) after incubation

PHB: polyhydroxybutyrate

PLA: polylactic acid

POPs: persistent organic pollutants

PP: polypropylene

PS: polystyrene

PTCE: phenol/1,1,2,2-tetrachloroethane solution

PVC: polyvinyl chloride

P&ID: piping and instrumentation diagram

SD: standard deviation

TES: trace element solution

TOC: total organic carbon

TPA: terephthalic acid

TSS: total suspended solids

UV: ultraviolet radiation

VSS: volatile suspended solids

WWTP: wastewater treatment plant

WWTPs: wastewater treatment plants

XPS: X-ray photoelectron spectroscopy

XRD: X-ray diffraction

1. INTRODUCTION

1.1. OVERVIEW

Plastic has become a necessity, with wide-ranging applications including commercial, industrial, and medicinal. From their outstanding durability and versatility to their low-cost production, plastics have become very popular with an increasing global production to satisfy high demands. In 2017 alone, the total global production of plastics was 348 million tonnes (PlasticsEurope, 2018). However, plastic wastes have been polluting the environment due to many factors such as insufficient recovery rates, increase of single-use plastic products, and littering. The pollution of marine environments by microplastics (MPs), which are generally defined as small plastic particles with a diameter of 5 mm or less (J. C. Anderson et al., 2016; Carr et al., 2016; Claessens et al., 2013), has increased concerns and have augmented substantially in the past hundred years. More than 5.25 trillion of floating macro and micro plastic pieces has been estimated to be in the open ocean (Eriksen et al., 2014) from which approximately 92.4 % are MPs (Santana et al., 2016).

In the following sections, the definition of microplastics and their impact on the environment and public health are discussed. Next, the significance and aim of the current study are presented.

1.2. MICROPLASTICS

Ever since the presence of small plastic fragments, fibres and pellets was detected, the term ‘microplastics’ has been used to collectively define these particles. Many size-ranges have been assigned to microplastics in different studies, for instance diameters of <10 mm, <5 mm, 2-6 mm, <2 mm, and <1 mm (Cole et al., 2011), although such inconsistency hindered the comparison of scientific data from diverse research works. Hence, they were defined as plastic particles of <5 mm in diameter by scientists at the first international research workshop on the occurrence, effects and fate of microplastic marine debris in 2008, hosted by the National Oceanic and Atmospheric Administration (NOAA; Arthur et al., 2009).

The main plastics found within MPs consist of thermoplastics like polyethylene (PE), polypropylene (PP), polystyrene (PS), polyvinyl chloride (PVC), and poly(ethylene terephthalate)

(PET, Andrady, 2017; Auta, Emenike, & Fauziah, 2017; Murphy, Ewins, Carbonnier, & Quinn, 2016). The latter is massively used in beverage and food packaging and when not properly disposed or recovered, it may end up in the oceans. The popularity of PET falls on its outstanding properties such as very high mechanical strength, low gas permeability, and highly resistance to atmospheric degradation. But the excellent properties that make PET chemically and physically durable also make it a major residue in the waste stream due to its high resistance to microbial and atmospheric attacks.

1.2.1. Types of microplastics

Microplastics are classified into two different types, depending on the way they were originated: primary and secondary **(Figure 1.1**.). Primary MPs are plastics that are manufactured to be within the microscopic size range; also known as microbeads, they are mainly used in medicines, industrial applications and personal care products such as facial scrubs and toothpastes. Moreover, other plastic particles that fall in this category include virgin pellets used as 'feedstock' in plastic manufacture, fibres from synthetic fabrics and tiny plastics from tire abrasion. Secondary MPs are the fragments that result from the weathering and degradation of larger plastics, mostly caused by UV-radiation (Li et al., 2018).

Primary and secondary MPs can originate from a wide variety of sources. For instance, according to Boucher & Friot, 2017, the biggest contributors (two-thirds) to the primary MPs, which make up to 30% of the total new plastic waste released into the oceans each year, are the abrasion of synthetic textiles occurred when laundry washing and abrasion of tires when driving.

The macroplastic litter that originates MPs in marine environments is produced in many ways; some of the different sources include coastal tourism, construction, agriculture, packaging, and plastic recyclers (UNEP, 2016). Furthermore, MPs can also be generated by leakages in waste handling and recycling activities, such as landfills, paper and plastic recycling, organic waste treatment, and food waste shredding (Sundt et al., 2014). Other than the land-based sources, MPs can also originate from activities at sea such as commercial fishing, nautical doings and aquaculture.

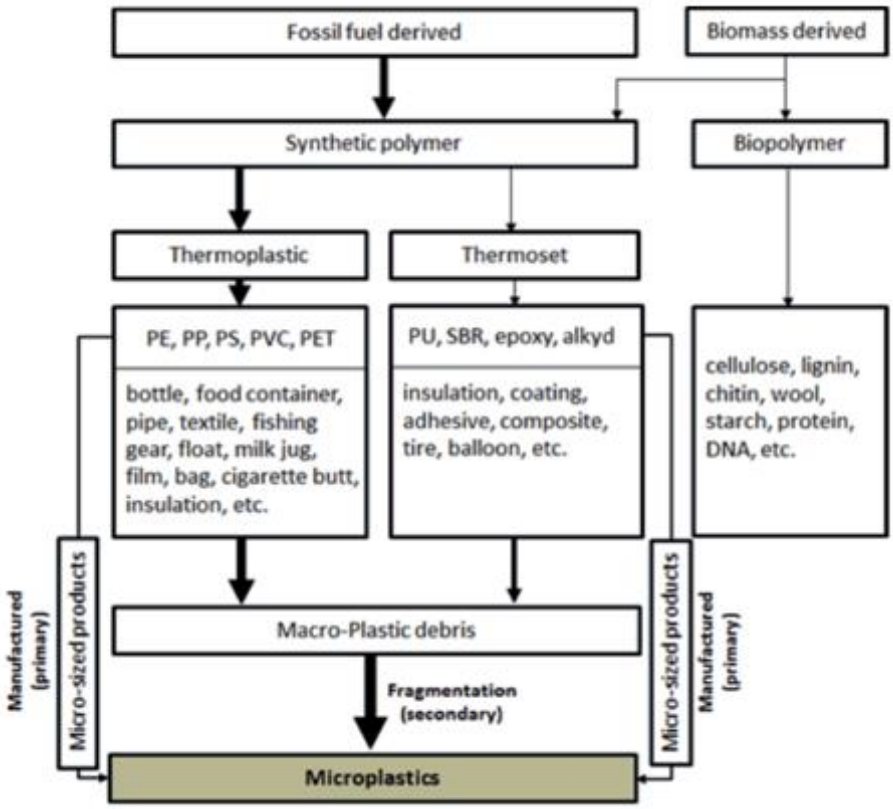

Figure 1.1. Types of microplastics. Production of the most common artificial and natural polymers, including typical applications. Microplastics (primary) are manufactured for particular applications. All plastics can be subject to fragmentation during environmental exposure and degradation into (secondary) microplastics (GESAMP, 2015)

1.2.2. Pathways of microplastics into the aquatic environment

Microplastics can enter the aquatic environment through many different pathways (**Figure 1.2**.) such as:

- Effluent discharge from Wastewater Treatment Plants (WWTPs)
- Untreated sewage
- Domestic discharges (laundry washing machines)
- Industrial activities
- Agricultural activities

- Wind transfer
- Road runoff
- Overflows in sanitary and storm sewers

For instance, though WWTPs are designed to retain macroplastics and small plastic particles with an efficiency of 90 – 98%, an important fraction of MPs remain in the effluents. This is because they treat such large volumes of wastewater daily, that even a small percentage of wastewater that was not properly treated would result in a significant amount of microplastics being released into the water stream. Different investigations have reported that WWTPs act as potential sources of microplastics (HELCOM, 2014; Magnusson & Norén, 2014; Talvitie et al., 2015). For example, an assessment of a WWTP in Scotland reported that, despite a high retention efficiency of 98.41%, 65 million MPs/day were released into the receiving water (Murphy et al., 2016). Likewise, the effluents of 17 different WWTPs across the United States were assessed by Mason et al. (2016), finding that the facilities discharge up to 15 million MPs/day into the receiving waters. In another study performed by Gies et al. (2018) in Vancouver, Canada, it was found that a WWTP releases approximately 82 million MPs/day through the effluent, despite of having a retention of microplastics of 97 – 99%. Some other plants may not be equipped with advanced filtration systems, as it is the case of many WWTPs in New York (Driedger, Dürr, Mitchell, & Van Cappellen, 2015).

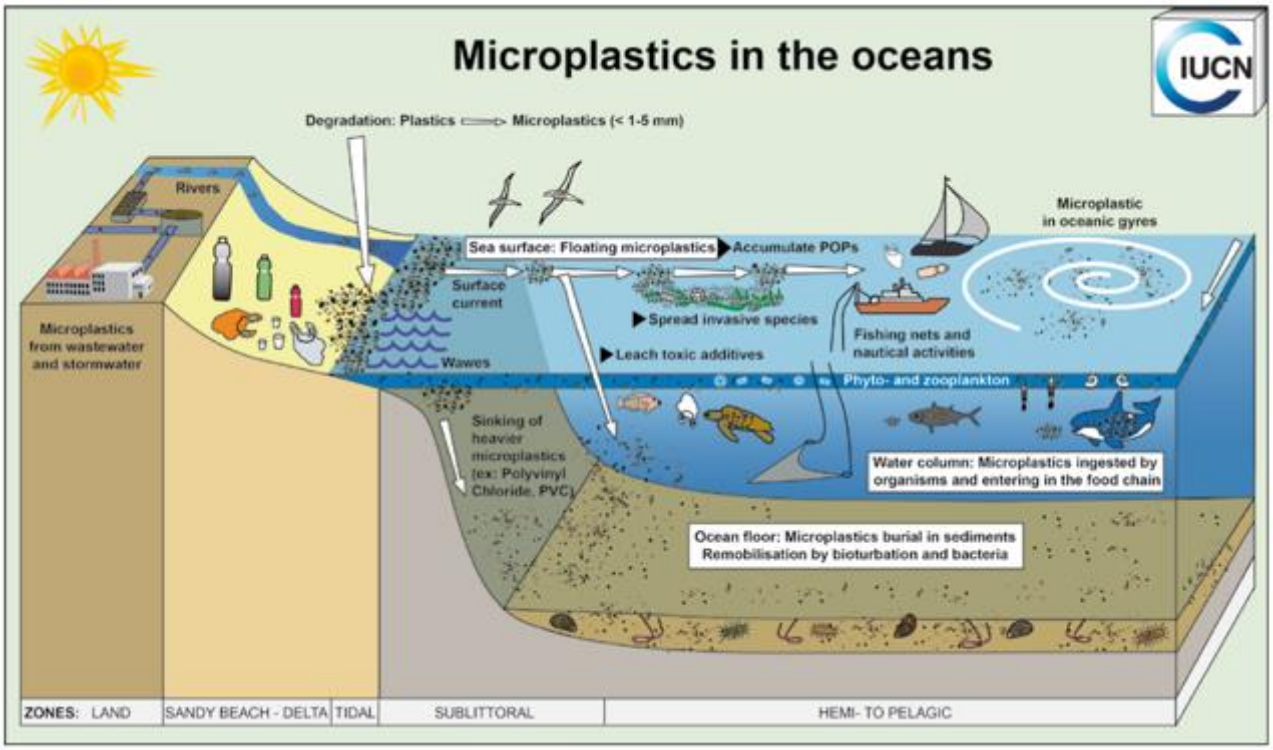

Figure 1.2. Schematic drawing showing the main sources and movement pathways for plastics debris in the oceans (Thevenon, 2014)

The MPs originated from the abrasion of tires are transported into the ocean via road runoff and wind transfer. Microbeads used both in cosmetics and industrial activities can also enter the water bodies through domestic or industrial drainage systems.

Other potential pathway through which MPs are transported to water bodies is overflows of wastewater in sanitary and storm sewers during high rain events. When the volume of municipal sewage and rainwater runoff carried in sewers increases and surpasses the WWTPs capacity, overflow points discharge wastewater directly into rivers or lakes so that the treatment plant is not overloaded. The untreated wastewater that is discharged can potentially carry MPs along with other alarming components such as pathogens, pharmaceuticals, heavy metals, and toxins. According to Environment Canada figures, nearly 120 million cubic metres of untreated sewage and runoff entered the waterways across Canada in 2017 (Cruickshank, 2018). Given the fact that enormous volumes of treated and untreated wastewater are discharged globally and only a fraction (60%) of municipal water is treated, massive quantities of MPs are expected to enter the environment via WWTP releases (Jingyi Li et al., 2018).

1.3. ENVIRONMENTAL IMPACT OF MICROPLASTICS

Perhaps the main environmental impact of microplastics is their accumulation in different ecosystems. MPs stand out for their chemical stability and durability which makes it easy for their extensive accumulation, especially in the aquatic environment (Gewert, Plassmann, & MacLeod, 2015). Their high bioavailability and capacity to adsorb toxic elements represent a threat to marine biota. These effects are discussed in detail in the following sections.

1.3.1. Accumulation of microplastics in the aquatic environment

Microplastics are accumulating in different marine ecosystems at increasing rates. Many quantitative reports of global abundances of MPs have been published (**Table 1.1**), indicating their presence in large ocean currents, sediments, water columns, surfaces and coastal areas (GESAMP, 2015). The observed trend is that MPs accumulate in areas that are close to cities or regions of high human activity. However, MPs have also been detected in very isolated areas such as the Arctic sea ice (Obbard et al., 2014), Tibetan Plateau remote lakes (K. Zhang et al., 2016) and in a mountain lake in Mongolia (Free et al., 2014). The concentration of microplastics is commonly measured as the number of plastic particles per unit of the area being sampled, or number of plastic particles per unit of the volume being sampled (which is estimated as the area times the depth of sampling).

- **Surface waters**

Several studies have been conducted to determine the abundance of MPs in global surface waters; although the amounts reported may vary significantly, high volumes have been found, going up to 5 $x10^6$ MPs/km^2. In one study performed in the eastern North and South Pacific Oceans, plastic debris was found in 42% of all surface samples collected between 2001 and 2012 (Law et al., 2014). The total weight of MPs floating in that region of the eastern Pacific Ocean was estimated to be as high as 21,290 tonnes with a maximum plastic concentration from individual tows exceeding 10^6 MPs/km^2. The occurrence and abundance of plastic debris has been also studied in surface waters from other ocean and sea areas such as the Mediterranean Sea (Fossi et al., 2012), Western North Atlantic Ocean and Caribbean Sea (Law et al., 2010), Western North Pacific Ocean (Yamashita & Tanimura, 2007), and Arctic Ocean (Obbard et al., 2014).

- **Lakes**

Similarly, some studies have characterized the amounts of MPs in surface water of lakes. Surface waters were sampled in 2016 to determine the abundance of MPs in the lakes Bolsena and Chiusi in Italy (Fischer, et al., 2016). These waters were found to contain up to 4 MPs/m^3 at the surface and up to 234 MPs/kg in sediment. Free et al. (2014) observed a high abundance of MPs in Lake Hovsgol, a large, remote, mountain lake in Mongolia in what it was the first study to characterize plastic particles in such remote area. An average of 20,264 MPs/km^2 was found in this lake, which indicates it is more heavily polluted than more developed lakes like the Laurentian Great Lakes (Free et al., 2014).

- **Sediments**

Microplastics in nearshore, beaches, and marine sediments have been also characterized along many coastlines around the world. Sandy beaches from 18 sites worldwide, including Chile, Portugal, Japan, South Africa, and United Kingdom, were found to be contaminated with up to 160,000 MPs/m^3 sediment (Browne et al., 2011). Another study found that beach sediments sampled at different depths along shorelines of São Paulo State, Brazil, contained high densities of microplastics of up to 8,867 MPs/m^3 sediment. A shocking total of approximately 762 million MPs was estimated to be present in the whole area (Turra et al., 2014).

- **Rivers**

As rivers have shown to be a significant pathway of microplastics to the ocean, many studies have been performed to measure the microplastic contamination on the surface and sediment of various rivers worldwide. Austria, UK, USA, Chile, Italy, South Korea, Germany, Canada, and China are some of the locations that have been assessed for microplastic abundance in rivers. Some of the rivers with the heavier densities include Los Angeles River, USA (1,1 x10^6 MPs/m^3); Nakdong River, South Korea (187,000 MPs/m^3); and St. Lawrence River, Canada (1.0 x10^6 MPs/m^3) (GESAMP, 2016). While MPs were reported for rivers in all the studied areas, concentrations varied considerably, up to a factor of 10^9, probably due to the use of different methodologies and the proximity to cities and sources.

Table 1.1. Global occurrence of microplastics in the aquatic environment

Location	Maximum observed concentration	Reference
Coastal areas and beaches		
Baltic Coast Germany, beach sediments	7 MPs/kg dry sediment 11 fibres/kg dry sediment	Stolte et al., 2015
Japan, sandy beaches	30 MPs/250 mL sediment	Browne et al., 2011
Chile, sandy beaches	20 MPs/250 mL sediment	Browne et al., 2011
Portugal, sandy beaches	31 MPs/250 mL sediment	Browne et al., 2011
South Africa, sandy beaches	30 MPs/250 mL sediment	Browne et al., 2011
United Kingdom	40 MPs/250 mL sediment	Browne et al., 2011
Brazil, sandy beaches	163 MPs/m^3	Turra et al., 2014
Belgium, beach sediments	93 MPs/kg dry sediment	Claessens et al., 2011
Australia, coastal surface	4,256 MPs/km^2	Reisser et al., 2013
Open ocean		
Eastern North Pacific ocean, surface water	$>10^6$ MPs/km^2	Law et al., 2014
Mediterranean Sea, surface water	10 MPs /m^3	Fossi et al., 2012
Western North Atlantic ocean and Caribbean sea, surface water	580,000 MPs/km^2	Law et al., 2010
Western North Pacific ocean, surface water	500 x 10^4 MPs/km^2	Yamashita & Tanimura, 2007
Arctic Ocean, sea ice	234 MPs/m^3 ice	Obbard et al., 2014
Lakes		
Lake Hovsgol, Mongolia, surface water	45,000 MPs/km^2	Free et al., 2014
Lake Vembanad, India, sediments	496 MPs/m^2	Sruthy & Ramasamy, 2017
Lake Bolsena, Italy	surface water 4 MPs/m^3 sediments 112 MPs/kg dry sediment	Fischer, et al., 2016
Lake Chiusi, Italy	surface water 3 MPs/m^3 sediments 234 MPs/kg dry sediment	Fischer, et al., 2016
Tibetan Plateau remote lakes, China, sediments	563 MPs/m^2	K. Zhang et al., 2016
Laurentian Great Lakes, US, surface water	466,000 MPs /km^2	Eriksen et al., 2013

1.3.2. Occurrence of microplastics in Canadian water bodies

Few studies have been conducted in Canada to characterize the quantities of MPs in aquatic environments. While most of these studies (**Table 1.2**) focused on several main regions, their outcome indicates that to date microplastics can be observed everywhere. The studies included analyses in coastal sediments and surface waters located at different regions of Canada and they are briefly explained below.

- **Central Canada**

One of the first assessments in MPs abundance in Canada was conducted by Zbyszewski & Corcoran in the province of Ontario in 2011. In this study, the presence of MPs in beaches around Lake Huron was assessed. Though the plastic particles were not quantified in all the sampled locations, the beach at Sarnia was reported to have 408 MPs/m^2 (Zbyszewski & Corcoran, 2011).

In 2014, Corcoran et al. assessed sediments from the Humber Bay region, located at the northwest shoreline of Lake Ontario – the smallest of the Laurentian Great Lakes. A total of 6,172 plastic pieces were collected within the samples, including polystyrene pieces, and pellets and fragments of mostly polyethylene and polypropylene (Corcoran et al., 2015). The accumulation rates of pellets and fragments found at the Humber Bay beach site were ~$26x10^6$ MPs/km^2 while in the case of polystyrene pieces, the accumulation rate was $1.7x10^6$ g/ km^2. Another study performed in the same year by Helm et al. analyzed samples collected at the surface water in Lake Ontario, Lake Erie, and urban streams entering Lake Ontario. These waters were found to contain between 90,000 and $6.7x10^5$ MPs/km^2 (Helm et al., 2016). Furthermore, Ballent et al. (2016) investigated microplastic pollution at Lake Ontario and found MPs in all the samples collected in nearshore, tributary and beach sediments. Abundances varied between 20 to 28,000 MPs/kg of dry sediment, with the highest abundance found at the mouth of Etobicoke Creek (Ballent, et al., 2016). Amounts of MPs in beach samples appeared to decrease with greater distance from Toronto; only at sites in the Greater Toronto Area (GTA) and offshore of Oakville, the microplastics abundance was of > 1000 MPs/kg.

Table 1.2. Occurrence of microplastics in water bodies in Canada

Location	Maximum observed concentration	Reference
Lake Huron (Sarnia beaches), shoreline sediments	408 MPs/m^2	Zbyszewski & Corcoran, 2011
Coastal British Columbia, sub-surface water	9200 MPs/m^3	Desforges, et al., 2014
St. Lawrence River, sediments	1.4 x 10^5 MPs/m^2	Castañeda, et al., 2014
McCormacks Beach and Rainbow Haven Beach, Nova Scotia, sediments	8000 MPs/kg sediment	Mathalon & Hill, 2014
Lake Ontario, shoreline sediments	~26 MPs/m^2	Corcoran et al., 2015
Lake Ontario and urban streams entering, surface waters	90,000 – 6,700,000 MPs/km^2	Helm et al., 2016
Bay of Fundy, New Brunswick and Nova Scotia, coastal sediments	1320 MPs/kg sediment	Forsythe, 2016
Lake Ontario, nearshore, tributary and beach sediments	~28,000 MPs/kg dry sediment	Ballent, et al., 2016
Lake Winnipeg, surface water	748,000 MPs/km^2	P. J. Anderson et al., 2017
Lambert Channel and Baynes Sound, British Columbia, sediments	25,000 microbeads/kg dry sediment 300 MPs/kg dry sediment	Kazmiruk et al., 2018

In one of the few studies conducted in Canadian freshwaters, Castañeda and colleagues collected sediment samples from ten sites in the St. Lawrence River between Lake St. Francis and Quebec City in 2013 (Castañeda, et al., 2014). Microplastics of 0.40 - 2.16 mm in diameter were discovered throughout the sites, with abundances that varied by four orders of magnitude across sites. The highest site density was 1.4 x 10^{11} MPs/km^2 which, according to the authors, is comparable to those concentrations of the world's most contaminated marine sediments. Similarly, surface waters of Lake Winnipeg – the 11th largest freshwater body in the world – were assessed to determine the densities of MPs. Anderson et al. collected samples at twelve locations between 2014 and 2016 and

found that all of them contained MPs. The abundances ranged from 53,000 to 748,000 MPs/km^2 which revealed that densities of MPs in Lake Winnipeg are similar or significantly greater to those reported in the Laurentian Great Lakes (P. J. Anderson et al., 2017).

- **The West Coast**

The coastal British Columbia was evaluated in two separate studies. In 2014, Desforges and co-workers documented the abundance, composition and distribution of MPs in sub-surface seawaters of the northeastern Pacific Ocean and coastal British Columbia. The density ranged from 8 to 9200 MPs/m^3. An increase of 6, 12 and 27-fold in concentration was found in west coast Vancouver Island, Strait of Georgia, and Queen Charlotte Sound, respectively, when compared to the lowest found in offshore Pacific waters (Desforges, et al., 2014). The MPs were composed of fibres or fragments of size in different ranges: <100, 100-500, 500-1000, >1000 µm; from which fibres accounted 75% of MPs on average.

The second study, in 2018, was conducted by Kazmiruk et al. and assessed the abundance and distribution of MPs within surface sediments of Lambert Channel and Baynes Sound. This area of British Columbia constitutes a key shellfish growing region in Canada. Microplastics were found at all 16 sampling locations indicating widespread contamination of this region with these particles. Three types of MPs were recovered: microbeads, microfibres and microfragments. The first one occurred in the greatest number within Baynes Sound, coincident with regions of intense shellfish aquaculture (up to 25,000 MPs/kg dry sediment). Microfibres and microfragments occurred in a much less number and in similar amounts (100-300 MPs/kg dry sediment) (Kazmiruk et al., 2018). These findings showed that the premier oyster growing region of British Columbia is highly contaminated with MPs and would directly impact the quality of the products that are being farmed and sold by the Canada's oyster farming industry (Kazmiruk et al., 2018).

- **The Atlantic Region**

The coastal sediments of the Atlantic Region were characterized to quantify amounts of MPs in two independent studies. In the first one (Mathalon & Hill, 2014), microplastic fibres were enumerated and compared within different reservoirs in the intertidal zone from three beaches on the outskirts of the urbanized Halifax Harbour in addition to an aquaculture site. Overall, all the sediments collected in the three beaches along Nova Scotia's Eastern Shore (one exposed beach and two protected beaches), contained an average concentration of up to 8,000 MPs/kg sediment.

The second study (Forsythe, 2016) characterized MPs concentrations and distribution in the Bay of Fundy. Sediment samples were collected from 15 intertidal sites along New Brunswick's southwestern coast; all the samples contained MPs with an average concentration of 268 MPs/kg sediment and had a total composition of 89% fibres, 8% fragments and 2% microbeads.

1.3.3. Presence of microplastics in marine biota

Once MPs enter the water bodies, they can be ingested by a wide range of marine organisms. Microplastic debris has infiltrated over 100 marine species of wildlife, including commercially important fish and shellfish (GESAMP, 2015). The high variety of these animals contaminated with MPs comprises cod, swordfish, anchovy, sardines, bluefin tuna, chinook salmon, haddock, mussels, oysters, and brown shrimp. For instance, several studies confirmed contamination of wild bivalves: blue mussels collected in Europe contained on average 0.2 to 0.5 MPs/g wet weight, mussels sampled in Canada contained 34 to 178 MPs/mussel, and commercially sold species of bivalves in China contained 4 to 57 MPs/bivalve (GESAMP, 2015).

A large variety of fish species have been documented to ingest MPs in the form of fibres, fragments, and pellets. Neves et al. (2015) examined the digestive tract contents of 263 individuals from 26 species of commercial fish of the Portuguese coast and found MPs in 19.8% of the fish. From this percentage, 32.7% had ingested more than one microplastic, with some species having an average of up to 1.66 MPs/fish (Neves et al., 2015). The presence of MPs was also detected in 9% and 28% of gastrointestinal tracts from fish sold at markets in the USA and Indonesia, respectively, with an average of abundance of 0.5 MPs/fish in the USA samples and 1.4 MPs/fish in the

Indonesian samples (Rochman et al., 2015) . Extensive research has been done to detect MPs in many other commercially targeted fish species.

Microplastics in the marine environment have the capacity to adsorb toxic elements such as metals, persistent organic pollutants (POPs), endocrine-disrupting compounds, and pharmaceuticals (Carr et al., 2016; GESAMP, 2015; Santana et al., 2016). Plastics contaminated with POPs such as polycyclic aromatic hydrocarbons (PAHs), polychlorinated biphenyls (PCBs) and dichlorodiphenyltrichloroethane (DDTs), are found globally from coastal areas to remote areas of subtropical gyres (Wang, Tan, Peng, Qiu, & Li, 2016). The impact of biota ingesting these chemicals is poorly understood. However, some of the harmful effects reported so far include endocrine disruption, reproductive failure, internal injuries, mortality, and delayed growth (Ogunola & Palanisami, 2016).

1.4. IMPACT OF MICROPLASCTICS ON PUBLIC HEALTH

The proven accumulation and abundance of microplastics in global water bodies have made possible for these micro pollutants to enter the human food chain and drinking water (**Figure 1.3**). For instance, MPs have been found in commercial fish and shellfish, bottled and tap water, and in foodstuff like table salt, beer, and honey.

- **Microplastics in fish and shellfish**

Microplastics have been observed in many wild marine species of commercial interest, including fish, mussels, clams, oysters and scallops. For example, a study confirmed MPs contamination in 9 species of bivalves from a fishery in China (Jiana Li, Yang, Li, Jabeen, & Shi, 2015). The abundance of MPs was in the range of 4.3 to 57.2 MPs/individual, with the species yesso scallop having the highest number of MPs (57.2 MPs/individual). The most common plastic was PE followed by PET and polyamide. The presence of MPs has been also confirmed in crustaceans such as brown shrimp and Norway lobster. In a study performed in Clyde, UK it was observed that 83% of 120 individuals contained plastics in their stomach, mainly MPs (Murray & Cowie, 2011).

A large variety of fish species have been documented to ingest MPs (GESAMP, 2016). For example, a study found that some fish species purchased from markets in the USA and Indonesia were contaminated with MPs (Rochman et al., 2015). From the samples purchased in the USA, 28% of individual fish and 55% of all species had MPs in their gastrointestinal tracts. Some of the species contaminated with MPs reported by this study include rockfish, Pacific anchovy, Pacific sanddab and Chinook salmon.

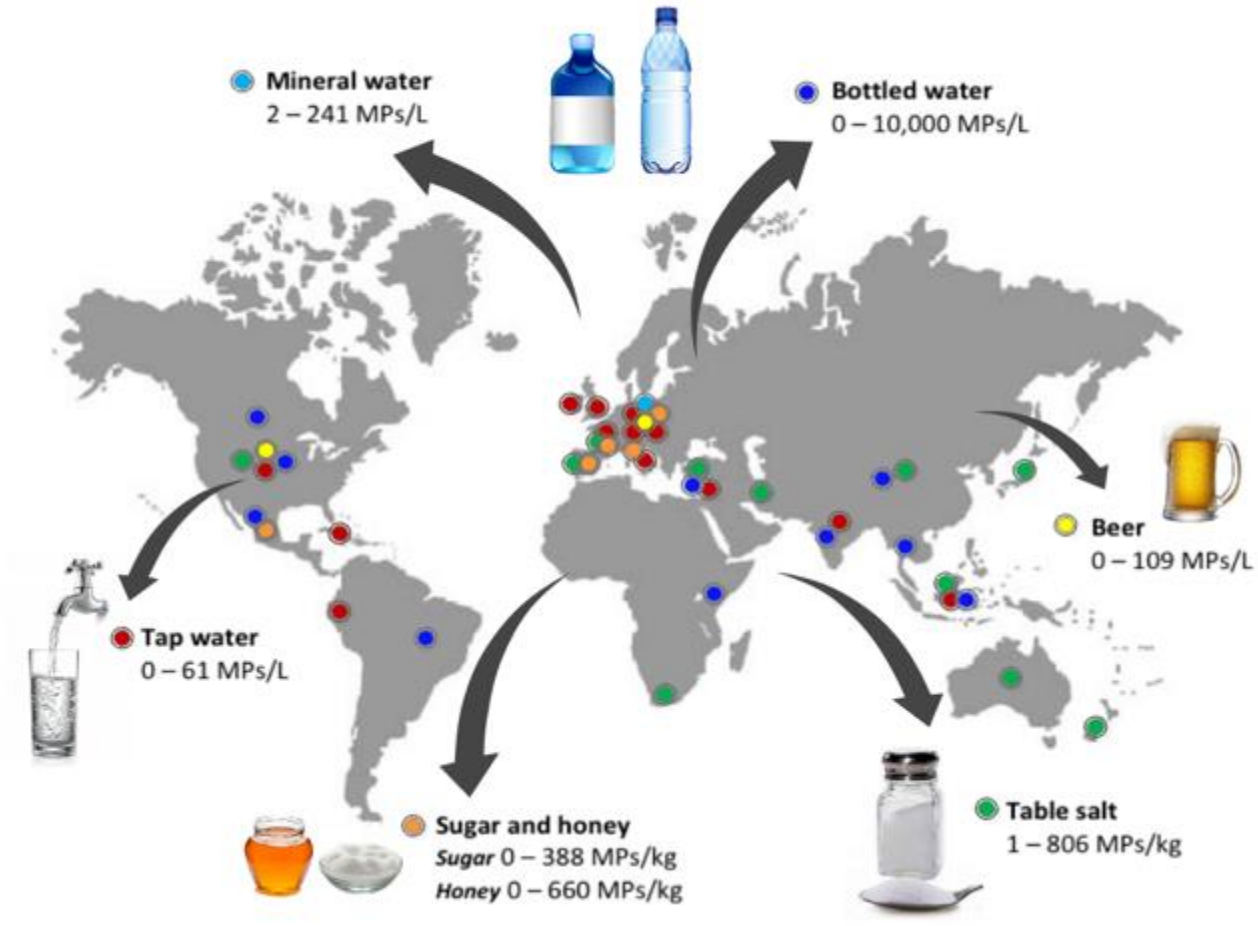

Figure 1.3. Occurrence of MPs in foodstuffs (excluding fish and shellfish) and drinking water (concentrations reported by Kosuth et al., 2018; Liebezeit & Liebezeit, 2014; Yang et al., 2015; Liebezeit & Liebezeit, 2013; Schymanski et al., 2018; Mason et al., 2018; Gündoğdu, 2018; Iñiguez et al., 2017; Karami et al., 2017)

Research shows that not only wild seafood is contaminated with MPs, but also cultured seafood. Farmed mussels purchased at a grocery store and produced in an aquaculture site of the west coast of Newfoundland and Labrador, Canada, were inspected against live mussels obtained from two beaches in Nova Scotia. The abundances of microfibers in farmed mussels were higher than in wild mussels, with an average of ~75 MPs/mussel in farmed mussels and of ~34 MPs/mussel in wild mussels (Mathalon & Hill, 2014).

- **Microplastics in foodstuffs**

Several recent studies around the world reported the occurrence of MPs in food items that include beer (Kosuth et al., 2018; Liebezeit & Liebezeit, 2014), honey (Liebezeit & Liebezeit, 2013, 2015), sugar (Liebezeit & Liebezeit, 2014), and table salt (Kosuth et al., 2018; Yang et al., 2015). The highest abundance of MPs was observed in table salt. Local supermarkets in China were reported to have table salt with up to 681 MPs/kg of sea salt and 364 MPs/kg of lake salt (Yang et al., 2015). Similarly, in some grocery stores and specialty shops in USA, table salt was found to have up to 806 MPs/kg (Kosuth et al., 2018).

Honey and sugar are next in abundance of MPs. The two products were tested by Liebezeit & Liebezeit in two different studies (2013 & 2015). The most recent and extensive study comprised the analysis of 47 honey samples originated in several countries from Europe and Latin America. Microplastics were found in all the honey samples analyzed with a concentration ranging between 2 to 336 MPs/kg (Liebezeit & Liebezeit, 2015). Likewise, the study performed in 2013 reported MPs in all the tested samples of honey and refined sugar, which originated from Germany, France, Italy, Spain and Mexico. The MPs concentration was of [0 – 660] MPs/kg for honey and of [0 – 388] MPs/kg for sugar (Liebezeit & Liebezeit, 2013).

Beer from twelve different North American brands was tested for MPs by Kosuth et al (2018). All of the beer samples were found to have MPs, with a mayority (98.4%) of those being fibres. The concentrations were in the range of 0 to 14.3 MPs/L (Kosuth et al., 2018).

- **Microplastics in drinking water**

Since drinking water to humans is significantly supplied from the continental surface freshwater resources (lakes and rivers), which have been proven to contain MPs, tap and commercial bottled water have been reported to be contaminated with these particles (Kosuth et al., 2018; Jingyi Li et al., 2018). Mineral water from 22 different bottles obtained in grocery stores located in Germany were inspected in 2018, and found to be contaminated with up to 241 MPs/L (Schymanski et al., 2018).

In another study conducted by Mason et al. in 2017, more than 250 water bottles from 11 leading brands worldwide revealed widespread contamination with plastic debris including polypropylene, nylon, and PET. A total of 93% of all the tested bottles were contaminated with MPs in an average of up to 314 MPs/L (Mason et al., 2018). In a study performed recently by researchers at McGill University, Canada, bottled water from five Canada's leading bottled water brands was tested for MPs. Thirty of the 50 bottles tested had MPs of different types, including polyethylene and PET, at an average of ~10 MPs/L with diameter >100µm. Although these results have not been published yet, the methodology for the detection of MPs and their estimated abundance are comparable to those from Mason et al. (2018). Kosuth et al. (2018) investigated the presence of MPs in 159 samples of globally sourced tap water. Microplastics were found in 81% of the tap water samples analyzed, with an evident majority being fibres (98.3%) between 0.1 – 5 mm (Kosuth et al., 2018). The concentration of microplastics was in the range of 0 to 61 MPs/L.

- **Toxicity and potential effects of microplastics on humans**

It is evident that humans are exposed to MPs through the consumption of marine foodstuffs, including fish, shellfish, and table salt. Furthermore, humans may be exposed to MPs via terrestrial foodstuffs (beer, honey, and sugar), drinking water and inhalation from air (Napper et al., 2015). One of the first studies to estimate the potential exposure of humans to MPs through the ingestion of plastic-contaminated seafood was done by van Cauwenberghe and Janssen in 2014. They calculated that the dietary exposure of European consumers can be up to 11,000 MPs/year (Van Cauwenberghe & Janssen, 2014).

This issue has raised concerns about the risks associated with the ingestion of MPs. However, the understanding of the possible effects that MPs may pose on human health, including the leaching of absorbed toxic chemicals, is still in the early stages. Research showed that nanoparticle toxicity is extremely complex and that the biological interactions of nanoparticles depend on several physicochemical properties such as particle size, shape, crystal structure, chemical composition, surface area and surface properties (GESAMP, 2016). Some effects from ingesting MPs have been demonstrated for a variety of marine organisms which include endocrine disruption and abnormal growth (Rochman et al., 2014). Nonetheless, to date, there have been no in vivo studies of the effects of microplastic consumption on humans (The Lancet Planetary Health, 2017).

Scientists speculate that only smaller MPs (≤ 20 μm) would be able to penetrate into organs, and if so, interactions of these particles with the immune system could potentially lead to immunotoxicity and thus trigger adverse effects such as immunosuppression, immune activation and abnormal inflammatory responses (Barboza et al. , 2018). Although designing robust studies to look at this issue might be experimentally and ethically difficult, toxicological studies are urgently needed to assess the health risks that MPs pose to humans.

1.5. SIGNIFICANCE OF THIS STUDY

Many scientific reports have assessed the sources, fate, effects, distribution, and behaviour of MPs (Barboza & Gimenez, 2015; GESAMP, 2015b, 2015a; Ogunola & Palanisami, 2016; UNEP, 2016; Wagner et al., 2014; Wang et al., 2016); nevertheless, methods to treat and/or reduce the amounts that contaminate water, marine biota, drinking-water, and food remain inconclusive. For instance, biological or microbial degradation has been proposed as a promising method to reduce recalcitrant polymers in the environment that is eco-friendly and effective. Microbes could be used to break down the typical long chains of the synthetic polymers to generate either hydrocarbons or monomers that can be later used or recycled (Ghosh, Pal, & Ray, 2013). Several studies have shown that some microorganisms can degrade plastics (Auta et al., 2017; Paço et al., 2017; J. Zhang et al., 2004) and it is believed that among the biological agents, microbial enzymes have the highest potential for the biodegradation of plastics (Bhardwaj et al., 2013).

Because of its non-biodegradability and high global production, PET MPs have been accumulating in the marine environment, affecting freshwater and marine ecosystems. Numerous organisms are not only ingesting MPs but are also exposed to the organic contaminants adsorbed onto the MPs (Wagner et al., 2014). The abiotic degradation of PET in the form of film, pellet, fibre, and powder is well documented. Several studies found that PET is susceptible to degradation by microbial polyester hydrolases (Wei & Zimmermann, 2017b); other studies found that certain fungal species have the ability to enzymatically degrade this polymer. Although part of these studies has shown the biotic (microbial) degradation of PET in the form of films or strips by bacterial species, there is scarce research focused on studying the biodegradation of PET microplastics. Furthermore, to the authors' knowledge, there are no reports on the biodegradation of PET MPs by naturally occurring bacteria in activated sludge from WWTPs.

Since biodegradation is an eco-friendly option to degrade plastic particles, identifying microbes that can potentially degrade MPs and gaining insights on the process can facilitate the development of methods to reduce and/or remove MPs from the environment. Microbes of different nature can be found in many natural habitats with different environmental conditions. For instance, activated sludge from Wastewater Treatment Plants (WWTPs) is a highly species-rich ecosystem with an abundant bacterial diversity. Given that municipal and industrial wastewaters, which are commonly polluted with MPs, undertake important biological treatments in WWTPs, probable plastic degraders may populate such ecosystems.

1.6. AIM OF THE STUDY

The primary objective of this study is to contribute to the development of strategies for the clean-up of PET MPs within wastewater and aquatic environments by isolating and investigating natural occurring bacteria in activated sludge with the potential to degrade PET MPs. As mentioned above, activated sludge from WWTPs may be a good potential source for microbes that are starting to adapt and develop PET-degrading capabilities, since the influents that undertake biological treatments are commonly contaminated with MPs. Four intermediate objectives were defined to achieve this end. These are:

1. Screening of microbial communities from activated sludge and selection of possible PET degraders. Here, the microbes are screened for their ability to utilize PET as the sole carbon and energy source for growth. An enrichment procedure is performed to create strong selective conditions using PET MPs to select for microbial strains with potential to thrive on PET.
2. Biodegradability assessment of PET MPs by the evolved carbon dioxide method. This involves the evaluation of the microbial communities for their capability to biodegrade PET MPs and generate carbon dioxide as an oxidation product. This objective also includes the engineering, procurement and construction of an experimental set-up for the biodegradation test in compliance with the standard ISO 14852.
3. Validation of the biodegradation extent through analytical methods and equipment located at the Ryerson University Analytical Centre and Mechanical Engineering Department. This includes characterization and comparison of morphology, chemical structure, and molecular weight of PET MPs before and after exposure to microbial interactions by means of Scanning Electron Microscopy (SEM), Fourier Transform Infrared (FTIR), Differential Scanning Calorimetry (DSC), and intrinsic viscosity. Additionally, the presence of soluble metabolites is evaluated through Reversed-phase high performance liquid chromatography (HPLC), and
4. Microbial analysis. Four bacterial strains, selected from the microbial community present in the bioreactor after the test, are evaluated for their ability to grow with PET MPs as the sole carbon source. This includes isolation of the bacterial strains, clear-zone test, growth analysis, and their identification using molecular techniques. The DNA sequencing was performed by ACGT Corporation.

The following chapters present the methodology, experimental results, and conclusions of the current study. That is:

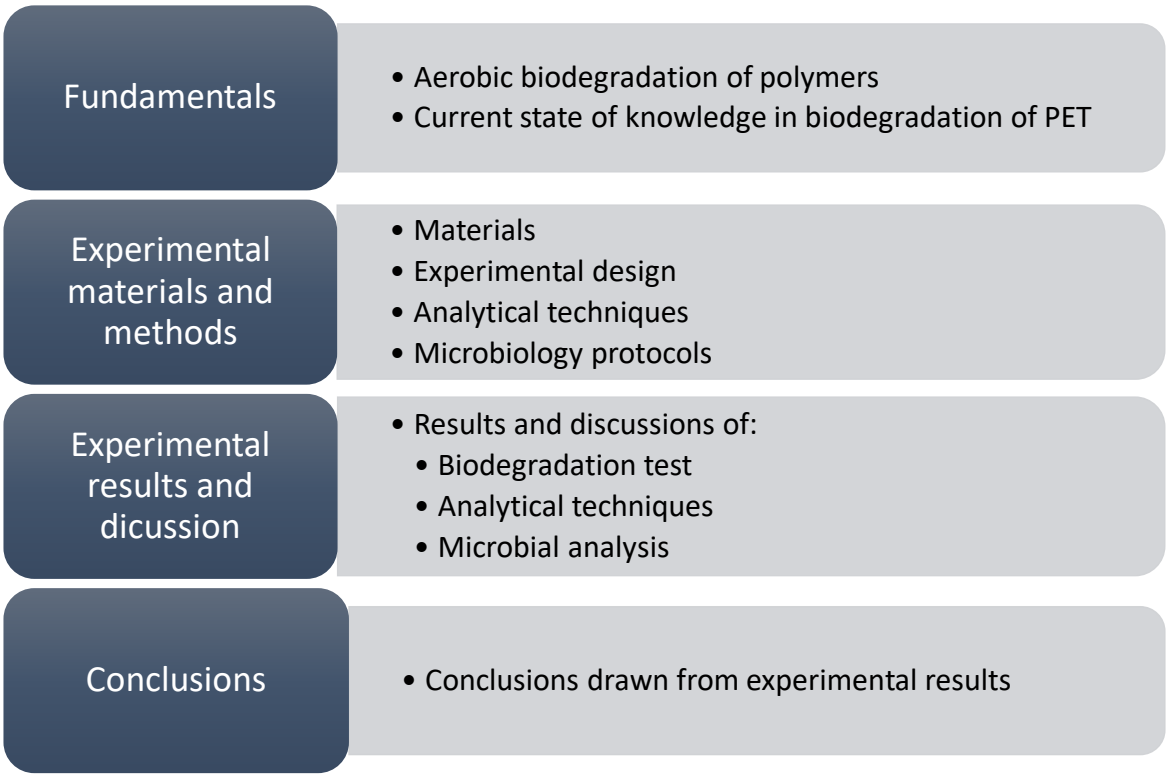

Figure 1.4. Description of the chapters presented in the current study

2. FUNDAMENTALS

2.1. OVERVIEW

This chapter aims to review the fundamentals of aerobic biodegradation of polymers and the current state of knowledge on the biodegradation of PET microplastics. It includes the aerobic biodegradation process, the description of PET and Poly(ε-caprolactone) (PCL) properties and applications, and the current state of research on the biodegradation of PET.

2.2. AEROBIC BIODEGRADATION OF POLYMERS

Organisms have developed many mechanisms to degrade organic materials because of millions of years of evolution. Bacteria, especially, possess extremely diverse metabolic activities and high adaptability, which make them valuable organisms with an endless potential for biological applications. Many remediation strategies for polluted environments have been developed with the aid of bacteria; for instance, clean-up of oil spills, polychlorinated biphenyls (PCBs), and heavy metals were all performed utilizing bacteria with adequate metabolic capabilities (Webb, 2012). Biodegradation has ever since been considered an attractive approach in treating pollutants in the environment and considerable attention has been put on the biodegradation of plastics as huge pollutants.

Plastics can be degraded in the presence or absence of oxygen. When the degradation occurs in the presence of oxygen and by the action of aerobic microorganisms such as bacteria and fungi the process is called aerobic biodegradation. In this process, microbes break down polymer chains and utilize the carbon for energy and growth generating, as ultimate end products, CO_2, water and biomass. The chemistry of the key degradation process is represented by the following equation (Weinreb & Moon, 2005):

$$Polymer + O_2 \xrightarrow{microbes} CO_2 + H_2O + Residue + Biomass$$

When the polymer is fully utilized by microbes, mineral salts are also produced and there is no residual polymer left (Kyrikou & Briassoulis, 2007). The biodegradation of plastics proceeds actively under soil or aquatic environments in different conditions and the responsible microorganisms differ from each other as they have their own optimal growth conditions and enzymatic biocatalysts. The process of bacterial biodegradation occurs via three key steps: bio-deterioration, bio-fragmentation, and bio-mineralization, which are described in detail in the following section.

2.2.1. Mechanism of aerobic biodegradation of polymers

The aerobic microbial biodegradation of plastics is a very slow oxidation process that comprises three different stages, as illustrated in **Figure 2.1**. Each stage is explained in detail below.

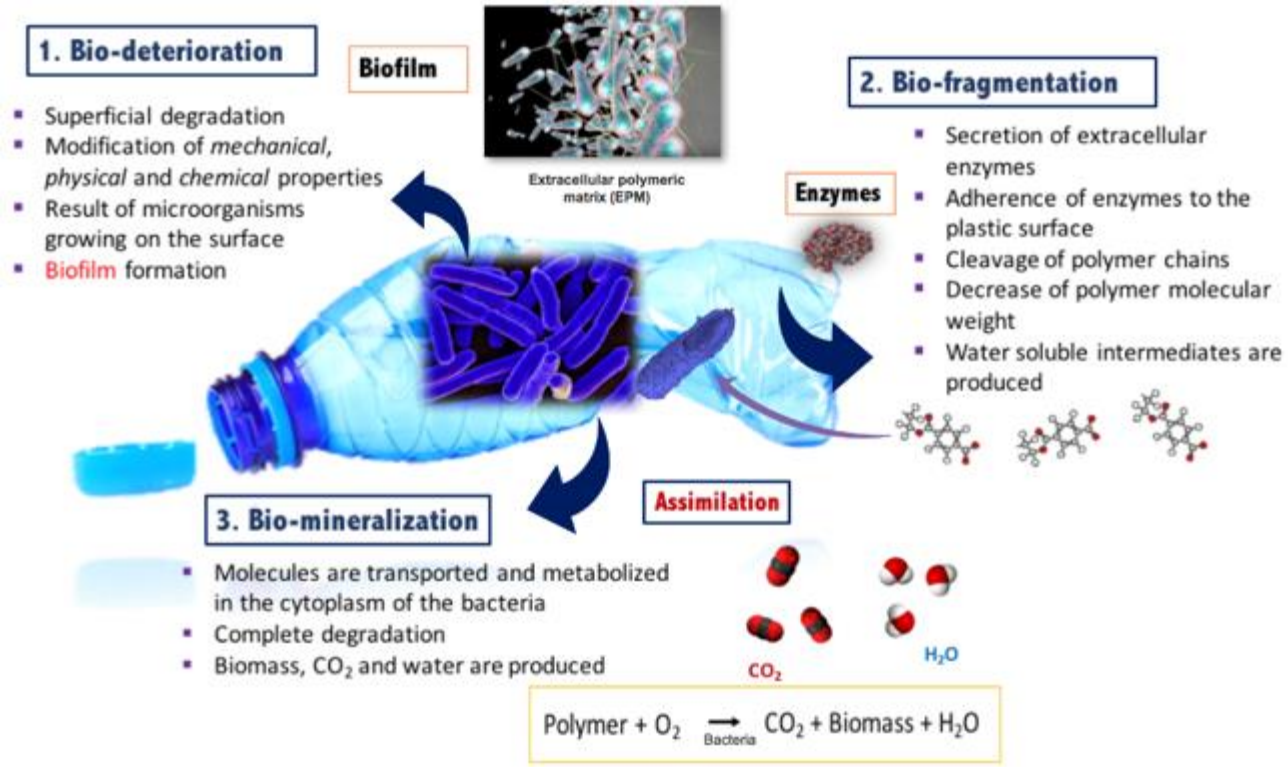

Figure 2.1. Mechanism of biodegradation of plastics by bacteria

1. Bio-deterioration: normally occurs outside the organism due to the size of the polymer chain and the insolubility of many of the polymers. It involves the combined action of bacterial communities and/or abiotic factors. The microbes colonize the polymer surface forming a high-cell density biofilm that facilitates their growth and survival, a process that is also called biofouling. The activity of microorganisms colonizing and growing on the surface of the plastic can degrade the material and modify its mechanical, physical and chemical properties (Lucas et al., 2008). Hence, it is believed that microbial biofilm formation triggers the degradation process and that it is a prerequisite for any substantial deterioration (Mohan & srivastava, 2011).

A bacterial *biofilm* is a hydrated matrix of polysaccharides and protein where bacterial cells can encase themselves to survive and grow. The formation of biofilm seems to be the favourite mode of growth of plastic degrading bacteria (Sivan, 2011). It is not only dependent on the composition, structure and hydrophobicity of the plastic but also on the environmental conditions. Once the biofilm is formed, it can provoke physical or chemical deterioration (Dussud & Ghiglione, 2015). Physical deterioration involves alteration of pore size and distribution, cracks and weakening of physical properties due to the action of secreted extracellular polymeric substances (EPS) that infiltrate the pores of the material and allow the microorganisms to grow inside. Chemical deterioration includes changes in the microstructure of the polymer matrix due to microbial released acid compounds - such as nitrous, nitric and sulphuric acid - that modifies the pH inside the pores and induces progressive degradation. The processes and effects of biofilms on polymer surfaces are illustrated in **Figure 2.2**.

The polymer bio-deterioration can be assessed by several methods; one can be the evaluation of macroscopic modifications in the material, like roughening of the surface, formation of holes and cracks, changes in colour, and development of microbes over the surface (Lucas et al., 2008). Another approach is to evaluate changes in rheological properties such as glass transition temperature, melting temperature, and crystallinity, which can be a sign of internal bio-deterioration.

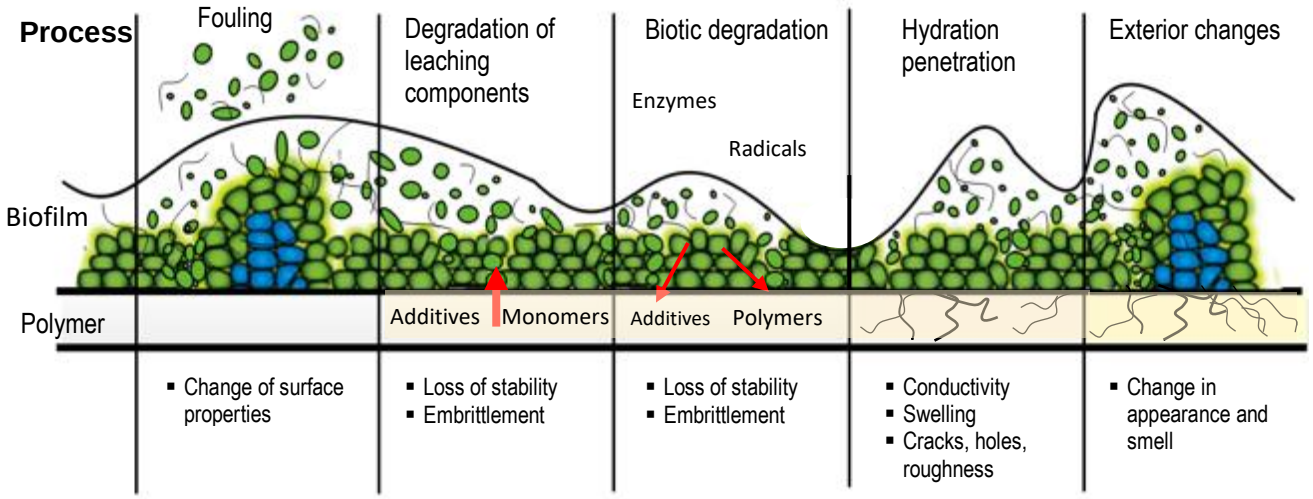

Figure 2.2. Processes and effects of biofilms on polymer surfaces pending

2. Bio-fragmentation: exo- or endo-enzymes (also called depolymerises) secreted by the microorganisms are responsible for this step, acting either through random cleavage on the internal linkages of the polymer chains, or through a sequential cleavage on the terminal monomer units in the main chain. Since polymers have high molecular weight, they are unable to cross the cell wall and/or cytoplasmic membrane. Hence, these microbial enzymes break down complex polymers yielding smaller molecules of short chains, that are smaller enough to pass the semi-permeable outer bacterial membranes, and subsequently be utilized as carbon and energy sources (Shah et al., 2008).

The bio-fragmentation of plastics can be verified by the presence of low molecular weight molecules or changes in molecular weight of the polymer, which can be detected using GPC analysis or intrinsic viscosity; also, functional chemical changes at the surface level are a sign of degradation that can be revealed by FTIR analysis. Other approaches include the 'clear zone' test, in which the microbial activity is screened for its ability to hydrolyze a specific polymer. In this test, the material scattered in agar plate is inoculated with the microorganism of interest and then incubated. If a clear-zone is formed around the colony, it indicates the solubilisation of the substrate as a result of the degradation caused by secreted enzymes (Cerdà-Cuéllar et al., 2004).

3. Bio-mineralization: once sufficiently small size oligomeric or monomeric fragments are formed they are transported into the cell where they are mineralized. At this stage, the transported molecules inside the cells are oxidized through aerobic respiration leading to the production of adenosine triphosphate (ATP) for energy, cell structure and new biomass. Primary and secondary metabolites are commonly excreted in this process, which may be further metabolized or transformed if the microorganism has the proper metabolic capability. The bio-mineralization is achieved when there is a complete degradation of primary and secondary metabolites into completely oxidized metabolites such as CO_2, salts, minerals, and water, as shown in **Figure 2.1**.

The assimilation of plastics is usually assessed through standardized respirometric tests, where the consumption of oxygen or the evolution of carbon dioxide are measured and compared to theoretical values. More details on these methods are presented in section 2.2.3.

Many variations of this general view of the biodegradation process can occur, depending on the polymer, the organisms, and the environment. Nonetheless, there will always be the involvement of enzymes. Enzymes exist in every living cell and hence in all microbes and are very specific in their action on substrates, so the different enzymes help in the degradation of various types of plastics (Bhardwaj et al., 2013). Some of the microbial enzymes from both fungi and bacteria that have been implicated in the biodegradation of plastics include laccase, manganese peroxidase, cutinase, esterase, lipase, proteinase K, pronase, and dehydrogenases (Ghosh et al. , 2013; Krueger et al., 2015).

2.2.2. Factors affecting the biodegradation of polymers

The biodegradation of plastics is governed by different factors that include polymer characteristics, type of organism, environmental conditions (temperature, humidity, pH), and nature of pre-treatment. The main polymer characteristics that affect the biodegradation process include the following (Tokiwa et al., 2009):

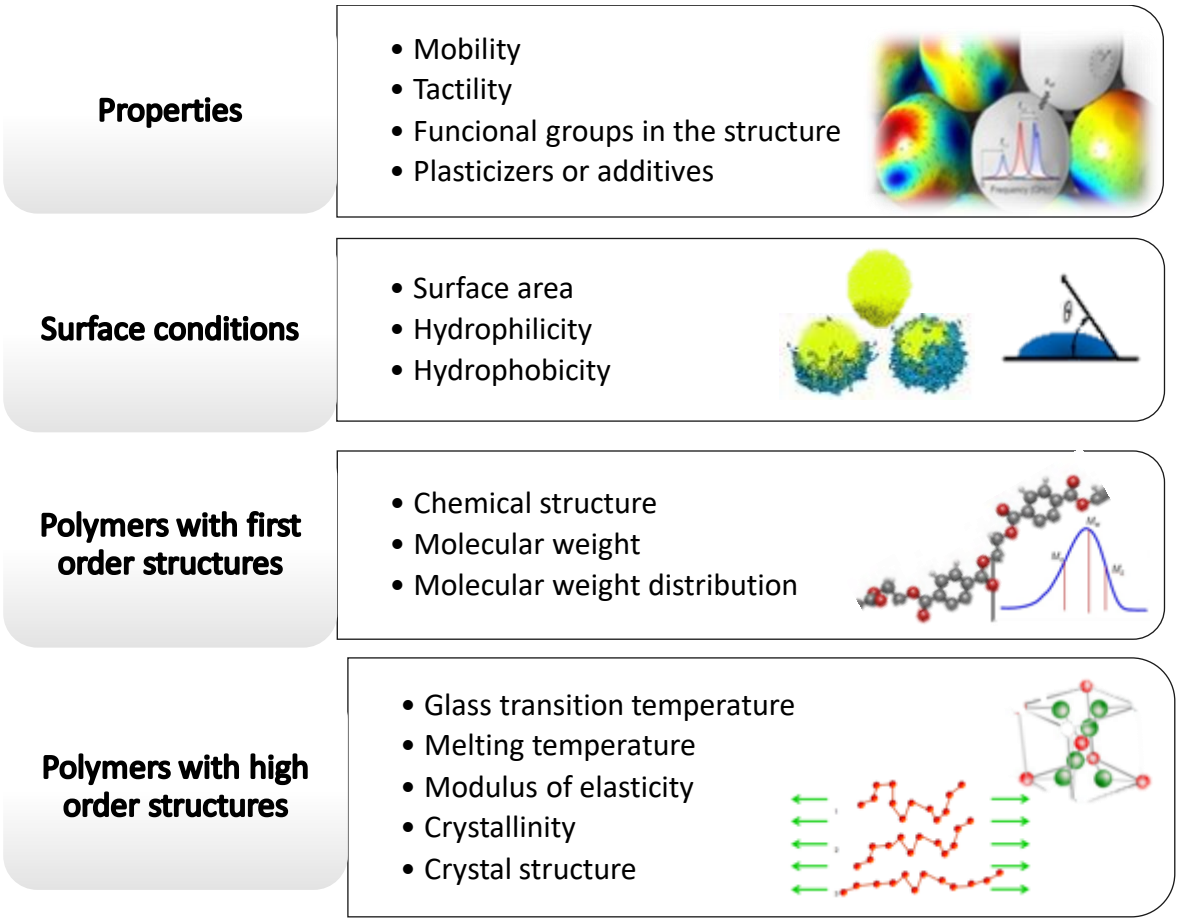

Figure 2.3. Polymer characteristics affecting biodegradation

The degree of crystallinity is a crucial factor affecting biodegradability, since enzymes mainly attack the amorphous domains of a polymer. The molecules in the amorphous region are loosely packed, and thus make it more susceptible to degradation. Conversely, the crystalline part of the polymers has a stiff structure that is very difficult to infiltrate, hence it is more resistant to biological action (Tokiwa et al., 2009).

2.2.3. Biodegradation assessment

Numerous methods for the experimental assessment of polymer biodegradability have been described in the scientific literature. The most common approaches that have been adopted to study the biodegradation process include monitoring the following variables (Van Der Zee, 2011):

1) Accumulation of biomass
2) Depletion of substrates
3) Reaction products
4) Changes in the substrate properties.

For instance, one of the most common and simple methods available to detect changes in the plastic substrate is visual observation. It is used to evaluate changes that can describe degradation, including roughening of the surface, formation of holes and cracks, de-fragmentation, changes in colour, or formation of biofilms on the surface (Shah et al., 2008). Although these changes might not prove that the polymer is being metabolized, they are the clear first indication of microbial attack.

Sophisticated spectroscopy techniques such as SEM provide high resolution images that can be used to obtain information on these changes; examples of modifications and biofilm formation on plastic surfaces caused by bacterial degradation can be seen in **Figure 2.4**. The micrograph **A**) shows the biofilm of a pure culture bacteria capable of utilizing polyethylene glycol as a source of carbon, while micrograph (**B**) shows the biofilm of a pure culture of bacteria capable of degrading water-soluble polyurethane (Gu, 2003). Evidence of cracks, pits, and bacterial adhesion on a HDPE strip and a LDPE strip incubated for 120 days can be observed in micrographs (**C**) and (**D**), respectively (Skariyachan et al., 2017).

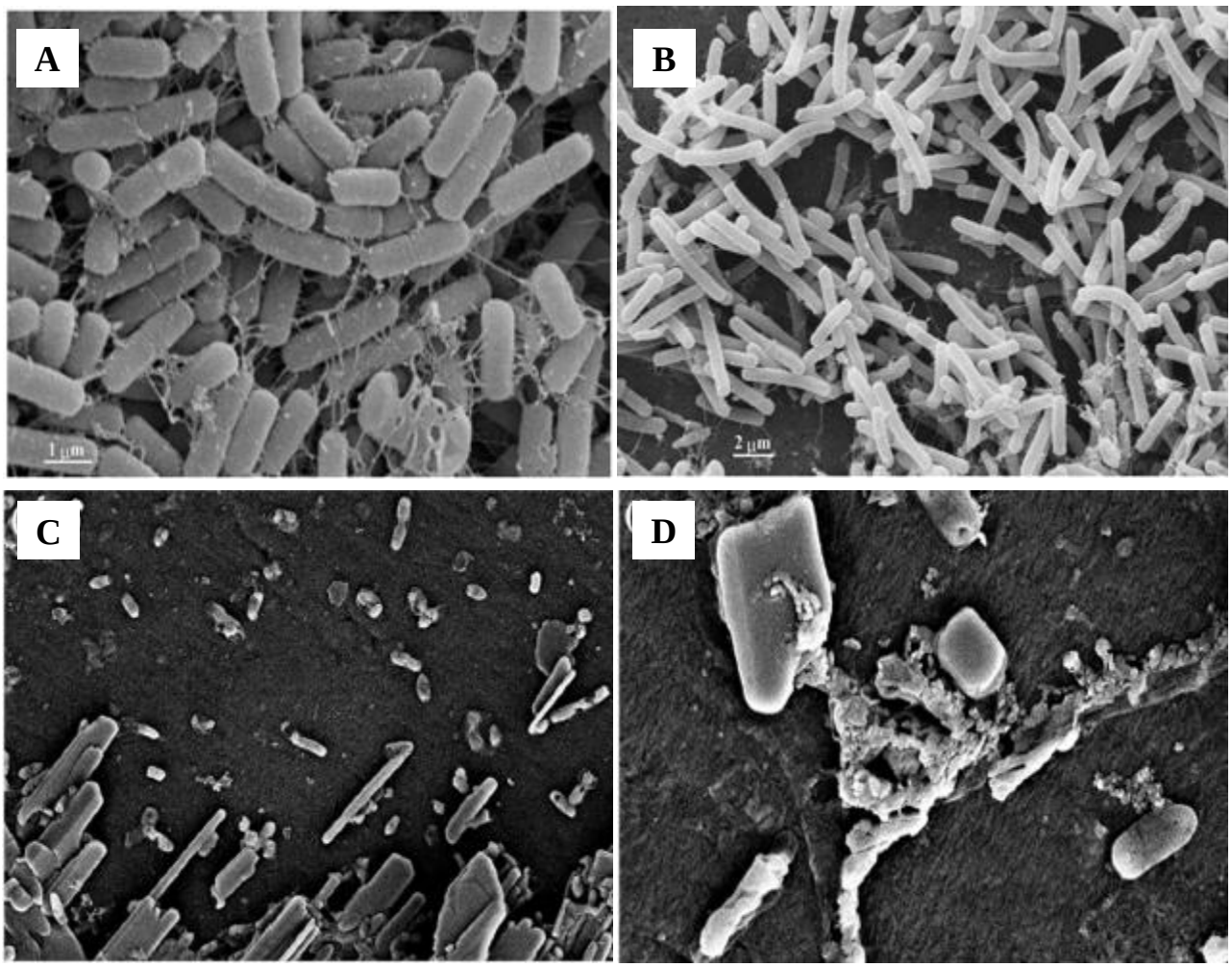

Figure 2.4. SEM micrographs of several biodegradation studies (Gu, 2003; Skariyachan et al., 2017).

A number of other analytical techniques can be employed to assess changes occurred on the plastic due to the biodegradation process such as FTIR, DSC, nuclear magnetic resonance spectroscopy (NMR), X-ray photoelectron spectroscopy (XPS), X-ray diffraction (XRD), contact angle, water uptake, among others (Jayasekara et al., 2005). Some of these techniques are explained later in detail in chapter 3. Although these measures are not themselves indicators of biodegradation, they can provide insight into the degradation process (Selke et al., 2015).

2.2.4. Biodegradation tests

Many standardized tests have been developed to measure the biodegradation of plastics in different environments and with the use of different analytical techniques. Such tests can be divided into three categories: field tests, simulation tests, and laboratory tests. The latter are conducted in a controlled reactor to simulate the degradation process in compost, soil or aqueous medium. The external parameters like temperature, pH, humidity, etc., are controlled and adjusted, and the analytical tools available are better than would be used for field tests. Examples of these tests are determination of CO_2 evolution (Sturm test), enzymes tests, O_2 consumption, etc. Other laboratory tests include plate tests (clear zone), respiration tests, radioactively labeled polymers, and laboratory-scale simulated accelerating environments (Van Der Zee, 2011).

2.2.4.1. CO_2 evolution test – ISO 14852

Microbes use oxygen to oxidize carbon and form carbon dioxide when they are under aerobic conditions. The formation of carbon dioxide, which is what is measured in CO_2 evolution tests, is the only indicator that the polymer is being assimilated by microbes. The assimilation is the unique event in which there is a real integration of atoms from fragments of polymeric materials inside microbial cells. This integration brings to microorganisms the necessary sources of energy, electrons and elements (i.e. carbon, nitrogen, oxygen, phosphorus, sulphur and so forth) for the formation of the cell structure.

Several test procedures for the estimation of aerobic biodegradation of polymer materials by measuring the oxygen uptake or CO_2 evolution are available and have been standardized for practical and legislative purposes (Strotmann et a., 2004). For instance, the International Standard ISO 14852 is specially designed to determine the ultimate aerobic biodegradability of plastic materials in an aqueous medium, including those plastics containing formulation additives. The test material is exposed in a synthetic medium under laboratory conditions to an inoculum from activated sludge, compost or soil (ISO, 2018). The degree of biodegradability is determined by comparing the experimental amount of evolved CO_2 from the degraded material with the theoretical amount during the aerobic microbial degradation process. An example of the system needed to perform such test is illustrated in **Figure 2.5.**

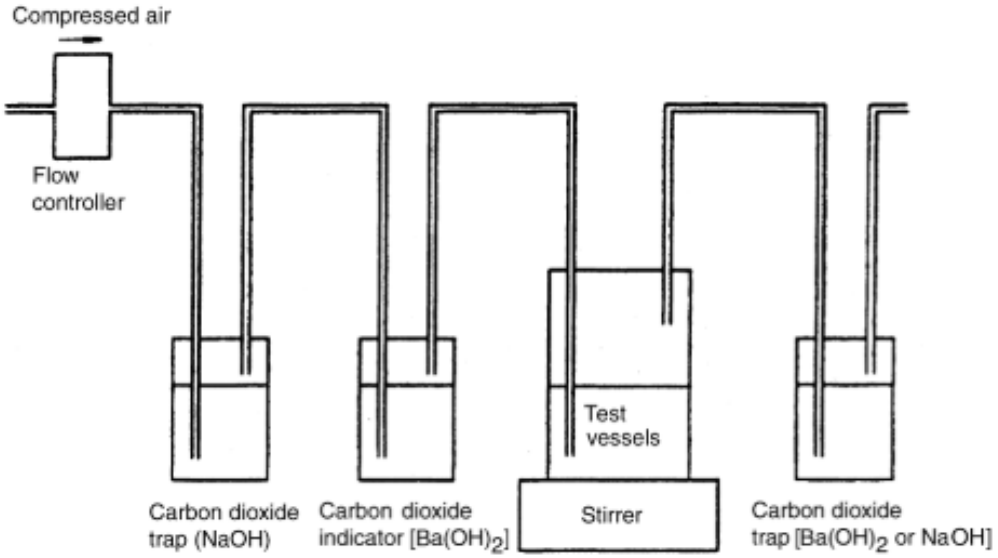

Figure 2.5. Principle of the CO_2 evolution test – ISO 14852 (Pagga et al., 2001)

2.3. POLY(ETHYLENE TEREPHTHALATE) AND POLY(ε – CAPROLACTONE)

In this section, the properties, manufacture and applications of PET and PCL are described. Furthermore, the degradation process of PET is explained.

2.3.1. Poly(ethylene terephthalate) (PET)

PET is the most common thermoplastic polymer resin of the polyester family and is used in fibres for clothing, thermoforming for manufacturing, engineering resins, and particularly in food and beverage packaging, mostly soft-drink and water bottles. It is strong and durable, chemically and thermally stable and has low gas permeability (Webb, 2012). PET consists of polymerized units of the monomer ethylene terephthalate, with repeating ($C_{10}H_8O_4$) units (**Figure 2.6**). Depending on the thermal history and the way it is processed, it can be amorphous or semi crystalline (Pirzadeh et al., 2007). The standard physical and chemical properties of commercial PET are specified in **Table 2.1.**

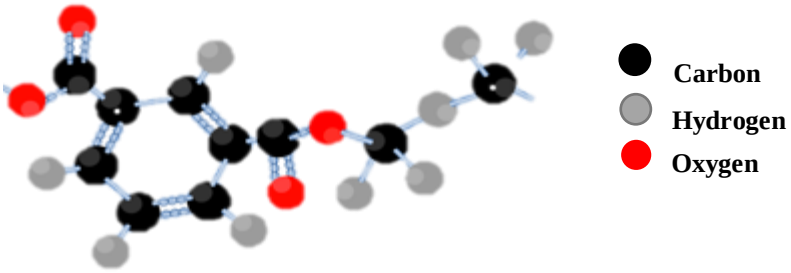

Figure 2.6. PET monomer structure (ethylene terephthalate)

Table 2.1. Physical and chemical properties of PET

Property	**Value (unit)**	**Reference**
Molecular weight (monomer)	192 (g/mol)	-
Weight-average MW	15,000 – 80,000	Mark, 1999; Al-Sabagh et al., 2016
Mark-Houwink parameters	K = 3.72 x 10^{-4} (dL/g) a = 0.73 $[\eta] = KM_v{}^a$ (Mark-Houwink equation)	Mark, 1999
Intrinsic viscosity	0.45 – 1.2 (dL/g)	Awaja & Pavel, 2005; Farah et al., 2015
Density	1.25 – 1.91 (g/cm^3)	Farah et al., 2015
Glass transition temperature	69 -115 (ºC)	Farah et al., 2015; Mark, 1999
Heat of fusion	166 (J/g)	Kannan, Grieshaber, & Zhao, 2016
Melting temperature	200-265 (ºC)	Farah et al., 2015; Mark, 1999
Breaking strength	50 (MPa)	Mark, 1999
Young's Modulus	1700 (MPa)	Awaja & Pavel, 2005

Commercial synthesis of PET is performed by two different reaction pathways (**Figure 2.7**). In the first one, terephthalic acid (TPA) is reacted with ethylene glycol (EG) at a temperature around 240-260 ºC and pressure 500 kPa. In the second, dimethyl terephthalate (DMT) is reacted with EG in a *trans*-esterification reaction at a temperature between 150-220 ºC and 100 kPa (Awaja & Pavel, 2005). Both reactions yield bis(hydroxyethyl) terephthalate (BHET) which is then polymerized in several steps, depending on the desired molecular weight (Webb, 2012).

Two types of PET grades are broadly synthetized and seem to dominate the global market: fibre-grade and bottle-grade. Each type is designed with a particular molecular weight, optical appearance, and intrinsic viscosity that meet specific requirements of each application (Al-Sabagh et al., 2016). For instance, fibre-grade PET used for textiles has a low molecular weight (15,000-20,000 g/mol) and an intrinsic viscosity between 0.55 and 0.67 dL/g. PET used for technical yarns has a higher molecular weight and an intrinsic viscosity over 0.95 dL/g. PET of bottle-grade has an even higher average molecular weight that goes from 24,000 to 36,000 g/mol, and intrinsic viscosities between 0.75 – 1.00 dL/g (Al-Sabagh et al., 2016).

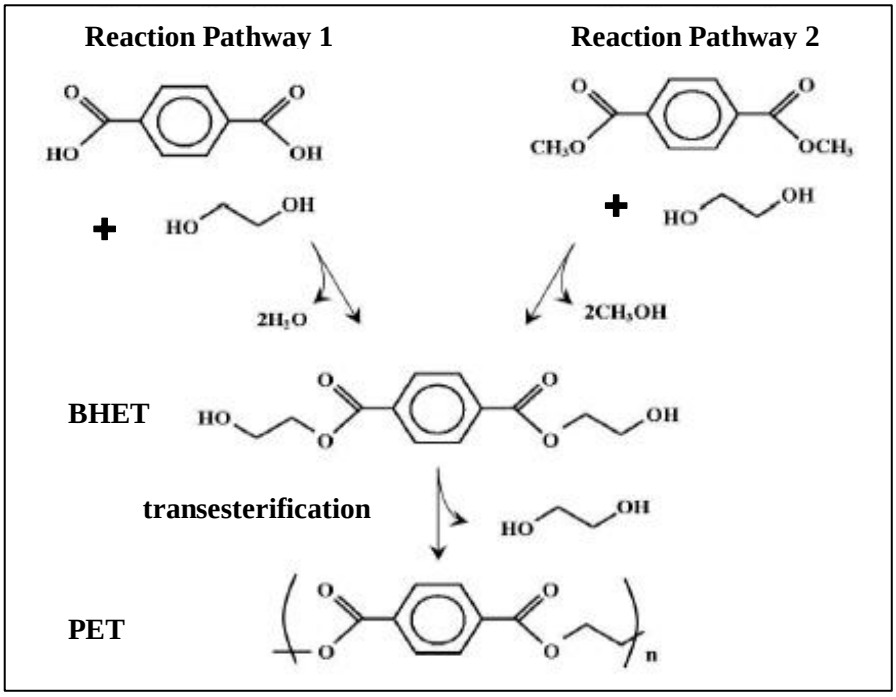

Figure 2.7. Chemical Reactions of PET manufacturing (Webb, 2012)

An enormous amount of PET is produced every year to meet the increasingly high demands. In 2015, an estimated of 58 million tonnes of plastics were produced in Europe only, from which PET comprised over 4 million tonnes (7.1%) for the manufacture of bottles for water, soft drinks, juices, cleaners, etc. (PlasticsEurope, 2016). Furthermore, PET fibres constitute more than 50% of the synthetic fibres manufactured around the world (Sinha et al., 2010).

2.3.2. Poly(*ε*-caprolactone) (PCL)

PCL is one of the major aliphatic polyesters that were developed as biodegradable plastics. It is semi-crystalline and made by the ring-opening polymerization of the monomer *ε*-caprolactone (Tokiwa & Calabia, 2007), which is depicted in **Figure 2.8**. Some of the chemical and physical properties of this polymer are listed in **Table 2.2**. Since PCL is non-toxic and biodegradable, it is commonly used for biomedical applications such as scaffold preparation and drug delivery systems (Gan, Fung, Jing, Wu, & Kuliche, 1999; Höglund, Hakkarainen, & Albertsson, 2007). After widely studied, PCL was proved to be readily biodegradable in various environments. For instance, some filamentous fungi, yeasts, bacteria and compost microorganisms were found to hydrolyze PCL (Guo et al., 2012; Hakkarainen & Albertsson, 2002; Leja & Lewandowicz, 2010). Due to its biodegradability, PCL is commonly used as a reference material in biodegradation tests, especially when the material to be tested is a recalcitrant polymer. Microbes active towards PCL are able to carry out esterase activity, which is a requirement for an efficient degradation of other polyesters (Mezzanotteet al., 2005).

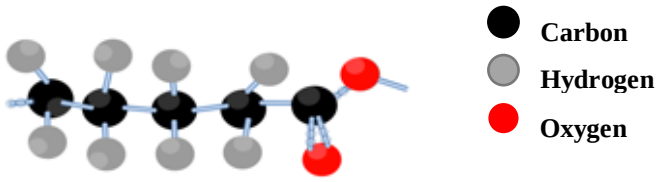

Figure 2.8. PCL monomer structure (*ε*-caprolactone)

Table 2.2. Physical and chemical properties of PCL

Property	Value (unit)	Reference
Molecular weight (monomer)	114 (g/mol)	-
Weight-average MW	74,000	Shuster, Narkis, & Siegmann, 1994
Intrinsic viscosity	0.9 (dL/g)	Chataniet al., 1970
Measured density	1.094 – 1.200 (g/cm^3)	Chataniet al., 1970
Melting temperature	331 (K)	Huarng, Min, & White, 1988
Glass transition temperature	201 (K)	Huarng et al., 1988
Heat of fusion	8.9 (kJ/mol)	Huarng et al., 1988

2.3.3. Degradation of PET

Widely used polymeric materials can undergo degradation processes of different nature when released to the environment. The chemical, physical, and biological processes by which plastics may degrade in the environment include photo-degradation, thermo-oxidative degradation, thermal and mechanical degradation, hydrolysis, and biodegradation (Andrady, 2011; Arutchelvi et al., 2008). All these degradation processes can occur separately or combined and are usually induced by several environmental factors - such as moisture, wind, high temperatures, light, high energy radiation - or the presence of microorganisms.

Under marine conditions, the degradation of plastics generally commence with photo-degradation, where solar UV radiation provides the activation energy necessary for the oxidation of the polymer chains (Andrady, 2011). Consequently, the material becomes more brittle and undergoes fragmentation, which eventually leads to low molecular weight particles or the so-called MPs. Polymers can also undergo degradation when subjected to mechanical stress like wave action and sand grinding, which results in physical abrasion, weathering and fragmentation (Wang et al., 2016). The MPs or fragments can endure further degradation by surrounding microbial communities that first colonize the surface and then metabolize the material, converting the carbon in the polymer into CO_2. The microbes may secrete catalytic agents that depolymerise the material and make it readily assimilable, depending on many factors such as surface hydrophilicity & roughness, oxygen availability, and microbial enzymatic processes (Lucas et al., 2008). Nevertheless, the entire process of complete degradation of MPs may take decades (Müller et al., 2001), especially because the low temperatures and oxygen availability found in the marine environment considerably reduce the photo-degradative effect (Wang et al., 2016; Webb, 2012).

PET MPs under marine environmental conditions can undergo abiotic degradation through photo, thermo-oxidative and hydrolytic degradation, as disclosed in **Figure 2.9**. Photo-degradation of PET occurs on exposure to ultraviolet light and leads to cross-linking and random cleavage of the ester bond forming carboxylic acid groups and a vinyl end group (Gewert et al., 2015). This degradation leads to deterioration in physical and mechanical properties, embrittlement, and development of an intense yellow colour.

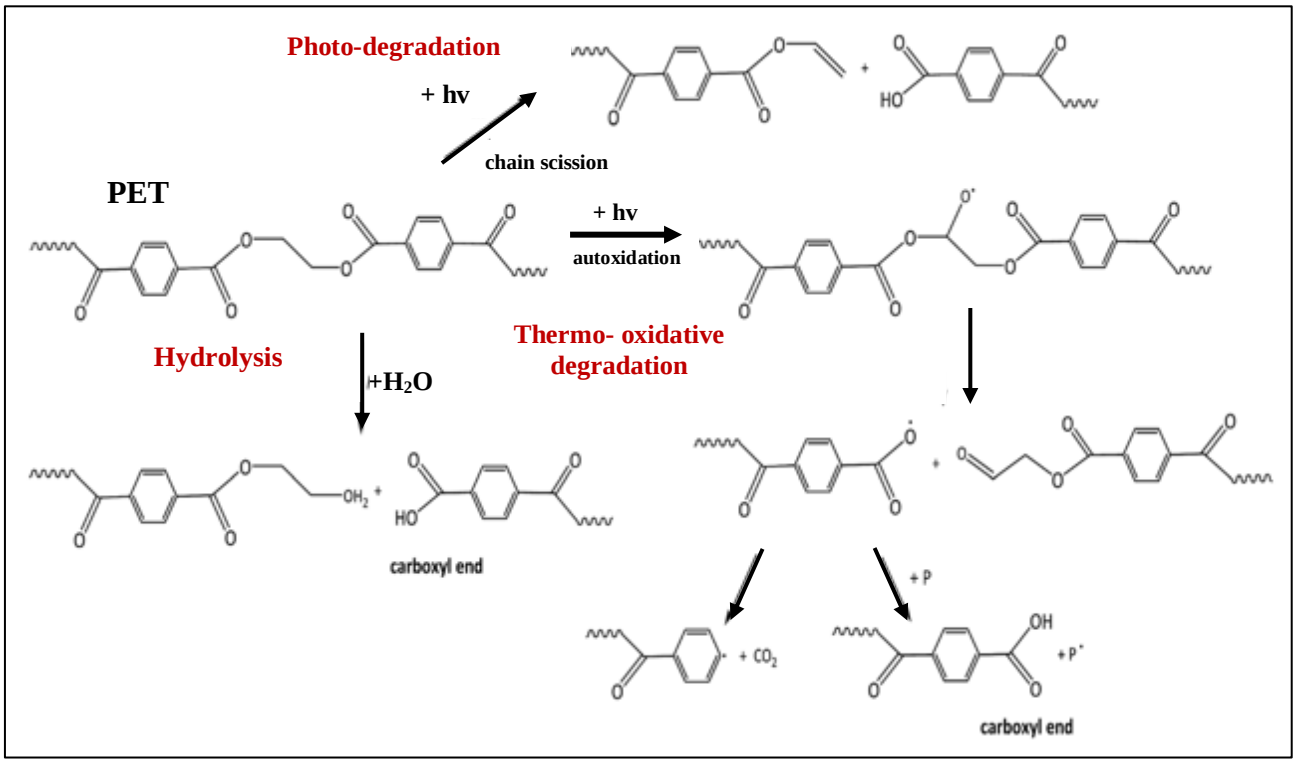

Figure 2.9. Abiotic degradation of PET: chain scission induced by radiation, photo-induced autoxidation, and hydrolytic degradation (Gewert et al., 2015)

Photo-degradation leads to thermo-oxidative degradation forming hydro-peroxide at the methylene group in the diester linkage of the polyester chain, as it is shown in **Figure 2.9**. The mechanism is not completely understood and it is believed to follow free radical reactions (Venkatachalam et al., 2012). As a consequence of this process, the molecular weight of the main polymer is reduced, and the carboxylic end groups are increased.

The latter effects are also generated in the hydrolysis of PET. The hydrolysis, as depicted in **Figure 2.9**, occurs as the reverse reaction of one part of the esterification of PET, where water produces the chemical scission of an ester linkage in the main chain forming carboxylic acid and alcohol functional groups. The rate of hydrolysis is known to be extremely slow under low temperature conditions, nonetheless it is the most important process in the degradation of PET within a low temperature range (Gewert et al., 2015).

The ester bonds present in the polymer chain of PET could normally be broken by several mechanisms, however, due to its aromatic groups, its structure tends to be resistant to degradation.

The characteristic aromatic ring of PET coupled with short aliphatic chain makes the polymer a stiff molecule with a relatively high thermal stability. Thus, PET is insensitive to any hydrolytic degradation under normal conditions (Müller et al., 2001; Venkatachalam et al., 2012; Webb, 2012). However, despite of its compact structure and high resistance to environmental degradation, several studies have reported the degradation of PET by some microorganisms and their specific enzymes, which is further discussed in section 2.4.

2.4. LITERATURE SURVEY ON PET BIODEGRADATION

Aliphatic polyesters like PCL, polylactic acid (PLA) and polyhydroxybutyrate (PHB) are known to be susceptible to microbial attack, biotransformation and bio-deterioration because they possess a flexible polymer chain that allows enzyme activity. Conversely, aromatic polyesters such as PET have high melting points and a low mobility of the polymer chains that inhibit enzyme activity and makes them very resistant to biodegradation. For this reason, PET has been long regarded as inert to biological degradation.

Many attempts have been made to increase PET hydrolytic susceptibility by introducing easily hydrolysable aliphatic components into the aromatic polyester chains (Müller et al., 2001). In early investigations, copolyesters of PET with different aliphatic components - glycolic acid, oxalic acid, adipic acid, ε-caprolactone, etc - were assessed for their susceptibility to biological degradation. For example, the enzymatic hydrolysis of a copolyester of PET with ε-caprolactone was studied by Tokiwa & Suzuki in 1981. After the polymer decomposition using lipase isolated from a strain Rhizopus delemar, it was found that the biodegradation rate decreased when increasing the amount of PET in the sample (Tokiwa & Suzuki, 1981).This result was comparable to others obtained in similar investigations (Jun et al., 1994; Nagata et al., 1997; Witt, Müller, & Deckwer, 1995) and all appeared to withdraw the same conclusion: significant degradation can be observed only at relatively low fractions of the aromatic component.

There are limited reports on the biodegradation of PET, most of which are related to its enzymatic degradation through hydrolysis, alcoholysis, ammonolysis and aminolysis (Janczak et al., 2018). Some examples are listed in **Table 2.3**.

Table 2.3. Various literature reports on enzymatic degradation of PET

PET				Reaction conditions			
Form	Crystallinity	Organism	Enzyme	Temperature	Incubation time	Degradation/ %weight loss	Reference
Film	10%	*Thermofibida fusca*	Hydrolase (TfH)	55ºC	3 weeks	≈ 50%	Müller et al., 2005
Films and granules	≤ 48.2%	*Fusarium solani pisi*	Cutinase	30 – 40 ºC	[15 – 72] h	Yes	Vertommen et al., 2005
Nano-particle	NR	*Candida cylindracea Pseudomonas sp.*	Lipases	40ºC	NR	Yes	Herzog et al., 2006
Yarn	NR	*Fusarium oxysporum*	Hydrolase	30ºC	168 h	Yes	Nimchua et al., 2007
Film	7%	Humicola insolens	Cutinase	70ºC	96 h	97%	Ronkvist et al., 2009
Film	NR	*Thermofibida cellulosilytica*	Cutinase	50ºC	120 h	Yes	Herrero Acero et al., 2011
Film	NR	*Thermofibida alba*	Cutinase	50ºC	2 h	Yes	Ribitsch et al., 2012
Film	NR	*Saccharomonospora viridis*	Cutinase	63ºC	3 days	Yes	Kawai et al., 2014
Film	NR	*Thermofibida fusca KW3*	Hydrolase	65ºC	50 h	≤ 45%	Wei et al., 2016
Film	36.5 – 37.4%	*Candida Antarctica Humicola insolens*	Lipase Cutinase	37 – 60ºC	≤ 28 days	Yes	Carniel et al., 2017
Film	NR	*Candida Antarctica Humicola insolens*	Lipase Cutinase	60ºC	14 days	Yes	Machado de Castro et al., 2017

NR: Not reported

In these reports, specific enzymes isolated from microorganisms are utilized to assess the biodegradation of PET. The enzymes involved in PET degradation are mainly alpha- and beta-hydrolases, like cutinases and related enzymes (Danso, Schmeisser, & Chow, 2018). In the 1970s, the enzymatic hydrolysis of polyester by a lipase was reported for the first time, which created the starting point for many other studies to identify enzymes that hydrolyze polyesters.

Marten et al. investigated important parameters in the hydrolysis of polyesters by lipases from *Pseudomonas* sp. (Marten et al., 2005). A fungal cutinase from *Fusarium solani pisi* (Nimchua et al., 2008; Vertommen et al., 2005) and hydrolase from *Fusarium oxysporum* (Nimchua et al., 2007) were detected to act on different solid PET substrates. A big discovery was the identification of bacterial enzymes with polyester activity from the thermophilic actinomycete *Thermobifida* sp. Other enzymes that were proven to effectively depolymerize PET include a hydrolase from *Thermofibida fusca,* (Müller et al., 2005) cutinases from *Thermofibida alba* (Ribitsch et al., 2012) and *Thermofibida cellulosilytica* (Herrero Acero et al., 2011), and a esterase from *Thermofibida halotolerans* (Ribitsch et al., 2012). A cutinase from *Humicola insolens* and lipase from *Candida Antarctica* were also evidenced to act both individually and synergistically on the hydrolysis of PET (Carniel et al., 2017).

Other reports shown in **Table 2.3** have discussed the combined action of multiple enzymes on the enzymatic degradation of PET as well as the different factors affecting the catalytic performance such as temperature and pH. A common conclusion drawn is that polyester hydrolases need to exhibit thermal stability properties at elevated temperatures (40 to 70 ºC) for the degradation of PET. This represents a great challenge for the environmental biodegradation of PET since typical ambient temperatures (< 30ºC) are much lower than what polyester hydrolases need (Krueger et al., 2015; Wei & Zimmermann, 2017a).

PET degradation by microbes

Although most studies have focused in the enzymatic degradation of PET in the form of film, pellet, fiber, and, in few cases, powder, a number of research studies have been done on the natural biodegradation of PET (**Table 2.4.**). In these studies, several fungi and bacteria were found to possess the capability to biodegrade PET. These microorganisms include *Penicillium funiculosum, Nocardia, Arthrobacter sulfonivorans, Serratia plymuthica, Clitocybe sp.,* and *Laccaria laccata*. For instance, Asmita et al. (2015) indicated the degradation of PET small strips by *Bacillus subtilis*, *Staphylococcus aureus*, *Streptococcus pyogenes*, and *Aspergillus niger*, present in different types of soil. The plastic strips incubated with these bacterial species exhibited weight loss of 74.59%, 8.75%, 3.92%, and 52.94% after 30 days, respectively. In another study, Auta et al. (2017) reported the potential of two bacterial strains taken from sediment, *Bacillus cereus* and *Bacillus gottheilii*, to biodegrade UV-treated PET microplastics. After 40 days of incubation, the weight loss percentage achieved for two individually cultured samples was of 6.6% for *Bacillus cereus* and 3.0% for *Bacillus gottheilii*.

In a recent research work by Yoshida et al. (2016), the biodegradability of was evaluated PET using 250 PET debris-contaminated environmental samples including sediment, soil, wastewater, and activated sludge from a PET bottle recycling. The microorganisms in the samples were first screened for their ability to use low-crystallinity (1.9%) PET film as the major carbon source for growth. One microbial consortium, named No. 46, was able to degrade the PET film surface and catabolize 75% of the PET film carbon into CO_2 in about 80 days. After performing enzyme essays, isolation, and RNA-sequencing, the bacterial strain responsible for the degradation and assimilation of PET represented a novel species of the genus *Ideonella*, that the researchers named *Ideonella Sakaiensis*. The investigators explained that, although few known examples of esterases, lipases, or cutinases are capable of hydrolyzing PET, the novel bacterium generated a specific PET-hydrolytic enzyme (PETase) that was able to breakdown the polymer to produce mono(2-hydroxyethyl) terephthalate acid (MHET) as a major product. Surprisingly, another enzyme was also secreted by this bacterium, MHETase, which was able to hydrolyze MHET to produce two monomers- ethylene glycol and terephthalic acid- used to make PET through polymerization. The biodegradation of PET by Ideonella sakaiensis is illustrated in **Figure 2.10**. On comparative analysis with other enzymes such as TfH (hydrolase from *Thermofibida fusca*), LC-cutinase (metagenome from plant compost), and FsC (cutinase from *F. solani*), PETase was found to have 120, 5.5, and 88 times more effective activity towards PET films at low temperatures (Koshti et al., 2018).

Table 2.4. Literature reports on biodegradation of PET

PET		Reaction conditions					
Form	Crystallinity	Temperature	Medium	Degradation / weight loss achieved	Source of microbes	Degrading microorganism	Reference
Fiber	NR	30ºC	Aqueous	very low	Activated sludge	NR	J. Zhang et al., 2004
Film	NR	30ºC	Agar	0.08%	Dump soil	*Penicillium funiculosum*	Nowak et al., 2011
Sheet	NR	Room temp.	Air	very low	Soil	*Nocardia*	Sharon & Sharon, 2012
Film	NR	Room temp.	Aqueous	≤ 1.43%	Seawater	*Alteromonas, Kordiimonas lacus, Thalassospira, Lentibacter*	Webb, 2012
Film	NR	Room temp.	Compost	5.191%	Garden soil	NR	Asmita et al., 2015
				74.59%	-	*Bacillus subtilis*	
			Aqueous	8.75%	-	*Staphylococcus aureus*	
			Aqueous	3.85%	-	*Streptococcus pyogenes*	
Film	NR	Ambient temp.	Compost	not significant	Soil	NR	(Selke et al., 2015)
Film	1.9%	28ºC	Aqueous	75%	Sediment	*Ideonella Sakaiensis*	Yoshida et al., 2016
Film	9.8%	12.5-13ºC	Compost	not significant	Soil	NR	Mercier et al., 2017
UV-treated powder (MPs)	NR	NR	Aqueous	6.6% 3.0%	Sediment	*Bacillus cereus* *Bacillus gottheilii*	Auta et al., 2017
Film	NR	NR	Compost	not significant	Soil	*Arthrobacter sulfonivorans, Serratia plymuthica, Clitocybe sp., Laccaria laccata*	Janczak et al., 2018

NR: Not reported; MPs: Microplastics

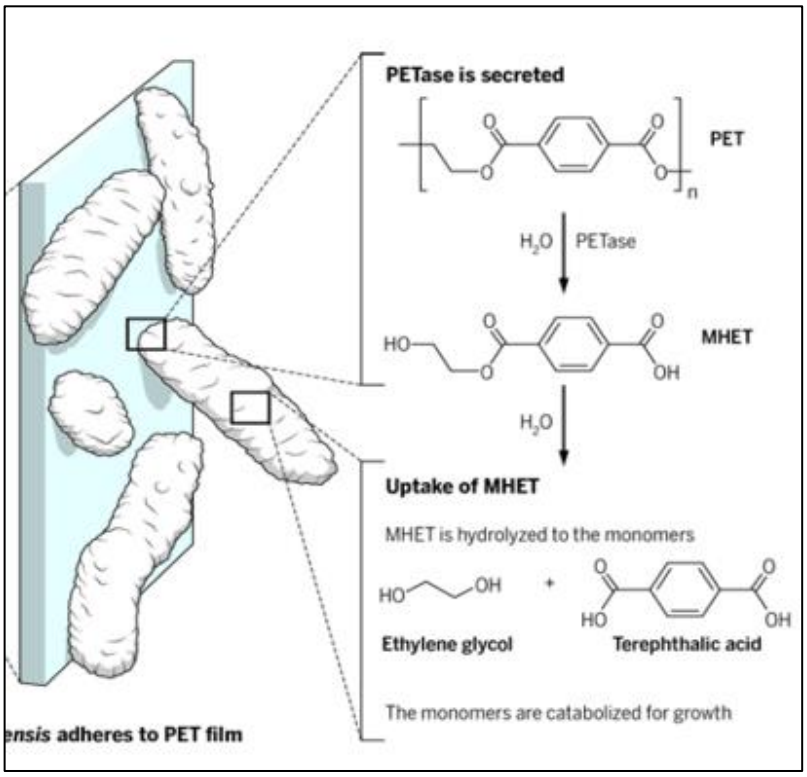

Figure 2.10. Biodegradation of PET by *I. Sakaiensis*(Bornscheuer, 2016)

The discovery of the bacterium *I. sakaiensis* proves the existence of bacterial strains with highly active PET-hydrolysing enzymes in environmental samples which suggests that other promising polyester degraders may also be found within this microbial biodiversity. In fact, new insights into the function and global distribution of PET-degrading bacteria and PET hydrolases in marine and terrestrial metagenomes were recently provided by Danso et al. (2018). In this work, the researchers developed a search algorithm that identified 504 possible PET hydrolase candidate genes from various databases. After clustering the 504 novel candidates based on amino-acids similarities, they found that all of the newly identified PET hydrolases occurred mainly in three bacterial phyla: *Actinobacteria, Proteobacteria*, and *Bacteroidetes*; and the main hosts within the *Proteobacteria* were the *Deltaproteobacteria, Gammaproteobacteria*, and *Betaproteobacteria* (Danso et al., 2018); *I. sakaiensis* is just one example of the possible PET degraders belonging to the latter class. Although PET hydrolases were found to be truly rare enzymes, they constitute promising candidates that can be further investigated as viable biocatalysts for environmental remediation and industrial PET recycling processes.

3. EXPERIMENTAL MATERIALS AND METHODS

3.1. Characteristics of microplastics

PET powder of 300 μm particle size was acquired from GoodFellow and used as the test material. PCL (Mn 2000) with TOC and size particle comparable to that of PET was supplied by Sigma Aldrich Chemical and used as a reference material in the biodegradation test. PCL waxy solids were mechanically crushed to obtain fine particles. PET and PCL particles were passed through two sieves to obtain microplastics with a narrow size distribution in the range of [300-425] μm (ASTM E11 test sieves mesh no. 40 and 50, Advantech, U.S.A.). PET microplastics were thermally treated at 100°C for 1 hour and tested for their crystallinity by means of DSC analysis (methodology in section 3.5.3). The mean crystallinity of the PET MPs was of 25%. The carbon content (C_C) and total organic carbon (TOC) of the microplastics were determined from the chemical formula (calculations in **Appendix C.2.1** and **C.2.2**) and the values are presented in **Table 3.1.** The PET microplastics were analyzed by optical microscopy. The image (**Figure 3.1**) shows a narrow size distribution of PET MPs in the range of [300-425] μm.

Table 3.1. Characteristics of microplastics

Polymer	Particle size (μm)	Cc	m (g)	TOC (mg C/L)	Crystallinity (%)
PET	300 – 425	0.625	2500	1645	25.1 ± 0.90
PCL	300 – 425	0.631	2500	1661	-

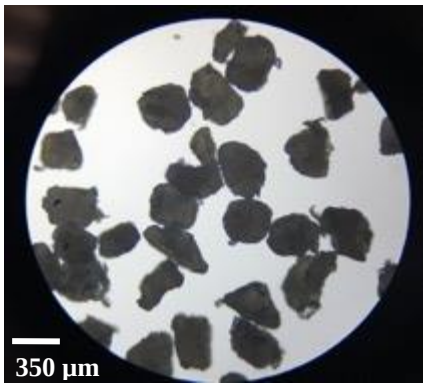

Figure 3.1. Optical image of PET microplastics

3.2. Growth medium

A growth medium with basic nutrients and minerals was use for the microbial screening and biodegradation test, with composition shown in **Table 3.2**. This medium is highly buffered, contains abundant inorganic nutrients that help to keep the pH constant throughout the biodegradation test. The solution contains about 360 mg/L of phosphorus (as phosphate ion) and 424 mg/L of nitrogen (as ammonium ion) with a pH of 7.2 – 7.4. The numerical calculations for the preparation of phosphate buffer saline and trace element solution are provided in **Appendix A**.

Table 3.2. Detailed composition of the growth medium

Growth medium solution	
$(NH_4)_2SO_4$	0.20 % w/v
Yeast extract	0.05 % w/v
Trace-element solution	1.00 % v/v
In Phosphate buffer saline (PBS) 10 mM	
Trace-element solution	**% w/v**
$FeSO_4 \times 7H_2O$	0.10
$MgSO_4 \times 7H_2O$	0.10
$CuSO_4 \times 5H_2O$	0.01
$MnSO_4 \times 5H_2O$	0.01
$ZnSO_4 \times 7H_2O$	0.01
In distilled water	

3.3. Experimental apparatus

The experimental data was generated by the apparatus shown in **Figure 3.4**. This unit was built in the Membrane Bioreactors Laboratory (KHN-111) of the Department of Chemical Engineering and was designed according to ISO 14852. It consisted of a series of batch bioreactors that are aerated in a closed system. All the parts and equipment were supplied by VWR International and the unit was constructed with the aid of the Technical Support Staff. Since the experimental apparatus allows determining the amount of evolved carbon dioxide in a biodegradation process, it can be operated to study the aerobic biodegradation of diverse materials, including microplastics. The laboratory possesses compressed air supply, which is used as the air source for this unit. In this study, the experimental apparatus was used to evaluate the biodegradation of PET microplastics by microbial communities from activated sludge. Both PET and activated sludge are described in Sections 3.1 and 3.4.1, respectively. Description of the process is given next and corresponds to the piping and instrumentation diagram (P&ID) shown in **Figure 3.4**.

The process starts with the aeration of the four batch bioreactors, which have been previously loaded with the test material (PET), reference material (PCL), inoculum and growth medium (See **Figure 3.3** for bioreactor configuration details). The valve (**V**-5) is slightly opened and air goes through (**1**) a carbon dioxide (CO_2) trap, where this component reacts with NaOH to generate carbonate and CO_2-free air (See **Figure 3.2** for CO_2 trap details). When pure oxygen is supplied, the valve regulator **(V-6**) is slightly opened and oxygen goes directly to the reactors. Then, the oxygen or air free of CO_2 splits into four streams to distribute the air to (**2**, **3**, **4**, **5**) the bioreactors in parallel. Valves (**V-1**, **V-2**, **V-3**, **V-4, V-6**) and flow meters (**F**) are set-up in each stream to regulate the airflow to each reactor, which is maintained in the range of 50-100 mL/min. Before entering each bioreactor, the air/oxygen is passed through a bottle containing $Ba(OH)_2$ which serves as a CO_2 indicator and is then bubbled into the bottom of the reactor. The air/oxygen exiting the reactor is passed through another CO_2 trap, consisting of bottles filled with $Ba(OH)_2$ to collect evolved CO_2 and is then released to ambient. The reactors are stirred throughout the process and their inner temperature monitored using temperature probes (**TT**) installed in their side arms and thermometers (**T**) set-up in a temperature panel (**6**). The cooling thermostat (**7**) or water recirculating bath continuously pumps water at the set-up temperature through the jackets of the bioreactors, which permits to maintain the desired temperature in the reaction vessels. The pinch valves (**V-7**, **V-8**, **V-**

9, **V-10**) of the sampling/injection mechanisms installed in the left-hand side arm of the reactors allow injecting and taking samples of media without compromising the air tightness of the system.

The selection of the reactor vessels, magnetic stirrers, tubing, flow-meters, thermometers and thermostat are based on various factors such as type of feed, flow rates, and temperature range. The model used as reactor vessels is a jacketed double sidearm spinner flask from Wheaton, which is specifically designed for suspension cell cultures and has an integral cap and magnetic impeller assembly. The magnetic stirrer used is a slow-speed model from VWR with a range of 0 to 150 rpm and it is selected to gently circulate the cells and avoid cell lysis. The tubing used for the airline is a non-permeable type Tygon® from Cole-Parmer, which does not absorb any carbon dioxide or oxygen from the air flowing in the system. Since stainless steel is an inert material that does not interact with chemical or biological substances, stainless steel tubing from RESTEK CORP is installed as the inlet and outlet lines of the absorber bottles and reactors (using two-hole rubber stoppers), and connected to the Tygon® tubing; the same stainless steel tubing with a smaller diameter is used for the sampling system. The flow meters are flow tubes from SP Scienceware that feature a borosilicate glass construction and a flow reading range from 2.80 up to 145 mL/min. The thermometers selected are Hi-accuracy dual thermometers from VWR that feature a stainless-steel probe, a monitor and a temperature range from -50 to 70°C. Finally, the LAUDA Alpha heating and cooling circulator from LAUDA-BRINKMANN INC provides a temperature range from – 25 to 100°C and stability of ±0.05°C. It is used to accurately maintain the desired inner temperature in the reactors.

Figures 3.2 and **3.3** show the configuration of the bioreactors and CO_2 traps while **Figure 3.4.** shows the P&ID of the experimental set-up. **Figure 3.5** shows photographs of the built bioreactor and experimental set-up.

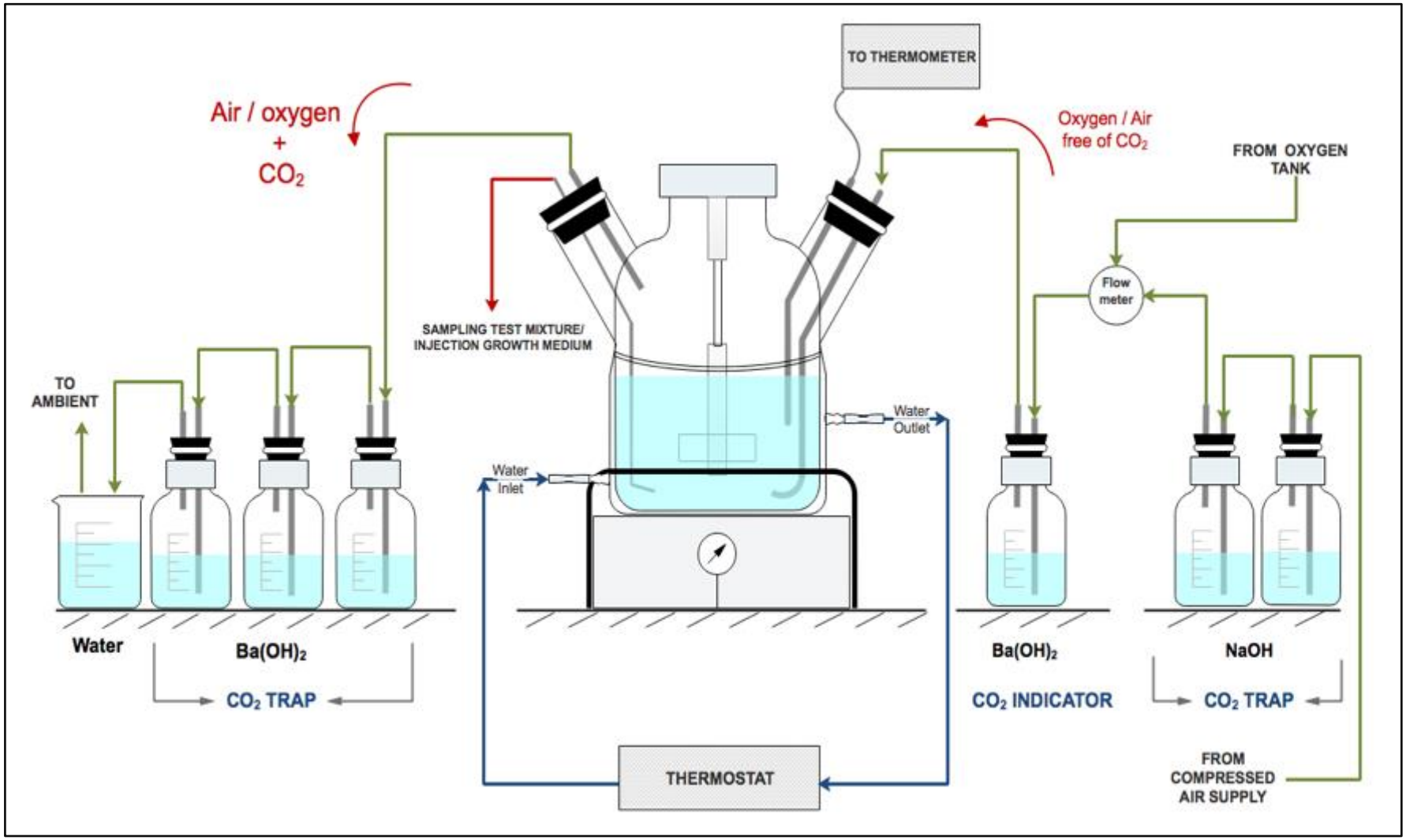

Figure 3.2. Details of CO_2 indicator and CO_2 trap of each batch bioreactor with either oxygen or air supply

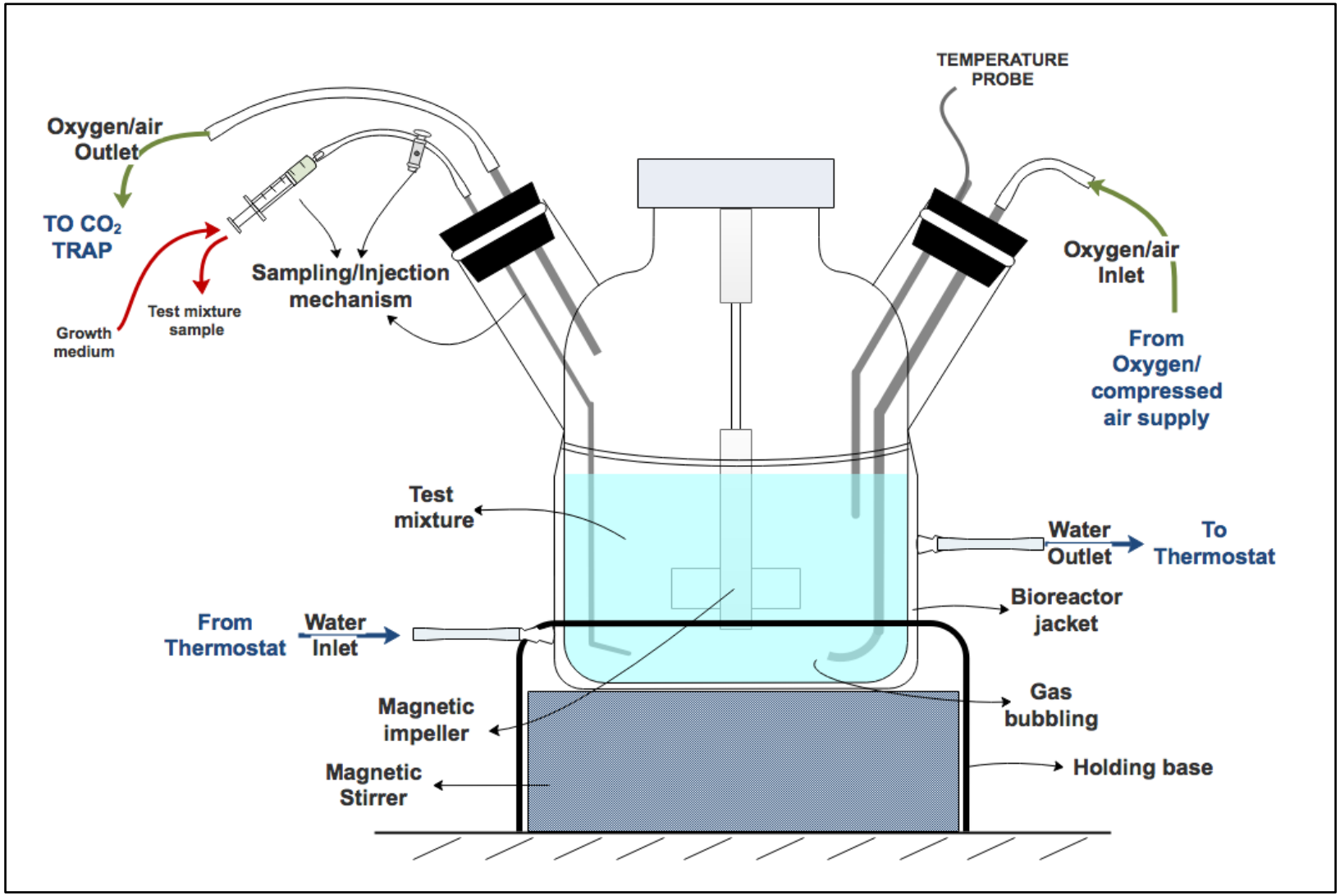

Figure 3.3. Bioreactor configuration

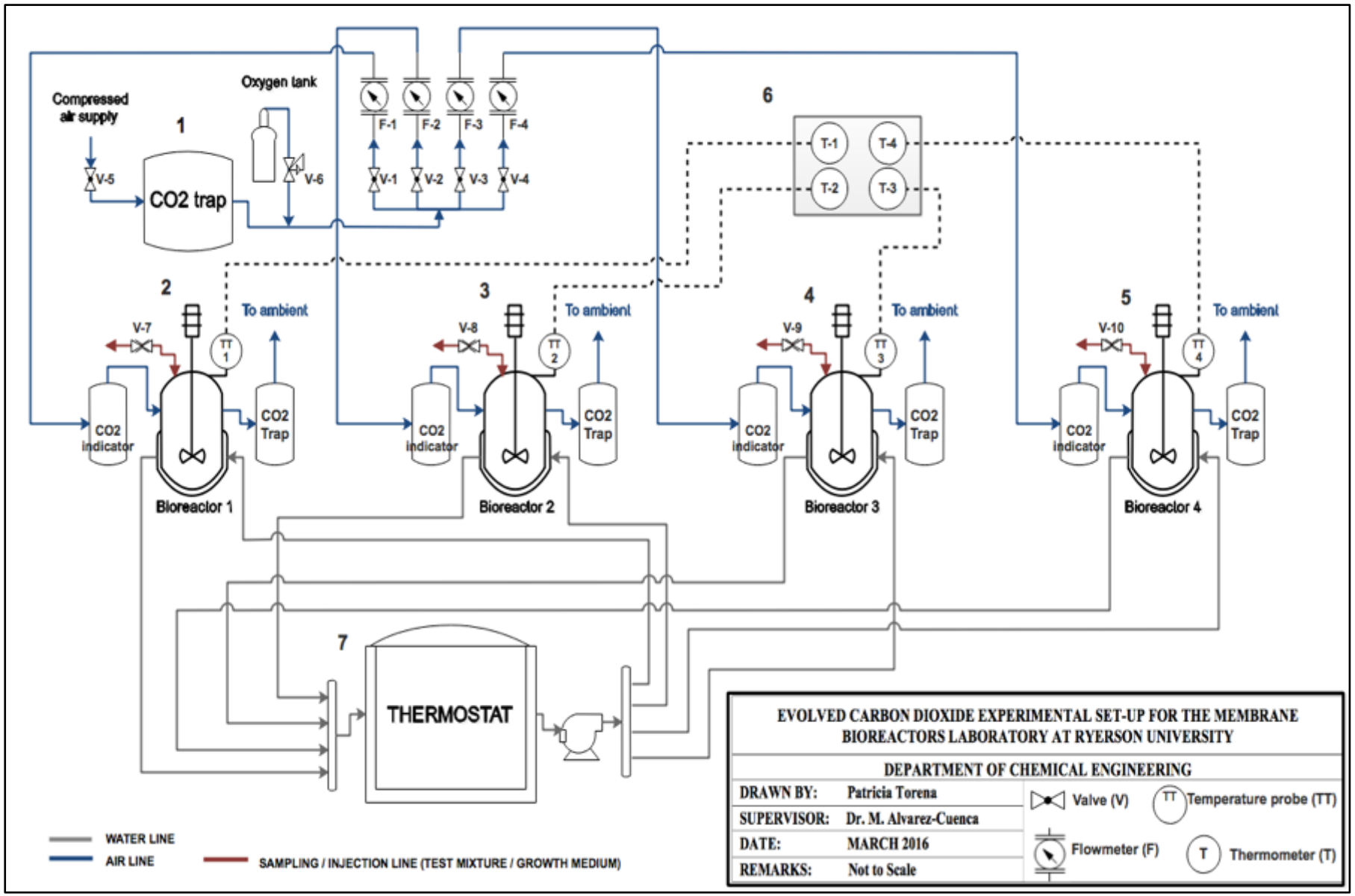

Figure 3.4. Process and instrumentation diagram (P&ID) of the experimental device constructed for the biodegradation assessment. The equipment/materials used to build the apparatus are tabulated in **Table 3.3.**

Figure 3.5. Photos of (**A**) the bioreactor configuration as shown in **Figure 3.3** and (**B**) the experimental apparatus as shown in **Figure 3.4**.

Table 3.3. Equipment used in the experimental unit and their description

Equipment	Company brand (Model)	Description
Bioreactor vessel	**Celstir® Wheaton** (356954)	**Body**: borosilicate glass, 360-degree water jacket, side arms size 45 mm. **Jacket**: inlet and outlet hose barb connections for 0.0635 m (1/4") I.D. tubing **Magnetic impeller**: 316 stainless-steel shaft and PTFE holders, paddle and bearings.
Cooling thermostat	**LAUDA Alpha** (97039-888)	**Temperature range**: -25 to 100°C **Temperature stability**: ±0.05°C **Heater power**: 1.5 kW **Cooling output at 20°C**: 0.225 kW **Pump type**: pressure pump, 1 step **Pump Pressure max.**: 0.2 bar **Pump flow max.**: 15 L/min **Bath volume**: 7.5 L **Power supply**: 115 V, 60 Hz.
Magnetic stirrer	**VWR® Slow speed magnetic stirrer** (12621-066)	**Speed range**: 1 to 150 rpm **Top plate material**: aluminum **Maximum vessel diameter**: 0.15 m **Maximum volume capacity**: 2 L **Controls**: stir knob, 1 to 10 dial markings **Power supply**: 120 V, 50/60 Hz, 7.2 W, 0.14 A
Thermometer and temperature probe	**Traceable® VWR®** (89204-742)	**Temperature range**: -50 to 70°C **Resolution**: 0.01°C **Accuracy**: ±0.3°C **Temperature probe**: stainless steel, diameter 0.125", stem length 6 ¼", accurate readings with tip penetration of 1/3-inch
Flow meter	**Riteflow® SP SCIENCEWARE®** (40400-0010)	**Flow rate range**: 2.80 to 145 mL/min **Flow tubes**: borosilicate glass, plain ends **Overall length**: 65 mm **Inlet/outlet connections**: compression glass fittings for 8.5 mm (3/8") I.D. tubing **Floats**: glass and stainless-steel **Float stops**: Teflon®
Absorber bottles	**VWR® Media/storage bottle with cap** (10754-816, 10754-818)	**Body**: borosilicate glass **Volume**: 250 and 500 mL **Diameter**: 0.07 and 0.086 m **Height**: 0.138 and 0.176 m
Silicone tubing (water line)	**VWR®** (89068-482)	**Material**: low-volatile grade, platinum-cured silicone **Temperature range**: -73 to 204°C **Durometer hardness**: Shore A, 50 **Wall thickness**: 0.063" **I.D.**: 1/4" **O.D.**: 3/8"

Continued from Table 3.3 .

Equipment	Company brand (Model)	Description
Lab tubing	**Tygon® Cole-Parmer** (06407-05, 06407-76)	**Material**: Tygon® E-3603 **Temperature range**: -50 to 74°C ***Air line:*** Wall thickness: 1/32" I.D.: ¼" O.D.: 5/16" ***Sampling/injection line:*** Wall thickness: 1/16" I.D.: 1/8" O.D.: ¼"
Stainless steel tubing	**Restek** (29034, 21512)	**Material**: instrument-grade 304 stainless steel ***Air line:*** I.D.: 0.21" O.D.: ¼" ***Sampling/injection line:*** I.D.: 0.085" O.D.: 1/8"
Rubber stopper	**VWR®** (59582-269)	**Material**: black rubber **Type**: two-hole **Size**: 6 ½ **Length**: 25 mm **Top diameter**: 34 mm **Bottom diameter**: 27 mm
Manifold -water	**APolloPEX™** (PXCM4PT)	**Material**: copper with brass Pex barb connection **Number of branches**: 4 (closed end) **Inlet O.D.**: 3/4" **Branches O.D.**: ½" **Branch spacing**: 2" on center
Manifold - Air	**Ecoplus®** (728460)	**Material**: chrome **Type**: T style **Number of ports**: 4 (close end) **Inlet I.D.**: ¼" **Outlets I.D.**: 3/16"
Pinch valve	**Talon® VWR® Regular pinchcock** (21573-155)	**Material**: stainless steel **Minimum to maximum grip**: 0 to 12 mm **Maximum tubing O.D.**: ½" **Clamp height**: 47 mm
Tubing connectors	**Mix and Match quick disconnects SCIENCEWARE®** (H19728-0000, H19729-0000)	**Material**: polyethylene **Type**: interchangeable with other to make reducing combinations **Temperature range**: up to 80 °C **O.D**.: 1/4 to 5/16" and 3/8 to 1/2"
Oxygen tank	**Oxygen grade 5.0 Linde Canada** (24060140)	**Pressure**: 2,640 psig **Size**:300 **Content**: 9.23 m^3 **Specifications**: Ar < 5 ppm, CO < 0.5 ppm, CO_2< 0.5 ppm, H_2O < 1 ppm, Kr < 1 ppm, N_2< 2 ppm
Oxygen regulator	**Regulator for Oxygen 5.0 Linde Canada** (11255629)	**Material**: brass **Type**: single stage **Pressure range**: 0-250 psig **Delivery side**: ¼" compression fitting with diaphragm valve

3.4. Isolation and screening of PET-degrading bacteria

This section provides details on the collection of activated sludge and isolation of bacteria with potential to degrade PET MPs.

3.4.1. Activated sludge collection and characterization

Activated sludge samples were collected from the aeration tank of North Toronto WWTP located in East York, Toronto, Ontario and used as source of potential PET-degrading microorganisms. The sample was placed in a container and transported to the laboratory (KHN 111) at Ryerson University for further analyses. After letting the sample settle, a volume of supernatant was tested for pH, total suspended solids (TSS), and volatile suspended solids (VSS), according to standard methods (APHA, 1998). The TOC was determined from the VSS value, since it is generally 58% of the VSS (Castro-Aguirre et al., 2017). All assessments were performed in triplicates, and average values are presented in **Table 3.4** (calculations shown in **Appendix C.2.3**)**.** The activated sludge sample was used for isolation and screening of PET-degrading bacteria within 72 hours of the day of collection.

Table 3.4. Characteristics of the activated sludge from North Toronto WWTP

pH	TSS (mg/L)	VSS (mg/L)	TOC (mg C/L)
6.56	847 ± 83.9	551 ± 69.3	320 ± 40.2

3.4.2. Screening of PET-degrading bacteria end enrichment culture

The microbial communities in activated sludge were screened for their ability to utilize PET as the sole carbon source for growth by measuring the biomass concentration (***X***) throughout the incubation with this polymer as the sole carbon and energy source. The VSS concentration, an approximate measure of biomass concentration (Ryu et al., 2014), was determined periodically throughout the incubation period of 60 days. A separate flask, which was prepared the same way but with PCL microplastics, was incubated under the same conditions and kept as a reference. The biomass concentration in this flask was also monitored to assess the capacity of the microbial community to utilize the reference material. Subsequently, an enrichment-culture technique was followed using PET microplastics (**Figure 3.6**) to isolate potential PET degraders.

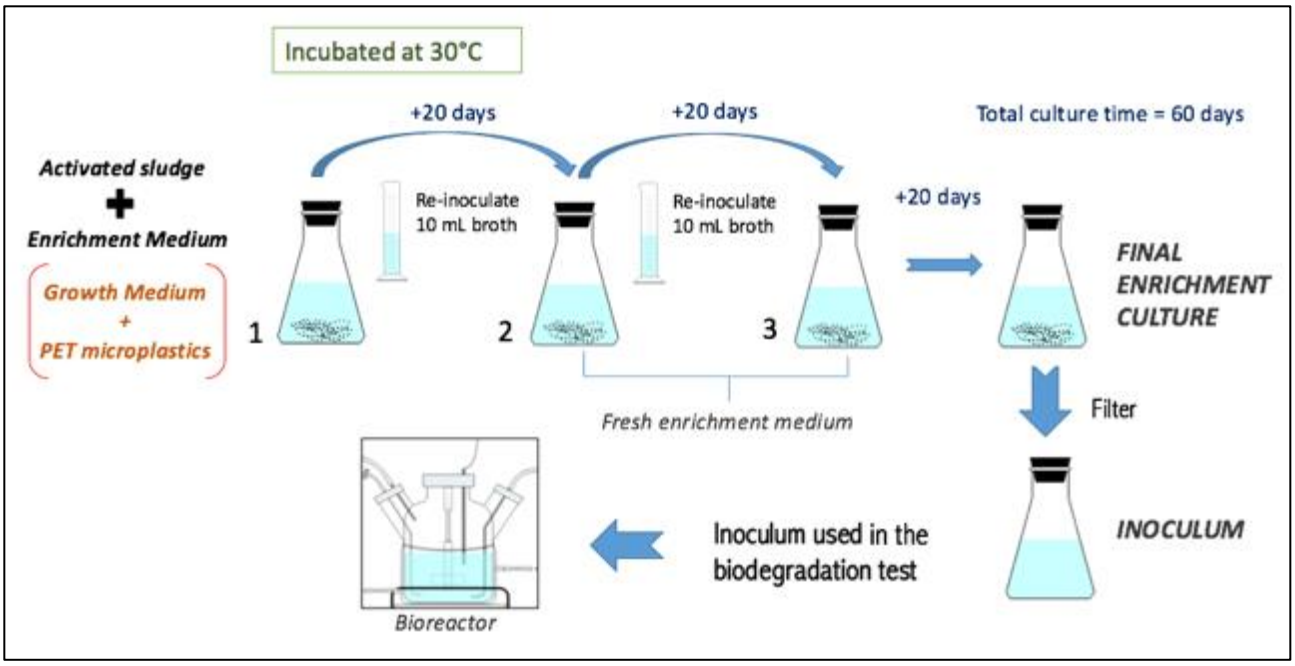

Figure 3.6. Schematic diagram of the enrichment-culture technique

The enrichment medium was prepared with 200 mL of growth medium and 400 mg of PET microplastics. The enrichment culture was started by mixing 50 mL of activated sludge with 200 mL of enrichment medium and incubated at 30°C for 20 days. Then, a volume of broth was taken from the flask and re-inoculated into fresh enrichment medium and cultivated under the same conditions for 20 days. The same procedure was repeated a third time. The final enriched broth, once filtered through filter paper to remove microplastics, constituted the inoculum for the biodegradation experiment.

3.5. Biodegradation assessment by analysis of evolved carbon dioxide

The biodegradation of PET microplastics was assessed by the method of evolved carbon dioxide standardized in ISO 14852 (ISO, 2018). In this method, the experimental amount of evolved CO_2 from degraded materials is compared with the theoretical amount during an aerobic microbial degradation process, which is calculated as 100% oxidation of the polymer from the chemical formula. In order to perform such assessment, an experimental set-up was designed, built, and commissioned in compliance with this standard, as presented in section 3.3. All the

details of the experimental feed, design parameters, biodegradation test protocol, calculations and kinetics evaluation are presented in the following sections.

3.5.1. Design parameters and experimental feed

To develop biological microplastics removal, several design parameters were adopted from the standard ISO 14852 and studies by other researchers like Yoshida et al. (2016).The batch reactors feed was composed of growth medium, microplastics and inoculum prepared as previously described. The exact composition of the experimental feed of each bioreactor is presented in **Table 3.5**.

Table 3.5. Composition of the feed

Bioreactor	PET (mg)	PCL (mg)	Growth medium (mL)	Inoculum (mL)
1	2500	-	800	150
2	2500	-	800	150
3	-	2500	800	150
4 (Blank)	-	-	800	150

The amount of polymeric material was set to be 2500 mg, which gives a total organic carbon (TOC) content of 1645 mg/L and a carbon to nitrogen ratio in the feed of 7:3 (calculations in **Appendix C.2** and **A**, respectively). The temperature was selected to be 30°C and pH between 7-7.5. The effect of oxygen supply in the biodegradation process was evaluated by varying the flowrates of oxygen to the system. Therefore, the experimental set-up worked under three different air flowrates: 48 mL/min of pure oxygen and 65 mL/min and 100 mL/min of air free of CO_2. Additionally, the effect of nutrient availability was assessed during the stage 3 where air was supplied at 100 mL/min. To do this, 15 mL of growth medium was injected to each reactor every 3 days.

Due to the slow nature of the biodegradation of polymeric materials such as PET, the residence time selected for the entire test was of 168 days, which would also make possible to evaluate the biodegradation process under three different aeration conditions and for at least 7 weeks each.

The complete set of design parameters are summarized in **Table 3.6**.

Table 3.6. Design parameters

Parameters	Value/ranges
Reactor type	Batch
Residence time	168 days
Air flow rate	48 –100 mL/min
Temperature	30°C
pH	7 – 7.5
Stirring speed	45 rpm
TOC	≈ 1700 mg/L
Phosphorus content (PO_4^-)	361 mg/L
Nitrogen content (NH_4^+)	424 mg/L
C:N	7:3
TSS (inoculum)	30 – 1000 mg/L

3.5.2. Start-up and test procedure

The engineering, procurement, and construction (EPC) of the evolved CO_2 test unit, including the commissioning, took approximately one year. The biodegradation test period took around 8 months (September 2017-May 2018), including the screening of PET-degrading bacteria and inoculum preparation. Commissioning was performed using only tap water to verify adequate flows of water and air through the entire system.

Assembly and installation of the experimental system

The test unit was assembled with the aid of the technical support staff and the following steps were taken (refer to the list of equipment in **Table 3.4** and to the system configuration in **Figures 3.3**, **3.4** and **3.5**).

1. The cooling thermostat LAUDA Alpha was put in place and the pump connection link (silicone tube) was removed. Two separate rubber hoses (O.D. 1") were connected to the

external circulation set, one to the return to bath and one to the pump outflow. Both connections were tightened and secured with hose clips.

2. The end of each hose was then connected to the inlet of one manifold. A stand and clamps were used to hold both manifolds horizontally. The manifold connected to the pump outflow was labeled as the "pumping water" and the one connected to the return to bath was labelled as "returning water".
3. The slow-speed magnetic stirrers (4 in total) where placed alongside the thermostat. A supporting base made with PVC and hand-tightening screws was designed and constructed to secure each bioreactor vessel onto the magnetic stirrer.
4. The bioreactor vessels were assembled (magnetic impeller and lid), placed and secured onto the magnetic stirrers using the supporting base.
5. Four pieces of PVC tubing (O.D. ¾") were connected to each branch of the manifold and each line was followed by plastic connectors (reduction from 3/8" to ¼") and a silicone tubing (I.D. ¼"). These connections were done for both manifolds.
6. Each of the four lines of the "pumping water" were connected to the inlet of the bioreactor's jacket and each of the four lines of the "returning water" were connected to the outlet of the corresponding bioreactor's jacket.
7. A piece of stainless-steel tubing (O.D. ¼") was molded to create the air inlet of each bioreactor, with a length long enough to reach the bottom of the vessel so that air can be bubbled into the test mixture in the reactor (**Figures 3.4**and **3.6-A**). The tubing was passed through one hole of a two-hole rubber stopper. This assembly was then used to tightly close the right-hand side arm of each bioreactor. Then, one temperature probe was bent and installed into the second hole of the stopper of each reactor. The wire of each probe was plugged into the corresponding thermometer, which was wall-mounted previously.
8. A piece of stainless steel tubing (O.D. 1/8") was molded to create the sampling/injection line of each bioreactor as shown in **Figures 3.4**and **3.6-A**, with a length long enough to reach the bottom of the vessel so that liquid samples can be taken out of the reactor and growth medium can be injected directly to the test mixture. The tubing was passed through one hole of a two-hole rubber stopper. This assembly was then used to tightly close the left-hand side arm of each bioreactor. A short piece of stainless-steel tubing

(O.D. 1/4") was installed into the second hole of the stopper and used as the air outlet for each bioreactor.

9. A piece of Tygon tubing (1/8") was used to connect a syringe to the exit of the stainless-steel tubing of the sampling/injection mechanism of each bioreactor, as shown in **Figure 3.4**. A pinch valve (pinchcock) was installed in the sampling/injection line of each reactor to pinch the flexible Tygon tubing and shut off flow. The pinch actuator can be manually opened to allow sampling of test medium or injection of growth medium.
10. APVC squared panel was used to wall-mount in parallel the four flow meters. The air manifold was mounted on the panel and each of its four outlets (I.D. 3/16") was connected to the bottom of a flowmeter using lab tubing. The top of each flow meter was connected to the air inlet of each bioreactor using Tygon lab tubing (1/4").
11. A piece of silicone tubing (I.D. ¼") was connected to the inlet of the air manifold and to both the compressed air valve (**V-5**) and the oxygen tank regulator (**V-6**). This line is used to aerate the entire experimental system.
12. The plastic caps of all the absorber bottles were prepared by cutting a hole to each cap and installing a two-hole rubber stopper. Two pieces of stainless-steel tubing (O.D. ¼") were molded and installed into the stopper of each absorber bottle as the air inlet and outlet. The tubes used as inlets were long enough to reach the bottom of the absorber bottles so that air can be bubbled into the solution contained in the bottle. The ones used as outlets were short to let the air from the bottle scape from the top.
13. Tygon lab tubing (1/4") was used to connect all the air outlets of the bioreactors to the absorber bottles to create the CO_2 traps and indicators, as shown in **Figures 3.3** and **3.6-B**. A 500 mL beaker was placed at the end of each CO_2 trap.

Commissioning of the experimental system

The start-up of the experimental set-up consisted of the following steps (refer to **Figures 3.3**, **3.4** and **3.5**):

1. Inspect the air Tygon tubing is properly connected to the compressed air supply (V-5), CO_2 trap bottles, CO_2 indicator bottles, beakers, and bioreactors.
2. Inspect all the air valves (V-1, V-2, V-3, V-4, V-5) and ensure they are closed.

3. Inspect the water line tubing and ensure is properly connected to the thermostat, manifolds, and bioreactors jackets.
4. Fill up the thermostat bath up to a maximum level of 20 mm below the bath bridge, approximately 9.5 L, with a mixture of distilled water and 0.1 g of sodium carbonate (Na_2CO_3) per liter of water
5. Connect the thermostat unit to a grounded main power socket with a power supply 120V and 15 A
6. Switch on the thermostat at the mains switch, then set the temperature set point to 30°C using the menu functions and enter keys
7. Verify water is flowing properly through the bioreactors jackets and there are no leakages in the tubing, connections or manifolds
8. Fill up each bioreactor [1 - 4] with 1 L of tap water, close them tight with their cap, making sure their magnetic impeller is centered and tightened
9. Turn on the magnetic stirrers and set up the speed at #3 (45 rpm); check for proper stirring in all bioreactors
10. Fill up all the absorber bottles and beakers with tap water and close the bottle caps tight
11. Turn on the air valve (V-5) and use valves V-1, V-2, V-3 and V-4 to adjust the airflow rate to each bioreactor to 50 mL/min
12. Inspect there is proper and constant air flow through all bioreactors and absorber bottles, as well as proper air release to ambient
13. Ensure there are no air leakages in air valves, connectors, and bottle caps
14. Take temperature readings from each bioreactor thermometer; adjust the thermostat set point temperature to achieve an inner temperature of 30°C in all bioreactors
15. Ensure the experimental unit operates continuously and consistently without supervision for at least 7 days

Biodegradation test protocol

After two weeks of troubleshooting, the bioreactors were fed with growth medium and microplastics and were inoculated on November 13th, 2017 with the final enrichment culture obtained as described in section 3.4.2. The troubleshooting and experimental protocol are detailed in **Appendix B**. All sample calculations for this test can be found in **Appendix C.2.4**.

3.5.3. Determination of percentage biodegradation

The percentage biodegradation of microplastics D_t was calculated from the amount of CO_2 evolved for each measurement interval using Equation **1** (ISO, 2018):

$$D_t = \frac{\sum(mCO_2)_T - \sum(mCO_2)_B}{ThCO_2} \times 100 \qquad (1)$$

where $(mCO_2)_T$ is the total amount of carbon dioxide evolved from microplastics in the bioreactor (mg), $(mCO_2)_B$ is the total amount of carbon dioxide evolved in the blank bioreactor (mg), and $ThCO_2$ is the theoretical amount of carbon dioxide evolved from microplastics (mg). This last term can be calculated from Equation **2**:

$$ThCO_2 = W_0 \times C_C \times \frac{44}{12} \qquad (2)$$

where W_0 is the initial weight of microplastics (mg), C_C is the carbon fraction in the microplastics, and *44*/*12* the ratio of molecular weight of CO_2 and atomic mass of carbon.

The evolved carbon dioxide reacts with $Ba(OH)_2$ and is precipitated as barium carbonate ($BaCO_3$), as shown in Equation **3**. Then, $(mCO_2)_T$ and $(mCO_2)_B$ are calculated by titrating the remaining $Ba(OH)_2$ in the absorber bottles with HCl (Equations **5** and **6**).

$$CO_2 + Ba(OH)_2 \rightarrow BaCO_3 + H_2O \qquad (3)$$

$$Ba(OH)_2 + 2HCl \rightarrow BaCl_2 + 2H_2O \qquad (4)$$

$$mCO_2 = \left(\frac{2c_B \times V_{B0}}{c_A} - V_A \times \frac{V_{Bf}}{V_{Bz}}\right) \times c_A \times 22 \qquad (5)$$

$$V_A = V_f - V_i \qquad (6)$$

where c_A is the concentration of HCl (M), c_B is the concentration of $Ba(OH)_2$ (M), V_{B0} is the volume of $Ba(OH)_2$ at the beginning of the test (mL), V_{Bf} is the volume of $Ba(OH)_2$ before titration (mL), V_{Bz} is the volume of aliquot of $Ba(OH)_2$ used for titration (mL), V_A is the volume

of HCl used for titration, and *22* is half the molecular mass of CO_2. For the titration and determination of V_A, V_f is the final and V_i the initial volume of HCl in the burette. A numerical example of the calculation of the amount of CO_2 evolved from the reactors is shown in **Appendix C.2.4**.

3.5.4. Kinetics evaluation

- *Kinetics in the enrichment procedure*

In batch cultures, the microbial growth shows an exponential phase that is defined as (Najafpour, 2007):

$$X = X_0 e^{\mu t} \qquad (7)$$

where X is the biomass concentration (mg VSS/L) at time t (d), X_0 is the initial biomass concentration (mg VSS/L), and μ is the specific growth rate (d^{-1}).

- *Kinetics in the biodegradation test*

The kinetic constant of microplastics reduction was calculated using the first-order kinetic model as shown below (Auta et al., 2017):

$$K = -\frac{1}{t}\left(ln\frac{W}{W_0}\right) \qquad (8)$$

where K is the first-order kinetic constant of MPs reduction (d^{-1}), t is the incubation time (d), W_0 is the initial weight of microplastics, and W is the weight of microplastics after incubation (mg), calculated from Eq. **(9)**:

$$W = W_0\left(1 - \frac{Dt}{100}\right) \qquad (9)$$

where *Dt* is the percentage biodegradation. After obtaining the microplastics reduction rate for both PET and PCL, the half-life ($t_{1/2}$) was calculated (Alaribe & Agamuthu, 2015) as follows:

$$t_{1/2} = \ln(2)/K \qquad (10)$$

Numerical examples of the calculations of kinetics are presented in **Appendix C.2.5**.

3.6. Analytical techniques and data analysis

This section discusses the different analytical techniques and data analysis tools employed throughout the experimental work. A TSS and VSS analysis was employed during the inoculum preparation and screening of PET-degrading microorganisms. Then, to validate and trace the degradation of PET MPs in the biodegradation test, a series of analytical techniques were performed to monitor modifications on the polymer. Since the deterioration of polymers is an interfacial process that takes place almost exclusively on the outer surface, techniques to characterize material properties at the surface level provide the most informative data. The different techniques employed to determine the morphological and structural changes include:

- Fourier transform infrared (FTIR)
- Differential Scanning Calorimetry (DSC)
- Intrinsic viscosity
- Scanning Electron Microscopy (SEM)

Additionally, Reversed-phase high performance liquid chromatography (HPLC) analysis was performed to detect the possible presence of soluble metabolites as a consequence of the biodegradation of PET, such as bis(2-hydroxyethyl) terephthalate (BHET) and terephthalic acid (TPA) (Gamerith et al., 2017). **Table 3.7** presents a summary of all the parameters that were determined with each analytical technique to evaluate the extent of each biodegradation stage. The SEM/EDS equipment used in this study was provided by the Mechanical Engineering department at Ryerson University. The DSC and HPLC equipment were provided by the Ryerson University Analytical Centre.

All the incubated PET samples were purified before the FTIR, DSC, and intrinsic viscosity analyses by removing the media and adhered cells as follows: a volume of 15 mL of media + PET MPs was taken from the bioreactors #1 and #2 (triplicates), placed in several 1.5 mL microtubes and centrifuged (Eppendorf Centrifuge 5424) at 7300 rpm for 5 minutes. The media was discarded, and the cells recovered from all tubes were supplemented with 20% glycerol and stored at –80 ºC until required. The microplastics were collected, washed with distilled water and ethanol, and dried in the oven at 60°C for one hour.

A numerical example of each of the calculations performed in all the analytical techniques is presented in **Appendix C.2.6**.

Table 3.7. Analytical techniques

Analytical technique	Parameter assessed
SEM/EDS	Attachment of bacteria Biofilm formation Polymer surface erosion Presence of mineral salts
DSC	Changes in rheological properties (melting temperature, crystallinity, glass transition temperature)
Intrinsic viscosity	Molecular weight changes
FTIR	Changes in molecular structure and chemical bonds at the polymer surface
HPLC	Presence of metabolites in solution

3.6.1. TSS and VSS analysis

The analysis of TSS and VSS was performed to characterize the inoculum to be used in the biodegradation test and to monitor microbial growth during the screening of PET-degrading microorganisms. TSS was determined from the weight difference of a glass fibre filter pad (0.45µm) before and after filtering the sample and drying the pad at 105°C to constant mass (Equation **11**). VSS was obtained by the loss-on-ignition method, in which residues after incineration at 550°C are subtracted from TSS (Equation **12**).

$$TSS = \frac{(B-A)\times 10^6}{V} \qquad (11)$$

$$VSS = \frac{(B-C)\times 10^6}{V} \qquad (12)$$

where TSS is the total suspended solids (mg/L), B is the weight of filter pad + residue dried at 105°C (g), A is the weight of filter pad (g), V is the volume of sample (mL), 10^6 is the conversion factor, VSS is the volatile suspended solids (mg/L), and C is the weight of filter pad + residue after ignition at 550°C (g).

3.6.2. Fourier-transform infrared (FTIR) spectroscopy analysis

Fourier-transform infrared spectroscopy is a technique used to obtain an infrared spectrum of absorption or emission of a solid, liquid or gas. It consists in passing light from the infrared region of the electromagnetic spectrum – typically the mid-infrared region – onto or through a sample, and measuring the decrease in the energy of the beam due to interaction with the sample as a function of the wavelength of the light (Webb, 2012). The result is a spectrum that contains absorption peaks that are characteristic of the vibrational energies of the chemical bonds in the sample, which is also referred to as a 'fingerprint'.

FTIR spectroscopy stands as powerful method for the characterization of polymers that has been widely used to study their degradation both qualitatively and quantitatively. For instance, the carbonyl and crystallinity indexes can be used to indicate the degradation behaviour of the polymer and are calculated using measurements of the IR peaks of interest. In the case of the crystallinity index, there are intensities of the morphologically specific absorption bands that are

assigned to crystalline parts of the polymer that could be measured before and after degradation to identify any modification.

Moreover, infrared spectroscopy facilitates the identification and quantification of degradation products. For example, FTIR is commonly used to inspect thermo- and photo-oxidized polyethylenes and detect a range of carbonyl-containing compounds that are usually formed after photo- and thermo-degradation (Stuart, 2004).

FTIR analysis (Perkin Elmer Spectrum One) was performed in the scanning range of 4000 to 450 cm^{-1} to inspect PET MPs before and after the biodegradation test. The FTIR spectra and characteristic peaks of the samples were compared to investigate possible changes in the molecular structure and chemical bonds at the polymer surface, associated with bio-deterioration during the incubation. The carbonyl index was calculated as the ratio of the vibration of the band at 1710 cm^{-1} (I_{1710}) to that of the 871 cm^{-1} (I_{871}), as shown in Equation **13** (Janczak et al., 2018):

$$Carbonyl\ index = \frac{I_{1710}}{I_{871}} \qquad (13)$$

The crystallinity index was determined as the ratio of peak areas at the bands 1341 cm^{-1}(A_{1341}) and 1410cm^{-1} (A_{1410}) (Herrero Acero et al., 2011).

$$Crystallinity\ index = \frac{A_{1341}}{A_{1410}} \qquad (14)$$

Each spectrum reported is the average of at least three spectra measured in different MPs samples.

3.6.3. Differential scanning calorimetry (DSC) analysis

The differential scanning calorimetry (DSC) is a thermo-analytical technique used to evaluate the response of polymers to heating in a controlled atmosphere. To this end, the difference in the amount of heat required to increase the temperature of a sample and a reference is measured as a function of time. The equipment to perform such analysis is composed of a measurement

chamber and a computer. The result of a DSC analysis is a curve of heat flux versus temperature or time that could show endothermic or exothermic peaks. This curve can be used for the calculation of enthalpies of transitions by integrating the peak of a given transition (Pungor & Horvai, 1994).

DSC is routinely used for investigation, selection, comparison, and end-use performance of materials. Some of the characteristic properties that are routinely measured include glass transition, melting point, freezing point, boiling point, crystallization, and crystallinity. The latter is one of the most important properties of semi-crystalline thermoplastics such as PET, nylon, polyethylene, and polypropylene. The percent crystallinity refers to the overall level of crystalline component in relationship to its amorphous component, and it is directly related to many other key properties exhibited by these thermoplastics: brittleness, toughness, stiffness, optical clarity, long term stability, among others.

Differential scanning calorimetry (DSC) analysis was carried out to PET MPs before and after incubation to verify possible changes in the rheological properties, such as fusion enthalpy and crystallinity degree. The analysis was performed under nitrogen atmosphere using Perkin Elmer Pyris Diamond equipment and 9 mg for all samples. The samples were heated at a linear rate to an elevated temperature of 300°C to erase previous thermal history, then cooled at a linear rate before heating again. First, each sample was heated from room temperature (35°C) to 300°C at a rate of 10°C/min. Then, samples were cooled to room temperature at 10°C/min and a second heating was performed under the same conditions to determine the crystallinity degree by means of Equation **15** (Bimestre & Saron, 2012).

$$\%crystallinity = \frac{\Delta H_m - \Delta H_c}{\Delta H_m^0} \times 100 \quad (15)$$

where ΔH_m is fusion enthalpy of the microplastics (J/g), ΔH_c is enthalpy of cold crystallization (J/g) and ΔH_m^0 is the hypothetical fusion enthalpy of the polymeric material 100% crystalline. ΔH_m is calculated from the area of the endothermic signal, while ΔH_m^0 for PET is 140 J/g (Kong & Hay, 2002). The thermal properties reported are the average of DSC thermal curves of at least two samples of MPs.

3.6.4. Intrinsic viscosity analysis

Inherent viscosity of PET microplastics (before and after incubation) was determined according to standard test ASTM D4603 (ASTM, 2015) using an Ubbelohde-1B viscometer. Each sample of PET microplastics (0.22 – 0.25 mg) was mixed with a prepared solvent mixture of 60/40 w/w phenol/1,1,2,2-tetrachloroethane (PTCE) for a total volume of 50 mL. The mixture was placed in a water bath set at 110°C and stirred for 5 hours to dissolve the microplastics. After complete solubilisation, the solutions were filtered, placed in the viscometer and tested in a 30°C water bath. The obtained flow times of the pure solvent (t_0) and of PET solutions (t) were used to obtain the relative (η_r) and inherent (η_{inh}) viscosities through the following equations (ASTM, 2015; Sanches, Dias, & Pacheco, 2005):

$$\eta_r = \frac{t}{t_0} \qquad (16)$$

$$\eta_{inh} = \frac{Ln(\eta_r)}{C} \qquad (17)$$

where t_0 is the flow time of pure solvent (s), t is the flow time of polymer solutions (s), C is the concentration of the polymer solution (g/dL), and η_{inh} is the inherent viscosity of the polymer (dL/g).

Intrinsic viscosity (η) was then calculated from a single measurement of the η_r by means of the Billmeyer relationship (Billmeyer, 1949):

$$\eta = 0.25(\eta_r - 1 + 3Ln\eta_r)/C \qquad (18)$$

Finally, the viscosity molecular weight M_v of the microplastics was calculated using the Mark-Houwink (ASTM, 2015) Equation **19**:

$$\eta = K{M_v}^a \qquad (19)$$

where the values of the constants K and a, for a system of 60/40 PTCE at 30°C, are (Hergenrother & Nelson, 1974):

$$K = 2.37 \times 10^{-4}$$

$$a = 0.73$$

The reported values of intrinsic viscosity and molecular weight are the average of at least two samples of PET MPs

3.6.5. Optical microscopy and Scanning electron microscopy (SEM) analysis

The optical microscope, or often called light microscope, provides enough magnification to distinguish between objects examined. The device uses a system of lenses and visible light to sharply magnify small detailed samples and project the image directly to the eye. The eyepiece and objective lenses provide the resolving and magnifying power of the microscope, while the condenser lens system, by focusing the light source onto the specimen, maximises the resolution of the systems by increasing the numerical aperture or light-capturing ability of the objective lenses (Nielsen et al., 2016). At highest magnifications, the resolution of the microscope is approximately 0.2 μm, which is suitable for viewing or studying most bacteria and other microorganisms(Nielsen et al., 2016). Light-optical microscopes are extensively used in research in areas such as microelectronics, nanophysics, biotechnology.

A scanning electron microscope (SEM), on the other hand, produces images of a sample by scanning the surface with a focused beam of electrons (Stokes, 2008). The electrons interact with atoms in the sample, producing various signals that contain information about the surface topography and composition of the sample. The electron beam is scanned, and its position is combined with the detected signal to produce an image. SEM can achieve high-resolution images with magnification up to 100,000X or 1 nm.

An energy-dispersive X-ray analyzer may be also interfaced to the SEM system, which allows for qualitative and semi-quantitative determination of elements (atomic number > 6) in powders and thin films or for mapping of compositional distribution of chemical compositions (Lobo & Bonilla, 2003). The preparation of the specimen for this technique is fairly simple; however, when specimens are insulating materials that may undergo electrostatic charging when exposed

to the electron probe, it is necessary to coat their surface with a thin film of conducting carbon or metal like gold (Egerton, 2006).

The samples of PET MPs were inspected by both optical microscopy and SEM analyses. A high-resolution scanning electron microscope model JEOL 638LV was used, equipped with Oxford energy dispersive X-ray spectroscopy (EDS), backscatter diffraction, and three-dimensional surface imaging. SEM/EDS analysis of PET microplastics was performed on three different sets of samples:

Set A (PET microplastics at 0 days): samples taken before the incubation with the microbial community. They were washed with ethanol and distilled water and dried in the oven at 60° for 1 hour; then coated with gold to improve the conductivity and examined.

Set B (Incubated PET microplastics): samples taken from the bioreactors after 168 days of incubation and prepared for assessment without removal of adhered cells. They were washed with distilled water and ethanol and dried in an oven at 60° for 1 hour; then gold-coated and examined.

Set C (Purified incubated PET microplastics): these samples were taken from the bioreactor after 168 days of incubation and purified to wash out the adhered cells, as previously described, then gold-coated and examined.

The first set (A) of samples comprised the microplastics in their original form without any biological treatment and served as a reference point. The second set (B) made possible to inspect for microbial colonization and biofilm formation onto the polymer surface after the biological treatment. The third set (C) made possible to observe the surface of the biologically treated polymer after washing out the attached cells and this way detect any morphological modification such as surface erosion, cracks and roughness. An elemental analysis was also performed to detect the precipitation of mineral salts onto the MPs surface.

3.6.6. Reversed-phase high performance liquid chromatography (HPLC)

HPLC is an analytical technique used to separate, identify and quantify each component of a mixture, in which a liquid solvent (mobile phase) containing a sample mixture is passed over a solid adsorbent material (stationary phase). The sample in solution form is injected into the liquid mobile phase contained in the instrument. Then, the mobile phase carries the sample through a packed or capillary column (stationary phase) and as the sample moves through the column, its components partition themselves between the mobile phase and the stationary phase. The elution or retention time is the amount of time between the injection of the sample and its elution from the column (Harvey, 2008; Nagy & Vékey, 2008). The separated solutes are detected at the exit of the column by a flow-through detector such as a Diode Array Detector.

The resultant chromatogram is a two-dimensional plot of the concentration in terms of the detector response versus the time. The detector gives response as a peak whose height is dependent on the concentration of the component or solute. The peak height or area under the peak are considered a measure of a component concentration. Each peak represents a compound present in the sample since different compounds have characteristic or standard retention times under the same operational conditions. In order to identify the component and quantify it, a calibration curve is constructed by injecting, under identical operational conditions, standard solutions with known concentrations of the component and recording the peak areas for each concentration. In most cases, there is a linear relationship between the height or area and the concentration of the component. Then, the concentration of the component in the sample in question is determined by comparing the peak area obtained to that of the calibration curve.

HPLC analysis (Perkin Elmer Series 200) was performed to samples of media taken from the reactors throughout the biodegradation test to evaluate the possible presence of PET degradation products BHET and TPA. Samples of liquid medium were taken at 6 different times (108, 120, 128, 148, 157, and 168 days) and centrifuged (Eppendorf Centrifuge 5424) at 7300 rpm for 5 minutes. The supernatant was filtered through a 0.22μm cellulose Acetate filter and brought to a 2 mL HPLC vial. A reversed phase column Supelco Discovery C18 was used.

To obtain good separation of the products, a linear gradient mixture of formic acid and methanol was used as the mobile phase with constant 10% 0.01N formic acid, starting with 85%

water and 5% methanol, gradual (3 min) to 10% methanol, gradual (to 16 min) to 50% methanol, and gradual (to 20 min) to 90% methanol (Gamerith et al., 2017; Machado de Castro et al., 2017; Vertommen et al., 2005). The total flow of the eluents was 0.85 mL/min while the column was maintained at 40°C.

The injection volume of the samples was 10µL and they were injected by means of an auto-sampler able to hold up to 100 samples. Detection of the analytes was performed with a photodiode array detector (DAD) (Perkin Elmer LC240) at a wavelength of 230 nm. Standards of TPA and BHET were prepared in distilled water in a range of (0.075-5.545) mM and treated the same way as samples. The analysis was performed in triplicate and the resulting retention times are reported as the average.

3.7. Statistical data analysis

All descriptive statistics were performed using Microsoft Excel and results are reported as mean value ± standard deviation (*M* ± *SD*). In the case of the cumulative CO_2 and % biodegradation of the PCL and blank reactors, the error is reported as the propagated instrumental uncertainty, since no replicates were used in the biodegradation test as a result of certain limitations in the experimental device constructed. Numerical examples of these calculations of uncertainties are presented in **Appendix C.2.7**.

3.8. Microbial analysis

3.8.1. Isolation of bacterial strains

The microbial cells were recovered from the PET microplastics after incubation and kept in saline and glycerol solution at –80ºC until their later use. A volume (100 µL) of these cells were serially diluted in saline solution (1% NaCl) to decrease the concentration of cells. A 100µL of the dilution of 10^{-3} was plated in Luria Broth (LB) agar and incubated at 30ºC for 48 hours. Four bacterial strains with distinct colony morphologies were identified and selected among all the colonies that grew, based on an apparent higher abundance. Two or three colonies of each morphology type were individually picked and re-streaked on LB agar, giving a total of 11 plates labelled as BS1, BS2, BS3, BS4, BS5, BS6, BS7, BS8, BS9, BS10, BS11. These plates were

incubated at 30ºC for 24 hours and the bacterial strains were re-streaked until pure isolates were obtained, which was confirmed by verifying that all colonies had the same morphology and that there was no contamination. The final distinct isolates obtained were bacterial strains BS3, BS6, BS10, and BS11. The colonies were characterized based on gram-staining and their morphology, according to taxonomy found in Bergey's Manual of Systematic Bacteriology.

3.8.2. Growth analysis

The isolates BS3, BS6, BS10, BS11 were analyzed to determine their ability to grow individually and as a community with PET MPs as the sole carbon and energy source. The isolates and the consortium formed by these 4 isolates (labelled as BST) were incubated in 20 mL of growth medium with 120 mg of UV-blasted PET MPs at 30ºC for 25 days. The growth curve of the batch cultures was constructed with the values of colony-forming units (CFU) and optical density (OD) measured at different times. The colony forming units (CFU mL^{-1}) of the sample volume were quantified by the dilution plate count technique. The measurement of OD or absorbance at 600 nm is a common method for estimating the concentration of bacterial cells in a liquid. The cell count CFU is performed to measure the number of viable cells within that sample.

Before initiating the growth analysis, overnight cultures of the isolates were prepared to ensure that all cells were at the same growth stage. To prepare the overnight cultures, one loop of each colony was individually transferred into 1 mL of LB broth, vortexed and transferred into 9 mL of LB broth. Then the mixture was vortexed and incubated on a shaker (100 rpm) at 30ºC overnight. The next day, the cells of each isolate were washed with saline1 % NaCl (Protocol in **Appendix B**) and the obtained pellet was mixed with 20 mL of growth medium and vortexed. One milliliter of each culture was transferred into a 1.5 mL cuvette to determine its OD (Eppendorf Biophotometer 8.5 mm) as a measure of bacterial cell density. Dilutions of these cultures were made with different ratios of growth medium to adjust their ODs to approximately the same value and to make a total of 20 mL of mixture. Approximately 120 mg of PET MPs, previously sterilized using UV-light for 30 minutes, were added to each tube.

The community formed by all bacterial strains (BST) culture was prepared with 2 mL of each culture BS3, BS6, BS10, BS11, plus 12 mL of growth medium and 120 mg of PET MPs. A

negative control was prepared with the consortium BST and growth medium (no PET MPs) and another negative control was prepared only with growth medium and PET MPs. All the cultures were incubated at 30ºC for 25 days, and their OD and CFU values determined at different time points. To determine the CFU, 100 µL of culture was serially diluted and the three most probable dilutions were spread-plated in LB agar and incubated at 30ºC for 48 hours. The resulting colonies from the best plate were counted, usually the plate with CFU in the range of 30-300. The OD measurements were performed in triplicates and the OD of the negative control was monitored to be zero throughout the test.

A second growth analysis was repeated for cultures BS3 and BS11 and for a period of 163 hours. The community made up of these two isolates was also analyzed, as well as the two negative controls.

3.8.3. Clear-zone test

The bacterial strains BS3, BS6, BS10, BS11 were tested using the clear-zone technique. The plates were prepared using two solid medium layers. The lower layer (15 mL) contained mineral-salt agar and the upper layer (10 mL) contained the polymer suspension, as described in **Appendix A**. The four isolates were serially diluted and then spread-plated and incubated for 20 days. The formation of clear zones around resulting colonies was monitored throughout the test.

3.8.4. Microbial identification by molecular techniques

The isolates were identified by means of molecular techniques as follows: all pure cultures were individually DNA extracted using Power Soil® DNA Isolation Kit (MO BIO Laboratories Inc., Canada) and the extractions were used in amplifying the 16S rRNA region using the polymerase chain reaction process (PCR) (Protocols in **Appendix B**). The resulting 16S rRNA gene fragments were sent to ACGT Corporation (Toronto, ON) for Sanger sequencing. The DNA sequences were identified using the Basic Local Alignment Search Tool (BLAST) of the National Center for Biotechnology Information (NCBI). The percent of confidence of each corresponding culture was recorded.

4. EXPERIMENTAL RESULTS AND DISCUSSIONS

This section discusses and analyzes as follows the experimental results obtained.

1. The main objective of this work was to evaluate the biodegradation of PET microplastics by bacterial communities from activated sludge and to gain insights on this process. The biological degradation is an important process that can be used as a potential tool for the removal of PET microplastics within wastewater and marine environments.
2. An experimental set-up was designed and constructed to perform the biodegradability assessment in compliance with the standard ISO 14852.
3. Bacterial communities from activated sludge with the potential to degrade PET MPs were isolated and screened. Their biomass concentration was determined to calculate the microbial growth rate. The final culture, enriched with potential PET-degrading bacteria, was used to inoculate the four bioreactors in the biodegradation test.
4. The biodegradability assessment test was performed, according to the standard ISO 14852. The aerobic biodegradation of PET microplastics by the enriched bacterial culture was assessed for a period of 168 days through the quantification of the carbon dioxide evolved throughout the entire test. The kinetics of the biodegradation process were also evaluated.
5. The biodegradation extent was validated through the assessment of morphological and structural changes on the microplastics by FTIR, DSC, intrinsic viscosity, and SEM analyses, as well as the presence of soluble metabolites through HPLC.
6. A microbial analysis of the final cultures in the (PET) bioreactors was performed to evaluate and identify bacterial strains involved in the biodegradation process.
7. All experimental results and uncertainties are expressed as the mean and standard deviation.

4.1. Isolation and screening of PET-degrading bacteria

The bacterial strains in activated sludge able to use PET MPs as the sole carbon and energy source were isolated using an enrichment-culture technique. This technique is used to encourage the growth of certain microorganisms under strong selective conditions and it has been successfully used to isolate microbial strains with potential to degrade certain polymers (Cerdà-Cuéllar et al., 2004).

Samples of activated sludge were incubated in growth medium supplemented with PET microplastics as the sole carbon source for 60 days (triplicates), as previously described. The bacterial biomass was monitored by measuring the VSS throughout the incubation time (Equation **12**). The raw data and calculations of biomass concentration at different times, for both PET and PCL are presented in **Appendix C.3** and mean values presented in **Table 4.1**. The VSS method, also known as the dry cell weight method, was chosen as a measure of bacterial biomass that was readily available, simple, economic and quick. The microbial growth rate (μ) in batch tests has been inferred before from the monitoring of the mass of volatile suspended solids (VSS), among other parameters (Ryu et al., 2014; Stasinakis et al., 2003). The dry cell weight or VSS, expressed in mg VSS L^{-1}, has been the traditional standard method for the direct determination of biomass.

Moreover, VSS is commonly used for quantifying bacterial mass in activated sludge, and even though it does not coincide with the effective bacterial biomass, it can be used as a rough measure

Table 4.1. Biomass profile throughout the incubation period

Substrate	PET microplastics	PCL microplastics
Time (days)	Biomass (mg VSS L^{-1})	Biomass (mg VSS L^{-1})
0	110 ±13.9	110.4 ± 13.9
11	91.7 ± 33.3	58.3 ± 35.4
29	203 ± 94.8	642 ± 82.5
39	347 ± 79.2	725 ± 35.4
42	614 ± 128	875 ± 200
53	650 ± 306	1025 ± 200
60	503 ± 66.8	-

of the amount of bacteria in any sample. Other researchers have successfully used this parameter as a measure of microbial biomass (Foladori et al., 2010; Kumar et al., 2016; Zhao et al., 2013;Horta et al., 2015).

The microbial biomass obtained throughout the incubation period is depicted in **Figure 4.1** as cell dry weight (mg VSS L^{-1}) versus time. The increasing trend indicates that the bacterial community was able to grow in the presence of both PET and PCL microplastics under the culture conditions. Further, the growth was statistically assessed using non-linear regression analysis. The exponential model fitted well to the experimental data, which is in agreement with the typical exponential phase of microbial growth in batch cultures (Najafpour, 2007). The consortium that was exposed to PET microplastics exhibited an exponential growth phase until day 53 of incubation, with a fitted regression line $X = 110.4e^{0.0321t}$ and an average regression coefficient of 0.8458. This exponential growth observed in the culture with PET as substrate suggests that there are potential PET degraders within the microbial community. After 53 days of incubation, the biomass started to decrease; this suggests that the consortium entered the death phase which could have been caused by, e.g., a depletion of nutrients. Likewise, the consortium that was exposed to PCL microplastics displayed an exponential phase with a fitted regression line $X = 110.4e^{0.0457t}$ and an average regression coefficient of 0.7894. The values of R2 were rather low, which can be explained by the

In batch cultures, the microbial growth is defined by Equation **7** which has an exponential form:

$$X = X_0 e^{\mu t} \qquad (7)$$

From linearizing Equation **7** and plotting Ln(X) vs time, it was also possible to obtain the specific microbial growth rates (μ) of 0.0344 d^{-1} for PET and 0.0551 d^{-1} for PCL. The kinetic equation for PET was $Ln(X) = 0.0344t + 4.4923$ (R^2 0.854) and for PCL was $Ln(X) = 0.0551t + 4.3241$ (R^2 0.823). A greater microbial growth rate was observed in the case of PCL, which can be explained by the fact that PCL is a biodegradable aliphatic polyester that has been shown to be degraded by microbes in many different environments, including activated sludge (Hakkarainen & Albertsson, 2002).

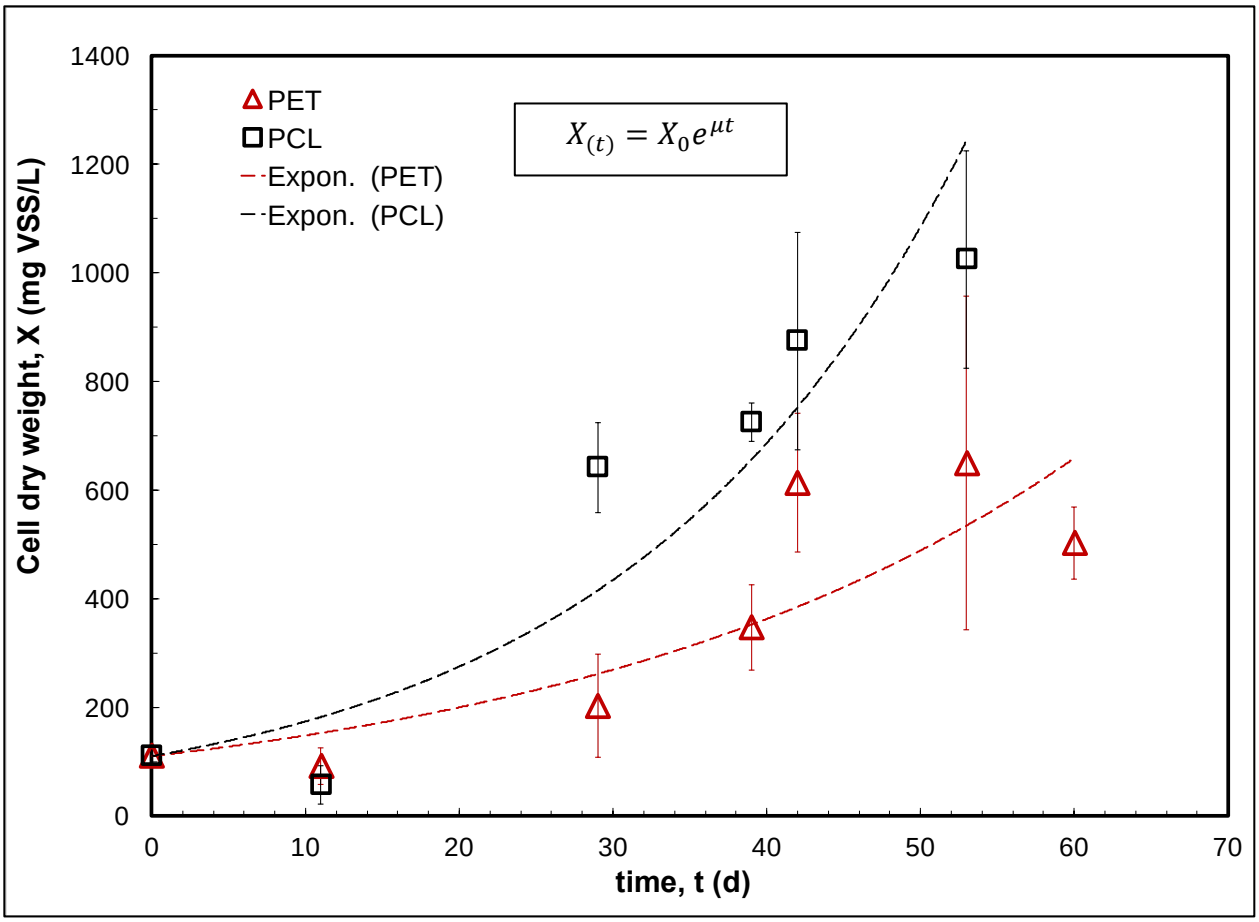

Figure 4.1. Biomass growth of enriched culture during the incubation with microplastics.

The possibly high amount of microplastics (400 mg) provided as a substrate to the bacterial community may have played an important role in the microbial growth. When the concentration of substrate available is high, the protein and enzyme synthesizing system of the organisms becomes stimulated, resulting in an increase growth rate. The species utilizing the substrate are favoured and therefore grow faster, which makes their proportion in the final culture to be higher. Therefore, the final culture reflects characteristics of the culture developed under the given conditions rather than the original one (Stasinakis et al., 2003).

This culture technique allowed to encourage the growth of potential PET-degrading microorganisms within the community from activated sludge and the final culture obtained, enriched with these microbes, was then used as inoculum for the biodegradation test. The inoculum had a TSS value of 683 mg/L (*SD* = 109) and VSS value of 503 mg/L (*SD* = 66.8).

4.2. Biodegradation results

An experimental set-up (as shown in **Figure 3.3**) built in compliance with ISO 14852 was used to perform the biodegradation test of PET microplastics and PCL as a reference, in which temperature, air flow rate, and pH were monitored over time (**Figure 4.2**, raw data presented in **Appendix C.1**). The temperature and pH were stable at 30°C and 6.10 – 7.31, respectively. Oxygen flow rate (F_{O2}) was adjusted to three different values throughout the testing period: pure oxygen was first supply at a rate of 47.2 mL/min for 50 days; then, CO_2-free air (21% O_2) was supplied at 65 mL/min for 58 days and finally at 100 mL/min for 60 days, which correspond to 10.2 mL/min and 21.0 mL/min of oxygen, respectively. During the last 60 days of the test, 15 mL of growth medium were supplied every 3 days to each bioreactor to provide microbes with fresh nutrients.

The standard ISO 14852 suggests the use of a well-defined biodegradable polymer such as cellulose or microcrystalline as the reference material for the biodegradation assessment. However, the microorganisms that are able to perform cellulolytic activity to biodegrade such polymers might not be equally able to carry out esterase activity to efficiently biodegrade materials like polyesters (Mezzanotte et al., 2005). Consequently, PCL, a degradable aliphatic polyester, was selected as a more suitable reference material as other authors like Funabashi et al., (2007) have suggested.

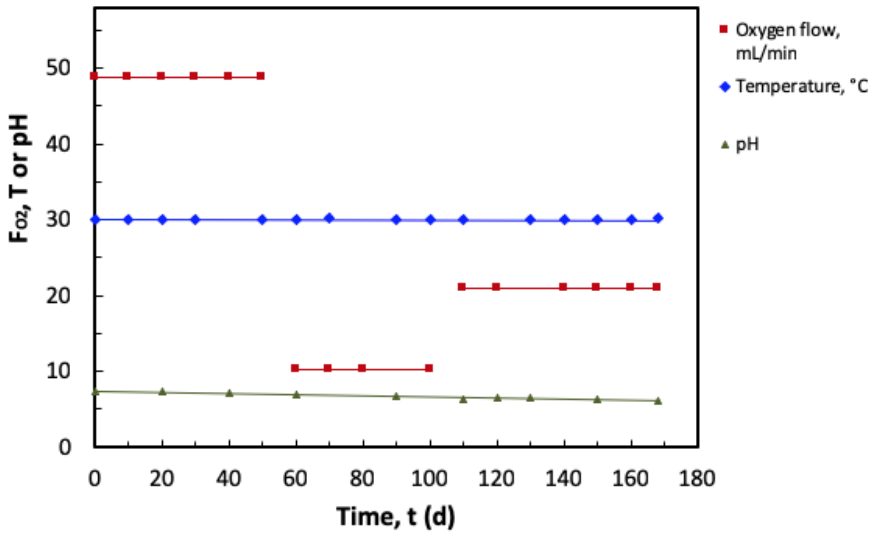

Figure 4.2. Operating conditions throughout the biodegradation tests.

For the data analysis, the experimental amount of CO_2 evolved in the bioreactors was periodically estimated through titrations of the absorber bottles and Equation **5**:

$$mCO_2 = \left(\frac{2c_B \times V_{B0}}{c_A} - V_A \times \frac{V_{Bf}}{V_{Bz}}\right) \times c_A \times 22 \qquad (5)$$

The percentage degradation of the microplastics (%Dt) was also determined using Equation **1**. Raw data, calculations, cumulative values and statistics for all the time points are presented in **Appendix C.2.4**.

The results of microplastics degradation by the microbial consortium are presented in **Table 4.2** and the cumulative values of CO_2 (mCO_2) and % Dt were plotted as a function of time as shown in **Figures 4.3** and **Figure 4.4**. The % biodegradation is a measurement of how much CO_2 can be evolved from the microplastics compared to the theoretical amount. For instance, 2500 mg of PET microplastics with a carbon content (Cc) of 62.5% gives, by means of Equation **2**, a theoretical amount of CO_2 that can be evolved from the material of 5729 mg, as shown in **Table 4.2**.

Table 4.2. Overall biodegradation and kinetic results of microplastics after incubation

	PET	PCL
Cc (%)	62.5	63.1
W_0 (mg)	2500 ± 0.0001	2500 ± 0.0001
$ThCO_2$ (mg)	5729 ± 0.23	5787 ± 0.23
mCO_2 (mg)	1756 ± 308	2771 ± 60.5
Dt (%)	17.07 ± 5.38	34.42 ± 0.012
R^2	0.8151	0.7926
K (day^{-1})	0.0011 ± 0.0004	0.0025 ± 0.0001
$t_{1/2}$ (day)	618 ± 227	280 ± 0.001

The total amount of CO_2 evolved in the blank was 778 mg (*SD* = 43.5) after 168 days of testing. This amount of CO_2 represents the background which was later subtracted to the amount evolved from the bioreactors with microplastics to determine the biodegradation, as shown in Equation **1**. This is the reason why the amount of CO_2 evolved from the blank bioreactor have a great influence on the final biodegradation values. During the test, there were some negative values of mCO_2 and Dt; although physically these values are absurd, they were possible since they were a consequence of specific days where there was a higher production of mCO_2 in the blank bioreactor with respect to the other reactors (Selke et al., 2015).

As depicted in **Figure 4.3**, the amount of CO_2 evolved from microplastics after 168 days of incubation was of 1756 mg (*SD* = 308) for PET and 2771 mg (*SD* = 60.5) for PCL. Overall, the microbial consortium degraded 34% of PCL and 17% of PET microplastics. The higher biodegradation rate found in PCL is reasonable and evident, since it is an aliphatic polymer [-$OCH_2(CH_2)_3CH_2$-CO-] that has been proved to be biodegradable in many different environments (Guo et al., 2012, 2010; Marten et al., 2005; Mueller, 2006), whereas PET is an aromatic polyester [-OCH_2CH_2-O-CO-⟨⊙⟩-CO-] that tends to be resistant to microbial attack (Webb, 2012). Nevertheless, this bacterial consortium also showed PET-degrading capability. The potential of the microbial community to significantly degrade the microplastics and produce CO_2 was compared with the rate of reduction constant *K*, and half-life.

The PCL microplastics experienced the highest reduction rate of 0.0025 day^{-1} (*SD* = 0.0001) during the incubation time, whereas PET showed a lower reduction rate of 0.0011 day^{-1} (*SD* = 0.0004). Since PCL presented a higher reduction rate, the half-life of 280 days was significantly lower than that of PET (618 days). These kinetic parameters further support the degree of microbial activities within the test medium and what they imply is that 0.0025 mg of PCL and 0.0011 mg of PET microplastics were taken up by the microbial consortium per day. Furthermore, the consortium will need approximately 618 days to reduce PET microplastics to its half and 280 days to reduce PCL microplastics to its half. The fact that the values of R^2 for the kinetics (**Table 4.2**) were rather low indicates that the first-order kinetic model used was not suitable. Other kinetic models such as Power Law Model, Michaelis-Menten inhibition model and Michaelis-Menten activation model could have been used to better predict the experimental data in the biodegradation of MPs; however, testing these models was beyond the scope of this investigation.

The use of a biodegradable polymer such as PCL in the biodegradation test was important to check the inoculum activity. If no activity is detected for a readily degradable polymer, likely the microorganisms will not interact with a more resistant material such as PET. Also, the degradation of the biodegradable polymer by an active inoculum represents an ideal process that was used as a reference point to compare with the degradation of the polymer of interest.

The enlarged available surface area provided by the micro-size of PET particles might have played an important role in the degradation of the polymer. Since biodegradation is usually an interfacial process that occurs at the surface level, materials in the form of powder typically degrade more easily due to the increased area/volume ratio (Castro-Aguirre et al., 2017; Eubeler, 2010). In this context, an improved degradation has been evidenced in some studies of enzymatic degradation of polyesters (Gamerith et al., 2017; Gan et al., 1999; Wu & Gan, 1998; Y. Zhao et al., 1999).

Apart from the particle size of the polymer, the low crystallinity (25%) of PET microplastics might have aided the biodegradation process as well, since higher activities have been reported towards the amorphous regions of polyester substrates (Herzog et al., 2006; Kint & Muñoz-Guerra, 1999; Marten, Müller, & Deckwer, 2003; Vertommen et al., 2005; Webb, 2012).

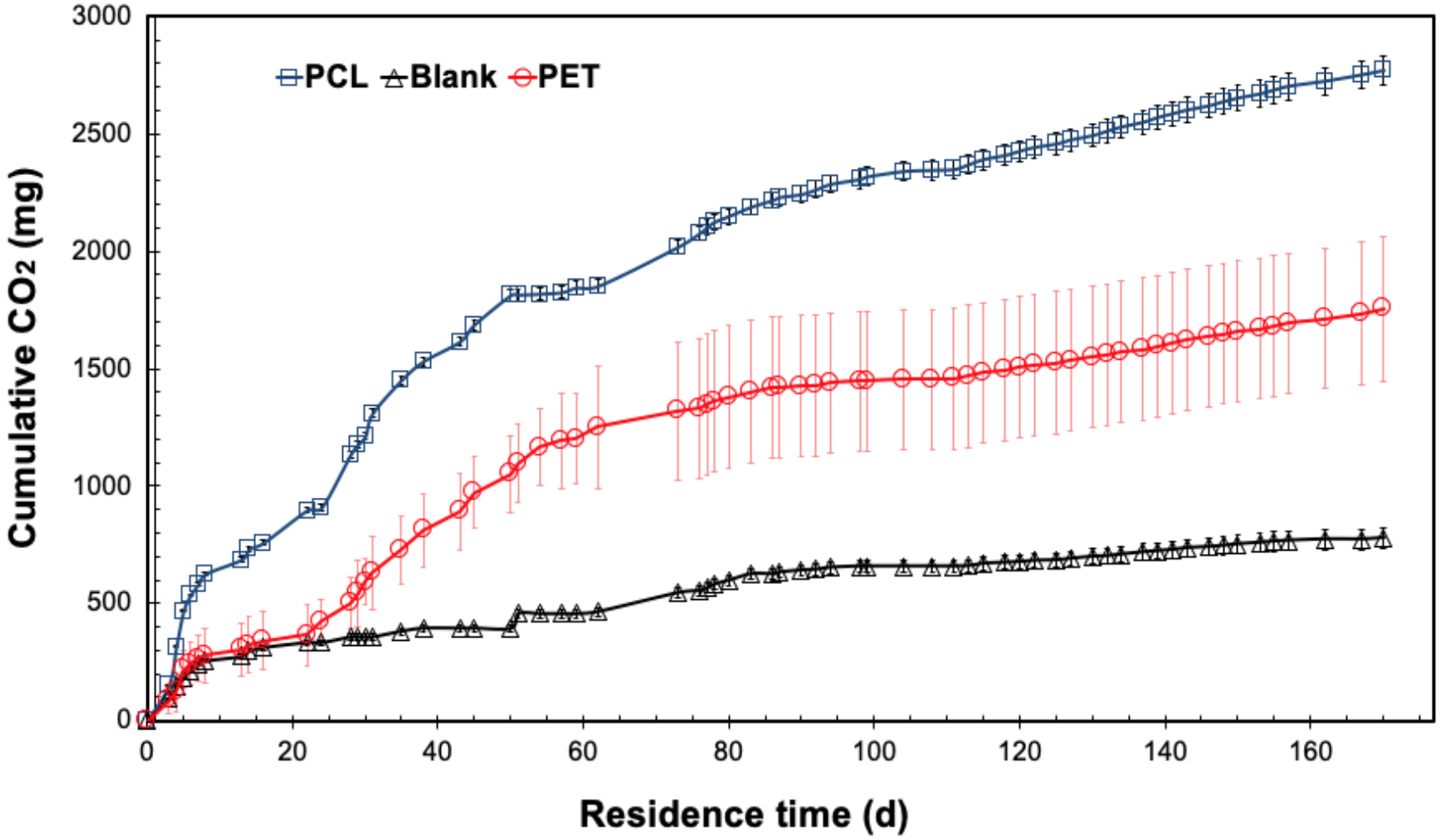

Figure 4.3. Cumulative evolved CO_2 profiles of PET, PCL and blank in the biodegradation test.

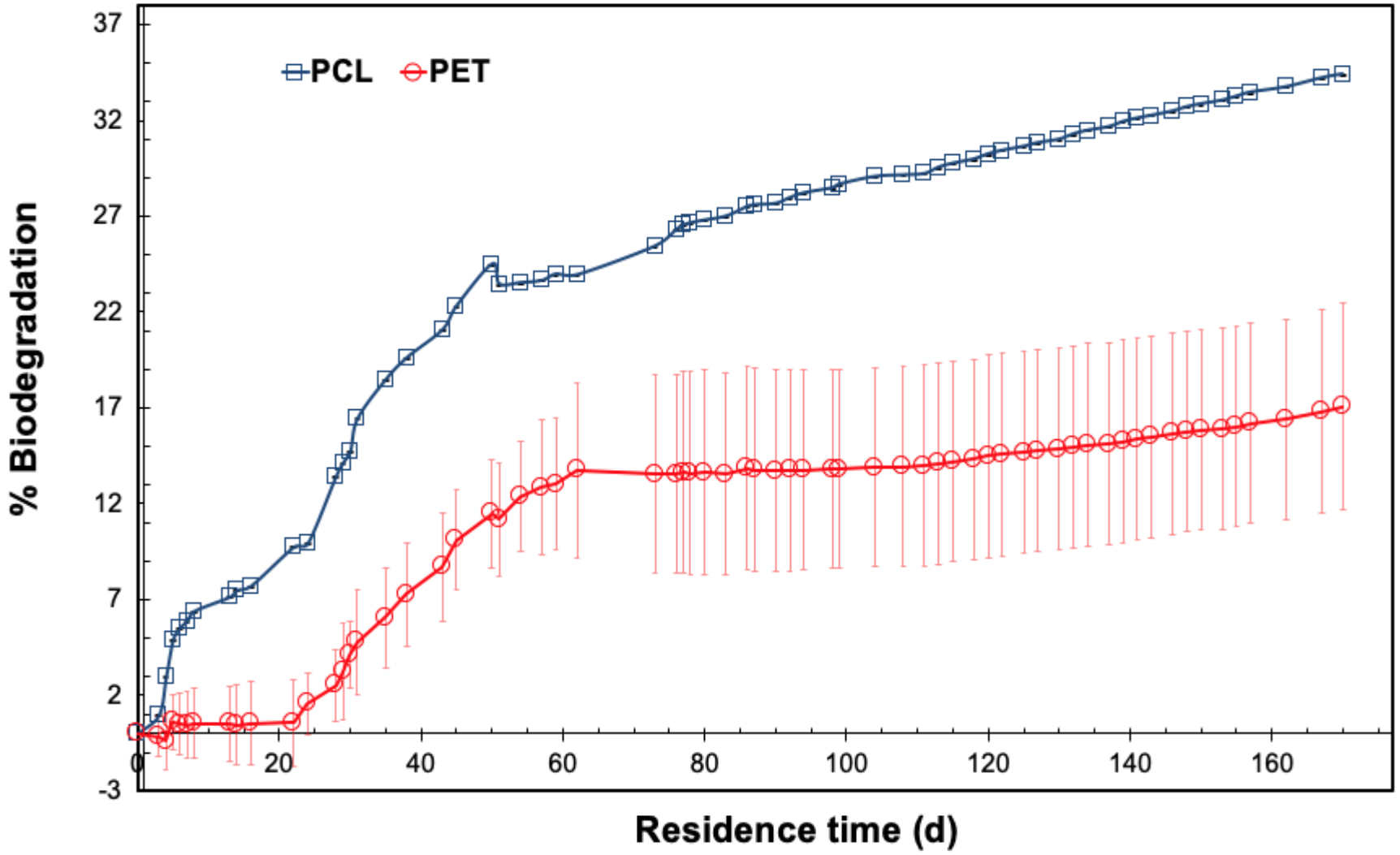

Figure 4.4. Biodegradation rates of PET and PCL microplastics in the biodegradation test

To investigate the influence of oxygen concentration on the biodegradation process, three different oxygen flow rates were supplied to the system during the incubation period in the following order: 47.8 mL/min (stage 1), 10.2 mL/min (stage 2), and 21.0 mL/min (stage 3). The %Dt of microplastics obtained during each stage is depicted in **Figure 4.5**. It was observed that the highest biodegradation for PET was of 11.5% (*SD* = 2.82) and for PCL of 24.5% (*SD* = 0.005), both achieved when the highest oxygen flowrate of 47.8 mL/min was supplied. When the oxygen rate was adjusted to 21.0 mL/min and fresh nutrients were supplied to the reactors every 3 days, the biodegradation achieved for both types of microplastics was of 3.1% (*SD* = 0.18) for PET and 5.3% (*SD* = 0.005) for PCL, much lower than that obtained when pure oxygen was supplied. The lowest polymer degradation, PET 2.5 ± 2.38% and PCL 4.4 ± 0.007%, was obtained at the lowest oxygen flowrate, 10.2 mL/min. These percentages were considerably lower than those attained with the highest oxygen flowrate at 47.8 mL/min. When comparing the biodegradation percentages of PET and PCL between the three different stages, it was observed that the higher the oxygen flow rate, the higher the biodegradation achieved.

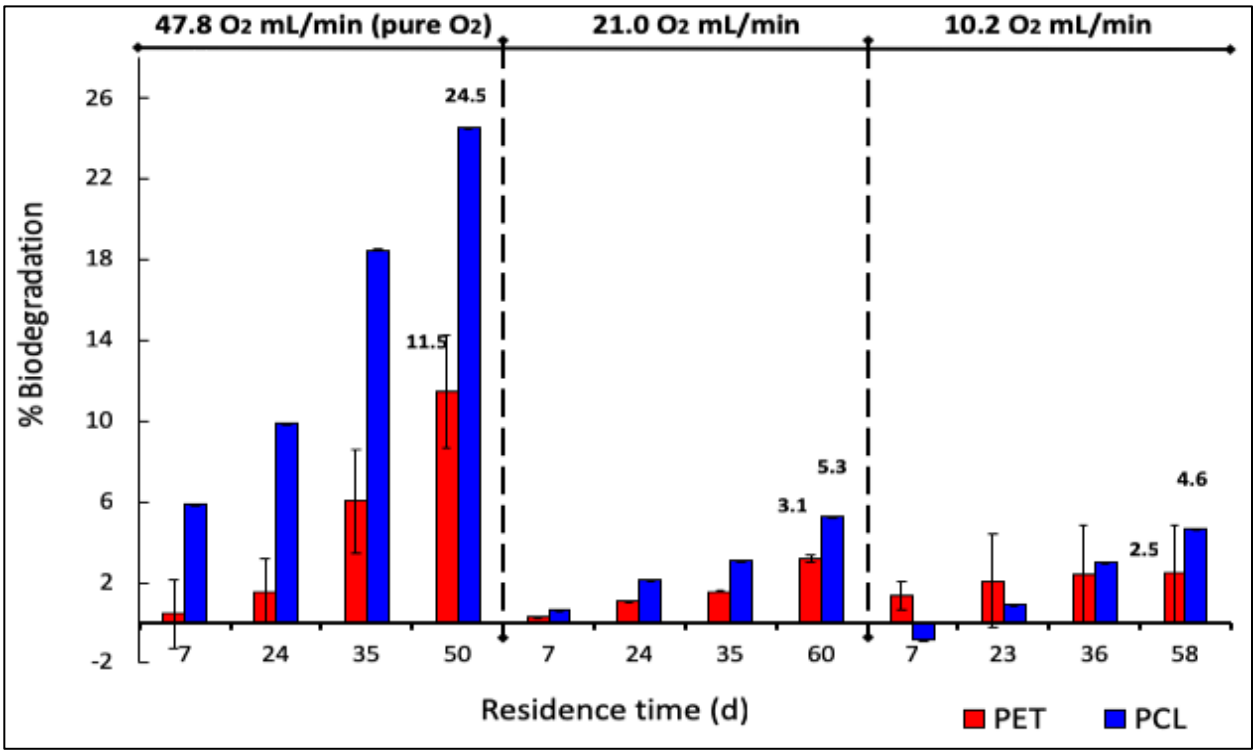

Figure 4.5. Graphical comparison of the biodegradation of microplastics at different oxygen flowrates.

The amounts of cumulative CO_2 yielded on each stage of PET and PCL biodegradation versus time were plotted (**Figure 4.6**) using the blank reactor as a background and then compared. The highest amount of evolved CO_2 from PET degradation (*M* = 1051 mg, *SD* = 161) occurred again in stage 1, with the highest oxygen flowrate. Moreover, the amounts of CO_2 obtained for both stage 2 (*M* = 404 mg, *SD* = 136 mg) and stage 3 (*M* = 300 mg, *SD* = 10) were similar. Although it was expected that stage 3 would yield more CO_2 due to a higher supply of oxygen, there are other factors that may have impacted the process that need to be considered as well. The fact that stage 2 was initiated consecutively to stage 1 – to which only pure oxygen was supplied –might have provided stage 2 with an oxygen-enriched medium to begin with. This can be further probed by inspecting the rate at which the CO_2 was yielded. The CO_2 production rate had a sharp increase during the first 12 days of stage 2 and thereafter, it started to decrease until it almost remained constant. The initial high oxygen availability could have encouraged the accelerated CO_2 production rate, and once it began to deplete, the rate slowed down until nearly unchanged. Stage 3, on the other hand, presented a consistent increasing CO_2 production rate, which might have been motivated by the higher oxygen concentration.

The reason why the biodegradation rates from stage 2 (2.5%) and stage 3 (3.1%) differ from each other, despite of both stages yielding similar amounts of CO_2, is the amount of CO_2 evolved from the blank. Numerically speaking, since this value is used as the background in the calculation of percentage biodegradation Dt (Equation **1**), low amounts of cumulative CO_2 in this reactor during stage 3 resulted in a higher percentage of biodegradation (3.1%), whereas, a higher amount evolved during stage 2 resulted in a lower percentage of biodegradation (2.5%).

A similar behaviour was observed on the cumulative CO_2 evolved from the incubation of PCL (**Figure 4.6**). Stage 1 presented the highest amount of CO_2 production (*M* = 1813 mg, *SD* = 22.86) and biodegradation percentage (24.5%). Different biodegradation percentages were observed in stage 2 (4.6%) and stage 3 (5.3%) although they exhibited similar CO_2 productions of 532±18.03 mg and 425±19.59 mg, respectively.

	Stage 1	Stage 3	Stage 2
O_2 flowrate	47.8 mL/min (**F1**)	21.0 mL/min (**F3**)	10.2 mL/min (**F2**)

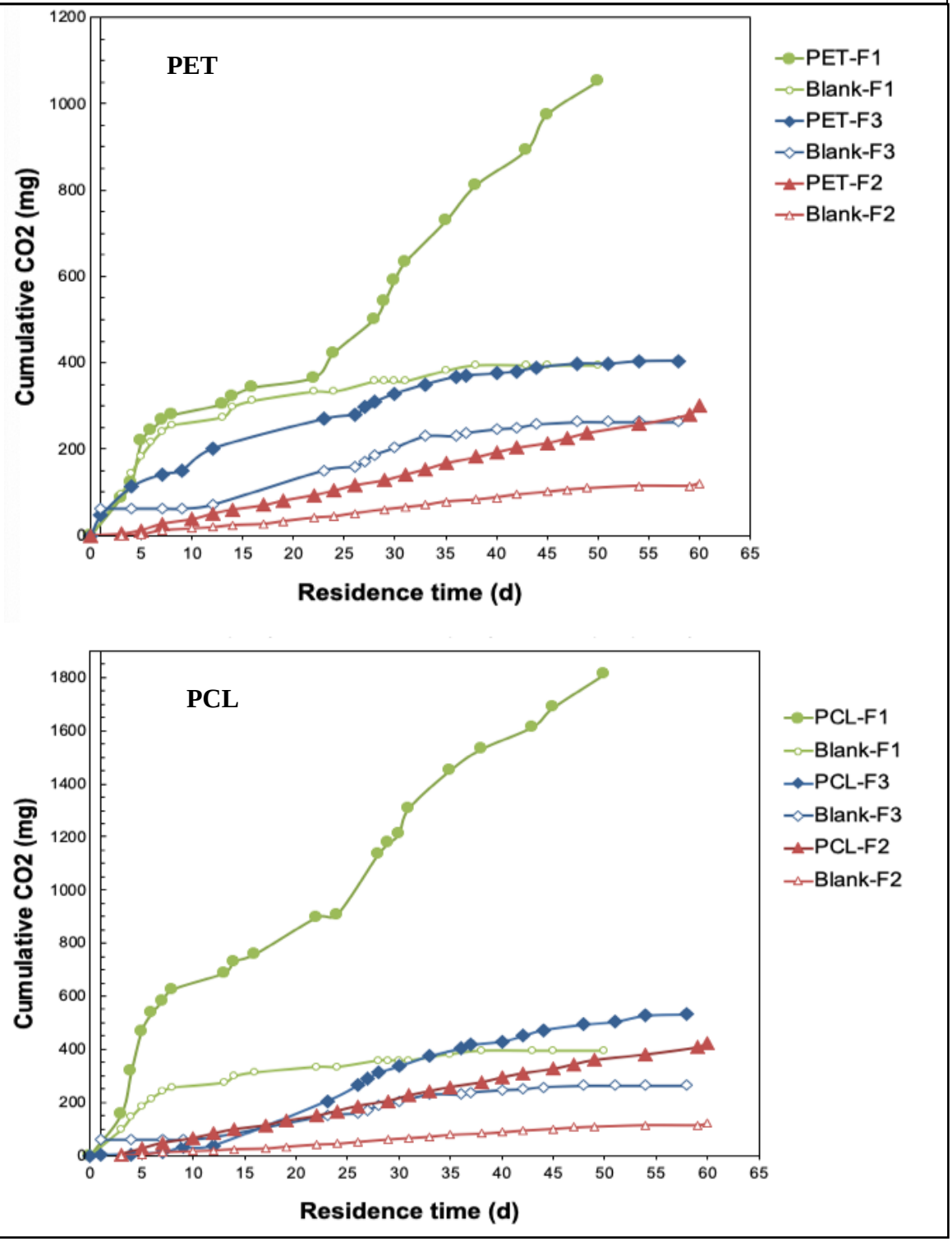

Figure 4.6. Cumulative evolved CO_2 in the biodegradation of PET (top) and PCL (bottom) at varied oxygen flow rates. The CO_2 evolved from the blank is included as the background.

When these results were compared with the calculated kinetic parameters (**Table 4.3**), the same trend was observed. The higher the oxygen availability, the higher the microplastic reduction rate. Also, a shorter half-time to reduce the polymers to their half was required by the consortium when more oxygen was available. According to these results, the order of biodegradability of the microplastics by the microbial community was as follows: for PET, Dt_{Stage1} (11.5%) > Dt_{Stage3} (3.1%) > Dt_{Stage2} (2.5%); for PCL, Dt_{Stage1} (24.5%) > Dt_{Stage3} (5.3%) > Dt_{Stage2} (4.6%) (See **Table 4.3**)

Although the effect of oxygen concentrations on the biodegradation of microplastics was assessed in series configuration, a common trend was clearly observed: higher biodegradation rates were obtained at higher oxygen concentrations. These results are reasonable since in the process of aerobic biodegradation microorganisms use oxygen to oxidize the carbon from the organic materials and produce CO_2, biomass, and water (Shah et al., 2008); when the oxygen availability is too low, oxygen becomes a limiting factor which in turn slows down the biodegradation process (Castro-Aguirre et al., 2017). The results suggest that the biodegradation of microplastics by aerobic microbial degraders could be greatly improved when the supplied oxygen concentration is increased.

The CO_2 evolution test is a standardized and well-stablished method to determine the aerobic biodegradability of polymers that has been successfully used for biological degradation studies for polyesters and other similar polymers (Funabashi, Ninomiya, & Kunioka, 2007; Guo et al., 2012, 2010; Selke et al., 2015). One preceding report (Yoshida et al., 2016) demonstrated the biodegradation of PET films by *Ideonella* species. The authors reported that an initial microbial consortium incubated for about 80 days degraded 75% of a PET film, and once the degrading strain was isolated and identified as *Ideonella sakaiensis*, it was then proved to completely degrade PET films in about 42 days (Yoshida et al., 2016). Likewise, although using the weight method, Asmita et al. (2015) reported degradation of PET small strips by microbial consortia in garbage soil (29.4%) in about 120 days.

Table 4.3. Biodegradation of MPs and kinetic parameters for varied oxygen flow rates

O_2 flowrate (mL/min)	**PET**			**PCL**		
	Dt (%)	MPs reduction constant K (d^{-1})	Half-life $t_{1/2}$ (d)	Dt (%)	MPs reduction constant K (d^{-1})	Half-life $t_{1/2}$ (d)
47.8	11.5 ± 2.82	0.0024 ± 0.0006	283 ± 77	24.5 ± 0.005	0.0056 ± 0.0001	123 ± 0.003
21.0	3.14 ± 0.18	0.00053 ± 0.00003	1303 ± 74	5.27 ± 0.005	0.00090 ± 0.0001	769 ± 0.001
10.2	2.46 ± 2.38	0.00043 ± 0.0004	1607 ± 300	4.64 ± 0.002	0.00082 ± 0.0001	846 ± 0.001

Though studies on the biodegradation of PET microplastics by natural occurring bacteria are very limited, one conducted by Auta et al. (2017) evaluated the degradation of these particles by two bacterial strains isolated from mangrove sediments. The study reported a degradation of 6.6% by *Bacillus cereus* and 3.0% by *Bacillus gottheilii* after 40 days of incubation. When comparing the current study with the latter report, it was observed that similar rates of PET degradation were obtained, specifically in the stages where lower oxygen rates were supplied to the cultures. The bacterial consortium degraded 2.46% of PET MPs in stage 2 (58 days), and 3.14% in stage 3 (60 days). However, a much higher degradation rate of 11.5% was observed when the cultures were incubated for 50 days with the highest oxygen flow rate of 47.8 mL/min. This degradation rate is almost twofold higher than the one by *Bacillus cereus* and fourfold higher than the one by *Bacillus gottheilii* from the referenced study.

The microbial consortium responsible for the biodegradation possess bacteria with PET-degrading capability that can be further investigated and used in bioremediation strategies.

4.3. Analytical results

The biodegradation extent was validated by assessment of morphological and structural changes on the microplastics through FTIR, DSC, intrinsic viscosity, and SEM analyses, as well as the presence of soluble metabolites through HPLC, as described in previous sections. These

analyses were also a measure that provided insights into the biodegradation process. In this section, the results from each analytical technique are presented.

4.3.1. Fourier-transform infrared spectroscopy results

Since FTIR spectroscopy is a powerful method for the structural characterization of polymers, FTIR analysis of the biodegraded PET MPs was performed in the scanning range of 4000 to 450 cm^{-1} to determine surface chemical and structural changes. The spectroscopic characterization of untreated PET MPs (PETo) was performed and then compared to the biodegraded PET (PET_i). The main spectral changes occurred were analyzed.

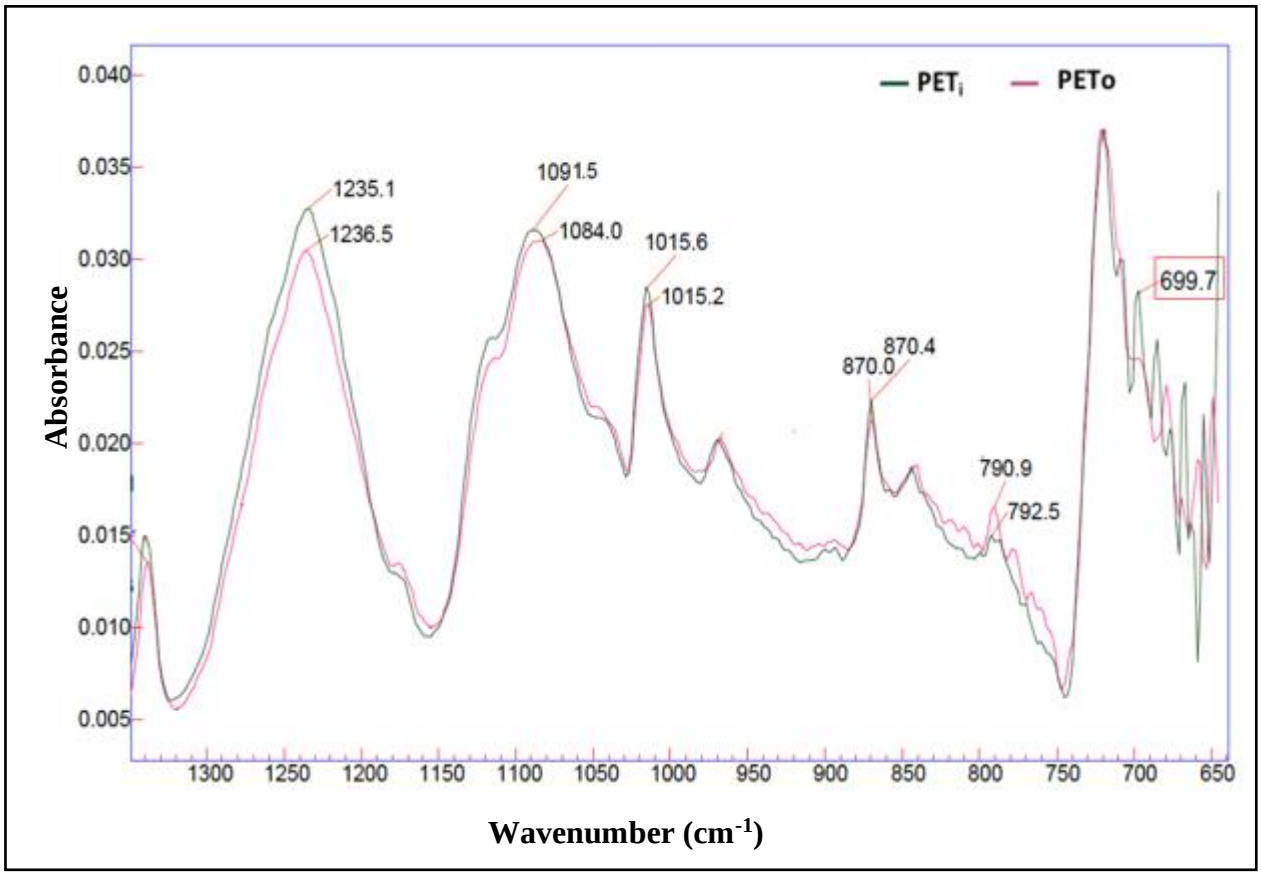

Figure 4.7. FTIR spectra of PET microplastics before (PETo) and after (PET_i) biodegradation by microbial consortium at wavenumber 1300-650 cm^{-1}. New evolved bands (highlighted in red) and elongations/shifts observed upon incubation are denoted.

The biodegradation extent of PET microplastics was further assessed by comparing the carbonyl index (%) and crystallinity index of PETo and PET_i. The FTIR spectra for the microplastics before and after incubation is shown in **Figure 4.7** (wavenumber 1300-650 cm^{-1}) and **Figure 4.8** (wavenumber 2500-1300 cm^{-1}). All the peaks and intensities are tabulated in **Appendix C.5**.

Main peaks of PET spectrum were identified at wavenumbers 1710, 1236, 1084, and 721 cm^{-1} which are carbonyl ketones (C=O), ether aromatic (C-O), ether aliphatic (C-O), and aromatic (C-H), respectively (Fotopoulou & Karapanagioti, 2015). Other characteristic peaks of PET (Gamerith et al., 2017; Holland & Hay, 2002; Nishikida & Coates, 2003; Umamaheswari & Murali, 2013) were also detected at: 1505 cm^{-1} and 841 cm^{-1}, assigned to aromatic C=C bond

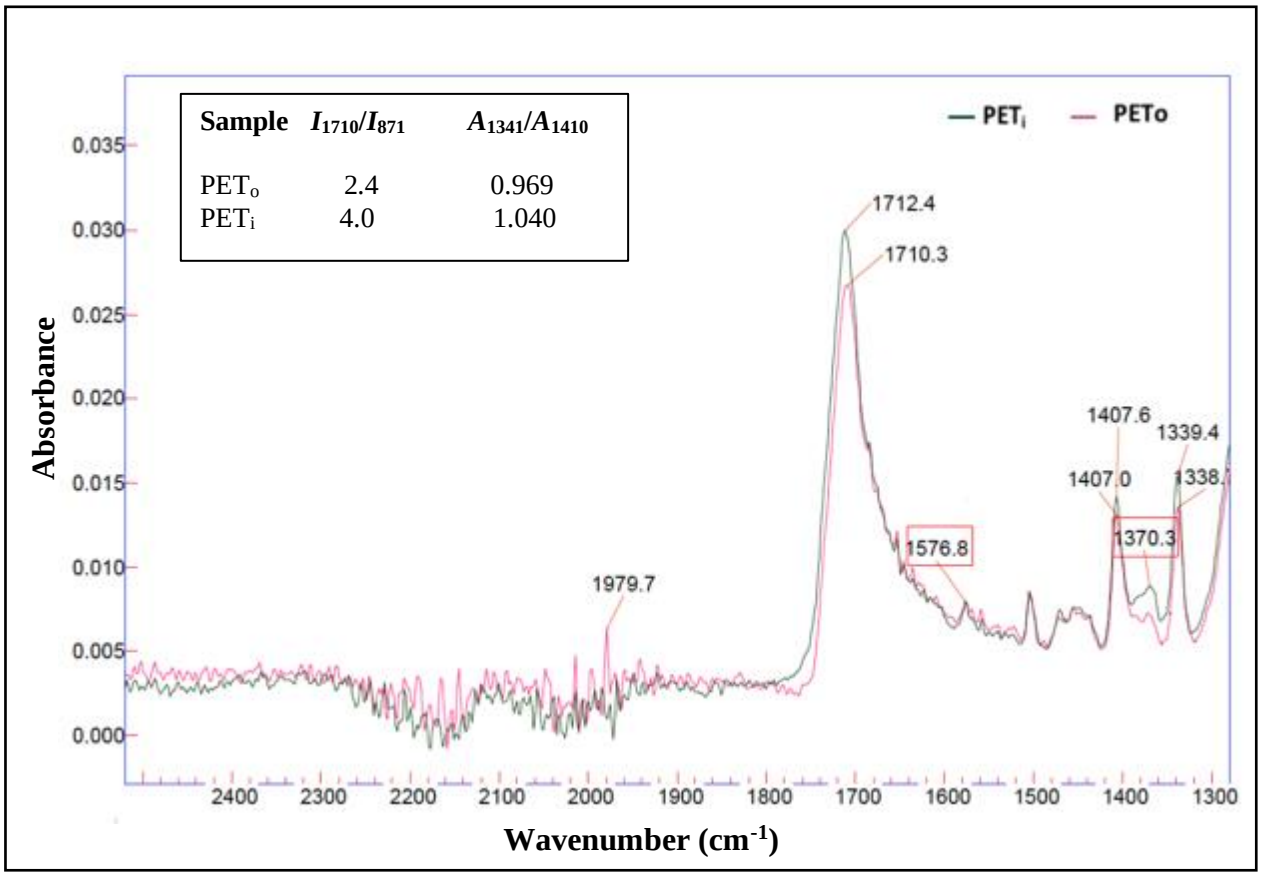

Figure 4.8. FTIR spectra of PET microplastics before (PETo) and after (PET_i) biodegradation by the microbial consortium at wavenumber 2500-1300 cm^{-1}. New evolved bands (highlighted in red) and elongations/shifts observed upon incubation are denoted. Inset: Carbonyl (I_{1710}/I_{871}) and crystallinity index (A_{1341}/A_{1410}) for both PETo and PET_i.

stretching; and 870 cm^{-1} and 969 cm^{-1}, assigned to aromatic C-H bending and O-CH_2 stretching of ethylene glycol segment.

Upon incubation, the PET microplastics underwent surface chemical and structural changes that were detected by FTIR. The bacterial strains induced a shift in several bands (illustrated in **Figure 4.7**): 1084 was shifted to 1091cm^{-1}, 1338 to 1339 cm^{-1}, and 841 to 846 cm^{-1}. They also induced higher intensities at the bands 1712, 1339,1235, 1091, 1015, 870, and 790 cm^{-1}, which confirms the interaction of the consortium with the polymer. The peak at 1979 was absent and new infrared bands evolved at 1577 cm^{-1}, 1370 cm^{-1}, and 699 cm^{-1} that can be associated with oxidation products formed at different frequencies. The addition or disappearance of functional groups have been related to microbial activities and are considered essential in elucidating the mechanism of plastic biodegradation (Auta et al., 2017; Khatoon et al., 2014; Skariyachan et al., 2017). Previous studies have effectively evaluated the biodegradation and microbial interactions towards polymers through FTIR analysis (Fotopoulou & Karapanagioti, 2015; Ioakeimidis et al., 2016; Umamaheswari & Murali, 2013).

The carbonyl index is a way to monitor changes in the carbonyl functional groups that has been used in similar biodegradation studies to quantify the degradation process. For instance, Janczak et al. (2018) reported an increase in the carbonyl index of PET films incubated in soil for 6 months that confirmed the biodegradation occurred. In this study, the carbonyl index was calculated as the ratio of the vibration of the band at 1710 cm^{-1} to that of the 871 cm^{-1} as shown in **Equation 13** (calculations in **Appendix C.2**). The carbonyl index of PET microplastics increased from the initial value of 2.4 to 4.0 after the biodegradation, which further validates the microbial interactions with the polymer. The FTIR analysis also revealed a change from 0.969 to 1.040 in the crystallinity index (A_{1340}/A_{1410}) upon incubation. Previous studies reported that an increase in PET crystallinity after a biological treatment is a consequence of microbial hydrolytic activity towards the amorphous regions of PET that leads to a more ordered state of the polymer chains at the surface, and it is therefore, a confirmation of biodegradation (Donelli et al., 2009; Herrero Acero et al., 2011).

All the surface chemical and structural changes detected by FTIR analysis confirm that PET microplastics underwent biodegradation after incubation with the microbial consortium.

4.3.2. Differential scanning calorimetry results

DSC analysis was performed to evaluate the thermal properties of the PET microplastics before and after the biodegradation process and detect any changes in crystallinity and melting temperature. The raw values obtained are Tabulated in **Appendix C.6**. The melting temperature of PET remained unchanged at 245ºC after incubation (**Table 4.4**). However, the % crystallinity (Equation **15**) of the PET particles increased from 25% (*SD* = 0.90) to 32% (*SD* = 0.62) after incubation with the microbial community. This is in agreement with the results obtained in the FTIR analysis, where the crystallinity calculated as the absorbance ratio A_{1341}/A_{1410}. showed an increase upon incubation. Some researchers have suggested that a polymer crystallinity may increase after a degradation process as a result of chain scission in the amorphous regions of the polymer that release small chain segments that later realign and crystallize (Pirzadeh et al., 2007).

4.3.3. Intrinsic viscosity results

The molecular weight of PET_o and PET_i was evaluated to determine if the polymer was fragmented into smaller molecules during the biodegradation process. The fragmentation can be verified when the molecular weight of the polymer decreases or when low molecular weight molecules are found in the media (Lucas et al., 2008). The viscosity average molecular weight M_v was calculated in terms of intrinsic viscosity by means of the Mark-Houwink equation (Equation **19**) with values of *K* and *a* taken from literature (Hergenrother & Nelson, 1974). The inherent and intrinsic viscosity of the microplastics was determined by viscometric measurements with a standard procedure (ASTM, 2015). The results are shown in **Table 4.4.** and numerical calculations are shown in **Appendix C.2**.

Previous studies have monitored molecular weight changes to determine the extent of biodegradation of polyesters and other polymers (Hakkarainen & Albertsson, 2002; Höglund, Hakkarainen, & Albertsson, 2007; Sheik et al., 2015). For instance, Sheik et al. (2015) measured the biodegradation extent of low-density polyethylene and polypropylene strips by endophytic fungi through the analysis of changes in molecular weight by viscometry. The authors reported a

Table 4.4. Results of thermal and viscometry analyses of PET MPs before and after biodegradation

Sample	Melting temperature, T_m (ºC)	Crystallinity (%)	Viscosity (dL/g)	Molecular weight
PET_o	245 ± 0.014	25.1 ± 0.90	0.6477± 0.024	27,512 ± 1417
PET_i	245 ± 0.12	32.4 ± 0.62	0.6427± 0.058	27,255 ± 3306

decrease in intrinsic viscosity and average molecular weight of strips which indicated fungal activity in plastic degradation (Sheik et al., 2015).

In this study, the calculated molecular weight of PET microplastics was observed to decrease slightly upon incubation from 27,512 (*SD* = 1417) to 27,255 (*SD* = 3306). Since the molecular weight change was not very significant, it is suggested that the degradation proceeded mostly at the microplastics surface level, as it has been stated in similar studies (Yoshida et al., 2016).

4.3.4. Scanning electron microscopy results

In the current study, surface modifications of PET microplastics after incubation were examined by means of SEM and EDS analyses; SEM is a well-stablished technique to examine topography of the material surface, biofilm development, morphology of bacterial adhesion, and the interactions between them (Khatoon et al., 2014). The results of SEM analysis on the test samples exhibited the development of pits, erosion and cavities as well as adhesion of bacterial colonies (**Figure 4.9**.). The clear formation of bacterial biofilm and the presence of salts on the surface of the microplastics indicate that these microorganisms were somehow involved in the biodegradation (**Figure 4.10**.). When comparing the SEM micrograph of PET at 0 days (**1**) with those at 168 days of incubation (**2**, **3** & **4**) in **Figure 4.9**, it was observed that the microplastics initially bared smooth surface, with no presence of erosion, pits or bacterial adhesion. After 168 days, the microplastics showed alterations and bacterial interactions, which suggests that the bacterial community played a crucial role in the biodegradation of PET.

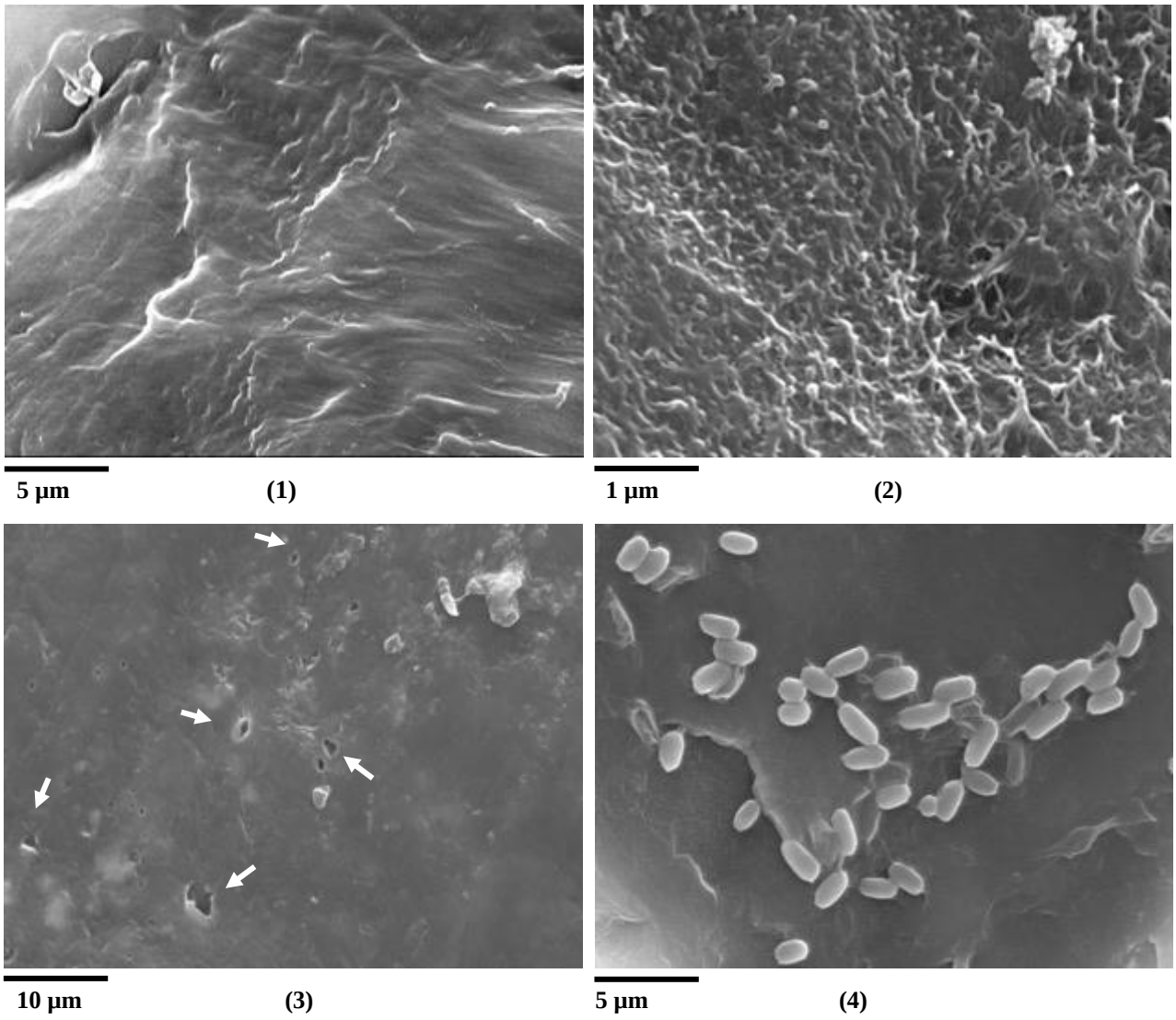

Figure 4.9. SEM analysis of surface erosion and bacterial adhesion PET microplastics. Micrograph **1** shows the smooth surface of PET without biological treatment. Micrographs **2**, **3** and **4** show the surface of degraded PET MPs presenting roughness, pits, and bacterial attachment.

Preceding reports have indicated that the presence of random cracks and pits on the surface of polyesters and other polymers may be attributed to biological degradation (Gewert et al., 2015; Jayasekara et al., 2005). Also, previous studies demonstrated the applicability of SEM to determine the extent of biodegradation of plastics by microorganisms (Fotopoulou & Karapanagioti, 2015; Ioakeimidis et al., 2016; Paço et al., 2017; Skariyachan et al., 2017).

In the micrographs **5, 6 & 7** taken at 168 days (shown in **Figure 4.10**) it was further detected that an assemblage of bacterial cells enclosed in a matrix, namely biofilm (Donlan, 2002), was also developed on the substrate. The formation of a biofilm is particularly important in the microbial degradation of polymeric materials since it is considered to be a prerequisite for their substantial deterioration and degradation (Dussud & Ghiglione, 2015; Mohan & srivastava, 2011). Numerous studies have investigated the correlation between the biofilm formation and degradation of plastics and proved that it promotes the biodegradation process (Tribedi, Gupta, & Sil, 2015; Webb et al., 2009). Aside from the biofilm formed on the PET microplastics during incubation, salts were also observed on their surface in micrograph **7**, which were further verified by elemental analysis. The EDS spectra taken after 168 days of incubation (**Figure 4.11**) showed concentrations of sodium (Na), chlorine (Cl) and calcium (Ca).

All the aforementioned results provide further evidence of the biodegradation extent of PET microplastics. Previous studies have utilized SEM to demonstrate biofilm formation and bacterial interactions taking part in the biodegradation of plastics. For example, Yoshida et al. (2016) reported SEM images of bacterial cells grown on PET film and the cell appendages to the plastic surface. Likewise, Khatoon et al. (2013) reported SEM images of biofilm development from activated sludge on polypropylene with degradative effects on the plastic.

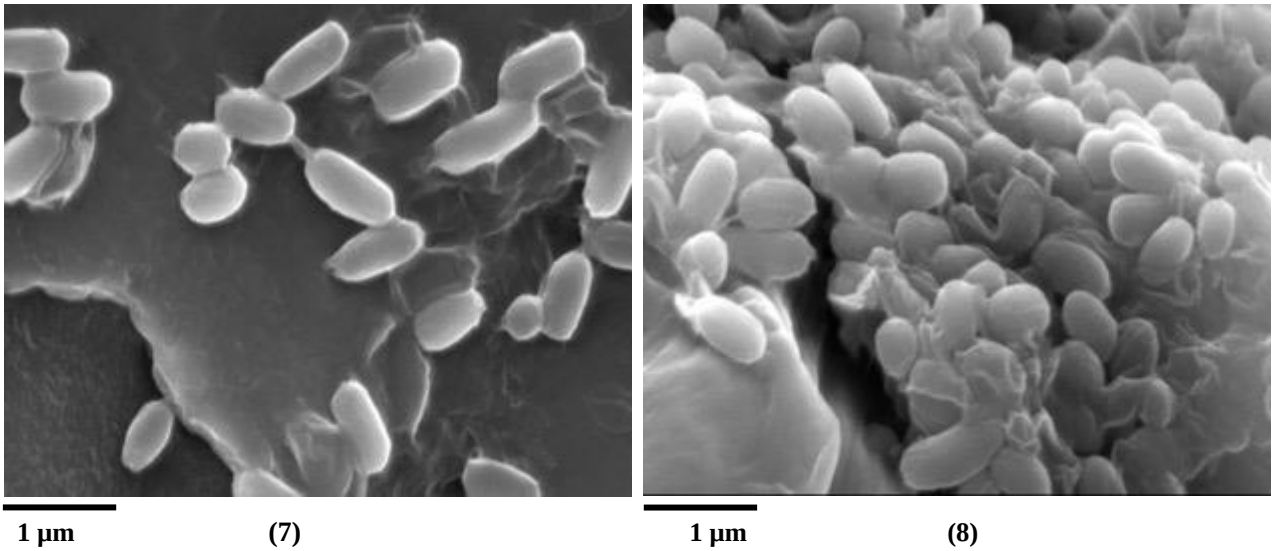

Figure 4.10. SEM analysis of biofilm formation and bacterial adhesion on PET microplastics. Micrographs **7**, **8** and **9** of PET after 168 days of incubation with the microbial consortium showing bacterial adhesion (**7**), bacterial biofilm (**8**), and salts (**9**).

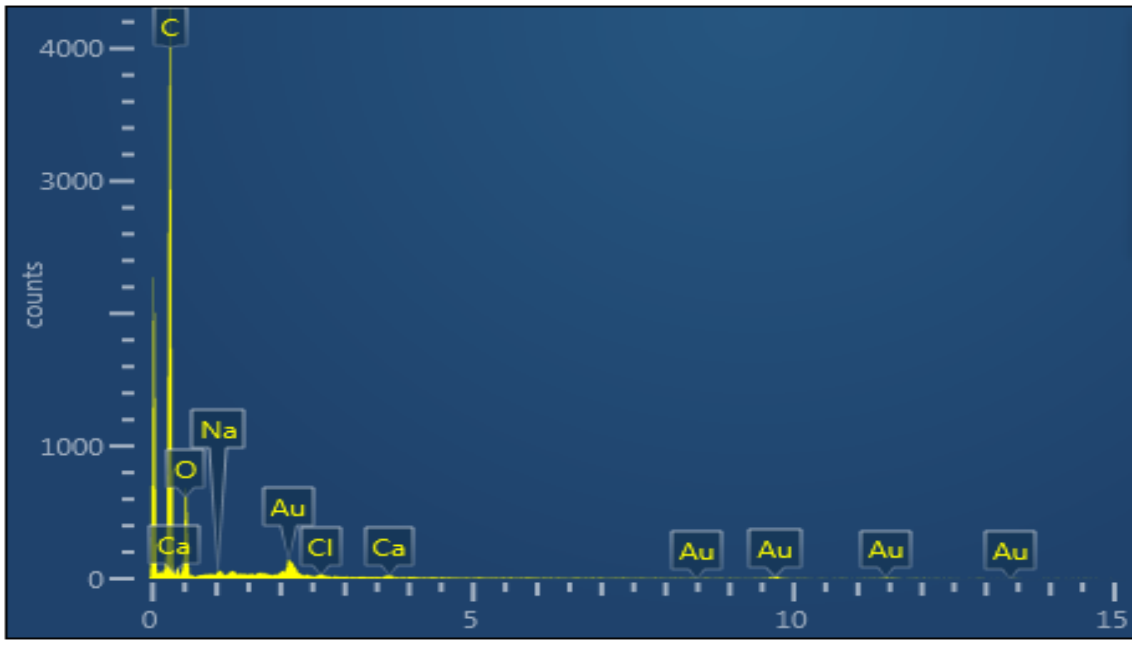

Figure 4.11. EDS spectra of PET microplastics after 168 days of incubation evidencing the presence of salts.

4.3.5. Reversed-phase high performance liquid chromatography results

HPLC analysis was performed to investigate the presence of BHET and TPA as potential PET degradation products released during incubation. The samples were taken at different times over incubation and their chromatograms were acquired at 230 nm. The typical retention time for the standard BHET was 18.3 min (*SD* = 0.018) and for TPA was 14.5 min (*SD* = 0.068).

All chromatograms of the (108, 120, 128, 148, 157 and 168 days) showed the same peaks, which were identical to the ones obtained for pure growth medium (values shown in **Appendix C.8**). These peaks were observed at 2.95 min (*SD* = 0.064), 3.15 min (*SD* = 0.031), 3.31 min (*SD* = 0.012), and 3.48 min (*SD* = 0.037). No peaks were detected at 18.3 or 14.5 min, which indicated the absence of the PET degradation products throughout the incubation period. However, this does not rule out the possibility that other degradation products not evaluated in this study, such as mono(ethylene terephthalate) (MHET), may have been released during the biodegradation process. Other authors reported the release of MHET during the degradation of PET film by bacterial species in significant higher concentrations than that of BHET and TPA (Yoshida et al., 2016).

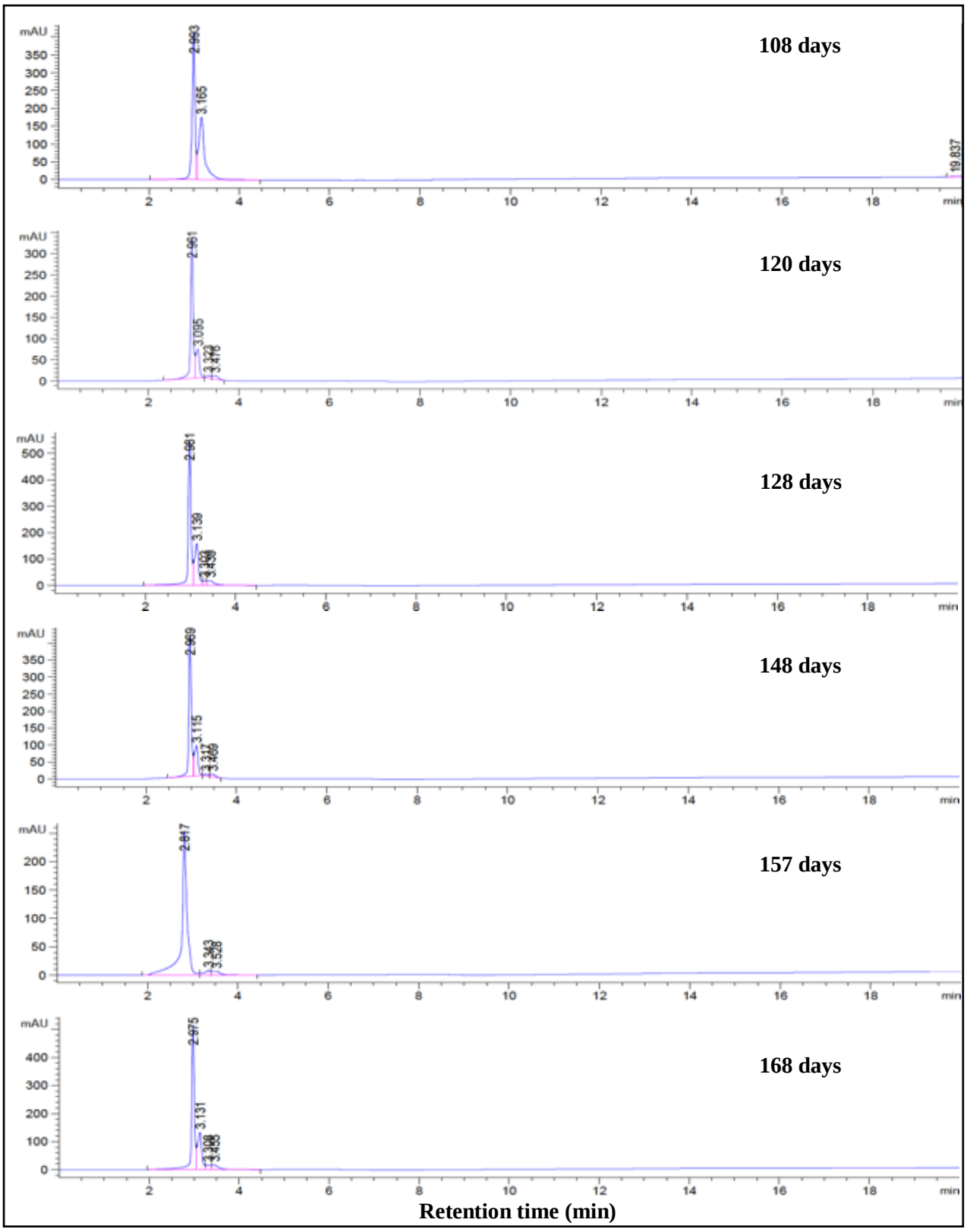

Figure 4.12. HPLC spectrum of test medium at intervals of the incubation of PET microplastics.

4.4. Microbial analysis

To identify the microorganisms that were involved in the biodegradation of PET, bacterial cells were recovered from the biodegraded PET MPs and further analyzed. Four bacterial strains labelled as BS3, BS6, BS10 and BS11 were isolated and characterized according to their phenotype based on colony morphologies; their characteristics are presented in **Table 4.5**.

The biodegradability potential of the bacterial isolates was further assessed in growth medium and PET MPs. Growth curves of each isolate and the community were constructed with the values of colony-forming units (CFU) and optical density (OD) measured at different times over incubation (**Figure 4.13**). Upon incubation, it was noted that the cultures BS6 and BS10 were contaminated with BS3, which means that the growth curves obtained correspond to these two combinations of isolates (BS3 + BS6) and (BS3 + BS10). As a result, it was not possible to evaluate the individual growth of the isolates BS6 and BS10 in the presence of PET MPs.

The culture BS3 presented an exponential growth in the first days, evidenced by a high turbidity and cell count. This suggests that the isolate can use PET MPs to grow. After 5 days, these values decreased and remained constant, which indicates that there was no more growth and the cells entered the stationary phase. It would be necessary to take more time points in the exponential growth phase to better understand the growth behaviour of this culture. At the end of

Table 4.5. Phenotypic characteristics of probable PET-degrading organisms isolated from activated sludge

Colony No.	**BS3**	**BS6**	**BS10**	**BS11**
Colour	White	Creamy-white	Creamy-white	deep-yellow
Edge	Filamentous	Entire	Entire	Entire
Elevation	Raised	Convex	Convex	Convex
Surface	Dry, powdery	Glistening	Glistening	Glistening
Shape	Circular	Circular	Circular	Circular
Size (diameter)	3 mm	3 mm	3 mm	0.5 mm
Gram nature	Positive	Positive	Positive	Positive

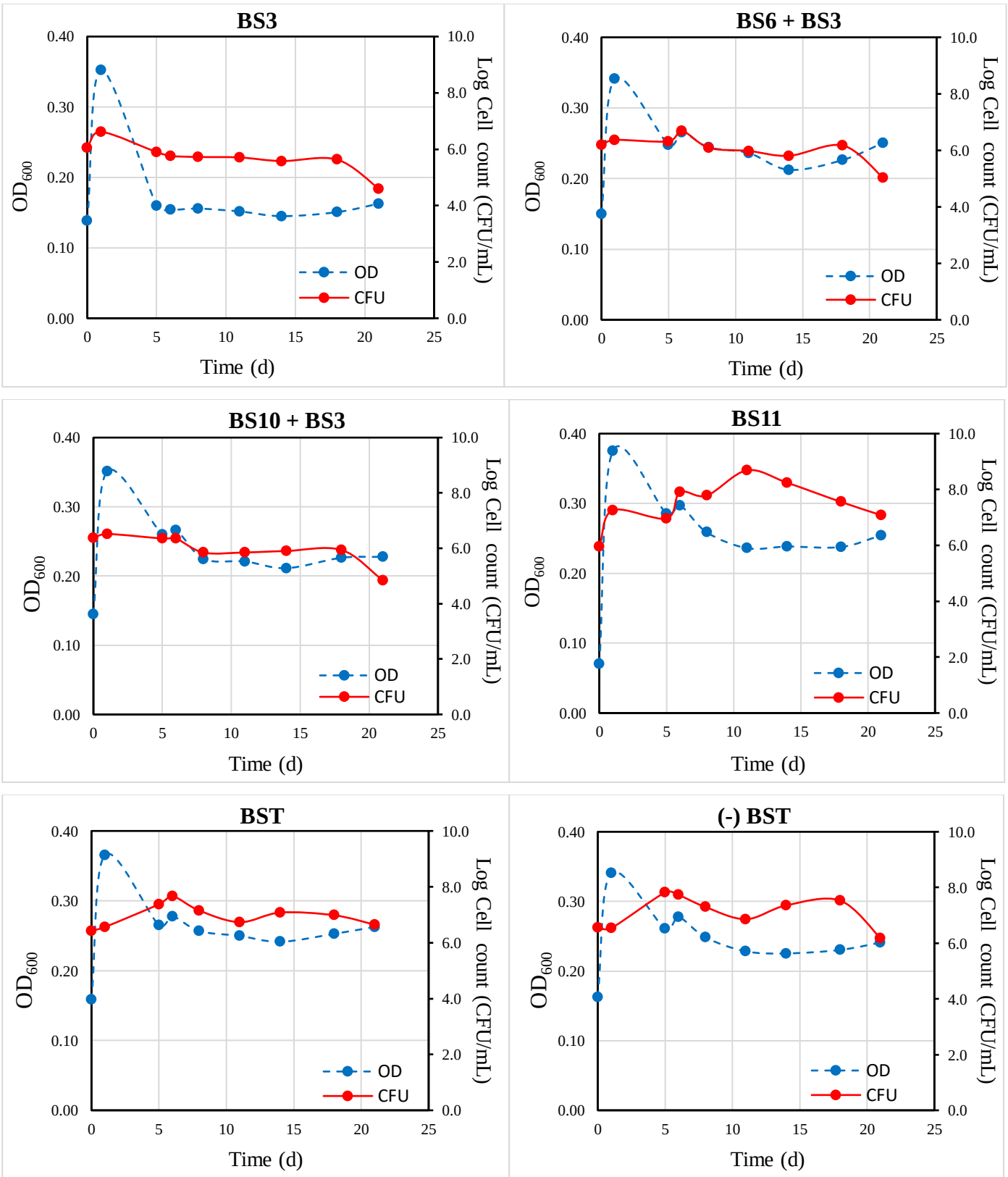

Figure 4.13. Growth curves of isolates (BS3, BS6, BS10, BS11), community BST and negative control (-) BST after 21 days of incubation with PET MPs. Optical density versus time.

the incubation period, the cells entered the death phase, which can be seen in the decrease of viable cells and increase of turbidity due to death of these cells.

The consortium BS6 + BS3 showed an initial spike in turbidity (OD) that was accompanied by a very slight increase in the cell count. After 5 days, the cell count remained almost unchanged, which suggests that the consortium did not grow significantly with PET MPs. Similarly, the consortium BS10 + BS3 initially showed a very slight increase in cell count; after 5 days the cell count remained unchanged until eventually started to decrease. This suggests that this consortium did not grow significantly in the presence of PET MPs.

On the other hand, the isolate BS11 showed viable cells that consistently grew until day 11 of incubation, from which point they started to decrease. This isolate also showed the highest increase in cell density the first few days of incubation. After 11 days, the cell density started to decline. These results suggest that the isolate BS11 can use PET MPs to grow, although more measurements would be necessary to better understand the growth behaviour in the exponential phase.

The community BST showed growth of viable cells and increase of OD until day 6. Thereafter, the cells did not change significantly and eventually started to die. A similar behaviour was observed for the negative control, which makes difficult to affirm that the growth seen in the community BST was due to the use of PET as a carbon source. It is unclear if the growth observed in the negative control was due to endogenous metabolism or to other factors.

To better understand the growth phase of the candidates BS3 and BS11 observed in the previous analysis, the two isolates were incubated under the same conditions for a shorter period of time of 161 hours. The consortium BS3 + BS1 and the two negative controls were also incubated and assessed as previously described. The OD and CFU measurements were done every few hours and the final growth curves obtained are presented in **Figure 4.14**. From the growth curves of the isolates BS3 and BS11, it can be observed that the exponential phase is better defined and evident. Both cultures showed growth in the presence of PET MPs. In the case of the consortium BS3 + BS11, it was not possible to conclude that the growth observed was due to the presence of PET as a substrate because the negative control showed a similar growth.

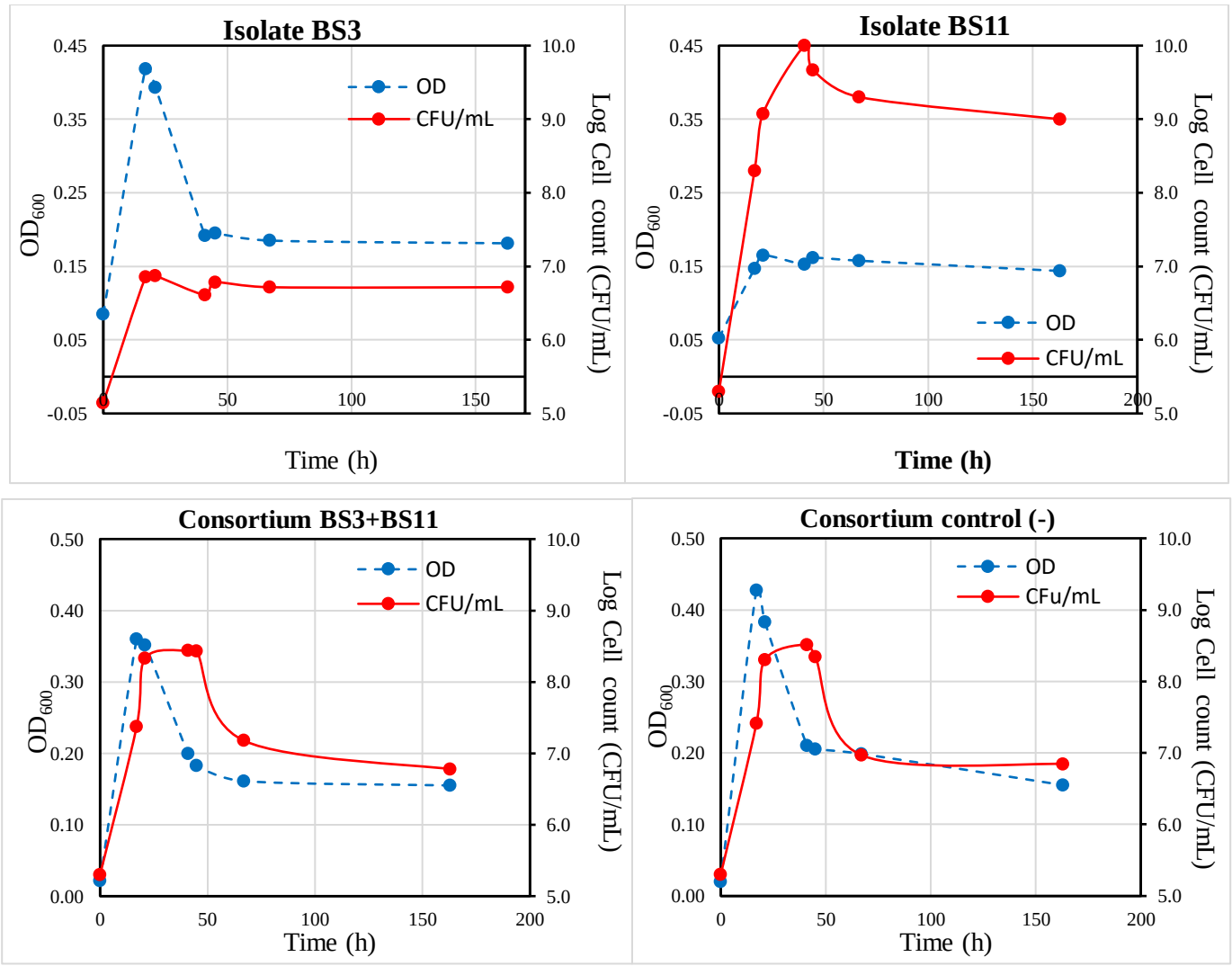

Figure 4.14. Growth curves of cultures BS3, BS11, consortium BS3+BS11 and negative control after 161 hours of incubation with PET MPs.

The clear-zone test was used to investigate enzymatic activity of the isolates upon exposure to PET. When a clear zone is formed around a colony, it is an indication that the substrate is being solubilized as a result of the degradation caused by secreted enzymes (Cerdà-Cuéllar et al., 2004). The mineral media and PET plates, prepared as described in section 3.6.3, were individually inoculated with the cultures BS3, BS6, BS10 and BS11 and incubated at 25º for 20 days. The culture BS3 was the only one that formed clear zones (**Figure 4.15**). This result indicated that the isolate BS3 can degrade the PET particles, however, this result could not be confirmed due to the absence of a negative control.

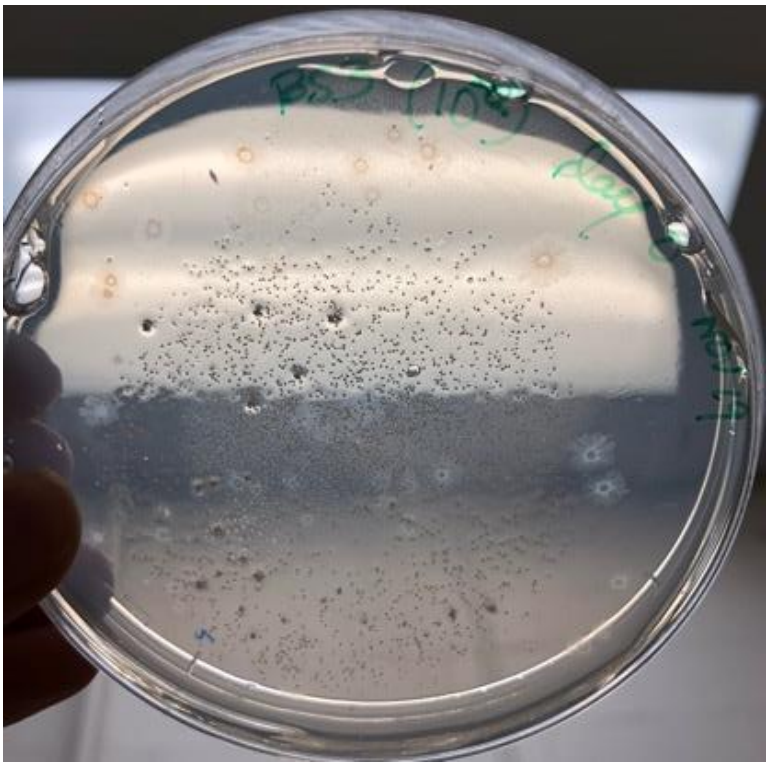

Figure 4.15. BS3 colonies and clear zones on a mineral media plate containing PET MPs. Culture at 25ºC for 20 days.

Molecular techniques were performed to identify the pure cultures BS3, BS6, BS10 and BS11. The DNA of all pure cultures was individually extracted and then amplified in the 16S rRNA region using the polymerase chain reaction process (PCR). The PCR was performed in Dr. Gilbride's laboratory with the aid of her graduate students. The PCR products were sequenced by ACGT Corporation and the resulting DNA sequences were analyzed using the Basic Local Assignment Search Tool (BLAST). The cultures were identified, all at 99% confidence, as:

- **BS3**: *Bacillus cereus* strain SEHD031MH (GenBank accession number MF927571.1)
- **BS6** and **BS10**: *Lysinibacillus macroides* strain RW13-2 (GenBank accession number KY569486.1)
- **BS11**: *Agromyces mediolanus* strain PNP3 (GenBank accession number MH169214.1)

Bacillus cereus and *Agromyces mediolanus* were the organisms that showed growth/interactions in the presence of PET MPs. The taxonomic hierarchy of the identified bacterial species from the microbial community with PET degrading activity is shown in **Figure 4.16**.

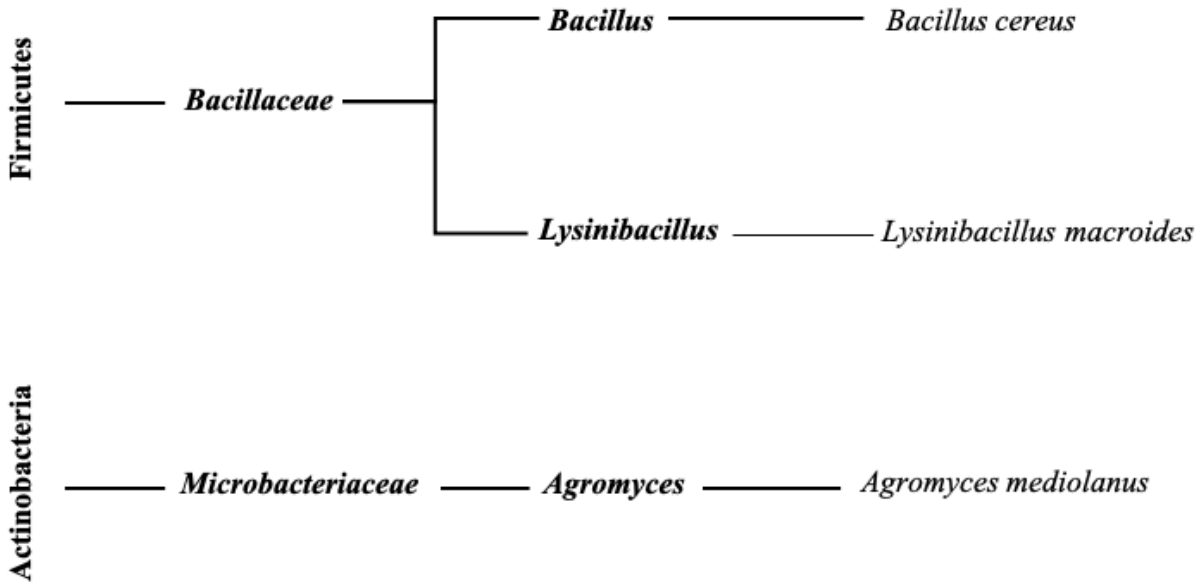

Figure 4.16. Taxonomic hierarchy of the identified bacterial species from the microbial community with PET degrading activity

Agromyces mediolanus is a gram-positive bacterium of the genus *Agromyces* that has not been yet related to the degradation of PET. Some strains of Agromyces *mediolanus*, however, are capable of assimilating aniline and oxidizing steroids (Evtushenko & Takeuchi, 2006). Other species from the genera *Agromyces* have been reported with the capacity to utilize certain hydrocarbons and plasticizers (Kawai, 2010; H. Zhao et al., 2016). These microorganisms seem to rapidly evolve by mutagenesis of existing genes that make possible adaptation to synthetic polymers introduced into the environment (Kawai, 2010).

Bacillus cereus is a gram-positive, rod-shaped, aerobic bacterium from the genus *Bacillus* that have been reported to degrade several polymers, including polyethylene and PET (Sowmya, H.V., Thippeswamy, 2014). One study performed by Auta et al. (2017) reported the degradation of UV-treated PET microplastics by *Bacillus cereus* isolated from sediment. After 40 days of incubation, the weight loss percentage achieved was 6.6%. The bacterial community used in the current investigation included a species from *Bacillus cereus* and showed rates of PET degradation that are comparable to the ones reported by Auta et al. This is especially true in the

stages where lower oxygen rates were supplied to the cultures; the bacterial consortium degraded 4.4% of PET MPs after 58 days in stage 2, and 5% after 60 days in stage 3. However, a higher degradation rate of 11% was observed when the consortium was incubated with the highest oxygen flow rate of 47.8 mL/min for 50 days, which suggests that its rate of PET biodegradation might be improved by increasing oxygen concentration.

The species *Lysinibacillus macroides* has not been related to the degradation of plastics, however, the strain MEW88 was reported to efficiently degrade organophosphorus pesticides (CN106566789A, 2016). Although the bacterial species *L. macroides* sp. RW13-2 was not individually assessed for its PET degrading capability, one may not overlook the possibility that it may have played a role during the biodegradation process. It is worth noting that the initial microbial community present in the activated sludge was subjected to a selective-enrichment procedure for the isolation of PET-dependent bacteria, after which it was used to inoculate the bioreactors in the biodegradation test. This means that the three bacterial species *Bacillus cereus*, *Agromyces mediolanus* and *Lysinibacillus macroides*, isolated from the resulting culture at the end of the biodegradation test, were able to thrive throughout the entire culture time having PET microplastics as the sole carbon and energy source. This result highlights the great potential that these bacteria, specially *B. cereus* SEHD031MH, have for the degradation of PET MPs.

5. CONCLUSIONS

This investigation was carried out between January 2016 and August 2018 at the Membrane Bioreactors Laboratory (KHN-111) of the Department of Chemical Engineering. From this work, the following conclusions were reached:

- An experimental unit was designed, installed, commissioned, and operated in compliance with standard ISO 14852. It consists of a series of batch bioreactors that are aerated in a closed system and its configuration allows to investigate the biodegradability of polymeric materials as well as other biological processes and cell cultures
- Bacterial communities found in activated sludge from the North Toronto WWTP were able to grow in mineral medium in the presence of poly(ethylene terephthalate) (PET) microplastics, evidenced by a growth in biomass concentrations
- PET microplastics were biologically degraded by a bacterial community (M = 17%; SD = 5.38) after 168 days of incubation
- PCL microplastics, taken as reference in the biodegradation test, were biodegraded 34% (SD = 0.012) by a bacterial community after 168 days of incubation
- Three bacterial strains among the degrading community were identified as *Bacillus cereus* SEHD031MH, *Agromyces mediolanus* PNP3 and *Lysinibacillus macroides* RW13-2
- PET microplastics underwent biological degradation that was validated by Fourier transform infrared spectroscopy, Differential scanning calorimetry and Scanning electron microscopy analyses
- Upon incubation, PET underwent surface chemical and structural changes, evidenced by an increase in crystallinity and the formation of new functional groups at the surface.
- PET microplastics also exhibited development of pits, cavities and roughness as well as adhesion of bacterial colonies after 168 days of incubation

- The effect of oxygen concentration was assessed throughout the biodegradation experiment and it was found that the highest biodegradation rate for both PET (11.5%) and PCL (24.5%) MPs was achieved when the highest oxygen rate 47.8 mL/min was supplied
- These results indicated that the biodegradation of microplastics by this bacterial community and potentially the bacterial strains *B. cereus* SEHD031MH, *A. mediolanus* PNP3 and *L. macroides* RW13-2 could be improved when the oxygen concentration supplied is increased, and
- *B. cereus* SEHD031MH showed a promising potential for degrading PET MPs as it grew in the presence of PET and formed clear zones as an indication of enzymatic activity

This study highlights the great potential of bacterial communities from activated sludge for the biodegradation of PET microplastics, thus responding to the existing and urgent need of bioremediation methods to reduce the presence of these pollutants in aquatic environments and wastewaters. The observed morphological and structural modifications on the biodegraded microplastics confirmed the presence of PET degraders within bacterial communities in activated sludge. Further, the strains *B. cereus* SEHD031MH and *A. mediolanus* PNP3, isolated from the community, have the potential to degrade PET microplastics.

The investigated bacterial strains have a promising PET-degrading activity that can be further investigated and applied in the development of effective biological treatments to eliminate MPs in water/wastewater. The application of these organisms to the elimination of microplastics in water, includes the design of innovative, effective, and large capacity reactors capable of efficiently treating effluents from industrial and domestic sources.

6. RECOMMENDATIONS FOR FUTURE RESEARCH

The design of the experimental unit in compliance with ISO 14852 provides many future research opportunities. The unit was carefully designed and built to allow determining the amount of carbon dioxide evolved in an aerobic biodegradation process. Its configuration offers the opportunity to study the aerobic biodegradation of any polymeric material in the form of pellet, film, or microparticles, as well as other biological processes and cell cultures. Further, studies of anaerobic biological processes and cultures can be done with this unit if all the inlets and outlets of the bioreactors are shutdown. The endless biological processes that can develop in this experimental unit are a source of further research, enhancement, process modeling and simulation.

Based on the operational experience and experimental results, I make the following recommendations for future research:

- One of the problems encountered during the operation of the unit was being subjected to sudden drops in pressure in the supply of compressed air caused by overloads in the main source of air. To overcome this issue and guarantee a continuous air supply to the cultures, a low-cost air pump and regulator can be installed in the unit.
- In addition, fine bubbling diffusers can be installed inside the bioreactors to provide substantial and efficient mass transfer of oxygen to the cultures. This will allow increasing the oxygen transfer efficiency to provide higher oxygen concentrations to the microbial culture.
- The effect of dissolved oxygen rates can be assessed to find the optimal values in which the bacterial consortium biodegrades PET. Dissolved oxygen meter and sensor can be installed in each bioreactor to be able to measure and monitor this variable.
- The effect of pure oxygen and air flow rates can be studied in order to enhance the biodegradation of microplastics. The bacterial strains can be assessed, as isolates and consortium, for their ability to degrade PET MPs utilizing different flow rates of pure oxygen and air.

- Other kinetic models such as Power Law Model, Michaelis-Menten inhibition model and Michaelis-Menten activation model can be tested to better predict the experimental data in the biodegradation of MPs
- The effect of temperature and pH can also be investigated in both bacterial consortium and isolates and the optimal values for a more efficient degradation can be found. To this end, a pH meter can easily be installed in each bioreactor.
- The composition of the entire bacterial community can be DNA sequenced and further investigated to find other PET degraders.
- Different combinations of bacterial isolates can be formulated and assessed to determine which shows the most efficient degradation.
- Enzyme assays can be performed to investigate the enzymes released by *Bacillus cereus*, *Agromyces mediolanus* and *Lysinibacillus macroides* that have PET hydrolytic activity. The catalytic activity of these enzymes can be later compared to other polyester hydrolases and cutinases such as *Thermobifida fusca* hydrolase TfH, leaf and branch compost cutinase LCC, and *F. solani* cutinase FsC.
- The investigation of the generation of by-products such as mono(2-hydroxyethyl) terephthalate acid (MHET) throughout the biodegradation of PET by this particular bacterial community and strains (*B. Cereus* SEHD031MH, *A. mediolanus* PNP3 and *L. macroides* RW13-2) can be performed to help determine the metabolic mechanisms in which these microbes degrade the polymer.
- As the results obtained in the scanning electron microscopy analysis demonstrated, bacterial biofilm was formed onto the surface of PET MPs. The role that bacterial biofilm plays in the biodegradation process can be further investigated; mathematical modeling of the biofilm on the surface of PET MPs can be performed and used to estimate, predict and control the degree and efficiency of the biodegradation process.
- Finally, an innovative, effective and large capacity reactor can be designed with these degrading microorganisms to efficiently treat and remove microplastics from industrial and domestic sources.

APPENDICES

APPENDIX A: Composition of prepared solutions

- ✓ **Phosphate buffer solution (PBS)**

Concentration required: 10 x 10^{-3} M = 10 mM

Total volume: 1 L

pH: 7.3

0.24 g of KH_2PO_4 (Potassium Phosphate Monobasic)

1.42 g of Na_2HPO_4 (Sodium Phosphate Dibasic)

8.00 g of NaCl (Sodium Chloride)

In distilled water added up to 1 L

<u>- Phosphorous concentration:</u>

Source: KH_2PO_4 and Na_2HPO_4

Molecular weights: P: 30.97 g/mol; KH_2PO_4: 136.086 g/mol; Na_2HPO_4:141.96 g/mol

$$g\ P = 0.24\ \text{g}\ KH_2PO_4 \times \frac{1\ mol\ KH_2PO_4}{136.086\ g\ KH_2PO_4} \times \frac{1\ mol\ P}{1\ mol\ KH_2PO_4} \times \frac{30.97\ g\ P}{1\ mol\ P} = 0.05462\ g\ P = 54.62\ mg\ P$$

$$g\ P = 1.42\ \text{g}\ Na_2HPO_4 \times \frac{1\ mol\ Na_2HPO_4}{141.96\ g\ Na_2HPO_4} \times \frac{1\ mol\ P}{1\ mol\ Na_2HPO_4} \times \frac{30.97\ g\ P}{1\ mol\ P} = 0.30979\ g\ P = 309.79\ mg\ P$$

Phosphorous concentration in PBS $= (54.62 + 309.79)\ mg = 364.41\ mg/L$

or 0.011767 mol/L

- ✓ **Trace element solution (TES)**

Total volume: 500mL

0.1% w/v $FeSO_4 \cdot 7H_2O$ (Iron (II) Sulfate Heptahydrate)

0.1% w/v $MgSO_4 \cdot 7H_2O$ (Magnesium Sulfate Heptahydrate)

0.01% w/v $CuSO_4 \cdot 5H_2O$ (Copper Sulfate Pentahydrate)

0.01% $MnSO_4 \cdot 5H_2O$ (Manganese Sulfate Pentahydrate)

0.01% $ZnSO_4 \cdot 7H_2O$ (Zinc Sulfate Heptahydrate)

In distilled water added up to 500 mL

Required amounts of reagents:

g $FeSO_4 \cdot 7H_2O = \frac{0.1\ g\ FeSO_4 \cdot 7H_2O}{100\ mL\ Solution} \times 500\ mL = 0.5$g $FeSO_4 \cdot 7H_2O$

g $MgSO_4 \cdot 7H_2O = \frac{0.1\ g\ MgSO_4 \cdot 7H_2O}{100\ mL\ Solution} \times 500\ mL = 0.5$g $MgSO_4 \cdot 7H_2O$

g $CuSO_4 \cdot 5H_2O = \frac{0.01\ g\ CuSO_4 \cdot 5H_2O}{100\ mL\ Solution} \times 500\ mL = 0.05$g $CuSO_4 \cdot 5H_2O$

g $MnSO_4 \cdot 5H_2O = \frac{0.01\ g\ MnSO_4 \cdot 5H_2O}{100\ mL\ Solution} \times 500\ mL = 0.05$g $MnSO_4 \cdot 5H_2O$

g $ZnSO_4 \cdot 7H_2O = \frac{0.01\ g\ ZnSO_4 \cdot 7H_2O}{100\ mL\ Solution} \times 500\ mL = 0.05$g $ZnSO_4 \cdot 7H_2O$

- ✓ **Growth medium**

Total volume: 1 L

0.2% w/v $(NH_4)_2SO_4$ (Ammonium Sulfate)

0.05% w/v Yeast extract

1% v/v Trace element solution (TES)

In PBS added up to 1 L (approximately 990 mL PBS)

Required amounts of reagents:

g $(NH_4)_2SO_4 = \frac{0.2\ g\ (NH_4)_2SO_4}{100\ mL\ Solution} \times 1000\ mL = 2.0$g $(NH_4)_2SO_4$

g Yeast extract = $\frac{0.05\ g\ \text{yeast extract}}{100\ mL\ Solution} \times 1000\ mL = 0.5$g Yeast extract

mL TES = $\frac{1\ \text{mL TES}}{100\ mL\ Solution} \times 1000\ mL = 10$mLTES

<u>- Phosphorous concentration:</u>

Source: PBS (990 mL)

$$mg\ P = \frac{0.011767\ \text{mol P}}{1000\ mL} \times 990\ mL \times \frac{30.97\ g\ P}{1\ mol\ P} = 0.36078\ g\ P = 360.78\ mg\ P$$

Phosphorous concentration in Growth medium = 360.78 mg/L

- Nitrogen concentration:

Source: $(NH_4)_2SO_4$ (2 g)

Molecular weights: N: 14 g/mol; $(NH_4)_2SO_4$: 132.14 g/mol

$$mg\ N = 2\ g\ (\mathrm{NH_4})_2\mathrm{SO_4} \times \frac{1\ mol\ (\mathrm{NH_4})_2\mathrm{SO_4}}{132.14\ g\ (\mathrm{NH_4})_2\mathrm{SO_4}} \times \frac{2\ mol\ N}{1\ mol\ (\mathrm{NH_4})_2\mathrm{SO_4}} \times \frac{14\ g\ N}{1\ mol\ N}$$

$$= 0.42380\ g\ N = 423.80\ mg\ N$$

Nitrogen concentration in Growth medium = 423.90 mg/L

- ✓ **Test medium**

- Composition: 2500 mg PET or PCL + 800 mL growth medium + 150 mL inoculum

- Carbon-Nitrogen ratio

Carbon content (provided by the PET)

$$mg\ C = mg\ PET \times Xc = 2500\ mg\ PET \times 0.625 = 1563\ mg\ C$$

Nitrogen content (provided by growth medium)

$$mg\ N = \frac{mg\ N}{L_{\ growth\ medium}} \times\ Volume_{growth\ medium\ used} = 423.90 \frac{mg\ N}{L} \times 0.8\ L = 339.04\ mg\ N$$

$$\frac{mg\ C}{mg\ N} = \frac{1563\ mg\ C}{339.04\ mg\ N} \approx \frac{7}{3}$$

(PET) Carbon to Nitrogen ratio is **7:3**

Similarly, for PCL:

(PCL) Carbon to Nitrogen ratio is **7:3**

- ✓ **Standard sodium carbonate solution**

Na_2CO_3 (Sodium Carbonate) solution volume: 500 mL

Concentration: 0.025 M Molecular weight: 105.99 g/mol

g Na_2CO_3= $\frac{0.025\ mol\ \mathrm{Na_2CO_3}}{L} \times \frac{105.99\ g\ \mathrm{Na_2CO_3}}{mol\ \mathrm{Na_2CO_3}} \times 0.5\ L = 1.324\ g\ \mathrm{Na_2CO_3}$

Distilled water added up to 500 mL

- ✓ **Hydrochloric Acid solution**

Total volume: 1 L

Different volumes (V_1) of HCl stock solution of molarity M_1were required to prepare1 L (V_2) of HCl solutions of varied concentrations (M_2). The following formula was used for the dilutions:

$$M_1 \times V_1 = M_2 \times V_2$$

Using HCl stock solution with concentration of 12M to prepare 1 L of 0.6 M HCl solution:

M_1 = 12 M V_2 = 1 L M_2 = 0.6 M

$$V_1 = \frac{M_2 \times V_2}{M_1} = \frac{0.6\ M \times 1\ L}{12\ M} = 0.05\ L = 50\ mL\ HCl$$

Thus, 50 mL of 12 M HCl solution and distilled water up to 1 L were needed to prepare the desired 0.6 M HCl solution.

After preparing the solutions, they were standardized with 0.025 M $NaCO_3$ standard solution to determine their exact molarity. To do this, the HCl solutions were titrated (triplicates) with the standard solution of $NaCO_3$and using methyl orange as indicator.

The reaction of both reactants occurs as follows:

$$Na_2CO_{3\,(aq)} + HCl_{(aq)} \rightarrow NaHCO_{3\,(aq)} + NaCl_{(aq)}$$

$$NaHCO_{3\,(aq)} + HCl_{(aq)} \rightarrow NaCl_{(aq)} + CO_{2\,(g)} + H_2O_{(l)}$$

<u>- Standardization of HCl solution:</u>

The exact molarity of HCl was found as shown in the following example:

Volume of Na_2CO_3 = 20 mL Assumed concentration of HCl = 0.05 M

Concentration of Na_2CO_3 = 0.025 M Volume of HCl used for titration (trial #2) = 0.0231 L

$$\text{mol } Na_2CO_3 = \frac{0.025\ mol\ Na_2CO_3}{L} \times 0.020\ L\ Na_2CO_3 = 0.0005\ mol\ Na_2CO_3$$

$$\text{mol HCl} = 0.0005\ mol\ Na_2CO_3 \times \frac{2\ mol\ \text{HCl}}{1\ mol\ Na_2CO_3} = 0.0010\ mol\ \text{HCl}$$

$$[HCl] = \frac{0.0010\ mol\ \text{HCl}}{0.0231\ L\ HCl} = 0.0433\ \text{M}$$

Only those volumes of HCl used in titration that were within ±0.4 mL were considered for calculations.

The following table summarizes the exact concentration of the HCl solutions as well as the volumes and molarities of the HCl stock solutions used.

HCl stock solution concentration (M)	Desired HCl concentration (M)	Volume of stock solution used (mL)	Standardized HCl (M)
12	0.6	50	0.4621
0.5	0.05	100	0.0433
0.5	0.06	120	0.0459
0.5	0.06	120	0.0414
0.5	0.06	120	0.0550
0.5	0.05	100	0.0466
0.5	0.04	80	0.0436
0.5	0.04	80	0.0432
0.5	0.04	80	0.0478
0.5	0.045	90	0.0484

- ✓ **Barium Hydroxide solution**

Solutions of Barium Hydroxide [$Ba(OH)_2$] of varied concentrations were prepared. An amount (m) of $Ba(OH)_2$granules was first weighed and placed in a 1 L volumetric flask. Distilled water was added up to 1 L and then the mixture was placed in a water bath at 106 ºF and stirred for 20 minutes to help dissolve the granules. The mixture was passed through a vacuum filtration system with an ashless filter paper to remove undissolved solids. Finally, the $Ba(OH)_2$solution was standardized using standard HCl solution.

The solutions prepared at the beginning of the biodegradation test were not placed in water bath nor filtered. Hence, greater amounts of granules were needed to achieve desired concentrations.

<u>- Standardization of $Ba(OH)_2$ solution:</u>

The exact molarity of prepared $Ba(OH)_2$solution was found as shown in the following example:

Volume of $Ba(OH)_2$ = 25 mL Assumed concentration of $Ba(OH)_2$ = 0.0125 M

Concentration of HCl = 0.0433 M Volume of HCl used for titration (trial #2) = 0.0149 L

$$\text{mol HCl} = \frac{0.0433\ mol\ \text{HCl}}{L} \times 0.0149\ L\ HCl = 0.000645\ mol\ \text{HCl}$$

$$\text{mol } Ba(OH)_2 = 0.000645\ mol\ \text{HCl} \times \frac{1\ mol\ Ba(OH)_2}{2\ mol\ \text{HCl}} = 0.000323\ mol\ Ba(OH)_2$$

$$[Ba(OH)_2] = \frac{0.000323\ mol\ Ba(OH)_2}{0.025\ L\ Ba(OH)_2} = 0.0127\ \text{M}$$

The following table shows the results for all the solutions of $Ba(OH)_2$ prepared and standardized.

$Ba(OH)_2$ solutions prepared without filtration

Mass of $Ba(OH)_2$(g)	Assumed$Ba(OH)_2$molarity (M)	Molarity of standard HCl (M)	Volume of standard HCl used (mL)	Standardized $Ba(OH)_2$ (M)
8	0.0050	0.4621	0.5	0.0231
4	0.0025	0.4621	0.2	0.0116
4	0.0030	0.4621	0.3	0.0139
11	0.0090	0.4621	0.9	0.0416
12	0.0110	0.4621	1.1	0.0508
8	0.0060	0.4621	0.6	0.0277
12	0.0125	0.4621	1.2	0.0578
11	0.0092	0.4621	1.1	0.0424
10	0.0083	0.4621	1.0	0.0385
9	0.0067	0.4621	0.8	0.0308

$Ba(OH)_2$ solutions prepared without filtration

Mass of $Ba(OH)_2$(g)	Desired $Ba(OH)_2$ molarity (M)	Molarity of standard HCl (M)	Volume of standard HCl used (mL)	Standardized $Ba(OH)_2$ (M)
8	0.0050	0.4621	0.6	0.0231
8	0.0058	0.4621	0.7	0.0270
8	0.0058	0.4621	0.7	0.0270
8	0.0042	0.4621	0.5	0.0193
8	0.0063	0.4621	0.7	0.0289
8	0.0054	0.4621	0.6	0.0250

$Ba(OH)_2$ solutions prepared with filtration

Mass of $Ba(OH)_2$(g)	Assumed $Ba(OH)_2$molarity (M)	Molarity of standard HCl (M)	Volume of standard HCl used (mL)	Standardized $Ba(OH)_2$ (M)
4.0	0.0125	0.0433	15.0	0.0130
4.0	0.0125	0.0433	14.7	0.0127
4.0	0.0125	0.0433	12.0	0.0130
4.0	0.0125	0.0433	12.2	0.0132
4.0	0.0125	0.0459	4.0	0.0093
4.0	0.0125	0.0459	4.1	0.0094
4.0	0.0125	0.0459	8.5	0.0097
4.0	0.0125	0.0414	8.6	0.0089
4.0	0.0125	0.0414	8.5	0.0088
4.0	0.0125	0.0414	8.6	0.0088
4.3	0.0125	0.0466	5.7	0.0132
4.3	0.0125	0.0466	6.3	0.0146
4.3	0.0125	0.0466	6.1	0.0141
4.3	0.0125	0.0436	6.3	0.0138
4.3	0.0125	0.0436	6.4	0.0139
4.3	0.0125	0.0432	6.5	0.0141
4.3	0.0125	0.0432	6.4	0.0139
4.3	0.0125	0.0478	6.0	0.0143
4.3	0.0125	0.0478	5.8	0.0137
4.3	0.0125	0.0484	5.7	0.0139
4.3	0.0125	0.0484	5.8	0.0140
4.3	0.0125	0.0484	5.6	0.0136

- ✓ **Sodium hydroxide solution**

Sodium hydroxide (NaOH) solution volume: 1 L

NaOH granules were slowly added into 1 L of distilled water while stirring. A water bath was used to help remove heat from the exothermic reaction of NaOH dissolution. Two different amounts of NaOH were required to prepare two concentrations:

Molecular weight NaOH: 39.997 g/mol

- 3.00 M NaOH solution:

$$\text{g NaOH} = \frac{3\ mol\ NaOH}{L} \times 1\ L \times \frac{39.997\ g\ NaOH}{1\ mol\ NaOH} = 120\ g\ NaOH$$

- 7.5 M NaOH solution:

$$\text{g NaOH} = \frac{7.5\ mol\ NaOH}{L} \times 1\ L \times \frac{39.997\ g\ NaOH}{1\ mol\ NaOH} = 300\ g\ NaOH$$

- ✓ **Mineral-salt medium**

Volume: 500 mL

0.35 g KH_2PO_4(Potassium Phosphate Monobasic)

0.35 g K_2HPO_2 (Potassium Phosphate Dibasic)

0.35 g $MgSO_4 \cdot 7H_2O$ (Magnesium Sulfate Heptahydrate)

0.5 g $(NH_4)_2SO_4$ (Ammonium sulfate)

0.0025 g NaCl (Sodium chloride)

0.001 g $FeSO_4 \cdot 7H_2O$ (Iron (II) Sulfate Heptahydrate)

0.001 g $ZnSO_4 \cdot 7H_2O$ (Zinc Sulfate Heptahydrate)

0.0005 g $MnSO_4 \cdot 5H_2O$ (Manganese Sulfate Pentahydrate)

1 mL Trace element solution

- ✓ **Mineral medium agar**

250 mL Mineral salt medium

5 g Agar-agar

- ✓ **Polymer suspension**

250 mL Mineral salt medium

0.75 g PET MPs

5 g Agar-agar

APPENDIX B: Experimental protocols and troubleshooting

Biodegradation test protocol

1. Empty the water completely from all the bioreactors and absorber bottles
2. Prepare the growth medium with the chemicals listed in **Table 3.2** (compositions and quantities in **Appendix A**), measure pH and add 800 mL of it to each bioreactor
3. Weight two samples of 2,500 mg of PET MPs and add each to bioreactors #1 and #2. Weight 2,500 mg of PCL MPs and add to the bioreactor #3. The bioreactor #4 carries no MPs and is used as negative control
4. Switch on the thermostat at the mains switch, then adjust the thermostat set point temperature to achieve an inner temperature of 30°C in all bioreactors
5. Prepare the barium hydroxide solution (concentrations in **Appendix A**); fill up the sixteen 250 mL absorber bottles with 100-150 mL of $Ba(OH)_2$ and immediately close the caps tight
6. Inoculate each bioreactor with 150 mL of the final enriched culture and measure the pH of the mixture
7. Turn on the magnetic stirrers and set up the speed at #3 (45 rpm) to keep the mixtures gently agitated
8. Fill up the beakers with more tap water, if necessary
9. Disconnect the air tubing from the compressed air supply (**V-5**) and connect it directly to the oxygen tank regulator(**V-6**) instead, omitting the NaOH bottles of the CO_2 trap (1) [**Figure 3.3**]. The system will be aerated with pure oxygen for the first 50 days (***stage 1***)
10. Use valves **V-1**, **V-2**, **V-3** and **V-4** to adjust the oxygen flow rate to each bioreactor to 48 mL/min
11. The test (***stage 1***) is started by bubbling oxygen through the bioreactors
12. Incubate for 50 days
13. During incubation, measure the carbon dioxide evolved from each first bottle of $Ba(OH)_2$ in the CO_2 traps at regular intervals by titration with standard HCl (every 2 days or when first bottle is turbid but before any precipitation is observed in the second bottle)

14. Seal the tubing immediately after removing the first absorber bottle so that no CO_2 from air enters the system. Move the two remaining absorber bottles one position closer to the bioreactor, and place one new bottle with fresh $Ba(OH)_2$ at the end of the series
15. Take readings of temperature and air flow rate on each bioreactor
16. Using the valves of the sampling/injection mechanisms (**V-7**, **V-8**, **V-9**, **V-10**), take small volumes (10 mL) of mixtures from the bioreactors and measure the pH (two times during ***stage 1***). To do this, connect a sterile syringe to the sampling/injection tubing (**Figure 3.4**), open the pinch actuator to allow the flow and start sucking out the medium until the syringe is filled up to 10 mL. Close the pinch actuator, remove the syringe and pour the sample into a 50 mL centrifuge tube for further testing.
17. Add more decalcified water to the thermostat water bath when required
18. Every week, remove temporarily the stainless-steel tubing in the absorber bottles for quick inspections and clean-ups to prevent accumulation of salts
19. After 50 days of incubation, shut down the oxygen flow using the regulator of the oxygen tank
20. Remove and titrate all the $Ba(OH)_2$ absorber bottles. Wash them, refill them with 100-150 mL of fresh $Ba(OH)_2$, cap and connect them back to the air line at the exit of the bioreactors
21. Prepare the sodium hydroxide solution (concentrations in **Appendix A**); fill up the two 500 mL absorber bottles and immediately close the caps tight. Place the bottles in position (1) [**Figure 3.3**]
22. Connect the air tubing back to the laboratory compressed air valve **V-5**
23. Use valves **V-1**, **V-2**, **V-3** and **V-4** to adjust the air flow rate to each bioreactor to 65 mL/min
24. The ***stage 2*** of the test is initiated by bubbling air through the bioreactors
25. Incubate for 58 days
26. Repeat steps (13 – 18)
27. Replace the NaOH solution in the CO_2 trap with one freshly made, when necessary
28. After 58 days of incubation, shut down the air flow using **V-5**
29. Remove and titrate all the $Ba(OH)_2$ absorber bottles. Wash them, refill them with 100-150 mL of $Ba(OH)_2$, cap and connect them back to the air line at the exit of bioreactors

30. Open the air valve **V-5**, increase the air flow rate in the system and adjust the flow rate to each bioreactor to 100 mL/min using valves **V-1**, **V-2**, **V-3** and **V-4**
31. The ***stage 3***of the test is begun by bubbling air through the bioreactors at a new flow rate
32. Repeat steps 12, 13, 14, 16 and 17
33. Using the sampling/injection mechanisms, take small volumes (15 mL) of mixtures from the bioreactors for pH measurement and HPLC analysis (six times in total during ***stage 3***)
34. Every three days, feed 15 mL of growth medium (prepared as described in section 3.2.) to each bioreactor. Measure the volume using a sterile syringe; connect it to the injection mechanism, open the pinchcock to allow the flow and start injecting the medium (Figure 3.4.). Close the pinchcock and remove the syringe.
35. Incubate for 60 days
36. After 60 days of incubation, shut down the air valves **V-5**, **V-1**, **V-2**, **V-3** and **V-4**
37. Remove and titrate all the $Ba(OH)_2$ absorber bottles
38. Remove the bioreactors lids and measure the pH. Take two samples of 15 mL from the middle and from the bottom (including settled microplastics) of each reactor for specific analyses

Troubleshooting

It was necessary to resolve several problems that arose during the operation of the test unit:

1. **Problem:** Clogging of stainless-steel tubing submerged in the absorber bottles due to build-up of $BaCO_3$ salts

   Solution: Temporary removal of tubing for regular inspections and clean-ups to prevent accumulation of salts
2. **Problem:** Rapid accumulation of $BaCO_3$ salts in the CO_2 indicator bottle of each bioreactor

   Solution: An additional absorber bottle filled with NaOH was placed before CO_2 indicator bottle of each bioreactor to absorb higher amounts of CO_2 from flowing air
3. **Problem:** Sudden drops in bioreactors inner temperature due to thermostat shut-offs caused by low bath water levels

Solution: Regular additions of decalcified water were done to the thermostat tank to make up for the evaporation losses and maintain the required minimum water level of 70 mm below the bath bridge

4. **Problem:** Sudden air flow disruption due to clogging of tubing submerged in NaOH from the first CO_2trap caused by decreased absorption capacity

   Solution: A higher concentration of NaOH solution (from 5 M to 10M) was used to increase the CO_2 absorption capacity of the NaOH solution and prevent frequent clogging

Microbiology protocols

Protocol to wash cells

1. Vortex each overnight culture and transfer from the 15 mL tube to a 50 mL centrifuge tube.
2. Weight all the tubes and pair the ones with similar weights. Adjust the weights so that the difference is ± 0.1 g. Use an additional tube with distilled water in case the number of cultures is odd.
3. Once all tubes have been paired, centrifuge at 7,000 x g for 10 minutes.
4. Carefully, pipette the LB broth out and leave the pellet in the tube.
5. Add enough saline solution (1% NaCl) to reach a volume of 30 mL in each tube and vortex to homogenize.
6. Repeat step 2.
7. Centrifuge at 10,000 x g for 10 minutes.
8. Pipette the saline solution out and leave the pellet.
9. Repeat steps 5 – 8.
10. Add growth medium to each pellet and vortex to homogenize.

- DNA Extraction

All pure culture isolates were individually DNA extracted using Power Soil® DNA Isolation Kit (MO BIO Laboratories Inc., Canada). The associated user protocol was followed with slight modification for better genomic DNA yield. Initial preparation of liquid samples was done through suspending the bacterial colonies in 500 µL of distilled water. This mixture was vortexed for 10 seconds for complete homogenization and was added to the PowerBead Tubes. Additional vortexing was done to incorporate bacteria throughout the PowerBead solution. Sixty microliters of solution C1 (containing sodium dodecyl sulfate (SDS) and disruption agents) was added to the PowerBead tubes and vortexed briefly. The PowerBead tubes were then horizontally secured on a flat-bed vortex pad and were subjected to 5 to 20 minutes at maximum speed depending on the isolate. Once the time had passed for mechanical lysis, tubes were centrifuged at 10,000 x g for 30 seconds at room temperature. The transfer of up to 500 µL of supernatant was placed into a clean 2 mL collection tube. To the collection tube, 250 µL of solution C2 (patented Inhibitor Removal Technology®) was added and vortexed for five seconds and incubated at 4 ℃ for 5 minutes. After incubation, the tubes were centrifuged at 10,000 x g for 1 minute. Avoiding the pellet, 600 µL of supernatant was transferred into a clean 2 mL collection tube with the addition of 200 µL solution C3 (patented Inhibitor Removal Technology®). The addition of solution C3 will produce a cloudy white mixture inside the collection tube. The tubes were vortexed for 5 seconds before incubating at 4 ℃ for 5 minutes. After 5 minutes, the collection tubes were centrifuged at 10,000 x g for 1 minute. Removal of 750 µL of supernatant was transferred into a clean 2 mL collection tube along with 1.2 mL of solution C4 (high concentration salt solution) avoiding overflow. The mixture was vortexed for 5 seconds for proper mixing. Once thoroughly mixed, 675 µL of supernatant solution was added onto the spin filter to be centrifuged at 10,000 x g for 30 seconds. The flow through was then discarded with another load of 675 µL of supernatant solution onto the spin filter. This step was repeated until all the supernatant solution was passed through spin filter. Once the process is done, 500 µL of solution C5 (ethanol-based wash solution) was added onto the spin filter and was centrifuged at 10,000 x g for 30 seconds. Discarding all flow through, an additional centrifugation at 10,000 x g for 1 minute was done to remove all residual wash solution. The spin filter was then carefully placed into a clean 2 mL collection tube and was directly added with 100 µL of solution C6 (sterile elution buffer). Solution C6 was then incubated at room temperature for 5 minutes for

maximum DNA yield. The collection tube underwent a final centrifugation at 10,000 x g for 30 seconds. The spin filter was then discarded from the collection tube and the remaining elution contained approximately 100 µL of DNA solution. DNA was stored at -20 ℃ ready for downstream application.

- Polymerase Chain Reaction of the 16S rRNA Gene

DNA extractions were used in amplifying the 16S rRNA region using the polymerase chain reaction process (PCR). Reactions were conducted on ice of a 25 µL total reaction which included a negative control with the absence of DNA. Forward primer U341F (CCTACGGGAGGCAGCAG) and reverse primer U785R (CTACCAGGGTATCTAATCC) were used in searching for the conserved region and were synthesized at the Peter Gilgan Centre for Research and Learning in Toronto, Canada.38

Each reaction contained 0.25 µL of Taq DNA polymerase (New England Biolabs, USA), 0.34 µL of 10 mg/mL BSA, 0.5 µL of 25 µM of forward and reverse primers, 0.5 µL of 10 mM of dNTPs, 5 µL of 10 X Taq Thermpol® buffer (New England Biolabs, USA), approximately 50 ng of DNA template with the remainder volume of sterile PCR-grade water. The reaction tubes were then positioned in the T100™ thermacycler (BioRad, Canada) to begin the PCR amplification.

The PCR protocol was executed by the thermocycler at the following settings: an initial denaturation temperature of 96 ℃ for 5 minutes continuing with the primary cycle. The primary cycle includes a denaturation of 94 ℃ for 1 minute, an annealing temperature of 65 ℃ for 1 minute with a decrease of 1 ℃ per cycle and an elongation of 3 minute at 72 ℃. The primary cycle is repeated for a total of 10 cycles. This is followed by the secondary cycle of a denaturation of 94 ℃ for 1 minute, annealing temperature at 55 ℃ for 1 minute with an elongation of 1 minute at 72 ℃. The secondary cycle is repeated for a total of 20 cycles which completes the protocol. PCR products are stored at 4 ℃ for gel electrophoresis and Sanger sequencing.

- Gel Electrophoresis

A 1% agarose gel was made to visually assess the quality of DNA in DNA extraction and PCR. Initially 0.65 g of Ultrapure™ agarose (Invitrogen, USA) is dissolved in 65 mL of 0.5 X of Tris-acetate EDTA (TAE) buffer. The solution is microwaved for approximately 2 minutes until all the agarose has dissolved. The solution is then cooled to around 40 °C where 1.08 µL of SYBR Safe (Thermo Fisher Scientific, Canada) is added and gently mixed throughout. The stained gel is poured into a gel tray with comb to fully solidify.

Once solidified, the gel is submerged into the Mupid-2plus gel electrophoresis system (Clonetech, USA) filled with 0.5X TAE buffer. DNA extractions products are first mixed with 8 µL of isolate genomic DNA and 2 µL of 6X loading dye. The DNA is loaded into each well alongside a 1 kb extended DNA ladder (New England Biolabs, USA) to determine quality and approximate amount of DNA. PCR products are loaded with a mixture of 4 µL of PCR products and 2 µL of 6X loading dye. The product is then loaded into the wells alongside a 100 bp DNA ladder (Froggabio, Canada). The gel electrophoresis apparatus is run at 100 V for 30 and 20 minutes respectively for DNA extractions and PCR products. The gel is then imaged and processed through Image Lab v5.1 (BioRad, Canada).

- Sanger Sequencing and BLAST

PCR products were sent to ACGT Corporation (Toronto, ON) for Sanger sequencing. PCR products were prepared with 100 µM of forward primer. Raw DNA sequences were sent back and analyzed using the Sequence Scanner v1.0 (Thermo Fisher Scientific, Canada). To determine the culture identity, DNA sequences were inputted into the Basic Local Alignment Search Tool (BLAST) online. The percent of confidence of each corresponding culture were recorded.

APPENDIX C. Recorded raw data and sample calculations

C.1. Operating conditions monitored in the biodegradation test

Time (days)	Temperature ºC	Oxygen flow rate (mL/min)	pH
0	30.10	48.7	7.35
10	30.10	48.7	-
20	30.10	48.7	7.30
30	30.12	48.7	-
40	25.00	48.7	7.05
50	30.13	48.7	-
60	30.10	10.2	6.94
70	30.17	10.2	-
80	21.00	10.2	-
90	30.09	5.0	6.72
100	30.05	10.2	-
110	30.06	21.0	6.33
120	22.00	21.0	6.46
130	30.08	21.0	6.44
140	30.09	21.0	-
150	30.10	21.0	6.22
160	30.07	21.0	-
168	30.18	21.0	6.10

C.2. Sample calculations

C.2.1. Carbon content, Cc

PET (monomer) Chemical formula: $C_{10}H_8O_4$

Atomic mass	Calculation	Total mass
C = 12.011	12.011 x 10	120.110
H = 1.008	1.008 x 8	8.064
O = 15.999	15.999 x 4	63.996
	Total mass $C_{10}H_8O_4$	192.170

$$Cc = \frac{Total\ mass\ Carbon}{Total\ mass\ monomer} = \frac{120.110}{192.170} = 0.625$$

PCL (monomer) Chemical formula: $C_6H_{10}O_2$

Atomic mass	Calculation	Total mass
C = 12.011	12.011 x 6	72.066
H = 1.008	1.008 x 10	10.080
O = 15.999	15.999 x 2	31.998
	Total mass $C_6H_{10}O_2$	114.144

$$Cc = \frac{Total\ mass\ Carbon}{Total\ mass\ monomer} = \frac{72.066}{114.144} = 0.631$$

C.2.2. Total organic carbon (TOC)

Total volume (*V*) of media in bioreactor: 0.95 L

Total mass (*m*) of PET and PCL added to the bioreactors: 2,500 mg

$$TOC = \frac{m \times Cc}{V}$$

PET: $$TOC = \frac{m \times Cc}{V} = \frac{2{,}500\ mg \times 0.625}{0.95\ L} = 1{,}644.737\ mg/L$$

PCL: $$TOC = \frac{m \times Cc}{V} = \frac{2{,}500\ mg \times 0.631}{0.95\ L} = 1{,}660.526\ mg/L$$

Activated sludge: TOC calculated as 58% of the total VSS (Castro-Aguirre et al., 2017)

VSS = 551.0 mg/L $TOC = 0.58 \times VSS = 0.58 \times 551.0 \frac{mg}{L} = 319.58 mg/L$

Inoculum:

VSS = 502.78 mg/L $TOC = 0.58 \times VSS = 0.58 \times 502.78 \frac{mg}{L} = 291.6 mg/L$

C.2.3. TSS AND VSS

Equation **11**: $TSS = \frac{(B-A)\times 10^6}{V}$ Equation **12**: $VSS = \frac{(B-C)\times 10^6}{V}$

-Activated sludge (Trial #1):

A = 0.1181 g

B = 0.1453 g $TSS = \frac{(0.1453-0.1181)g \times 10^6}{30mL} \times \left(\frac{mg \times mL}{g \times L}\right) = 907\ mg/L$

V = 30 mL

B = 0.1453 g

C = 0.1273 g $VSS = \frac{(0.1453-0.1273)g \times 10^6}{50\ mL} \times \left(\frac{mg \times mL}{g \times L}\right) = 600\ mg/L$

V = 50 mL

- Enrichment procedure: sample at 0 days

The enrichment medium consisted of 50 mL of activated sludge (847 mg TSS /L and 551 mg VSS /L) and 200 mL of growth medium, therefore:

$$TSS \text{ in 50 mL of inoculum} = 847 \frac{mg}{L} \times 0.05L = 42.4\ mg$$

Since V = 0.250 L, then:

$$TSS = \frac{42.4\ mg}{0.250\ L} = 169.4\ mg/L$$

$$VSS \text{ in 50 mL of inoculum} = 551 \frac{mg}{L} \times 0.05L = 27.6\ mg$$

Since V = 0.250 L, then:

$$VSS = \frac{27.6\ mg}{0.250\ L} = 110.4\ mg/L$$

These initial values of TSS and VSS also apply for the medium with PCL microplastics.

C.2.4. BIODEGRADATION TEST

Theoretical amount of evolved carbon dioxide

Equation **2**: $ThCO_2 = W_0 \times X_C \times \frac{44}{12}$

- For PET:

W_0 = 2,500 mg

X_C = 0.625 $ThCO_2 = 2{,}500\ mg \times 0.625 \times \frac{44}{12} = 5{,}729.167\ mg$

Mass of carbon dioxide evolved in the bioreactors

Equation **5**: $mCO_2 = \left(\frac{2c_B \times V_{B0}}{c_A} - V_A \times \frac{V_{Bf}}{V_{Bz}}\right) \times c_A \times 22$

- For PET (Bioreactor #1) at 7 days of incubation:

c_A = 0.4621 M

c_B = 0.0116 M Equation **6**: $V_A = V_f - V_i = (23.8 - 16.4)mL = 7.4\ mL$

V_{B0} = 200 mL

V_{Bf} = 200 mL

V_{Bz} = 200 mL $mCO_2 = \left(\frac{2 \times 0.0116 \times 200}{0.4621} - 7.4 \times \frac{200}{200}\right) \times 0.4621 \times 22 = 26.4295\ mg$

V_i = 16.4 mL

V_f = 23.8 mL

Percentage biodegradation

Equation **1**: $D_t = \frac{\sum(mCO_2)_T - \sum(mCO_2)_B}{ThCO_2} \times 100$

- For PET (Bioreactor #1) at 7 days:

$ThCO_2$ = 5729.167 mg

$(mCO_2)_B$ = 24.3887 mg $\quad D_t = \frac{(26.4295 - 24.3887)mg}{5729.167\ mg} \times 100 = 0.0356\%$

$(mCO_2)_T$ = 26.4295 mg

Final weight of microplastics

Equation **9**: $W = W_0\left(1 - \frac{Dt}{100}\right)$

- For PET after 168 days of incubation:

W_0 = 2,500 mg

Dt = 17.07% $\quad W = 2{,}500\ mg \times \left(1 - \frac{17.07}{100}\right) = 2{,}073\ mg$

C.2.5. KINETICS

Rate constant of microplastics reduction rate

Equation **8**: $K = -\frac{1}{t}\left(ln\frac{W}{W_0}\right)$

- For PET after 168 days of incubation:

t = 168 days

W = 2,073 mg $\quad K = -\frac{1}{168\ days}\left(ln\frac{2{,}073\ mg}{2{,}500\ mg}\right) = 0.00112\ days^{-1}$

W_0 = 2,500 mg

Half-life of microplastics

Equation **10**: $(t_{1/2}) = \ln(2)\,/K$

- For PET after 168 days of incubation:

K = 0.00112 days^{-1} $(t_{1/2}) = \frac{\ln(2)}{0.00112\ days^{-1}} = 618\ days$

C.2.6. ANALYTICAL TECHNIQUES

Crystallinity of microplastics

Equation **15**: $\%crystallinity = \frac{\Delta H_m - \Delta H_c}{\Delta H_m^0} \times 100$

- For PET microplastics after 168 days of incubation, trial #2:

ΔH_m = 35.03 J/g

ΔH_c = 10.92 J/g $\%crystallinity = \frac{(35.03-10.92)\,J/g}{140.1\,J/g} \times 100 = 32.80\%$

ΔH_m^0 = 140.1 J/g

Carbonyl and crystallinity indexes

Equation **13**: $Carbonyl\ index = \frac{I_{1710}}{I_{871}}$

Equation **14**: $Crystallinity\ index = \frac{A_{1341}}{A_{1410}}$

- For PET microplastics after 168 days of incubation:

I_{1710} = 0.044 $Carbonyl\ index = \frac{0.044}{0.011} = 4$

I_{871} = 0.011

A_{1341} = 0.157 $\quad\quad Crystallinity\ index = \frac{0.157}{0.151} = 1.04$

A_{1410} = 0.151

Relative viscosity of PET microplastics

Equation **16**: $\quad \eta_r = \frac{t}{t_0}$

- For PET microplastics after 168 days of incubation, trial #1:

t = 105 s

t_0 = 76 s $\quad\quad \eta_r = \frac{105\ s}{76\ s} = 1.3772$

Intrinsic viscosity of PET microplastics

Equation **18**: $\quad \eta = 0.25(\eta_r - 1 + 3Ln\eta_r)/C$

- For PET microplastics after 168 days of incubation, trial #1:

η_r = 1.3772

C= 0.5 g/dL $\quad\quad \eta = \frac{0.25[1.3772-1+3\times Ln(1.3772)]}{0.5\ ^{g}/_{dL}} = 0.6687\ dL/g$

Viscosity molecular weight of PET microplastics

Equation **19**: $\quad [\eta] = K{M_v}^a\ \therefore\ M_v = \left(\frac{\eta}{K}\right)^{1/a}$

- For PET microplastics after 168 days of incubation, trial #1:

η = 0.6687 dL/g $\quad\quad M_v = \left(\frac{0.6687}{0.000372}\right)^{1/0.73} = 28{,}737$

K = 0.000372; $\quad a$ = 0.73

C.2.7. UNCERTAINTY

Propagation of uncertainties (mCO2, %Dt) of PCL and Blank reactors

The following formulas were used for the calculation of uncertainties, depending on the type of function (Harvey, 2008).

Function	Error (u_R)
$R = k \times A$	$u_R = k \times u_A$
$R = A + B$	$u_R = \sqrt[2]{{u_A}^2 + {u_B}^2}$
$R = A - B$	$u_R = \sqrt[2]{{u_A}^2 + {u_B}^2}$
$R = A \times B$	$u_R = \sqrt[2]{\left(\frac{u_A}{A}\right)^2 + \left(\frac{u_B}{B}\right)^2}$
$R = \frac{A}{B}$	$u_R = \sqrt[2]{\left(\frac{u_A}{A}\right)^2 + \left(\frac{u_B}{B}\right)^2}$

Where:

R: calculated variable

u_R: uncertainty of calculated variable

A: variable 1

u_A: uncertainty of A

B: variable 2

u_B: uncertainty of B

Sample calculation of uncertainty of mCO_2 evolved in PCL reactor

Equation **5**: $$mCO_2 = \left(\frac{2c_B \times V_{B0}}{c_A} - V_A \times \frac{V_{Bf}}{V_{Bz}}\right) \times c_A \times 22$$

For titration performed on November 20th:

c_A = 0.4621 M

c_B = 0.0116 M

V_{B0}= 100 mL

V_{Bf} = 100 mL

V_{BZ} = 100 mL

$V_A = V_f - V_i = (51.2 - 47.8)mL = 3.9\ mL$

$$mCO_2 = \left(\frac{2(0.0116 \times 100}{0.4621} - 3.9 \times \frac{100}{100}\right) \times 0.4621 \times 22 = 67.1mg\ CO_2$$

R = 67.1 mg

From numerator of Equation 6: $(2c_B \times V_{B0}) = (2c_B \times 100) = 200 \times c_B$

- Uncertainty of $(200 \times c_B)$ Function: $k \times A$

$$u = 200 \times u_{c_B} = 200 \times 0.000065 = 0.013$$

- Uncertainty of $\left(\frac{200 \times c_B}{c_A}\right)$ Function: $\frac{A}{B}$

A = $200 \times c_B$

B = c_A

$$u = \sqrt[2]{\left(\frac{u_A}{A}\right)^2 + \left(\frac{u_B}{B}\right)^2} = \sqrt[2]{\left(\frac{0.013}{2.3103}\right)^2 + \left(\frac{0.0002}{0.4621}\right)^2} = 0.028$$

- Uncertainty of $\left(V_A \times \frac{V_{Bf}}{V_{Bz}}\right)$:

Since $V_{Bf} = V_{Bz}$ then $\frac{V_{Bf}}{V_{Bz}} = 1$

No calculation of uncertainty needed for this operation.

- Uncertainty of $\left(\frac{200 \times c_B}{c_A} - V_A\right)$ Function: $A - B$

A= $\frac{200 \times c_B}{c_A}$

B = V_A

$$u = \sqrt[2]{{u_A}^2 + {u_B}^2} = \sqrt[2]{0.028^2 + 0.07^2} = 0.076$$

- Uncertainty of $\left(\frac{200\times c_B}{c_A} - V_A\right) \times c_A$ Function: $A \times B$

A = $\left(\frac{200\times c_B}{c_A} - V_A\right)$

B = c_A

$$u = \sqrt[2]{\left(\frac{u_A}{A}\right)^2 + \left(\frac{u_B}{B}\right)^2} = \sqrt[2]{\left(\frac{0.076}{1.5995}\right)^2 + \left(\frac{0.0002}{0.4621}\right)^2} = 0.0528$$

- Uncertainty of $\left(\frac{200\times c_B}{c_A} - V_A\right) \times c_A \times 22$ Function: $k \times A$

k = 22

A = $\left(\frac{200\times c_B}{c_A} - V_A\right) \times c_A$

$$u = k \times u_A = 22 \times 0.0528 = 1.16$$

Finally, the mCO_2 evolved from the PCL reactor on November 20th is reported as:

$mCO_2 = (67.1 \pm 1.16)$ mg

C.3. Recorded data and results of Biomass concentration (X_{VSS})

- Activated sludge:

Sample	V (mL)	A (g)	B (g)	C (g)	**TSS (mg/L)**	**VSS (mg/L)**
#1	30.0	0.1181	0.1453	0.1273	907	600
#2	50.0	0.1174	0.1568	0.1317	788	502
				M	**847**	**551**
				SD	**83.9**	**69.3**

- PET:

0 days 169.5 mg TSS/L 110.4 mg VSS/L

Time: **11 days**						
Sample	V (mL)	A (g)	B (g)	C (g)	**TSS (mg/L)**	**VSS (mg/L)**
#1	6.00	0.1167	0.1172	0.1167	83.3	91.7
#2	6.00	0.1166	0.1170	0.1166	66.7	58.3
#3	6.00	0.1164	0.1174	0.1167	175	125
				M	**108**	**91.7**
				SD	**58.3**	**33.3**

Time: **29 days**						
Sample	V (mL)	A (g)	B (g)	C (g)	**TSS (mg/L)**	**VSS (mg/L)**
#1	6.00	0.1161	0.1172	0.1162	183	175
#2	6.00	0.1162	0.1168	0.1160	91.7	125
#3	6.00	0.1161	0.1186	0.1168	417	308
				M	**231**	**203**
				SD	**168**	**94.8**

Time: **39 days**						
Sample	V (mL)	A (g)	B (g)	C (g)	**TSS (mg/L)**	**VSS(mg/L)**
#1	6.00	0.1157	0.1170	0.1154	225	267
#2	6.00	0.1159	0.1182	0.1156	375	425
#3	6.00	0.1164	0.1187	0.1166	383	350
				M	**328**	**347**
				SD	**89.1**	**79.2**

Time: **42 days**						
Sample	V (mL)	A (g)	B (g)	C (g)	**TSS (mg/L)**	**VSS (mg/L)**
#1	6.00	0.1152	0.1197	0.1156	742	675
#2	6.00	0.1165	0.1209	0.1167	733	700
#3	6.00	0.1165	0.1172	0.1172	592	467
				M	**689**	**614**
				SD	**84.3**	**128**

Time: **53 days**						
Sample	V (mL)	A (g)	B (g)	C (g)	**TSS (mg/L)**	**VSS (mg/L)**
#1	6.00	0.1162	0.1224	0.1172	1033	867
#2	6.00	0.1165	0.1203	0.1177	633	433
				M	**833**	**650**
				SD	**283**	**306**

Time: **60 days**						
Sample	V (mL)	A (g)	B (g)	C (g)	**TSS (mg/L)**	**VSS (mg/L)**
#1	6.00	0.1149	0.1184	0.1158	583	433
#2	6.00	0.1159	0.1199	0.1165	667	567
#3	6.00	0.1153	0.1201	0.1171	800	508
				M	**683**	**503**
				SD	**109**	**66.8**

- PCL:

0 days 169.5 mg TSS/L 110.4 mg VSS/L

		Mean values					
Time (d)	V (mL)	A (g)	B (g)	C (g)	TSS (mg/L)	VSS (mg/L)	*SD*(VSS)
11	6.00	0.1157	0.1161	0.1158	66.7	58.3	35.4
29	6.00	0.1162	0.1202	0.1163	658	642	82.5
39	6.00	0.1152	0.1198	0.1155	775	725	35.4
42	6.00	0.1162	0.1228	0.1175	1092	875	200
46	6.00	0.1110	0.1199	0.1118	1483	1342	11.8
53	6.00	0.1162	0.1240	0.1179	1300	1025	200

C.4. Raw data and results of titrations, evolved CO_2 and %Dt on each reactor during the biodegradation test

Ca: concentration of HCl. **Cb**: concentration of BaOH. **Vb0**: initial volume of BaOH.
Vbf: final volume of BaOH. **Vbz**: volume aliquot of BaOH.
Va: volume of HCl used for titration.

$$mCO_2 = \left(\frac{2C_B \times V_{B0}}{C_A} - V_A \times \frac{V_{Bf}}{V_{BZ}}\right) \times C_A \times 22$$

	REACTOR 1 (PET)										
Date	Time (d)	Ca (mol/L)	Cb (mol/L)	Vb0 (mL)	Vbf (mL)	Vbz (mL)	Vf (mL)	Vi (mL)	Va (mL)	mCO2 (mg)	Dt (%)
14-Nov	0	0.4621	0.0116	100	100	100	50	0.000	10.0	0.000	0.000
		0.4621	0.0116	100	100	100	full		0.000	50.8	
17-Nov	3	0.4621	0.0116	100	100	100	36.5	36.2	0.30	47.8	0.57
		0.4621	0.0116	100	100	100	45.4	43.4	2.00	30.5	
18-Nov	4	0.4621	0.0116	200	200	200	4.90	0.000	4.90	51.8	0.071
19-Nov	5	0.4621	0.0116	100	100	100	full		0.0	50.8	0.98
		0.4621	0.0116	200	200	200	36.0	30.4	5.60	44.7	
20-Nov	6	0.4621	0.0116	200	200	200	47.8	41.0	6.80	32.5	0.018
21-Nov	7	0.4621	0.0116	200	200	200	23.8	16.4	7.40	26.4	0.036
22-Nov	8	0.4621	0.0116	200	200	200	16.2	8.50	7.70	23.4	0.142
27-Nov	13	0.4621	0.0116	200	200	200	30.2	22.6	7.60	24.4	0.089
28-Nov	14	0.4621	0.0116	200	200	200	7.90	0.30	7.60	24.4	0.018
30-Nov	16	0.4621	0.0116	200	200	200	7.80	0.000	7.80	22.4	0.142
06-Dec	22	0.4621	0.0116	200	200	200	14.8	7.50	7.30	27.4	0.11
08-Dec	24	0.4621	0.0231	200	200	200	50.0	36.7	17.1	29.5	0.51
12-Dec	28	0.4621	0.0416	150	150	150	18.7	0.60	18.1	90.5	1.16
13-Dec	29	0.4621	0.0231	150	150	150	13.9	5.50	8.40	67.1	1.17
14-Dec	30	0.4621	0.0139	150	150	150	35.8	28.5	7.30	17.3	0.30
15-Dec	31	0.4621	0.0508	150	150	150	50.0	28.0	25.1	80.8	1.41
19-Dec	35	0.4621	0.0400	200	200	200	50.0	43.1	25.8	89.7	1.14

22-Dec	38	0.4621	0.0578	150	150	150	50.0	42.4	25.8	88.4	1.32
27-Dec	43	0.4621	0.0424	150	150	150	45.5	26.6	18.9	87.4	1.53
29-Dec	45	0.4621	0.0385	150	150	150	27.1	9.20	17.9	72.2	1.26
03-Jan	50	0.4621	0.0308	200	200	200	33.4	15.1	18.3	85.0	1.48
04-Jan	51	0.4621	0.0231	150	150	150	21.4	11.5	9.90	51.8	-0.17
07-Jan	54	0.4621	0.0270	150	150	150	1.90	0.50	11.4	62.0	1.08
10-Jan	57	0.4621	0.0270	150	150	150	8.85	6.80	12.1	55.4	0.97
12-Jan	59	0.4621	0.0193	150	150	150	20.1	18.15	12.0	5.60	-0.56
26-Jan	73	0.4621	0.0289	150	150	150			12.4	64.6	1.41
		0.4621	0.0250	150	150	150			13.5	28.0	
29-Jan	76	0.0433	0.0130	100	100	100	49.0	0.000	49.0	10.5	0.030
30-Jan	77	0.0433	0.0130	100	100	100	39.1	0.000	39.1	19.9	0.13
31-Jan	78	0.0433	0.0127	100	100	100	43.6	0.000	43.6	14.3	-0.009
02-Feb	80	0.0459	0.0130	100	100	100	36.5	0.000	36.5	20.3	0.065
05-Feb	83	0.0459	0.0132	100	100	100	36.8	0.000	36.8	20.9	0.37
08-Feb	86	0.0459	0.0132	100	100	100	40.8	0.000	40.8	16.9	0.29
09-Feb	87	0.0459	0.0093	100	100	100	37.6	0.000	37.6	3.00	-0.081
12-Feb	90	0.0414	0.0093	100	100	100	40.1	0.10	40.0	4.50	-0.071
14-Feb	92	0.0414	0.0094	100	100	100	41.0	0.000	41.0	4.10	0.014
16-Feb	94	0.0414	0.0094	100	100	100	36.9	0.000	36.9	7.80	-0.008
20-Feb	98	0.0414	0.0097	100	100	100	38.2	0.000	38.2	7.90	0.045
23-Feb	101	0.0550	0.0097	100	100	100	35.1	1.60	33.5	2.10	0.037
26-Feb	104	0.0550	0.0097	100	100	100	33.6	0.20	33.4	2.27	0.040
02-Mar	108	0.0466	0.0100	100	100	100	40.8	0.000	40.8	2.17	0.038
05-Mar	111	0.0466	0.0100	100	100	100	38.6	1.00	37.6	0.20	0.003
07-Mar	113	0.0466	0.0132	100	100	100	47.2	0.000	47.2	9.70	0.13
09-Mar	115	0.0436	0.0132	100	100	100	46.6	0.000	46.6	13.4	0.072
12-Mar	118	0.0436	0.0132	100	100	100	49.2	0.000	49.2	10.9	0.11
14-Mar	120	0.0436	0.0146	100	100	100	52.0	0.000	52.0	14.4	0.20
16-Mar	122	0.0436	0.0141	100	100	100	54.8	0.000	54.8	9.50	0.079

19-Mar	125	0.0436	0.0138	100	100	100	53.5	0.000	53.5	9.40	0.12
21-Mar	127	0.0432	0.0138	100	100	100	52.3	0.000	52.3	11.0	0.084
24-Mar	130	0.0432	0.0139	100	100	100	51.4	0.000	51.4	12.3	0.071
26-Mar	132	0.0432	0.0139	100	100	100	52.9	0.000	52.9	10.9	0.14
28-Mar	134	0.0478	0.0141	100	100	100	47.1	0.000	47.1	12.5	0.010
31-Mar	137	0.0478	0.0141	100	100	100	47.8	0.000	47.8	11.8	0.041
02-Apr	139	0.0478	0.0139	100	100	100	45.4	0.000	45.4	13.4	0.15
04-Apr	141	0.0478	0.0139	100	100	100	46.7	0.000	46.7	12.1	0.12
06-Apr	143	0.0484	0.0143	100	100	100	47.0	0.000	47.0	12.9	0.091
09-Apr	146	0.0484	0.0143	100	100	100	46.3	0.000	46.3	13.6	0.15
11-Apr	148	0.0484	0.0137	100	100	100	47.1	0.000	47.1	10.1	0.087
14-Apr	151	0.0484	0.0137	100	100	100	46.4	0.000	46.4	10.9	0.081
16-Apr	153	0.0484	0.0139	100	100	100	46.9	0.000	46.9	11.2	0.080
18-Apr	155	0.0484	0.0139	100	100	100	46.3	0.000	46.3	11.9	0.12
20-Apr	157	0.0484	0.014	100	100	100	47.2	0.000	47.2	11.3	0.14
25-Apr	162	0.0484	0.014	100	100	100	39.5	0.000	39.5	19.5	0.24
30-Apr	167	0.0484	0.0136	100	100	100	32.1	0.000	32.1	25.7	0.45
03-May	170	0.0484	0.0136	100	100	100	33.9	0.000	33.9	23.7	0.31

	REACTOR 2 (PET)										
Date	Time (d)	Ca (mol/L)	Cb (mol/L)	Vb0 (mL)	Vbf (mL)	Vbz (mL)	Vf (mL)	Vi (mL)	Va (mL)	mCO2 (mg)	Dt (%)
14-Nov	0	0.4621	0.0116	100	100	100	0.000	0.000	0.000	0.000	0.000
17-Nov	3	0.4621	0.0116	100	100	100	30.2	27.4	2.8	22.4	-0.905
		0.4621	0.0116	100	100	100	48.6	45.4	2.8	22.4	
18-Nov	4	0.4621	0.0116	100	100	100	5.20	4.90	3.20	18.3	-0.51
19-Nov	5	0.4621	0.0116	200	200	200	24.3	16.1	0.30	98.6	1.03
20-Nov	6	0.4621	0.0116	200	200	200	9.50	1.20	8.20	18.3	-0.23
21-Nov	7	0.4621	0.0116	200	200	200	40.1	31.4	8.30	17.3	-0.12
27-Nov	13	0.4621	0.0116	200	200	200	37.5	30.2	7.30	27.4	0.14
28-Nov	14	0.4621	0.0116	200	200	200	16.6	7.90	8.70	13.2	-0.18
30-Nov	16	0.4621	0.0116	200	200	200	16.2	7.80	8.40	16.3	0.036
06-Dec	22	0.4621	0.0116	200	200	200	22.9	14.8	8.10	19.3	-0.036
08-Dec	24	0.4621	0.0416	150	150	150	22.4	3.80	18.6	85.4	1.49
12-Dec	28	0.4621	0.0231	150	150	150	27.2	18.7	8.50	66.1	0.73
13-Dec	29	0.4621	0.0139	150	150	150	21.4	13.9	7.50	15.2	0.27
14-Dec	30	0.4621	0.0508	150	150	150	50.0	35.8	25.0	81.3	1.42
19-Dec	35	0.4621	0.0578	200	200	4	19.7	18.9	0.80	102	1.35
22-Dec	38	0.4621	0.0424	150	150	150	50.0	42.7	19.8	78.3	1.14
27-Dec	43	0.4621	0.0385	200	200	200	40.6	14.7	25.9	75.5	1.32
29-Dec	45	0.4621	0.0308	200	200	200	44.9	27.1	17.8	90.1	1.57
03-Jan	50	0.4621	0.0231	200	200	200	46.5	33.4	13.1	70.1	1.22
04-Jan	51	0.4621	0.0270	200	200	200	49.1	33.7	19.4	40.0	-0.38
07-Jan	54	0.4621	0.0270	200	200	200	3.30	1.90	16.4	70.5	1.23
10-Jan	57	0.4621	0.0193	150	150	150	11.2	8.85	12.3	2.03	0.036
12-Jan	59	0.4621	0.0300	150	150	150	26.1	8.1	18.0	15.0	0.26
15-Jan	62	0.4621	0.0250	150	150	150	16.0	0.000	16.0	2.54	-0.11
26-Jan	73	0.4621	0.0300	150	150	150	15.0	0.000	15.0	45.5	-0.61

29-Jan	76	0.0433	0.0130	100	100	100	50.0	0	51.3	8.29	-0.008
30-Jan	77	0.0433	0.0130	100	100	100	45.0	0.10	44.9	14.4	0.029
31-Jan	78	0.0433	0.0127	100	100	100	46.7	0.000	46.7	11.4	-0.061
02-Feb	80	0.0459	0.0130	100	100	100	38.9	0.000	38.9	17.9	0.023
05-Feb	83	0.0459	0.0132	100	100	100	35.5	0.000	35.5	22.2	0.39
08-Feb	86	0.0459	0.0132	100	100	100	39.9	0.000	39.9	17.8	0.31
09-Feb	87	0.0459	0.0093	100	100	100	37.8	0.000	37.8	2.75	-0.085
12-Feb	90	0.0414	0.0093	100	100	100	39.6	0.000	39.6	4.85	-0.065
14-Feb	92	0.0414	0.0094	100	100	100	39.2	0.1.000	39.1	5.75	0.043
16-Feb	94	0.0414	0.0094	100	100	100	41.5	6.00	34.6	9.90	0.030
20-Feb	98	0.0414	0.0097	100	100	100	35.9	0.000	35.9	9.98	0.081
23-Feb	101	0.0500	0.0097	100	100	100	40.2	6.10	34.1	5.17	0.090
26-Feb	104	0.0550	0.0097	100	100	100	34.5	0.1	34.4	1.12	0.019
02-Mar	108	0.0466	0.0100	100	100	100	42.3	0.0	42.3	0.63	0.011
05-Mar	111	0.0466	0.0120	100	100	100	50.0	0.0	50.0	1.54	0.027
07-Mar	113	0.0466	0.0132	100	100	100	50.0	2.00	49.0	7.85	0.10
09-Mar	115	0.0436	0.0132	100	100	100	43.2	0.10	44.1	15.8	0.11
12-Mar	118	0.0436	0.0146	100	100	100	50.2	0.000	55.8	10.7	0.11
14-Mar	120	0.0436	0.0141	100	100	100	53.3	0.000	53.3	10.9	0.14
16-Mar	122	0.0436	0.0141	100	100	100	54.0	0.000	54.0	10.2	0.093
19-Mar	125	0.0432	0.0138	100	100	100	53.4	0.000	53.4	9.97	0.13
21-Mar	127	0.0432	0.0138	100	100	100	52.4	0.000	52.4	10.9	0.082
24-Mar	130	0.0432	0.0139	100	100	100	51.0	0.000	51.0	12.7	0.078
26-Mar	132	0.0432	0.0139	100	100	100	53.0	0.000	53.0	10.8	0.13
28-Mar	134	0.0478	0.0141	100	100	100	48.0	0.000	48.0	11.6	0.083
31-Mar	137	0.0478	0.0141	100	100	100	47.5	0.000	47.5	12.1	0.047
02-Apr	139	0.0478	0.0139	100	100	100	46.0	0.000	46.0	12.8	0.14
04-Apr	141	0.0478	0.0139	100	100	100	46.3	0.000	46.3	12.5	0.13
06-Apr	143	0.0484	0.0143	100	100	100	45.5	0.000	45.5	14.5	0.12
09-Apr	146	0.0484	0.0143	100	100	100	44.8	0.10	44.7	15.3	0.18
11-Apr	148	0.0484	0.0137	100	100	100	44.8	0.000	44.8	12.6	0.13

14-Apr	151	0.0484	0.0137	100	100	100	47.6	0.000	47.6	9.60	0.059
16-Apr	153	0.0484	0.0139	100	100	100	47.5	0.000	47.5	10.6	0.069
18-Apr	155	0.0484	0.0139	100	100	100	46.4	0.000	46.4	11.8	0.12
20-Apr	157	0.0484	0.014	100	100	100	46.2	0.000	46.2	12.4	0.16
25-Apr	162	0.0484	0.014	100	100	100	39.1	0.000	39.1	20.0	0.25
30-Apr	167	0.0484	0.0136	100	100	100	37.7	0.000	37.7	19.7	0.34
03-May	170	0.0484	0.0136	100	100	100	40.6	0.000	40.6	16.6	0.19

	REACTOR 3 (PCL)										
Date	Time (d)	Ca (mol/L)	Cb (mol/L)	Vb0 (mL)	Vbf (mL)	Vbz (mL)	Vf (mL)	Vi (mL)	Va (mL)	mCO2 (mg)	Dt (%)
14-Nov	0	0.4621	0.0116	100	100	100			10.0	0.000	0.000
17-Nov	3	0.4621	0.0116	100	100	100			0.000	50.8	
		0.4621	0.0116	100	100	100			0.000	50.8	
		0.4621	0.0116	100	100	100			0.000	50.8	0.98
		0.4621	0.0116	100	100	100	41.4	36.5	4.90	1.01	
18-Nov	4	0.4621	0.0116	200	200	200			0.000	101	1.98
		0.4621	0.0116	200	200	200	16.1	12.1	4.00	61.0	
19-Nov	5	0.4621	0.0116	200	200	200	full		0.000	101	1.95
		0.4621	0.0116	200	200	200	41.0	36.0	5.00	50.8	
20-Nov	6	0.4621	0.0116	200	200	200	51.2	47.8	3.40	67.1	0.61
21-Nov	7	0.4621	0.0116	200	200	200	45.7	40.1	5.60	44.7	0.35
22-Nov	8	0.4621	0.0116	200	200	200	22.5	16.9	5.60	44.7	0.51
27-Nov	13	0.4621	0.0116	200	200	200	41.4	37.5	3.90	62.0	0.74
28-Nov	14	0.4621	0.0116	200	200	200	22.3	16.6	5.70	43.7	0.35
30-Nov	16	0.4621	0.0116	200	200	200	23.5	16.2	7.30	27.4	0.23
02-Dec	18	0.4621	0.0116	200	200	200	40.4	33.0	7.40	26.4	0.46
04-Dec	20	0.4621	0.0231	200	200	200	50.0	42.9	13.6	65.0	1.12

06-Dec	22	0.4621	0.0231	100	100	100	28.3	22.9	5.40	46.8	0.44
08-Dec	24	0.4621	0.0289	150	150	150	40.0	22.4	17.6	11.7	0.20
10-Dec	26	0.4621	0.0416	150	150	150	41.7	23.2	18.5	86.4	2.70
		0.4621	0.0231	150	150	150	49.9	41.7	8.20	69.6	
12-Dec	28	0.4621	0.0231	150	150	150	35.2	27.2	8.00	71.1	0.81
13-Dec	29	0.4621	0.0231	100	100	100	27.4	21.4	6.00	40.7	0.70
14-Dec	30	0.4621	0.0139	150	150	150	26.5	21.0	5.50	35.8	0.61
15-Dec	31	0.4621	0.0508	150	150	150	50.0	28.4	23.4	97.6	1.69
19-Dec	35	0.4621	0.0277	200	200	200	41.3	22.8	18.6	55.4	2.04
		0.4621	0.0578	200	200	7	21.7	20.3	1.50	87.1	
22-Dec	38	0.4621	0.0424	150	150	150	34.9	15.2	19.7	79.3	1.15
27-Dec	43	0.4621	0.0424	150	150	150	50.0	45.5	19.2	84.4	1.46
29-Dec	45	0.4621	0.0385	150	150	150	50.0	41.2	17.9	72.2	1.25
03-Jan	50	0.4621	0.0308	200	200	200	15.0	0.70	14.3	125	2.17
04-Jan	51	0.4621	0.0231	200	200	200	11.5	0.70	19.9	0.10	-1.05
07-Jan	54	0.4621	0.0270	150	150	150	15.0	3.30	17.1	4.05	0.07
10-Jan	57	0.4621	0.0270	150	150	150	23.0	11.15	16.9	6.59	0.11
12-Jan	59	0.4621	0.0193	150	150	150	30.3	26.7	10.6	19.3	-0.32
15-Jan	62	0.4621	0.0270	150	150	150	43.2	39.2	16.8	7.10	-0.03
26-Jan	73	0.4621	0.0250	150	150	150	50.0	37.4	12.6	36.9	1.50
		0.1092	0.0250	150	150	150	50.0	38.5	50.0	44.9	
		0.1092	0.0250	150	150	150	50.0	16.8	33.2	85.2	
29-Jan	76	0.0433	0.0130	200	200	200	50.0	0.000	58.0	59.1	0.87
30-Jan	77	0.0433	0.0130	100	100	100	34.1	1.00	33.1	25.6	0.22
31-Jan	78	0.0433	0.0127	100	100	100	36.0	0.000	36.0	21.6	0.12
02-Feb	80	0.0459	0.0130	100	100	100	47.5	15.65	31.9	25.0	0.15
05-Feb	83	0.0459	0.0132	100	100	100	19.5	0.10	19.4	38.5	0.67
08-Feb	86	0.0459	0.0132	100	100	100	28.9	0.000	28.9	28.9	0.50
09-Feb	87	0.0459	0.0093	100	100	100	27.7	0.000	27.7	12.9	0.093
12-Feb	90	0.0414	0.0093	100	100	100	30.9	0.000	30.9	12.8	0.073

13-Feb	91	0.0414	0.0094	100	100	100	49.4	17.1	32.3	11.9	0.21
14-Feb	92	0.0414	0.0094	100	100	100	36.1	0.0	36.1	8.5	0.090
15-Feb	93	0.0414	0.0093	100	100	100	46.0	10.0	36.0	8.1	0.14
16-Feb	94	0.0414	0.0094	100	100	100	29.5	0.10	29.4	14.6	0.11
20-Feb	98	0.0414	0.0097	100	100	100	34.0	10.0	24.0	20.8	0.27
21-Feb	99	0.0414	0.0097	100	100	100	34.8	0.0	34.8	11.0	0.19
23-Feb	101	0.0414	0.0089	100	100	100	43.9	21.5	24.9	16.5	0.28
26-Feb	104	0.055	0.0089	100	100	100	47.0	20.0	27.0	6.49	0.11
28-Feb	106	0.0539	0.0100	100	100	100	48.1	11.0	37.1	0.007	0.000
02-Mar	108	0.0466	0.0097	100	100	100	37.0	0.0	37.0	4.75	0.082
05-Mar	111	0.0466	0.0097	100	100	100	37.6	0.0	37.6	4.13	0.071
07-Mar	113	0.0466	0.0132	100	100	100	36.1	0.0	36.1	21.1	0.33
09-Mar	115	0.0436	0.0132	100	100	100	38.5	0.0	38.5	21.2	0.21
12-Mar	118	0.0436	0.0146	100	100	100	48.4	0.0	48.4	17.8	0.23
14-Mar	120	0.0436	0.0141	100	100	100	50.0	5.40	45.7	18.2	0.26
16-Mar	122	0.0436	0.0141	100	100	100	47.3	0.0	48.4	15.6	0.18
19-Mar	125	0.0436	0.0138	100	100	100	47.8	0.0	47.8	14.9	0.21
21-Mar	127	0.0432	0.0138	100	100	100	46.0	0.0	46.0	17.0	0.19
24-Mar	130	0.0432	0.0139	100	100	100	44.5	0.0	44.5	18.9	0.18
26-Mar	132	0.0432	0.0139	100	100	100	44.7	0.0	44.7	18.7	0.27
28-Mar	134	0.0478	0.0141	100	100	100	41.9	0.0	41.9	18.0	0.19
31-Mar	137	0.0478	0.0141	100	100	100	39.5	0.0	39.5	20.5	0.19
02-Apr	139	0.0478	0.0139	100	100	100	39.0	0.0	39.0	20.1	0.26
04-Apr	141	0.0478	0.0139	100	100	100	43.2	0.0	43.2	15.7	0.19
06-Apr	143	0.0478	0.0143	100	100	100	44.8	0.0	44.8	15.8	0.14
09-Apr	146	0.0484	0.0143	100	100	100	42.3	0.0	42.3	17.9	0.23
11-Apr	148	0.0484	0.0137	100	100	100	39.8	0.0	39.8	17.9	0.22
14-Apr	151	0.0484	0.0137	100	100	100	42.3	0.0	42.3	15.2	0.16
16-Apr	153	0.0484	0.0139	100	100	100	42.0	1.00	41.0	17.5	0.19
18-Apr	155	0.0484	0.0139	100	100	100	41.5	0.0	41.5	17.0	0.21

20-Apr	157	0.0484	0.014	100	100	100	43.0	0.0	43.0	15.8	0.22
25-Apr	162	0.0484	0.014	100	100	100	37.5	0.0	37.5	21.7	0.28
30-Apr	167	0.0484	0.0136	100	100	100	31.0	0.0	31.0	26.8	0.46
03-May	170	0.5	0.0136	100	100	100	21.8	18.0	3.80	18.0	0.21

	REACTOR 4 (Blank)										
Date	Time (d)	Ca (mol/L)	Cb (mol/L)	Vb0 (mL)	Vbf (mL)	Vbz (mL)	Vf (mL)	Vi (mL)	Va (mL)	mCO2b (mg)	Total mCO2b (mg)
14-Nov	0	0.4621	0.0116	100	100	100	50.0	0.000	0.000	0	
17-Nov	3	0.4621	0.0116	100	100	100	30.8	30.2	0.60	44.7	96.6
		0.4621	0.0116	100	100	100	45.4	43.4	2.00	30.5	
		0.4621	0.0116	100	100	100	45.3	42.4	2.90	21.3	
18-Nov	4	0.4621	0.0116	100	100	100	5.20	4.90	0.30	47.8	47.8
19-Nov	5	0.4621	0.0116	200	200	200	30.4	24.3	6.10	39.6	39.6
20-Nov	6	0.4621	0.0116	200	200	200	16.4	9.50	6.90	31.5	31.5
21-Nov	7	0.4621	0.0116	200	200	200	31.4	23.8	7.60	24.4	24.4
22-Nov	8	0.4621	0.0116	200	200	200	8.50	0.000	8.50	15.2	15.2
27-Nov	13	0.4621	0.0116	200	200	200	49.5	41.4	8.10	19.3	19.3
28-Nov	14	0.4621	0.0116	200	200	200	30.0	22.3	7.70	23.4	23.4
30-Nov	16	0.4621	0.0116	200	200	200	32.1	23.5	8.60	14.2	14.2
06-Dec	22	0.4621	0.0116	200	200	200	36.2	28.3	7.90	21.3	21.3
12-Dec	28	0.4621	0.0416	150	150	150	50.0	35.2	21.1	24.0	24.0
19-Dec	35	0.4621	0.0231	150	150	10	22.3	21.7	0.60	24.4	24.4
22-Dec	38	0.4621	0.0139	150	150	150	42.7	34.9	7.80	12.7	12.7
04-Jan	51	0.4621	0.0424	100	100	100	33.7	21.4	12.3	61.5	61.5
15-Jan	62	0.4621	0.0270	100	100	100	8.70	0.000	8.70	9.04	9.04
26-Jan	73	0.4621	0.0250	150	150	150			15.1	11.7	80.3
		0.4621	0.0289	150	150	150			12.0	68.6	
29-Jan	76	0.0433	0.0130	100	100	100	43.0	0.000	50.8	8.76	8.76

30-Jan	77	0.0433	0.013	100	100	100			46.7	12.7	12.7
31-Jan	78	0.0459	0.0127	100	100	100	40.6	0.000	40.6	14.9	14.9
02-Feb	80	0.0459	0.0130	100	100	100	40.2	0.000	40.2	16.6	16.6
09-Feb	87	0.0459	0.0132	100	100	100	50.0	0.000	50.0	7.59	34.27
12-Feb	90	0.0414	0.0094	100	100	100	36.0	0.000	36.0	8.57	8.57
14-Feb	92	0.0414	0.0094	100	100	100	41.8	0.000	41.8	3.29	3.29
16-Feb	94	0.0414	0.0097	100	100	100	38.0	0.15	37.9	8.21	8.21
20-Feb	98	0.0414	0.0097	100	100	100	43.0	2.00	41.0	5.34	5.34
07-Mar	113	0.0466	0.0132	100	100	100	50.0	0.000	54.7	2.00	2.00
09-Mar	115	0.0436	0.0146	100	100	100	50.0	0.000	57.3	9.28	9.28
12-Mar	118	0.0436	0.0141	100	100	100	59.9	0.000	59.9	4.58	4.58
14-Mar	120	0.0436	0.0141	100	100	100	61.6	0.000	61.6	2.95	2.95
16-Mar	122	0.0436	0.0138	100	100	100	58.2	0.000	58.2	4.94	4.94
19-Mar	125	0.0432	0.0138	100	100	100	61.1	0.000	61.1	2.65	2.65
21-Mar	127	0.0432	0.0139	100	100	100	57.8	0.000	57.8	6.23	6.23
24-Mar	130	0.0432	0.0139	100	100	100	55.7	0.000	55.7	8.22	8.22
26-Mar	132	0.0432	0.0141	100	100	100	62.0	0.000	62.0	3.12	3.12
28-Mar	134	0.0478	0.0141	100	100	100	52.5	0.000	52.5	6.83	6.83
31-Mar	137	0.0478	0.0139	100	100	100	49.2	0.000	49.2	9.42	9.42
02-Apr	139	0.0478	0.0139	100	100	100	53.4	0.000	53.4	5.00	5.00
04-Apr	141	0.0478	0.0143	100	100	100	55.1	0.000	55.1	4.98	4.98
06-Apr	143	0.0484	0.0143	100	100	100	51.9	0.000	51.9	7.66	7.66
09-Apr	146	0.0484	0.0137	100	100	100	52.1	0.000	52.1	4.80	4.80
11-Apr	148	0.0484	0.0137	100	100	100	51.8	0.000	51.8	5.12	5.12
14-Apr	151	0.0484	0.0139	100	100	100	51.6	0.000	51.6	6.22	6.22
16-Apr	153	0.0484	0.0139	100	100	100	51.2	0.000	51.2	6.64	6.64
18-Apr	155	0.0484	0.014	100	100	100	53.1	0.000	53.1	5.06	5.06
20-Apr	157	0.0484	0.014	100	100	100	54.7	0.000	54.7	3.36	3.36
25-Apr	162	0.0484	0.0136	100	100	100	51.0	0.000	51.0	5.54	5.54
03-May	170	0.5	0.0136	100	100	100	26.7	21.8	4.90	5.94	5.94

- Descriptive statistics and data analysis

		Evolved CO_2 (mg)								%Biodegradation (Dt)					
Date	Residence Time (d)	Reactor 1 PET 1	Reactor 2 PET 2	PET *M*	PET *SD*	Reactor 3 PCL	PCL Error	Reactor 4 blank	Blank error	Reactor 1 PET 1	Reactor 2 PET 2	PET *M*	PET *SD*	Reactor 3 PCL	PCL Error
Nov 14	0	0.000	0.000	0.000	0.000	0.000	0.000	0.000	0.000	0.000	0.000	0.000	0.000	0.000	0.000
Nov 17	3	129	44.7	86.9	59.6	153	1.17	96.6	1.17	0.57	-0.90	-0.17	1.04	0.98	0.0003
Nov 18	4	51.8	18.3	35.1	23.7	163	1.17	47.8	1.17	0.071	-0.51	-0.22	0.41	1.98	0.0003
Nov 19	5	95.6	98.6	97.1	2.12	152	1.16	39.6	1.15	0.98	1.03	1.01	0.035	1.95	0.0003
Nov 20	6	32.5	18.3	25.4	10.0	67.1	1.16	31.5	1.15	0.018	-0.23	-0.11	0.18	0.61	0.0003
Nov 21	7	26.4	17.3	21.9	6.43	44.7	1.15	24.4	1.15	0.036	-0.12	-0.042	0.11	0.35	0.0003
Nov 22	8	23.4	-	23.4	-	44.7	1.15	15.2	1.14	0.14	-	0.14		0.51	0.0003
Nov 27	13	24.4	27.4	25.9	2.12	62.0	1.16	19.3	1.15	0.089	-0.12	0.11	0.036	0.74	0.0003
Nov 28	14	24.4	13.2	18.8	7.92	43.7	1.15	23.4	1.15	0.018	-0.18	-0.081	0.14	0.35	0.0003
Nov 30	16	22.4	16.3	19.4	4.31	27.4	1.15	14.2	1.14	0.14	0.036	0.088	0.074	0.23	0.0003
Dec 06	22	27.4	19.3	23.4	5.73	138	1.16	21.3	1.15	0.11	-0.036	0.037	0.10	2.02	0.0003
Dec 08	24	29.5	85.4	57.5	39.5	11.7	1.12	-	-	0.51	1.49	1.00	0.69	0.20	0.0002
Dec 12	28	90.5	66.1	78.3	17.3	227	1.15	24.0	1.11	1.16	0.73	0.95	0.30	3.51	0.0003
Dec 13	29	67.1	15.2	41.2	36.7	40.7	1.15	-	-	1.17	0.27	0.72	0.64	0.70	0.0002
Dec 14	30	17.3	81.3	49.3	45.3	35.6	1.15	-	-	0.30	1.42	0.86	0.79	0.61	0.0002
Dec 15	31	80.8	-	80.8	-	97.6	1.10	-	-	1.41	-	1.41		1.69	0.0002
Dec 19	35	89.7	101.6	95.7	-	143	1.14	24.4	1.17	-	1.35	1.35		2.04	0.0003
Dec 22	38	88.4	78.3	83.4	7.14	79.3	1.11	12.7	1.15	1.32	1.14	1.23	0.13	1.15	0.0003
Dec 27	43	87.4	75.5	81.5	8.41	84.4	1.11	-	-	1.53	1.32	1.43	0.15	1.46	0.0002
Dec 29	45	72.2	90.1	81.2	12.7	72.2	1.12	-	-	1.26	1.57	1.42	0.22	1.25	0.0002
Jan 03	50	85.0	70.1	77.6	10.5	126	1.13	-	-	1.48	1.22	1.35	0.18	2.17	0.0002
Jan 04	51	51.8	40.0	45.9	8.34	1.00	1.11	61.5	1.13	-0.17	-0.38	-0.28	0.15	-1.05	-0.0003
Jan 07	54	62.0	70.5	66.3	6.01	4.05	1.12	-	-	1.08	1.23	1.16	0.11	0.070	0.0002
Jan 10	57	55.4	2.03	28.7	37.7	6.59	1.12	-	-	0.97	0.036	0.50	0.66	0.11	0.0002

Jan 12	59	5.60	15.0	10.3	-	19.3	1.14	-	1.12	0.098	0.26	-0.56		0.33	-0.0003
Jan 15	62	96.6	2.54	49.6	-	7.10	1.12	9.04	1.14	1.53	-0.11	-0.11		-0.034	-0.0003
Jan 26	73	92.5	45.5	69.0	38.5	167	0.91	80.3	1.13	0.21	-0.608	0.94	0.67	1.50	0.0003
Jan 29	76	10.5	8.29	9.40	1.56	59.1	0.74	8.76	0.77	0.030	-0.008	0.011	0.027	0.87	0.0002
Jan 30	77	19.9	14.4	17.2	3.89	25.6	0.83	12.7	0.78	0.13	0.029	0.080	0.071	0.22	0.0002
Jan 31	78	14.3	11.4	12.9	2.05	21.6	0.82	14.9	0.80	-0.009	-0.061	-0.035	0.037	0.12	0.0002
Feb 02	80	20.3	17.9	19.1	1.70	25.0	0.83	16.6	0.80	0.065	0.023	0.044	0.030	0.15	0.0002
Feb 05	83	20.9	22.2	21.6	0.92	38.5	0.88	26.7	-	-0.10	-0.078	0.38	0.014	0.20	0.0002
Feb 08	86	16.9	17.8	17.4	0.64	28.9	0.85	-	-	0.29	0.31	0.30	0.014	0.50	0.0001
Feb 09	87	2.95	2.75	2.85	0.14	12.9	0.83	7.59	0.77	-0.081	-0.085	-0.083	0.003	0.093	0.0002
Feb 12	90	4.50	4.85	4.68	0.25	12.8	0.82	8.57	0.80	-0.071	-0.065	-0.068	0.004	0.073	0.0002
Feb 14	92	4.06	5.75	4.91	1.20	20.4	0.80	3.29	0.78	0.014	0.043	0.029	0.021	0.090	0.0002
Feb 16	94	7.75	9.89	8.82	1.51	14.6	0.83	8.21	0.80	-0.008	0.029	0.011	0.026	0.11	0.0002
Feb 20	98	7.89	9.98	8.94	1.48	20.8	0.85	5.34	0.79	0.045	0.081	0.063	0.025	0.27	0.0002
Feb 23	99	2.15	5.17	3.66	2.14	16.5	0.85	-	-	0.037	0.090	0.064	0.037	0.19	0.0001
Feb 26	104	2.27	1.12	1.69	-	6.49	0.83	-	-	0.040	0.019			0.40	0.0001
Mar 02	108	2.17	0.634	1.40	-	4.75	0.79	-	-	0.038	0.011			0.082	0.0001
Mar 05	111	5.45	1.54	3.49	-	4.13	0.79	-	-	0.095	0.027	0.003		0.071	0.0001
Mar 07	113	9.69	7.85	8.77	1.30	21.07	0.82	2.00	0.75	0.134	0.102	0.12	0.021	0.33	0.0002
Mar 09	115	13.4	15.8	14.6	1.70	21.15	0.81	9.28	0.75	0.072	0.114	0.091	0.027	0.21	0.0002
Mar 12	118	10.9	10.7	10.8	0.14	17.81	0.79	4.58	0.74	0.110	0.107	0.11	0.000	0.23	0.0002
Mar 14	120	14.4	10.9	12.7	2.47	18.20	0.79	2.95	0.73	0.199	0.139	0.17	0.042	0.26	0.0002
Mar 16	122	9.48	10.2	9.84	0.51	15.61	0.78	4.94	0.74	0.079	0.093	0.086	0.010	0.18	0.0002
Mar 19	125	9.40	9.97	9.69	0.40	14.87	0.78	2.65	0.73	0.118	0.128	0.13	0.007	0.21	0.0002
Mar 21	127	11.0	10.9	11.0	0.07	17.00	0.79	6.23	0.75	0.084	0.082	0.083	0.001	0.19	0.0002
Mar 24	130	12.3	12.7	12.5	0.28	18.87	0.80	8.22	0.76	0.071	0.078	0.075	0.005	0.18	0.0002
Mar 26	132	10.9	10.8	10.9	0.07	18.68	0.80	3.12	0.73	0.136	0.134	0.14	0.007	0.27	0.0002
Mar 28	134	12.5	11.6	12.1	0.64	17.98	0.80	6.83	0.76	0.099	0.083	0.091	0.011	0.19	0.0002
Mar 31	137	11.8	12.1	12.0	0.21	20.50	0.81	9.42	0.77	0.041	0.047	0.044	0.004	0.19	0.0002
Apr 02	139	13.4	12.8	13.1	0.42	20.15	0.81	5.00	0.75	0.147	0.136	0.15	0.007	0.26	0.0002

Apr 04	141	12.1	12.5	12.3	0.28	15.73	0.79	4.98	0.75	0.124	0.131	0.13	0.007	0.19	0.0002
Apr 06	143	12.9	14.5	13.7	1.13	15.81	0.79	7.66	0.76	0.091	0.119	0.11	0.021	0.14	0.0002
Apr 09	146	13.6	15.3	14.5	1.20	17.88	0.80	4.80	0.76	0.154	0.184	0.17	0.021	0.23	0.0002
Apr 11	148	10.1	12.6	11.4	1.77	17.90	0.80	5.12	0.76	0.087	0.130	0.11	0.030	0.22	0.0002
Apr 13	150	10.9	9.60	10.3	0.92	15.24	0.79	6.22	0.76	0.081	0.059	0.070	0.016	0.16	0.0002
Apr 16	153	11.2	10.6	10.9	0.42	17.50	0.80	6.64	0.76	0.080	0.069	0.075	0.008	0.19	0.0002
Apr 18	155	11.9	11.8	11.9	0.071	16.97	0.80	5.06	0.76	0.119	0.117	0.12	0.000	0.21	0.0002
Apr 20	157	11.3	12.4	11.9	0.78	15.81	0.79	3.36	0.75	0.139	0.158	0.15	0.014	0.22	0.0002
Apr 25	162	19.5	20.0	19.8	0.35	21.67	0.81	5.54	0.76	0.245	0.252	0.25	0.007	0.28	0.0002
Apr 30	167	25.7	19.7	22.7	4.24	26.83	0.84	-	-	0.449	0.344	0.40	0.078	0.46	0.0001
May 03	170	23.7	16.6	20.2	5.02	18.04	1.20	5.94	1.19	0.311	0.186	0.25	0.085	0.21	0.0003

		Cumulative evolved CO2 (mg)								Cumulative %Biodegradation (Dt)					
Date	Residence Time (d)	Reactor 1 PET 1	Reactor 2 PET 2	PET *M*	PET *SD*	Reactor 3 PCL	PCL Error	Reactor 4 blank	Blank error	Reactor 1 PET 1	Reactor 2 PET 2	PET *M*	PET *SD*	Reactor 3 PCL	PCL Error
Nov 14	0	0.0	0.0	0.0	0.00	0	0	0	0	0.00	0.0	0.00	0.00	0.00	0
Nov 17	3	129.1	44.7	86.9	59.7	153	1.17	96.6	1.17	0.57	-0.9	-0.2	1.04	0.98	0.0003
Nov 18	4	180.9	63.0	122.0	83.4	316	2.33	144	2.34	0.64	-1.4	-0.4	1.46	2.97	0.0006
Nov 19	5	276.5	161.6	219.1	81.2	469	3.50	184	3.49	1.62	-0.4	0.6	1.42	4.92	0.0009
Nov 20	6	309.0	179.9	244.5	91.3	536	4.66	215	4.64	1.63	-0.6	0.5	1.59	5.53	0.001
Nov 21	7	335.5	197.2	266.3	97.8	580	5.81	240	5.79	1.67	-0.7	0.5	1.71	5.88	0.001
Nov 22	8	358.8	197.2	278.0	114	625	6.97	255	6.93	1.81	-0.7	0.5	1.81	6.39	0.002
Nov 27	13	383.2	224.6	303.9	112	687	8.13	274	8.08	1.90	-0.9	0.5	1.96	7.13	0.002
Nov 28	14	407.6	237.8	322.7	120	731	9.28	298	9.22	1.92	-1.0	0.4	2.10	7.48	0.002
Nov 30	16	430.0	254.1	342.0	124	758	10.4	312	10.4	2.06	-1.0	0.5	2.17	7.71	0.003
Dec 06	22	457.4	273.4	365.4	130	896	11.6	333	11.5	2.17	-1.0	0.6	2.27	9.73	0.003
Dec 08	24	486.9	358.8	422.8	90.6	908	12.7	333	11.5	2.68	0.4	1.6	1.58	9.93	0.003
Dec 12	28	577.4	424.8	501.1	108	1135	13.8	357	12.6	3.84	1.2	2.5	1.88	13.44	0.003
Dec 13	29	644.5	440.1	542.3	145	1176	15.0	357	12.6	5.01	1.4	3.2	2.52	14.14	0.003
Dec 14	30	661.8	521.4	591.6	99.3	1212	16.2	357	12.6	5.32	2.9	4.1	1.73	14.76	0.004
Dec 15	31	742.6	521.4	632.0	156	1309	17.3	357	12.6	6.73	2.9	4.8	2.73	16.44	0.004
Dec 19	35	832.3	623.0	727.6	148	1452	18.4	382	13.8	7.87	4.2	6.0	2.59	18.48	0.004
Dec 22	38	920.7	701.2	811.0	155	1531	19.5	394	14.9	9.19	5.4	7.3	2.71	19.64	0.004
Dec 27	43	1008.2	776.8	892.5	164	1615	20.6	394	14.9	10.72	6.7	8.7	2.86	21.09	0.005
Dec 29	45	1080.3	866.9	973.6	151	1687	21.7	394	14.9	11.98	8.3	10.1	2.64	22.34	0.005
Jan 03	50	1165.4	937.0	1051.2	162	1813	22.9	394	14.9	13.46	9.5	11.5	2.82	24.51	0.005
Jan 04	51	1217.2	977.0	1097.1	170	1814	24.0	456	16.1	13.29	9.1	11.2	2.97	23.47	0.005
Jan 07	54	1279.2	1047.4	1163.3	163.9	1818	25.1	456	16.1	14.38	10.3	12.4	2.86	23.54	0.005
Jan 10	57	1334.6	1049.5	1192.0	202	1825	26.2	456	16.1	15.35	10.4	12.9	3.52	23.65	0.005
Jan 12	59	1340.2	1064.5	1202.3	195	1844	27.3	456	17.2	15.44	10.6	13.0	3.41	23.98	0.005

Jan 15	62	1436.8	1067.0	1251.9	261	1851	28.5	465	18.3	16.97	10.5	13.7	4.57	23.95	0.005
Jan 26	73	1529.3	1112.5	1320.9	295	2018	29.4	545	19.5	17.19	9.9	13.5	5.15	25.45	0.005
Jan 29	76	1539.8	1120.8	1330.3	296	2077	30.1	554	20.2	17.22	9.9	13.6	5.17	26.32	0.005
Jan 30	77	1559.7	1135.2	1347.5	300	2103	30.9	567	21.0	17.34	9.9	13.6	5.24	26.54	0.005
Jan 31	78	1574.1	1146.6	1360.3	302	2124	31.8	582	21.8	17.33	9.9	13.6	5.28	26.66	0.005
Feb 02	80	1594.4	1164.5	1379.5	304	2149	32.6	598	22.6	17.40	9.9	13.6	5.31	26.80	0.006
Feb 05	83	1615.3	1186.7	1401.0	303	2188	33.5	625	22.6	17.30	9.8	13.6	5.29	27.00	0.006
Feb 08	86	1632.2	1204.5	1418.4	302	2217	34.3	625	22.6	17.59	10.1	13.9	5.28	27.50	0.006
Feb 09	87	1635.2	1207.3	1421.2	303	2230	35.2	633	23.4	17.51	10.0	13.8	5.28	27.60	0.006
Feb 12	90	1639.7	1212.1	1425.9	302	2243	36.0	641	24.2	17.44	10.0	13.7	5.28	27.67	0.006
Feb 14	92	1643.7	1217.9	1430.8	301	2263	36.8	644	25.0	17.45	10.0	13.7	5.26	27.97	0.006
Feb 16	94	1651.5	1227.8	1439.6	300	2286	37.6	653	25.8	17.44	10.0	13.7	5.23	28.22	0.007
Feb 20	98	1659.4	1237.7	1448.5	298	2307	38.4	658	26.6	17.49	10.1	13.8	5.21	28.48	0.007
Feb 23	99	1659.4	1237.7	1448.5	298	2318	39.3	658	26.6	17.49	10.1	13.8	5.21	28.67	0.007
Feb 26	104	1663.8	1244.0	1453.9	297	2340	40.1	658	26.6	17.57	10.2	13.9	5.18	29.07	0.007
Mar 02	108	1665.9	1244.7	1455.3	298	2345	40.9	658	26.6	17.60	10.2	13.9	5.20	29.15	0.007
Mar 05	111	1671.4	1246.2	1458.8	301	2349	41.7	658	26.6	17.70	10.3	14.0	5.25	29.22	0.007
Mar 07	113	1681.1	1254.0	1467.6	302	2370	42.5	660	27.3	17.83	10.4	14.1	5.27	29.55	0.008
Mar 09	115	1694.5	1269.8	1482.1	300	2392	43.3	669	28.1	17.90	10.5	14.2	5.24	29.76	0.008
Mar 12	118	1705.4	1280.5	1492.9	300	2409	44.1	674	28.8	18.01	10.6	14.3	5.25	29.99	0.008
Mar 14	120	1719.7	1291.5	1505.6	303	2428	44.9	677	29.5	18.21	10.7	14.5	5.29	30.25	0.008
Mar 16	122	1729.2	1301.7	1515.4	302	2443	45.7	682	30.3	18.29	10.8	14.6	5.28	30.43	0.008
Mar 19	125	1738.6	1311.7	1525.1	302	2458	46.5	684	31.0	18.41	11.0	14.7	5.27	30.65	0.009
Mar 21	127	1749.6	1322.6	1536.1	302	2475	47.3	691	31.8	18.49	11.0	14.8	5.27	30.83	0.009
Mar 24	130	1761.9	1335.3	1548.6	302	2494	48.1	699	32.5	18.57	11.1	14.8	5.27	31.02	0.009
Mar 26	132	1772.8	1346.1	1559.4	302	2513	48.9	702	33.2	18.70	11.2	15.0	5.27	31.28	0.009
Mar 28	134	1785.3	1357.6	1571.5	302	2531	49.7	709	34.0	18.80	11.3	15.1	5.28	31.48	0.009
Mar 31	137	1797.1	1369.7	1583.4	302	2551	50.5	718	34.8	18.84	11.4	15.1	5.28	31.67	0.010
Apr 02	139	1810.5	1382.5	1596.5	303	2571	51.3	723	35.5	18.99	11.5	15.3	5.29	31.93	0.010
Apr 04	141	1822.6	1395.0	1608.8	302	2587	52.1	728	36.3	19.11	11.6	15.4	5.28	32.12	0.010

Apr 06	143	1835.4	1409.4	1622.4	301	2603	52.9	736	37.0	19.20	11.8	15.5	5.26	32.26	0.010
Apr 09	146	1849.0	1424.8	1636.9	300	2621	53.7	741	37.8	19.36	11.9	15.7	5.24	32.48	0.010
Apr 11	148	1859.2	1437.3	1648.3	298	2639	54.5	746	38.6	19.44	12.1	15.8	5.21	32.70	0.010
Apr 13	150	1870.0	1446.9	1658.5	299	2654	55.2	752	39.3	19.53	12.1	15.8	5.22	32.86	0.011
Apr 16	153	1881.3	1457.5	1669.4	300	2671	56.0	759	40.1	19.61	12.2	15.9	5.23	33.05	0.011
Apr 18	155	1893.1	1469.3	1681.2	300	2688	56.8	764	40.8	19.73	12.3	16.0	5.23	33.25	0.011
Apr 20	157	1904.5	1481.7	1693.1	299	2704	57.6	767	41.6	19.86	12.5	16.2	5.22	33.47	0.011
Apr 25	162	1924.0	1501.6	1712.8	299	2726	58.5	773	42.3	20.11	12.7	16.4	5.22	33.75	0.011
Apr 30	167	1949.7	1521.3	1735.5	303	2753	59.3	773	42.3	20.56	13.1	16.8	5.29	34.21	0.012
May 03	170	1973.5	1538.0	1755.7	308	2771	60.5	778	43.5	20.87	13.3	17.07	5.38	34.42	0.012

C.5. Recorded peaks and intensities from FTIR analysis

PET_o			PET_i		
Peak	Area	Height	Peak	Area	Height
1979.7	0.051	0.004	-	-	-
1710.3	0.527	**0.012**	1712.4	2.005	**0.044**
-	-	-	1577.2	0.042	0.003
1505.4			1504.4	0.042	0.005
1456.3	0.058	0.002	1455.8	0.114	0.004
1407.0	**0.099**	0.007	1407.6	**0.151**	0.013
-	-	-	**1370.3**	0.042	0.003
1338.7	**0.096**	0.008	1339.4	**0.157**	0.014
1236.5	1.367	0.023	1235.1	2.523	0.041
1084.0	0.838	0.016	1091.5	1.470	0.029
1015.2	0.126	0.009	1015.6	0.231	0.017
968.6	0.052	0.003	968.9	0.080	0.004
870.0	0.051	**0.005**	870.4	0.105	**0.011**
841.4	0.034	0.002	846.0	0.041	0.003
790.9	0.063	0.003	792.5	0.061	0.004
721.2	0.684	0.026	721.2	0.964	0.042
-	-	-	**699.7**	0.030	0.003

C.6. Recorded thermal properties and results from DSC analysis

Sample	Trial	Weight (mg)	Tg (°C)	Tg (°C) *M*	*SD*	Tm (°C)	Tm (°C) *M*	*SD*	ΔHm (J/g)	ΔHc (J/g)	Cryst. (%)	cryst. (%) *M*	*SD*
PET_o	1	9.97	81.1	**81.1**	**0.014**	245.4	**245.4**	**0.014**	34.30	0	24.48	**25.12**	**0.90**
	2	12.0	81.1			245.4			33.84	2.237	25.75		
PET_i	1	11.124	80.5	**80.9**	**0.54**	245.3	**245.3**	**0.12**	33.35	11.37	31.92	**32.36**	**0.62**
	2	11.814	81.3			245.2			35.03	10.92	32.80		

C.7. Recorded values and results of molecular weight from intrinsic viscosity analysis

Sample	Weight (g)	*C* (g/dL)	t_0 (s)	Average t_0 (s)	t (s)	Average t (s)	η_{rel}	η_{inh} (dL/g)	η(dL/g)	M_V
Solvent	-	-	77 75 76	76	-	-	-	-	-	-
PET_0	0.2522	0.5	-	-	105 103 103		1.38 1.36 1.36	0.65 0.61 0.61	0.68 0.63 0.63	29,148 26,695 26,695
PET_i (trial 1)	0.252	0.5	-	-	105 105 104	105	1.38	0.64	0.67	28,737
PET_i (trial 2)	0.2525	0.5	-	-	105 106 105	105	1.39	0.65	0.68	29,560
PET_i (trial 3)	0.1108	0.5	-	-	102 100 99	100	1.32	0.56	0.58	23,467
									($M_V PET_0$) *M*	**27,512**
									SD	**1417**
									(M_V PET_i) *M*	**27,255**
									SD	**3306**

C.8. Recorded values and descriptive statistics for HPLC analysis

- Standards (Retention times)

TPA				BHET			
Concentration (mM)	Retention time (min)	***M***	***SD***	Concentration (mM)	Retention time (min)	***M***	***SD***
0.075	14.57	14.5	0.068	0.866	18.29	18.3	0.018
0.382	14.53			1.738	18.28		
0.485	14.55			3.261	18.28		
0.766	14.42			4.406	18.27		
-	-			5.545	18.25		

- Standards (Peak heights)

TPA Retention time = (14.5 ± 0.068) min						**BHET** Retention time = (18.3 ± 0.018) min					
Concentration (mM)	Peak Height (mAU)					Concentration (mM)	Peak Height (mAU)				
	Trial #1	Trial #2	Trial #3	***M***	***SD***		Trial #1	Trial #2	Trial #3	***M***	***SD***
0.075	11.1	10.8	-	10.9	0.21	0.866	223	235	236	231	7.01
0.382	86.8	87.0	-	86.9	0.14	1.738	460	516	514	497	31.5
0.485	104	94.5	96.6	98.3	4.77	3.261	921	1027	1028	992	61.6
0.766	73.4	86.5	86.7	82.2	7.58	4.406	1205	1377	1374	1319	98.4
-						5.545	2133	1552	1558	1748	334

- Samples

	Retention time (min)							
Days of incubation	108	120	128	148	157	168	*M*	*SD*
Peak 1	2.99	2.96	2.98	2.97	2.82	2.98	2.95	0.064
Peak 2	3.19	3.11	3.16	3.13		3.14	3.15	0.031
Peak 3		3.31	3.30	3.30	3.33	3.31	3.31	0.012
Peak 4		3.49	3.45	3.47	3.54	3.46	3.48	0.037

- Growth medium

Retention time (min)					
	Trial #1	Trial #2	Trial #3	***M***	**SD**
Peak 1	2.94	2.97	2.97	2.96	0.014
Peak 2	3.14	3.14	3.14	3.14	0.001
Peak 3	3.37	3.30	3.30	3.32	0.040
Peak 4		3.48	3.48	3.48	0.000

APPENDIX D: Calibration curves and DNA sequencing

HPLC analysis calibration

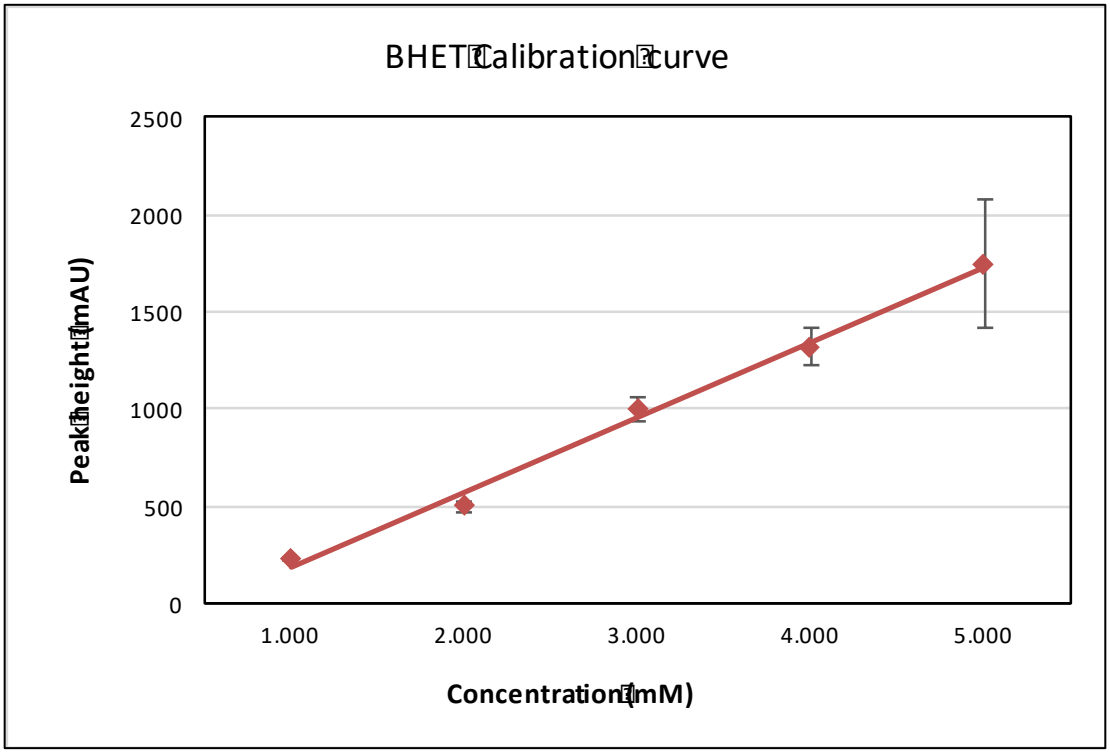

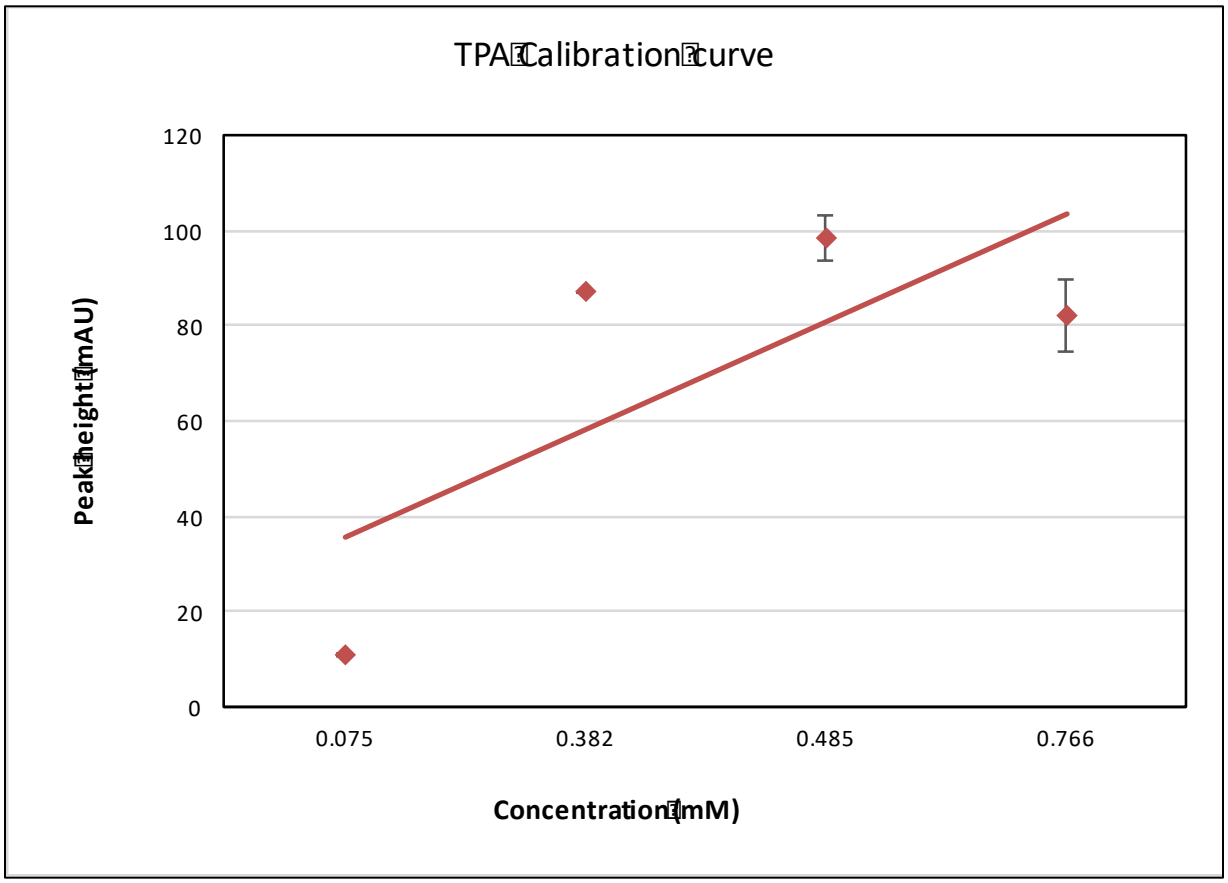
TPA Calibration curve
120
100
80
60
40
20
0
Peak height (mAU)
0.075
0.382
0.485
0.766
Concentration (mM)

DNA Sequencing performed by ACGT Corporation

1. Complete all sections of DNA Sequencing Order Form
2. Email 1 copy to order@acgtcorp.com
3. Print & enclose 1 copy with your samples.

Reset Form

ACGT CORP.

DNA Sequencing Order Form

Shipping Information:

Date: NOVEMBER 26TH, 2018
Name*: PATRICIA TORONO
Institution*: RYERSON UNIVERSITY
Ship Address*: 350 VICTORIA STREET TORONTO ON M5B 2K3 LABORATORY MAN-111
Phone*:
Email*: PATRICIA.TORONO@RYERSON.CA

Billing Information: ☐ same as shipping information

Quote No.:
Name:
Institution:
Bill Address:
Phone:
Email:

OFFICE USE: PAYMENT INFORMATION ☐ Credit Card Information on File			
PO Number:			
C.C Type:		C.C. Name:	
C.C Number:		C.C. Exp. Date:	

Sequencing Samples:

* refer to the ACGT website (www.acgtcorp.com) for recommended sample submission quantities
* refer to the ACGT website (www.acgtcorp.com) for a list of universal primers available at no additional charge
* custom primers used for sequencing can be ordered on this form
* use 1 row per reaction

Sample Name (max 15 characters)	Sample Conc. (ng/µl)	Vector Name[1] or PCR Product[2]	Length (bases)	Primer Name (max 20 characters)	Primer Conc.[3] (mg/µl)	GMP[4] (Y/N)	OFFICE USE ONLY: Seq ID	Temp. OD	Primer OD	Shipped
B3	see		~500bp	U341F	25 ng	No				
B6	see				6 pm	No				
B10	page					No				
B11	↓	↓	↓	↓	↓	No				
						No				
						No				
						No				
						No				
						No				
						No				
						No				
						No				

ACGT CORP. ◆ 700 BAY ST, SUITE 1100 ◆TORONTO, ON M5G 1Z6
TEL: 416-977-2228 or 1-800-735-0847; FAX 416-977-7122

Form CSF-720.02 rev. 1.0

1. Complete all sections of DNA Sequencing Order Form
2. Email 1 copy to order@acgtcorp.com
3. Print & enclose 1 copy with your samples.

ACGT CORP.

Sequencing Samples: CONTINUED

Sample Name (max 25 characters)	Sample Conc. (ng/µl)	Vector Name[1] or PCR Product	Length (bases)	Primer Name (max 20 characters)	Primer Conc.[2] (ng/µl)	GMP[3] (Y/N)	OFFICE USE ONLY: Seq#	Temp OD	Primer OD	Delivered
						No				
						No				
						No				
						No				
						No				
						No				
						No				
						No				
						No				
						No				
						No				
						No				

1. Provide vector name if applicable. Otherwise, indicate as PCR product
2. Provide primer concentration for custom primers synthesized externally; universal internal primers do not require concentration
3. Manufactured under a Quality System designed to meet the requirements of ISO 13485:2003. Additional charges may apply.

Select Data Delivery Options: All sequencing results are sent by email. (Please select only one option)

☑ ($5.00) Unedited Sequence Results [Chromatogram Trace]

☐ ($5.00) Unedited Sequence Results [Text + Chromatogram Trace]

☐ ($10.00) Edited Sequence Results [Text Data]

☐ ($10.00) Edited Sequence Results [Text Data + Chromatogram trace]

** No editing option available for GMP results.

Custom Primers to be Synthesized & Used for Sequencing

Primer Name	Scale	Sequence			Purification	GMP (Y/N)
	--Select One--	5'		3'	--Select One--	No
	--Select One--	5'		3'	--Select One--	No
	--Select One--	5'		3'	--Select One--	No
	--Select One--	5'		3'	RP-Cartridge	No

Additional Notes:

ACGT CORP. ❖ 700 BAY ST, SUITE 1100 ❖ TORONTO, ON M5G 1Z6
TEL: 416-977-2228 or 1-800-735-0847; FAX 416-977-7122

Save Order | Submit Order

PCR PRODUCTS

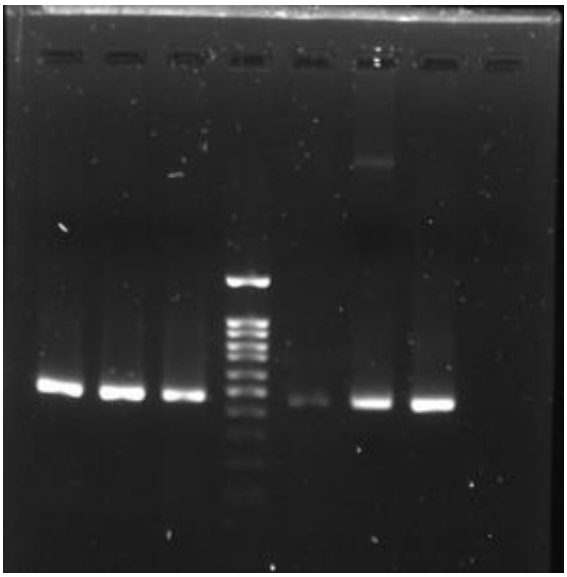

Agarose gel electrophoresis of PCR products of the 16S rRNA gene of bacterial isolates. From left to right: BS3, BS6, BS10, ladder, BS11, BS11 (redo), positive control, and negative control (distilled water).

Score	Expect	Identities	Gaps	Strand
750 bits(406)	0.0	413/416(99%)	2/416(0%)	Plus/Plus

```
Query  1    GGAGC-ACGCCGCGTGAGTGGATGAAGGCTTTCGGGTCGTAAAACTCTGTTGTTAGGGAA  59
            ||||| ||||||||||||| ||||||||||||||||||||||||||||||||||||||||
Sbjct  356  GGAGCAACGCCGCGTGAGT-GATGAAGGCTTTCGGGTCGTAAAACTCTGTTGTTAGGGAA  414

Query  60   GAACAAGTGCTAGTTGAATAAGCTGGCACCTTGACGGTACCTAACCAGAAAGCCACGGCT  119
            ||||||||||||||||||||||||||||||||||||||||||||||||||||||||||||
Sbjct  415  GAACAAGTGCTAGTTGAATAAGCTGGCACCTTGACGGTACCTAACCAGAAAGCCACGGCT  474

Query  120  AACTACGTGCCAGCAGCCGCGGTAATACGTAGGTGGCAAGCGTTATCCGGAATTATTGGG  179
            ||||||||||||||||||||||||||||||||||||||||||||||||||||||||||||
Sbjct  475  AACTACGTGCCAGCAGCCGCGGTAATACGTAGGTGGCAAGCGTTATCCGGAATTATTGGG  534

Query  180  CGTAAAGCGCGCGCAGGTGGTTTCTTAAGTCTGATGTGAAAGCCCACGGCTCAACCGTGG  239
            ||||||||||||||||||||||||||||||||||||||||||||||||||||||||||||
Sbjct  535  CGTAAAGCGCGCGCAGGTGGTTTCTTAAGTCTGATGTGAAAGCCCACGGCTCAACCGTGG  594

Query  240  AGGGTCATTGGAAACTGGGAGACTTGAGTGCAGAAGAGGAAAGTGGAATTCCATGTGTAG  299
            ||||||||||||||||||||||||||||||||||||||||||||||||||||||||||||
Sbjct  595  AGGGTCATTGGAAACTGGGAGACTTGAGTGCAGAAGAGGAAAGTGGAATTCCATGTGTAG  654

Query  300  CGGTGAAATGCGTAGAGATATGGAGGAACACCAGTGGCGAAGGCGACTTTCTGGTCTGTA  359
            ||||||||||||||||||||||||||||||||||||||||||||||||||||||||||||
Sbjct  655  CGGTGAAATGCGTAGAGATATGGAGGAACACCAGTGGCGAAGGCGACTTTCTGGTCTGTA  714

Query  360  ACTGACACTGAGGCGCGAAAGCGTGGGGAGCAAACAGGATTAGATCCCCCTGGTAG  415
            |||||||||||||||||||||||||||||||||||||||||||| ||||||||||
Sbjct  715  ACTGACACTGAGGCGCGAAAGCGTGGGGAGCAAACAGGATTAGATACCCCTGGTAG  770
```

Bacillus cereus strain SEHD031MH 16S ribosomal RNA gene, partial sequence

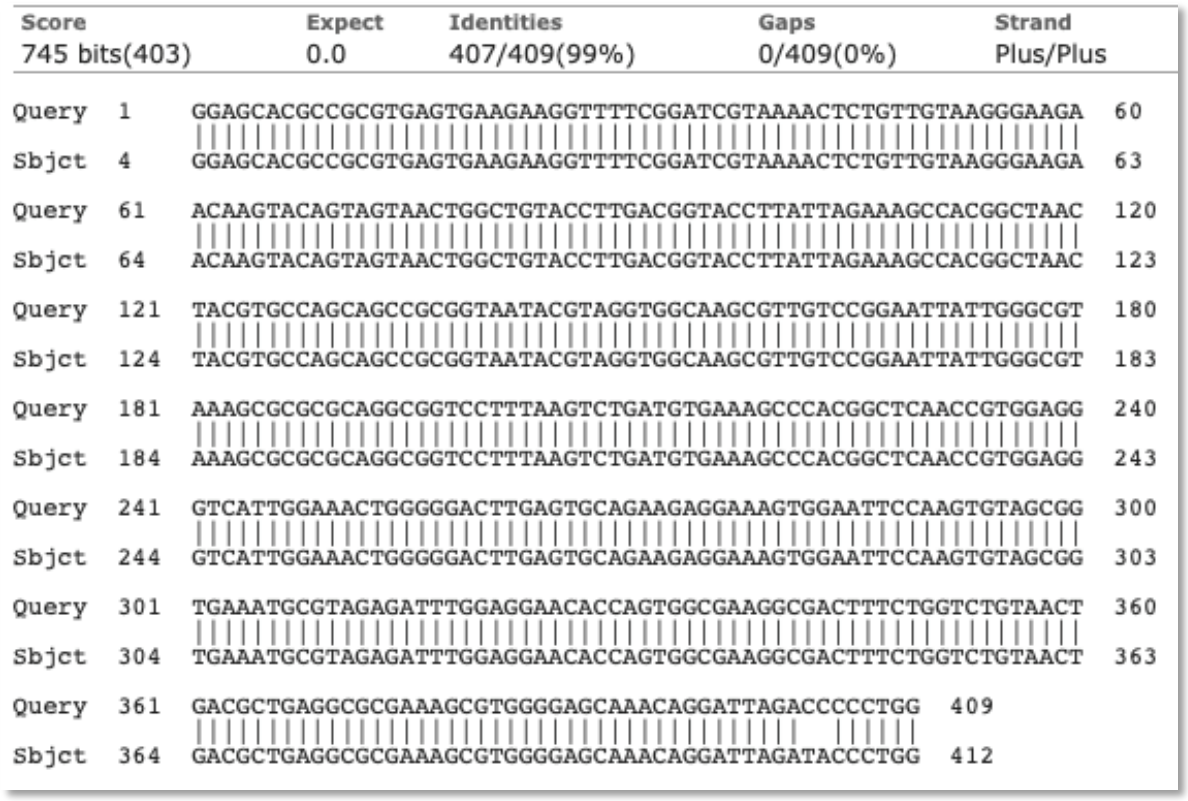

Score	Expect	Identities	Gaps	Strand
745 bits(403)	0.0	407/409(99%)	0/409(0%)	Plus/Plus

```
Query  1    GGAGCACGCCGCGTGAGTGAAGAAGGTTTTCGGATCGTAAAACTCTGTTGTAAGGGAAGA  60
            ||||||||||||||||||||||||||||||||||||||||||||||||||||||||||||
Sbjct  4    GGAGCACGCCGCGTGAGTGAAGAAGGTTTTCGGATCGTAAAACTCTGTTGTAAGGGAAGA  63

Query  61   ACAAGTACAGTAGTAACTGGCTGTACCTTGACGGTACCTTATTAGAAAGCCACGGCTAAC  120
            ||||||||||||||||||||||||||||||||||||||||||||||||||||||||||||
Sbjct  64   ACAAGTACAGTAGTAACTGGCTGTACCTTGACGGTACCTTATTAGAAAGCCACGGCTAAC  123

Query  121  TACGTGCCAGCAGCCGCGGTAATACGTAGGTGGCAAGCGTTGTCCGGAATTATTGGGCGT  180
            ||||||||||||||||||||||||||||||||||||||||||||||||||||||||||||
Sbjct  124  TACGTGCCAGCAGCCGCGGTAATACGTAGGTGGCAAGCGTTGTCCGGAATTATTGGGCGT  183

Query  181  AAAGCGCGCGCAGGCGGTCCTTTAAGTCTGATGTGAAAGCCCACGGCTCAACCGTGGAGG  240
            ||||||||||||||||||||||||||||||||||||||||||||||||||||||||||||
Sbjct  184  AAAGCGCGCGCAGGCGGTCCTTTAAGTCTGATGTGAAAGCCCACGGCTCAACCGTGGAGG  243

Query  241  GTCATTGGAAACTGGGGGACTTGAGTGCAGAAGAGGAAAGTGGAATTCCAAGTGTAGCGG  300
            ||||||||||||||||||||||||||||||||||||||||||||||||||||||||||||
Sbjct  244  GTCATTGGAAACTGGGGGACTTGAGTGCAGAAGAGGAAAGTGGAATTCCAAGTGTAGCGG  303

Query  301  TGAAATGCGTAGAGATTTGGAGGAACACCAGTGGCGAAGGCGACTTTCTGGTCTGTAACT  360
            ||||||||||||||||||||||||||||||||||||||||||||||||||||||||||||
Sbjct  304  TGAAATGCGTAGAGATTTGGAGGAACACCAGTGGCGAAGGCGACTTTCTGGTCTGTAACT  363

Query  361  GACGCTGAGGCGCGAAAGCGTGGGGAGCAAACAGGATTAGACCCCCTGG  409
            ||||||||||||||||||||||||||||||||||||||||||  ||||||
Sbjct  364  GACGCTGAGGCGCGAAAGCGTGGGGAGCAAACAGGATTAGATACCCTGG  412
```

Lysinibacilus macroides strain RW13-2 16S ribosomal RNA gene, partial sequence

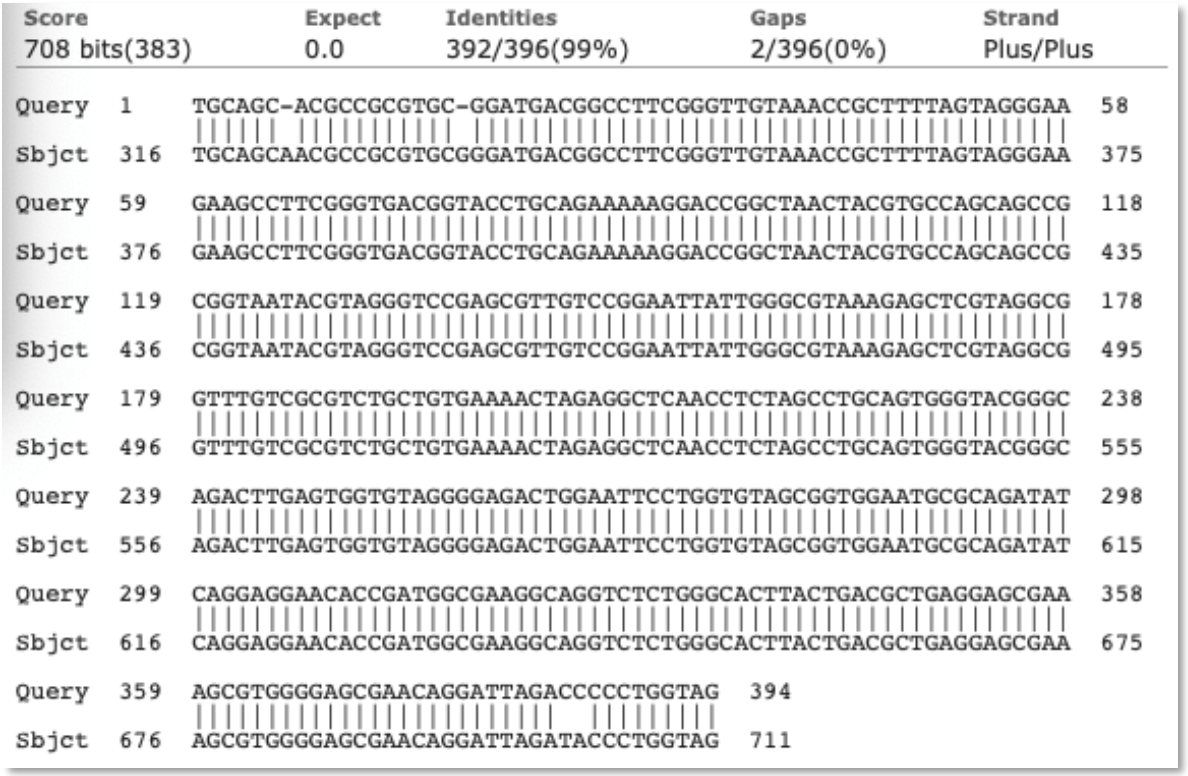

Score	Expect	Identities	Gaps	Strand
708 bits(383)	0.0	392/396(99%)	2/396(0%)	Plus/Plus

```
Query  1    TGCAGC-ACGCCGCGTGC-GGATGACGGCCTTCGGGTTGTAAACCGCTTTTAGTAGGGAA  58
            |||||| |||||||||||| ||||||||||||||||||||||||||||||||||||||||
Sbjct  316  TGCAGCAACGCCGCGTGCGGGATGACGGCCTTCGGGTTGTAAACCGCTTTTAGTAGGGAA  375

Query  59   GAAGCCTTCGGGTGACGGTACCTGCAGAAAAAGGACCGGCTAACTACGTGCCAGCAGCCG  118
            ||||||||||||||||||||||||||||||||||||||||||||||||||||||||||||
Sbjct  376  GAAGCCTTCGGGTGACGGTACCTGCAGAAAAAGGACCGGCTAACTACGTGCCAGCAGCCG  435

Query  119  CGGTAATACGTAGGGTCCGAGCGTTGTCCGGAATTATTGGGCGTAAAGAGCTCGTAGGCG  178
            ||||||||||||||||||||||||||||||||||||||||||||||||||||||||||||
Sbjct  436  CGGTAATACGTAGGGTCCGAGCGTTGTCCGGAATTATTGGGCGTAAAGAGCTCGTAGGCG  495

Query  179  GTTTGTCGCGTCTGCTGTGAAAACTAGAGGCTCAACCTCTAGCCTGCAGTGGGTACGGGC  238
            ||||||||||||||||||||||||||||||||||||||||||||||||||||||||||||
Sbjct  496  GTTTGTCGCGTCTGCTGTGAAAACTAGAGGCTCAACCTCTAGCCTGCAGTGGGTACGGGC  555

Query  239  AGACTTGAGTGGTGTAGGGGAGACTGGAATTCCTGGTGTAGCGGTGGAATGCGCAGATAT  298
            ||||||||||||||||||||||||||||||||||||||||||||||||||||||||||||
Sbjct  556  AGACTTGAGTGGTGTAGGGGAGACTGGAATTCCTGGTGTAGCGGTGGAATGCGCAGATAT  615

Query  299  CAGGAGGAACACCGATGGCGAAGGCAGGTCTCTGGGCACTTACTGACGCTGAGGAGCGAA  358
            ||||||||||||||||||||||||||||||||||||||||||||||||||||||||||||
Sbjct  616  CAGGAGGAACACCGATGGCGAAGGCAGGTCTCTGGGCACTTACTGACGCTGAGGAGCGAA  675

Query  359  AGCGTGGGGAGCGAACAGGATTAGACCCCCTGGTAG  394
            |||||||||||||||||||||||||  |||||||||
Sbjct  676  AGCGTGGGGAGCGAACAGGATTAGATACCCTGGTAG  711
```

Agromyces mediolanus strain PNP3 16S ribosomal RNA gene, partial sequence

REFERENCES

Al-Sabagh, A. M., Yehia, F. Z., Eshaq, G., Rabie, A. M., & ElMetwally, A. E. (2016). Greener routes for recycling of polyethylene terephthalate. *Egyptian Journal of Petroleum*, *25*(1), 53–64.

Alaribe, F. O., & Agamuthu, P. (2015). Assessment of phytoremediation potentials of Lantana camara in Pb impacted soil with organic waste additives. *Ecological Engineering*, *83*, 513–520.

Anderson, J. C., Park, B. J., & Palace, V. P. (2016). Microplastics in aquatic environments: Implications for Canadian ecosystems. *Environmental Pollution*, *218*, 269–280.

Anderson, P. J., Warrack, S., Langen, V., Challis, J. K., Hanson, M. L., & Rennie, M. D. (2017). Microplastic contamination in Lake Winnipeg, Canada. *Environmental Pollution*, *225*, 223–231.

Andrady, A. L. (2011). Microplastics in the marine environment. *Marine Pollution Bulletin*, *62*(8), 1596–1605.

Andrady, A. L. (2017). The plastic in microplastics: A review. *Marine Pollution Bulletin*, *119*(1), 12–22.

APHA, AWWA, & WPCF. (1998). *Standard Methods for the Examination of Water and Wastewater* (20th Editi). Washington DC, USA: American Public Health Association/American Water Works Association/Water Environment Federation.

Arthur, C., Baker, J., & Bamford, H. (2009). Proceedings of the International Research Workshop on the Occurrence , Effects , and Fate of Microplastic Marine Debris. Sept 9-11, 2008. *NOAA Technical Memorandum NOS-OR&R-30*.

Arutchelvi, J., Sudhakar, M., Arkatkar, A., Doble, M., Bhaduri, S., & Uppara, P. V. (2008). Biodegradation of polyethylene and polypropylene. *Indian Journal of Biotechnology*, *7*(January), 9–22.

Asmita, K., Shubhamsingh, T., Tejashree, S., Road, D. W., & Road, D. W. (2015). Isolation of Plastic Degrading Micro-organisms from Soil Samples Collected at Various Locations in Mumbai , India. *International Research Journal of Environment Sciences*, *4*(3), 77–85.

ASTM. (2015). Standard Test Method for Determining Inherent Viscosity of Poly (Ethylene Terephthalate) (PET) by Glass Capillary Viscometer. *Astm*, *i*(April 2003), 1–7.

Auta, H. S., Emenike, C. U., & Fauziah, S. H. (2017). Screening of Bacillus strains isolated from mangrove ecosystems in Peninsular Malaysia for microplastic degradation. *Environmental Pollution*, *231*, 1552–1559.

Awaja, F., & Pavel, D. (2005). Recycling of PET. *European Polymer Journal*, *41*(7), 1453–1477.

Ballent, A., Corcoran, P. L., Madden, O., Helm, P. A., & Longstaffe, F. J. (2016). Sources and sinks of microplastics in Canadian Lake Ontario nearshore, tributary and beach sediments. *Marine Pollution Bulletin*, *110*(1), 383–395.

Barboza, L. G. A., Dick Vethaak, A., Lavorante, B. R. B. O., Lundebye, A. K., & Guilhermino, L. (2018). Marine microplastic debris: An emerging issue for food security, food safety and human health. *Marine Pollution Bulletin*, *133*(June), 336–348.

Barboza, L. G. A., & Gimenez, B. C. G. (2015). Microplastics in the marine environment: Current trends and future perspectives. *Marine Pollution Bulletin*, *97*(1–2), 5–12.

Bhardwaj, H., Gupta, R., & Tiwari, A. (2013). Communities of Microbial Enzymes Associated with Biodegradation of Plastics. *Journal of Polymers and the Environment*, *21*, 575–579.

Billmeyer, F. W. (1949). Methods for estimating intrinsic viscosity. *Journal of Polymer Science*, *4*, 83–86.

Bimestre, B. H., & Saron, C. (2012). Chain extension of poly (ethylene terephthalate) by reactive extrusion with secondary stabilizer. *Materials Research*, *15*(3), 467–472.

Bornscheuer, U. T. (2016). Feeding on plastic. *Science*, *351*(6278), 1154–1155.

Browne, M. A., Crump, P., Niven, S. J., Teuten, E., Tonkin, A., Galloway, T., & Thompson, R. (2011). Accumulation of microplastic on shorelines woldwide: Sources and sinks. *Environmental Science and Technology*, *45*(21), 9175–9179.

Carniel, A., Valoni, É., Nicomedes, J., Gomes, A. da C., & Castro, A. M. de. (2017). Lipase from Candida antarctica (CALB) and cutinase from Humicola insolens act synergistically for PET hydrolysis to terephthalic acid. *Process Biochemistry*, *59*, 84–90.

Carr, S. A., Liu, J., & Tesoro, A. G. (2016). Transport and fate of microplastic particles in wastewater treatment plants. *Water Research*, *91*, 174–182.

Castañeda, R. A., Avlijas, S., Simard, M. A., Ricciardi, A., & Smith, R. (2014). Microplastic pollution in St. Lawrence River sediments. *Canadian Journal of Fisheries and Aquatic Sciences*, *71*(12), 1767–1771.

Castro-Aguirre, E., Auras, R., Selke, S., Rubino, M., & Marsh, T. (2017). Insights on the aerobic biodegradation of polymers by analysis of evolved carbon dioxide in simulated composting conditions. *Polymer Degradation and Stability*, *137*, 251–271.

Cerdà-Cuéllar, M., Kint, D. P. R., Muñoz-Guerra, S., & Marqués-Calvo, M. S. (2004). Biodegradability of aromatic building blocks for poly(ethylene terephthalate) copolyesters. *Polymer Degradation and Stability*.

Chatani, Y., Okita, Y., Tadokoro, H., & Yamashita, Y. (1970). Structural Studies of Polyesters. III. Crystal Structure of Poly-ε-caprolactone. *Polymer Journal*, *1*(5), 555–562.

Claessens, M., De Meester, S., Van Landuyt, L., De Clerck, K., & Janssen, C. R. (2011). Occurrence and distribution of microplastics in marine sediments along the Belgian coast. *Marine Pollution Bulletin*, *62*(10), 2199–2204.

Claessens, M., Van Cauwenberghe, L., Vandegehuchte, M. B., & Janssen, C. R. (2013). New techniques for the detection of microplastics in sediments and field collected organisms. *Marine Pollution Bulletin*, *70*(1–2), 227–233.

Cole, M., Lindeque, P., Halsband, C., & Galloway, T. S. (2011). Microplastics as contaminants in the marine environment: A review. *Marine Pollution Bulletin*, *62*(12), 2588–2597.

Corcoran, P. L., Norris, T., Ceccanese, T., Walzak, M. J., Helm, P. A., & Marvin, C. H. (2015). Hidden plastics of Lake Ontario, Canada and their potential preservation in the sediment record. *Environmental Pollution*, *204*, 17–25.

Cruickshank, A. (2018, April 11). Untreated sewage pollutes water across the country. *StarMetro Vancouver*.

Danso, D., Schmeisser, C., & Chow, J. (2018). New Insights into the Function and Global Distribution of Polyethylene Terephthalate (PET)-Degrading Bacteria and Enzymes in Marine and Terrestrial Metagenomes. *Applied and Environmental Microbiology*, *84*(8), 1–13.

Desforges, J. P. W., Galbraith, M., Dangerfield, N., & Ross, P. S. (2014). Widespread distribution of microplastics in subsurface seawater in the NE Pacific Ocean. *Marine Pollution Bulletin*, *79*, 94–99.

Donelli, I., Taddei, P., Smet, P. F., Poelman, D., Nierstrasz, V. A., & Freddi, G. (2009). Enzymatic surface modification and functionalization of PET: A water contact angle, FTIR, and fluorescence spectroscopy study. *Biotechnology and Bioengineering*, *103*(5), 845–856.

Donlan, R. M. (2002). Biofilms: Microbial life on surfaces. *Emerging Infectious Diseases*, *8*(9), 881–890.

Driedger, A. G. J., Dürr, H. H., Mitchell, K., & Van Cappellen, P. (2015). Plastic debris in the Laurentian Great Lakes: A review. *Journal of Great Lakes Research*, *41*, 9–19.

Dussud, C., & Ghiglione, J.-F. (2015). Bacterial degradation of synthetic plastics.

Egerton, R. F. (2006). *Physical Principles of Electron Microscopy : An Introduction to TEM, SEM, and AEM*. Springer Science+Business Media, Inc.

Eriksen, M., Lebreton, L. C. M., Carson, H. S., Thiel, M., Moore, C. J., Borerro, J. C., … Reisser, J. (2014). Plastic Pollution in the World's Oceans: More than 5 Trillion Plastic Pieces Weighing over 250,000 Tons Afloat at Sea. *PLoS ONE*, *9*(12), 1–15.

Eriksen, M., Mason, S. A., Wilson, S., Box, C., Zellers, A., Edwards, W., … Amato, S. (2013). Microplastic pollution in the surface waters of the Laurentian Great Lakes. *Marine Pollution Bulletin*, *77*(1–2), 177–182.

Eubeler, J. P. (2010). *Biodegradation of Synthetic Polymers in the aquatic environment*. Universität Bremen.

Evtushenko, L., & Takeuchi, M. (2006). The Family Microbacteriaceae. In M. Dworkin, S. Falkow, E. Rosenberg, K.-H. Schleifer, & E. Stackebrandt (Eds.), *The Prokaryotes* (Third, pp. 1020–1098).

Farah, S., Kunduru, K. R., Basu, A., & Domb, A. J. (2015). Molecular Weight Determination of Polyethylene Terephthalate. In S. Ebnesajjad (Ed.), *Poly(Ethylene Terephthalate) Based Blends, Composites and Nanocomposites* (pp. 143–165).

Fischer, E. K., Paglialonga, L., Czech, E., & Tamminga, M. (2016). Microplastic pollution in lakes and lake shoreline sediments - A case study on Lake Bolsena and Lake Chiusi (central Italy). *Environmental Pollution*, *213*, 648–657.

Foladori, P., Bruni, L., Tamburini, S., & Ziglio, G. (2010). Direct quantification of bacterial biomass in influent, effluent and activated sludge of wastewater treatment plants by using flow cytometry. *Water Research*, *44*(13), 3807–3818.

Forsythe, C. (2016). *The Quantification of Microplastics in Intertidal Sediments in the Bay of Fundy, Canada*. Royal Roads University.

Fossi, M. C., Panti, C., Guerranti, C., Coppola, D., Giannetti, M., Marsili, L., & Minutoli, R. (2012). Are baleen whales exposed to the threat of microplastics? A case study of the Mediterranean fin whale (Balaenoptera physalus). *Marine Pollution Bulletin*, *64*(11), 2374–2379.

Fotopoulou, K. N., & Karapanagioti, H. K. (2015). Surface properties of beached plastics. *Environmental Science and Pollution Research*, *22*(14), 11022–11032.

Free, C. M., Jensen, O. P., Mason, S. A., Eriksen, M., Williamson, N. J., & Boldgiv, B. (2014). High-levels of microplastic pollution in a large, remote, mountain lake. *Marine Pollution Bulletin*, *85*(1), 156–163.

Funabashi, M., Ninomiya, F., & Kunioka, M. (2007). Biodegradation of polycaprolactone powders proposed as reference test materials for international standard of biodegradation evaluation method. *Journal of Polymers and the Environment*, *15*(1), 7–17.

Gamerith, C., Zartl, B., Pellis, A., Guillamot, F., Marty, A., Acero, E. H., & Guebitz, G. M. (2017). Enzymatic recovery of polyester building blocks from polymer blends. *Process Biochemistry*, *59*, 58–64.

Gan, Z., Fung, J. T., Jing, X., Wu, C., & Kuliche, W. K. (1999). A novel laser light-scattering study of enzymatic biodegradation of poly(ε-caprolactone) nanoparticles. *Polymer*, *40*(8), 1961–1967.

GESAMP. (2015). *Sources, fate and effects of microplastics in the marine environment – a global assessment*.

GESAMP. (2016). Sources, Fate and Effects of Microplastics in the Marine Environment: Part 2 of a Global Assessment, 1–220.

Gewert, B., Plassmann, M. M., & MacLeod, M. (2015). Pathways for degradation of plastic polymers floating in the marine environment. *Environmental Science. Processes & Impacts*, *17*(9), 1513–1521.

Ghosh, S. K., Pal, S., & Ray, S. (2013). Study of microbes having potentiality for biodegradation of plastics. *Environmental Science and Pollution Research International*, *20*, 4339–4355.

Gu, J. D. (2003). Microbiological deterioration and degradation of synthetic polymeric materials: Recent research advances. *International Biodeterioration and Biodegradation*, *52*(2), 69–91.

Guo, W., Tao, J., Yang, C., Song, C., Geng, W., Li, Q., … Wang, S. (2012). Introduction of Environmentally Degradable Parameters to Evaluate the Biodegradability of Biodegradable Polymers. *PLoS ONE*, *7*(5), e38341.

Guo, W., Tao, J., Yang, C., Zhao, Q., Song, C., & Wang, S. (2010). The rapid evaluation of material biodegradability using an improved ISO 14852 method with a microbial community. *Polymer Testing*, *29*(7), 832–839.

Hakkarainen, M., & Albertsson, A. (2002). Heterogeneous biodegradation of polycaprolactone–low molecular weight products and surface changes. *Macromolecular Chemistry and Physics*, *203*(10-11), 1357–1363.

Harvey, D. (2008). *Modern Analytical Chemistry*. McGraw Hill.

HELCOM. (2014). *BASE project 2012-2014: Preliminary study on synthetic microfibers and particles at a municipal waste water treatment plant*.

Helm, P., Zimmer, G., Stones, M., Thibeau, J., Sims, A., Thorburn, B., & Page, W. (2016). Microplastics in and entering nearshore surface waters of the lower Great Lakes. In *Abstract submitted for the 59th Annual Conference on Great Lakes Research, International Association for Great Lakes Research (IAGLR)*. Guelph, Ontario.

Hergenrother, W. L., & Nelson, C. J. A. Y. (1974). Viscosity-Molecular Weight Relationship for Fractionated Poly (ethylene Terephthalate). *Polymer*, *12*, 2905–2915.

Herrero Acero, E., Ribitsch, D., Steinkellner, G., Gruber, K., Greimel, K., Eiteljoerg, I., … Guebitz, G. (2011). Enzymatic surface hydrolysis of PET: Effect of structural diversity on kinetic properties of cutinases from Thermobifida. *Macromolecules*, *44*(12), 4632–4640.

Herzog, K., Müller, R. J., & Deckwer, W. D. (2006). Mechanism and kinetics of the enzymatic hydrolysis of polyester nanoparticles by lipases. *Polymer Degradation and Stability*, *91*(10), 2486–2498.

Höglund, A., Hakkarainen, M., & Albertsson, A. C. (2007). Degradation profile of poly(ε-caprolactone)-the influence of macroscopic and macromolecular biomaterial design. *Journal of Macromolecular Science, Part A: Pure and Applied Chemistry*, *44*(9), 1041–1046.

Holland, B. J., & Hay, J. N. (2002). The thermal degradation of poly (vinyl acetate) measured by thermal analysis-Fourier transform infrared spectroscopy. *Polymer*, *43*, 1835–1847.

Hong, N., Cheng, L., Juan, W., Mengjun, T., & Yong, S. (2016). *CN106566789A*. China.

Horta, A. C. L., Da Silva, A. J., Sargo, C. R., Cavalcanti-Montaño, I. D., Galeano-Suarez, C. A., Velez,

A. M., … Zangirolami, T. C. (2015). On-line monitoring of biomass concentration based on a capacitance sensor: Assessing the methodology for different bacteria and yeast high cell density fed-batch cultures. *Brazilian Journal of Chemical Engineering*, *32*(4), 821–829.

Huarng, J. C., Min, K., & White, J. L. (1988). Phase equilibrium in the binary and ternary blend system: Polycaprolactone-polyvinyl chloride-styrene acrylonitrile copolymer. *Polymer Engineering and Science*, *28*(24), 1590–1599.

Iñiguez, M. E., Conesa, J. A., & Fullana, A. (2017). Microplastics in Spanish Table Salt. *Scientific Reports*, *7*(1), 1–7.

Ioakeimidis, C., Fotopoulou, K. N., Karapanagioti, H. K., Geraga, M., Zeri, C., Papathanassiou, E., … Papatheodorou, G. (2016). The degradation potential of PET bottles in the marine environment: An ATR-FTIR based approach. *Scientific Reports*, *6*(October 2015).

ISO. (2018). *ISO 14852:2018 - Determination of ultimate aerobic diodegradability of plastic materials in and aqueous medium - Method by analysis of evolved carbon dioxide*.

Janczak, K., Hrynkiewicz, K., Znajewska, Z., & Dąbrowska, G. (2018). Use of rhizosphere microorganisms in the biodegradation of PLA and PET polymers in compost soil. *International Biodeterioration and Biodegradation*, *130*(April), 65–75.

Jayasekara, R., Harding, I., Bowater, I., & Lonergan, G. (2005). Biodegradability of a selected range of polymers and polymer blends and standard methods for assessment of biodegradation. *Journal of Polymers and the Environment*, *13*(3), 231–251.

Jun, H. S., Kim, B. O., Kim, Y. C., Chang, H. N., & Woo, S. I. (1994). Synthesis of copolyester containing poly(ethylene terephthalate) and poly(ε-caprolactone) units, and its biodegradability. *Studies in Polymer Science*, *12*(7), 498–504.

Kannan, G., Grieshaber, S. E., & Zhao, W. (2016). Themorplastic Polyesters. In O. Olabisi & K. Adewale (Eds.), *Handbook of thermoplastics* (Second). CRC Press.

Karami, A., Golieskardi, A., Keong Choo, C., Larat, V., Galloway, T. S., & Salamatinia, B. (2017). The presence of microplastics in commercial salts from different countries. *Scientific Reports*, *7*(March), 1–11.

Kawai, F. (2010). The biochemistry and molecular biology of xenobiotic polymer degradation by microorganisms. *Bioscience, Biotechnology, and Biochemistry*, *74*(9), 1743–1759.

Kawai, F., Oda, M., Tamashiro, T., Waku, T., Tanaka, N., Yamamoto, M., … Tanokura, M. (2014). A novel Ca2+-activated, thermostabilized polyesterase capable of hydrolyzing polyethylene terephthalate from Saccharomonospora viridis AHK190. *Applied Microbiology and Biotechnology*, *98*(24), 10053–10064.

Kazmiruk, T. N., Kazmiruk, V. D., & Bendell, L. I. (2018). Abundance and distribution of microplastics

within surface sediments of a key shellfish growing region of Canada. *PLoS ONE*, *13*(5), 1–17.

Khatoon, N., Naz, I., Ali, M. I., Ali, N., Jamal, A., Hameed, A., & Ahmed, S. (2014). Bacterial succession and degradative changes by biofilm on plastic medium for wastewater treatment. *Journal of Basic Microbiology*, *54*(7), 739–749.

Kint, D., & Muñoz-Guerra, S. (1999). A review on the potential biodegradability of poly(ethylene terephthalate). *Polymer International*, *48*(5), 346–352.

Kong, Y., & Hay, Y. N. (2002). The measurement of cristalinity of polymers by DSC. *Polymer*, *43*(1), 3873–3878.

Koshti, R., Mehta, L., & Samarth, N. (2018). Biological Recycling of Polyethylene Terephthalate: A Mini-Review. *Journal of Polymers and the Environment*, *26*(8), 3520–3529.

Kosuth, M., Mason, S. A., & Wattenberg, E. V. (2018). Anthropogenic contamination of tap water, beer, and sea salt. *PLoS ONE*, *13*(4), 1–18.

Krueger, M. C., Harms, H., & Schlosser, D. (2015). Prospects for microbiological solutions to environmental pollution with plastics. *Applied Microbiology and Biotechnology*, *99*(21), 8857–8874.

Kumar, G., Sivagurunathan, P., Park, J. H., Park, J. H., Park, H. D., Yoon, J. J., & Kim, S. H. (2016). HRT dependent performance and bacterial community population of granular hydrogen-producing mixed cultures fed with galactose. *Bioresource Technology*, *206*, 188–194.

Kyrikou, I., & Briassoulis, D. (2007). Biodegradation of agricultural plastic films: A critical review. *Journal of Polymers and the Environment*, *15*(2), 125–150.

Law, K. L., Morét-Ferguson, S. E., Goodwin, D. S., Zettler, E. R., Deforce, E., Kukulka, T., & Proskurowski, G. (2014). Distribution of surface plastic debris in the eastern pacific ocean from an 11-year data set. *Environmental Science and Technology*, *48*(9), 4732–4738.

Law, K. L., Morét-Ferguson, S., Maximenko, N. A., Proskurowski, G., Peacock, E. E., Hafner, J., & Reddy, C. M. (2010). Plastic accumulation in the North Atlantic subtropical gyre. *Science*, *329*(5996), 1185–1188.

Leja, K., & Lewandowicz, G. (2010). Polymer biodegradation and biodegradable polymers - A review. *Polish Journal of Environmental Studies*, *19*(2), 255–266.

Li, J., Liu, H., & Paul Chen, J. (2018). Microplastics in freshwater systems: A review on occurrence, environmental effects, and methods for microplastics detection. *Water Research*, *137*, 362–374.

Li, J., Yang, D., Li, L., Jabeen, K., & Shi, H. (2015). Microplastics in commercial bivalves from China. *Environmental Pollution*, *207*, 190–195.

Liebezeit, G., & Liebezeit, E. (2013). Non-pollen particulates in honey and sugar. *Food Additives and Contaminants - Part A Chemistry, Analysis, Control, Exposure and Risk Assessment*, *30*(12), 2136–

2140.

Liebezeit, G., & Liebezeit, E. (2014). Synthetic particles as contaminants in German beers. *Food Additives and Contaminants - Part A Chemistry, Analysis, Control, Exposure and Risk Assessment*, *31*(9), 1574–1578.

Liebezeit, G., & Liebezeit, E. (2015). Origin of synthetic particles in honeys. *Polish Journal of Food and Nutrition Sciences*, *65*(2), 143–147.

Lobo, H., & Bonilla, J. V. (2003). General Introduction to Plastics Analysis. In H. Lobo & J. V. Bonilla (Eds.), *Handbook of Plastics Analysis*. Marcel Dekker, Inc.

Lucas, N., Bienaime, C., Belloy, C., Queneudec, M., Silvestre, F., & Nava-Saucedo, J. E. (2008). Polymer biodegradation: Mechanisms and estimation techniques - A review. *Chemosphere*, *73*(4), 429–442.

Machado de Castro, A., Carniel, A., Nicomedes Junior, J., da Conceição Gomes, A., & Valoni, É. (2017). Screening of commercial enzymes for poly(ethylene terephthalate) (PET) hydrolysis and synergy studies on different substrate sources. *Journal of Industrial Microbiology and Biotechnology*, *44*(6), 835–844.

Magnusson, K., & Norén, F. (2014). Screening of microplastic particles in and down-stream a wastewater treatment plant. *IVL Swedish Environmental Research Institute*, *C 55*(C), 22.

Mark, J. E. (1999). *Polymer Data Handbook*. (J. E. Mark, Ed.), *October*. Oxford University Press, Inc.

Marten, E., Müller, R. J., & Deckwer, W. D. (2003). Studies on the enzymatic hydrolysis of polyesters - I. Low molecular mass model esters and aliphatic polyesters. *Polymer Degradation and Stability*, *80*(3), 485–501.

Marten, E., Müller, R. J., & Deckwer, W. D. (2005). Studies on the enzymatic hydrolysis of polyesters. II. Aliphatic-aromatic copolyesters. *Polymer Degradation and Stability*, *88*, 371–381.

Mason, S. A., Welch, V., & Neratko, J. (2018). *Synthetic polymer contamination in bottled water*. *Fredonia State University of New York*.

Mathalon, A., & Hill, P. (2014). Microplastic fibers in the intertidal ecosystem surrounding Halifax Harbor, Nova Scotia. *Marine Pollution Bulletin*, *81*(1), 69–79.

Mercier, A., Gravouil, K., Aucher, W., Brosset-Vincent, S., Kadri, L., Colas, J., … Ferreira, T. (2017). Fate of Eight Different Polymers under Uncontrolled Composting Conditions: Relationships between Deterioration, Biofilm Formation, and the Material Surface Properties. *Environmental Science and Technology*, *51*(4), 1988–1997.

Mezzanotte, V., Bertani, R., Innocenti, F. D., & Tosin, M. (2005). Influence of inocula on the results of biodegradation tests. *Polymer Degradation and Stability*, *87*(1), 51–56.

Mohan, K., & srivastava, T. (2011). Microbial deterioration and degradation of Polymeric materials.

Journal of Biochemical Technology, *2*(4), 210–215.

Mueller, R. J. (2006). Biological degradation of synthetic polyesters-Enzymes as potential catalysts for polyester recycling. *Process Biochemistry*, *41*(10), 2124–2128.

Müller, R. J., Kleeberg, I., & Deckwer, W. D. (2001). Biodegradation of polyesters containing aromatic constituents. *Journal of Biotechnology*.

Müller, R. J., Schrader, H., Profe, J., Dresler, K., & Deckwer, W. D. (2005). Enzymatic degradation of poly(ethylene terephthalate): Rapid hydrolyse using a hydrolase from T. fusca. *Macromolecular Rapid Communications*, *26*, 1400–1405.

Murphy, F., Ewins, C., Carbonnier, F., & Quinn, B. (2016). Wastewater Treatment Works (WwTW) as a Source of Microplastics in the Aquatic Environment. *Environmental Science and Technology*, *50*(11), 5800–5808.

Murray, F., & Cowie, P. R. (2011). Plastic contamination in the decapod crustacean Nephrops norvegicus (Linnaeus, 1758). *Marine Pollution Bulletin*, *62*(6), 1207–1217.

Nagata, M., Kiyotsukuri, T., Minami, S., Tsutsumi, N., & Sakai, W. (1997). Enzymatic degradation of poly(ethylene terephthalate) copolymers with aliphatic dicarboxylic acids and/or poly(ethylene glycol). *European Polymer Journal*, *33*(10–12), 1701–1705.

Nagy, K., & Vékey, K. (2008). Separation methods. In *Medical Applications of Mass Spectrometry* (pp. 61–92).

Najafpour, G. (2007). Growth Kinetics. In *Biochemical Engineering and Biotechnology* (pp. 81–140).

Napper, I. E., Bakir, A., Rowland, S. J., & Thompson, R. C. (2015). Characterisation, quantity and sorptive properties of microplastics extracted from cosmetics. *Marine Pollution Bulletin*, *99*(1–2), 178–185.

Neves, D., Sobral, P., Ferreira, J. L., & Pereira, T. (2015). Ingestion of microplastics by commercial fish off the Portuguese coast. *Marine Pollution Bulletin*, *101*(1), 119–126.

Nielsen, J. L., Sevious, R. J., & Nielsen, P. H. (2016). *Experimental Methods in Wastewater Treatment*. (M. C. M. van Loosdrecht, P. H. Nielsen, C. M. Lopez-Vazquez, & D. Brjanovic, Eds.) (First). IWA Publishing.

Nimchua, T., Eveleigh, D. E., Sangwatanaroj, U., & Punnapayak, H. (2008). Screening of tropical fungi producing polyethylene terephthalate- hydrolyzing enzyme for fabric modification. *Journal of Industrial Microbiology and Biotechnology*, *35*(8), 843–850.

Nimchua, T., Punnapayak, H., & Zimmermann, W. (2007). Comparison of the hydrolysis of polyethylene terephthalate fibers by a hydrolase from Fusarium oxysporum LCH I and Fusarium solani f. sp. pisi. *Biotechnology Journal*, *2*, 361–364.

Nishikida, K., & Coates, J. (2003). Infrared And Raman Analysis Of Polymers. In H. Lobo & J. V.

Bonilla (Eds.), *Handbook of Plastics Analysis* (Vol. 68, p. 650). Marcel Dekker, Inc.

Nowak, B., Pajak, J., Labuzek, S., Rymarz, G., & Talik, E. (2011). Biodegradation of PET modified with polyester Bionolle by Penicillium funiculosum. *Polimery*, *56*(1), 35–44.

Obbard, R. W., Sadri, S., Wong, Y. Q., Khitun, A. A., Baker, I., & Richard, C. (2014). Global warming releases microplastic legacy frozen in Arctic Sea ice. *Earth's Future*, *2*(6), 315–320.

Ogunola, O. S., & Palanisami, T. (2016). Microplastics in the Marine Environment: Current Status, Assessment Methodologies, Impacts and Solutions. *Journal of Pollution Effects & Control*, *04*(02).

Paço, A., Duarte, K., da Costa, J. P., Santos, P. S. M., Pereira, R., Pereira, M. E., … Rocha-Santos, T. A. P. (2017). Biodegradation of polyethylene microplastics by the marine fungus Zalerion maritimum. *Science of the Total Environment*, *586*, 10–15.

Pagga, U., Schäfer, A., Müller, R. J., & Pantke, M. (2001). Determination of the aerobic biodegradability of polymeric material in aquatic batch tests. *Chemosphere*, *42*, 319–331.

Pirzadeh, E., Zadhoush, A., & Haghighat, M. (2007). Hydrolytic and thermal degradation of PET fibers and PET granule: The effects of crystallization, temperature, and humidity. *Journal of Applied Polymer Science*, *106*(3), 1544–1549.

PlasticsEurope. (2016). Plastics – the Facts 2016. An analysis of European plastics production, demand and waste data. *Association of Plastic Manufacturers, Brussels*.

PlasticsEurope. (2018). *Plastics – the Facts 2018. An analysis of European plastics production, demand and waste data*.

Pungor, E., & Horvai, G. (1994). *A Practical Guide to Instrumental Analysis*. CRC Press.

Reisser, J., Shaw, J., Wilcox, C., Hardesty, B. D., Proietti, M., Thums, M., & Pattiaratchi, C. (2013). Marine plastic pollution in waters around Australia: Characteristics, concentrations, and pathways. *PLoS ONE*, *8*(11), 1–11.

Ribitsch, D., Acero, E. H., Greimel, K., Dellacher, A., Zitzenbacher, S., Marold, A., … Guebitz, G. M. (2012). A new esterase from Thermobifida halotolerans hydrolyses polyethylene terephthalate (PET) and polylactic acid (PLA). *Polymers*, *4*(1), 617–629.

Ribitsch, D., Acero, E. H., Greimel, K., Eiteljoerg, I., Trotscha, E., Freddi, G., … Guebitz, G. M. (2012). Characterization of a new cutinase from Thermobifida alba for PET-surface hydrolysis. *Biocatalysis and Biotransformation*, *30*(1), 2–9.

Rochman, C. M., Kurobe, T., Flores, I., & Teh, S. J. (2014). Early warning signs of endocrine disruption in adult fish from the ingestion of polyethylene with and without sorbed chemical pollutants from the marine environment. *Science of the Total Environment*, *493*, 656–661.

Rochman, C. M., Tahir, A., Williams, S. L., Baxa, D. V., Lam, R., Miller, J. T., … Teh, S. J. (2015). Anthropogenic debris in seafood: Plastic debris and fibers from textiles in fish and bivalves sold for

human consumption. *Scientific Reports*, *5*(September), 1–10.

Ronkvist, Å. M., Xie, W., Lu, W., & Gross, R. A. (2009). Cutinase-Catalyzed hydrolysis of poly(ethylene terephthalate). *Macromolecules*, *42*(14), 5128–5138.

Ryu, B. G., Kim, J., Farooq, W., Han, J. I., Yang, J. W., & Kim, W. (2014). Algal-bacterial process for the simultaneous detoxification of thiocyanate-containing wastewater and maximized lipid production under photoautotrophic/photoheterotrophic conditions. *Bioresource Technology*, *162*, 70–79.

Sanches, N. B., Dias, M. L., & Pacheco, E. B. A. V. (2005). Comparative techniques for molecular weight evaluation of poly (ethylene terephthalate) (PET). *Polymer Testing*, *24*(6), 688–693.

Santana, M. F. M., Ascer, L. G., Custódio, M. R., Moreira, F. T., & Turra, A. (2016). Microplastic contamination in natural mussel beds from a Brazilian urbanized coastal region: Rapid evaluation through bioassessment. *Marine Pollution Bulletin*, *106*(1–2), 183–189.

Schymanski, D., Goldbeck, C., Humpf, H. U., & Fürst, P. (2018). Analysis of microplastics in water by micro-Raman spectroscopy: Release of plastic particles from different packaging into mineral water. *Water Research*, *129*, 154–162.

Selke, S., Auras, R., Nguyen, T. A., Castro Aguirre, E., Cheruvathur, R., & Liu, Y. (2015). Evaluation of biodegradation-promoting additives for plastics. *Environmental Science and Technology*, *49*(6), 3769–3777.

Shah, A. A., Hasan, F., Hameed, A., & Ahmed, S. (2008). Biological degradation of plastics: A comprehensive review. *Biotechnology Advances*, *26*(3), 246–265.

Sharon, C., & Sharon, M. (2012). Studies on Biodegradation of Polyethylene terephthalate: A synthetic polymer. *Journal of Microbiology and Biotechnology Research*, *2*(2), 248–257.

Sheik, S., Chandrashekar, K. R., Swaroop, K., & Somashekarappa, H. M. (2015). Biodegradation of gamma irradiated low density polyethylene and polypropylene by endophytic fungi. *International Biodeterioration and Biodegradation*, *105*, 21–29.

Shuster, M., Narkis, M., & Siegmann, A. (1994). Polymeric antiplasticization of polycarbonate with polycaprolactone. *Polymer Engineering and Science*, *34*(21), 1613–1618.

Sinha, V., Patel, M. R., & Patel, J. V. (2010). Pet waste management by chemical recycling: A review. *Journal of Polymers and the Environment*, *18*(1), 8–25.

Sivan, A. (2011). New perspectives in plastic biodegradation. *Current Opinion in Biotechnology*, *22*, 422–426.

Skariyachan, S., Setlur, A. S., Naik, S. Y., Naik, A. A., Usharani, M., & Vasist, K. S. (2017). Enhanced biodegradation of low and high-density polyethylene by novel bacterial consortia formulated from plastic-contaminated cow dung under thermophilic conditions. *Environmental Science and Pollution*

Research, *24*(9), 8443–8457.

Sowmya, H.V., Thippeswamy, B. (2014). Biodegradation of Polyethylene by Bacillus cereus. *Advances in Polymer Science and Technology: An International Journal*, *4*(2), 28–32.

Sruthy, S., & Ramasamy, E. V. (2017). Microplastic pollution in Vembanad Lake, Kerala, India: The first report of microplastics in lake and estuarine sediments in India. *Environmental Pollution*, *222*, 315–322.

Stasinakis, A. S., Mamais, D., Paraskevas, P. A., & Lekkas, T. D. (2003). Evaluation of Different Methods for the Determination of Maximum Heterotrophic Growth Rates. *Water Environment Research*, *75*(6), 549–552.

Stokes, D. (2008). *Principles and Practice of Variable Pressure : Environmental Scanning Electron Microscopy (VP-ESEM)*. (M. Rainforth, Ed.). John Wiley & Sons, Inc.

Stolte, A., Forster, S., Gerdts, G., & Schubert, H. (2015). Microplastic concentrations in beach sediments along the German Baltic coast. *Marine Pollution Bulletin*, *99*(1–2), 216–229.

Strotmann, U., Reuschenbach, P., Schwarz, H., & Pagga, U. (2004). Development and Evaluation of an Online CO 2 Evolution Test and a Multicomponent Biodegradation Test System. *Applied and Environmental Microbiology*, *70*(8), 4621–4628.

Stuart, B. H. (2004). *Infrared Spectroscopy: Fundamentals and Applications*. *Methods* (Vol. 8). Wiley.

Sundt, P., Schultze, P.-E., & Syversen, F. (2014). *Sources of microplastic- pollution to the marine environment Project report. (Miljødirektoratet), Norwegian Environment Agency*. https://doi.org/M-321|2015

Talvitie, J., Heinonen, M., Pääkkönen, J. P., Vahtera, E., Mikola, A., Setälä, O., & Vahala, R. (2015). Do wastewater treatment plants act as a potential point source of microplastics? Preliminary study in the coastal Gulf of Finland, Baltic Sea. *Water Science and Technology*, *72*(9), 1495–1504.

The Lancet Planetary Health. (2017). Microplastics and human health—an urgent problem. *The Lancet Planetary Health*, *1*(7), e254.

Theobald, D. (2014). The measurement of suspended solids.

Thevenon, F. (2014). Plastics in the marine environment. In F. Thevenon, C. Carroll, & J. Sousa (Eds.), *Plastic debris in the ocean: the characterization of marine plastics and their environmental impacts, situation analysis report* (p. 52 pp). IUCN, Gland, Switzerland.

Tokiwa, Y., & Calabia, B. P. (2007). Biodegradability and Biodegradation of Polyesters. *Journal of Polymers and the Environment*, *15*(4), 259–267.

Tokiwa, Y., Calabia, B. P., Ugwu, C. U., & Aiba, S. (2009). Biodegradability of plastics. *International Journal of Molecular Sciences*, *10*(9), 3722–3742.

Tokiwa, Y., & Suzuki, T. (1981). Hydrolysis of copolyesters containing aromatic and aliphatic ester

blocks by lipase. *Journal of Applied Polymer Science*, *26*(2), 441–448.

Tribedi, P., Gupta, A. Das, & Sil, A. K. (2015). Adaptation of Pseudomonas sp. AKS2 in biofilm on low-density polyethylene surface: an effective strategy for efficient survival and polymer degradation. *Bioresources and Bioprocessing*, *2*(1), 2–14.

Turra, A., Manzano, A. B., Dias, R. J. S., Mahiques, M. M., Barbosa, L., Balthazar-Silva, D., & Moreira, F. T. (2014). Three-dimensional distribution of plastic pellets in sandy beaches: Shifting paradigms. *Scientific Reports*, *4*(4435), 1–7.

Umamaheswari, S., & Murali, M. (2013). FTIR spectroscopic study of fungal degradation of poly (ethylene terephthalate) and polystyrene foam. *Elixir Chemical Engineering*, *64*, 19159–19164.

UNEP. (2016). *Marine plastic debris and microplastics - Global lessons and research to inspire action and guide policy change*.

Van Cauwenberghe, L., & Janssen, C. R. (2014). Microplastics in bivalves cultured for human consumption. *Environmental Pollution*, *193*, 65–70.

Van Der Zee, M. (2011). Analytical Methods for Monitoring Biodegradation Processes of Environmentally Degradable Polymers. *Handbook of Biodegradable Polymers: Isolation, Synthesis, Characterization and Applications*, 263–281.

Venkatachalam, S., Nayak, S. G., Lade, J. V., Gharal, P. R., Rao, K., & Kelkar, A. K. (2012). Degradation and recyclability of Poly(ethylene terephthalate). In *Polyester* (pp. 75–98). Intech Open.

Vertommen, M. A. M. E., Nierstrasz, V. A., Veer, M. Van Der, & Warmoeskerken, M. M. C. G. (2005). Enzymatic surface modification of poly(ethylene terephthalate). *Journal of Biotechnology*, *120*(4), 376–386.

Wagner, M., Scherer, C., Alvarez-Muñoz, D., Brennholt, N., Bourrain, X., Buchinger, S., … Reifferscheid, G. (2014). Microplastics in freshwater ecosystems: what we know and what we need to know. *Environmental Sciences Europe*, *26*(1), 12.

Wang, J., Tan, Z., Peng, J., Qiu, Q., & Li, M. (2016). The behaviors of microplastics in the marine environment. *Marine Environmental Research*, *113*, 7–17.

Webb, H. K. (2012). *Biodegradation of poly(ethylene terephthalate) by marine bacteria, and strategies for its enhancement*. Swinburne University Technology.

Webb, H. K., Crawford, R. J., Sawabe, T., & Ivanova, E. P. (2009). Poly(ethylene terephthalate) polymer surfaces as a substrate for bacterial attachment and biofilm formation. *Microbes and Environments / JSME*, *24*(1), 39–42.

Wei, R., Oeser, T., Schmidt, J., Meier, R., Barth, M., Then, J., & Zimmermann, W. (2016). Engineered bacterial polyester hydrolases efficiently degrade polyethylene terephthalate due to relieved product

inhibition. *Biotechnology and Bioengineering*, *113*(8), 1658–1665.

Wei, R., & Zimmermann, W. (2017a). Biocatalysis as a green route for recycling the recalcitrant plastic polyethylene terephthalate. *Microbial Biotechnology*, *10*(6), 1302–1307.

Wei, R., & Zimmermann, W. (2017b). Microbial enzymes for the recycling of recalcitrant petroleum-based plastics: how far are we? *Microbial Biotechnology*, *10*(6), 1308–1322.

Weinreb, D., & Moon, D. (2005). *Handbook of Biodegradable Polymers*. (C. Bastioli, Ed.) (First). Rapra Technology Limited.

Witt, U., Müller, R. J., & Deckwer, W. D. (1995). New biodegradable polyester-copolymers from commodity chemicals with favorable use properties. *Journal of Environmental Polymer Degradation*, *3*(4), 215–223.

Wu, C., & Gan, Z. (1998). A novel method of studying polymer biodegradation. *Polymer*, *39*(18), 4429–4431.

Yamashita, R., & Tanimura, A. (2007). Floating plastic in the Kuroshio Current area, western North Pacific Ocean. *Marine Pollution Bulletin*, *54*(4), 485–488.

Yang, D., Shi, H., Li, L., Li, J., Jabeen, K., & Kolandhasamy, P. (2015). Microplastic Pollution in Table Salts from China. *Environmental Science and Technology*, *49*(22), 13622–13627.

Yoshida, S., Hiraga, K., Takanaha, T., Taniguchi, I., Yamaji, H., Maeda, Y., … Oda, K. (2016). A bacterium that degrades and assimilates poly(ethyleneterephthalate). *Science*, *351*(6278), 1196–1199.

Zbyszewski, M., & Corcoran, P. L. (2011). Distribution and degradation of fresh water plastic particles along the beaches of Lake Huron, Canada. *Water, Air, and Soil Pollution*, *220*(1–4), 365–372.

Zhang, J., Wang, X., Gong, J., & Gu, Z. (2004). A study on the biodegradability of polyethylene terephthalate fiber and diethylene glycol terephthalate. *Journal of Applied Polymer Science*, *93*(3), 1089–1096.

Zhang, K., Su, J., Xiong, X., Wu, X., Wu, C., & Liu, J. (2016). Microplastic pollution of lakeshore sediments from remote lakes in Tibet plateau, China. *Environmental Pollution*, *219*, 450–455.

Zhao, H., Du, H., Lin, J., Chen, X., Li, Y.-W., Li, H., … Wong, M. (2016). Complete degradation of the endocrine disruptor di-(2-ethylhexyl) phthalate by a novel Agromyces sp. MT-O strain and its application to bioremediation of contaminated soil. *Science of The Total Environment*, *562*, 170–178.

Zhao, L., Delatolla, R., & Mohammadian, A. (2013). Nitrification kinetics and modified model for the Rideau River, Canada. *Water Quality Research Journal of Canada*, *48*(2), 192–201.

Zhao, Y., Hu, T., Lv, Z., Wang, S., & Wu, C. (1999). Laser light-scattering studies of poly(caprolactone-b-ethylene oxide-b-caprolactone) nanoparticles and their enzymatic biodegradation. *Journal of Polymer Science, Part B: Polymer Physics*, *37*(23), 3288–3293.